A STUDY OF THE FUNCTION AND DISTRIBUTION OF α_1-ADRENOCEPTORS IN THE MOUSE CAROTID ARTERY

Laura Methven BSc (Hons)

Submitted for the degree of Doctor of Philosophy (PhD) in the Faculty of Science, University of Glasgow.

January 2007

ProQuest LLC.
789 East Eisenhower Parkway
P.O. Box 1346
Ann Arbor, MI 48106 – 1346

Abstract

The primary objective of these experiments was to examine the function and distribution of the α_1-adrenoceptor (α_1-AR) subtypes in the mouse carotid artery. The aims were achieved by using wire myography for the functional studies and confocal microscopy for the studies of α_1-AR distribution. For both types of study, single and double knockouts of the α_1-AR subtypes were employed, in addition to pharmacological analysis, to provide an insight into the α_1-ARs in the wild type (WT) mouse.

The aim of the first two studies presented in this thesis (Chapters Three and Four) was to establish whether an α_{1A}-AR-mediated and/or α_{1B}-AR-mediated contractile response exist in the mouse carotid artery, in addition to the predominant α_{1D}-AR. It was found that the α_{1A}-AR had a contractile role in this vessel based on pharmacological analysis in the WT mouse and knockout mice. Firstly, an α_1-AR-mediated contractile response was identified in the $\alpha_{1B/D}$-KO. Secondly, the α_{1D}-AR and another α_1-AR subtype were identified as mediating the phenylephrine-induced response by employing subtype selective antagonists. Thirdly, the A-61603-induced response was found to be mediated by the α_{1A}-AR and the α_{1D}-AR using subtype selective antagonists. This also demonstrated that this α_{1A}-AR selective agonist had an action on the α_{1D}-AR. In the absence of α_{1B}-AR selective compounds, comparison of the agonist responses in the WT mouse and knockout mice revealed that a minor α_{1B}-AR-mediated response was also present. Thus, the α_{1D}-AR predominantly mediates the vasoconstriction of the mouse carotid artery but the α_{1A}-AR and α_{1B}-AR appear to contribute to the contractile response.

The aim of Chapter Five was to assess the effect of nitric oxide (NO) on the α_1-AR-mediated contractile response in the mouse carotid artery. The contractile response to both phenylephrine and A-61603 was augmented by the nitric oxide synthase inhibitor L-NAME. This suggested that the α_1-AR-mediated contractile response was suppressed by NO. An attempt was made to determine whether NO was released spontaneously in this vessel or in response to α_1-AR stimulation. There was no evidence of constitutive NO release. The effect of L-NAME was greater with increasing concentrations of α_1-AR agonist and a non-adrenergic response was shown to be unaffected by L-NAME. From these findings it is evident that in the mouse carotid artery activation of α_1-ARs triggers NO release, which suppresses the α_1-AR-mediated contractile response.

Chapter Six aimed to examine the distribution of the α_1-AR subtypes in the media of the mouse carotid artery. A protocol was developed to determine optimum conditions to visualise the binding distribution of the fluorescent α_1-AR ligand Quinazoline Piperazine Bodipy (QAPB) in the media of this vessel. Comparison of QAPB binding in the WT mouse with the α_1-AR knockout mice demonstrated that the α_{1D}-AR was a major component of the α_1-AR population. The use of non-fluorescent subtype selective antagonists to compete for QAPB binding sites revealed that the α_{1A}-AR and α_{1B}-AR also appeared to exist in the media of the WT mouse. Comparison of the QAPB subcellular binding distribution in the WT mouse and knockout mice suggested that the α_{1B}-AR may be predominantly located on the cell surface, while, in the absence of the α_{1B}-AR, the α_{1A}-AR and α_{1D}-AR may be predominantly located at intracellular sites.

The final study in this thesis (Chapter seven) aimed to establish whether α_1-ARs exist on the endothelium of the mouse carotid artery. Evidence of α_1-ARs on endothelial cells (EC) was found both in the WT and knockout mice through the use of QAPB and non-fluorescent subtype selective antagonists. The proportion of EC with QAPB binding was reduced in the knockout mice indicative of the loss of an entire α_1-AR population compared to the WT mouse. Comparing QAPB binding in the WT mouse and knockout mice in the presence of the non-fluorescent antagonists provided evidence that all three α_1-AR subtypes are present on the endothelium in the carotid artery of the WT mouse.

Collectively, the findings of the studies presented in this thesis demonstrate that all three α_1-ARs are present and are functional in the mouse carotid artery. The α_{1D}-AR is confirmed as being the predominant contractile α_1-AR subtype but both the α_{1A}-AR and α_{1B}-AR do have minor contractile roles in this vessel. Furthermore, the activation of α_1-ARs on the endothelium may result in the release of NO and subsequently cause the suppression of the α_1-AR-mediated contractile response.

Table of Contents

List of Tables

List of Figures

Acknowledgements

First of all I would like to thank Professor Ian McGrath, whose enthusiasm for and knowledge of adrenoceptors, and science in general, is inspiring. His guidance and advice is invaluable and much appreciated. Thank you so much.

I would also like to thank my second supervisor Dr Craig Daly for his input into my studies and comments on my thesis.

The lab has been a great place to work. Not only has Melissa made the lab a fun place, useful advice was also much appreciated. Thank you to Joyce for always going out of her way to help. I would like to thank those I still consider members of Lab 440 even though they have now moved on: Jude, Clare, Zeeshan, Angela and Simon. You have all made my PhD an enjoyable experience and taught me a lot.

I would also like to thank Jose Maria for training me in confocal microscopy during his visit from Spain.

Helen deserves huge thanks for putting up with long rants about my thesis, whether in the flat or during our long training runs for the half marathon.

I would like to thank my family for their valuable support and for always having confidence in me. In particular, Mum and Dad's positive way of thinking means a lot. Thank you to Alison for the frequent phone calls checking up on me (as a big sis does), and for keeping me up to date with the latest arrivals at Topshop.

Robert, thank you for going through everything with me. You deserve a medal! I hope you are as proud of me as I am of you.

Finally, I would like to acknowledge the financial support of the Ann B. McNaught Bequest and the British Heart Foundation.

Author's Declaration

I hereby declare that this thesis has been composed by myself, and that the work of which it is a record has been done by myself, except where specifically acknowledged. I also confirm that it has not been submitted in any previous application for a higher degree and that all sources of information have been specifically acknowledged by means of references.

Some of the results contained in this thesis have been published in peer-reviewed journals as follows:

Deighan C, **Methven L,** Naghadeh M.M, Wokoma A, MacMillan J, Daly C.J, Tanoue A, Tsujimoto G, McGrath J. C. (2005). Insights into the functional roles of alpha1-adrenoceptor subtypes in mouse carotid arteries using knockout mice. *Br J Pharmacol*, 144: 558-565.

Methven L, Daly C and McGrath JC (2006). Visualisation of endothelial α1-adrenoceptors in the murine carotid artery. Published at *Proceedings of the British Pharmacological Society* at http://www.pA2online.org/abstracts/Vol3Issue4abst144P.pdf.

Abbreviations

α_{1A}-KO	α_{1A}-adrenoceptor knockout mouse
α_1-AR	Alpha$_1$-adrenoceptor
α_{1b}	Denotes a receptor cloned, then expressed in a cell line
α_{1B}	Denotes a receptor subtype that has been classified pharmacologically
$\alpha_{1B/D}$-KO	$\alpha_{1B/D}$-adrenoceptor knockout mouse
α_{1B}-KO	α_{1B}-adrenoceptor knockout mouse
α_{1D}-KO	α_{1D}-adrenoceptor knockout mouse
µm	Micrometer
µM	Micromolar
$[Ca^{2+}]_i$	Intracellular Ca^{2+} concentration
5-HT	5-hydroxytryptamine
5MeU	5-methylurapidil
A-61603	N-[5-(4,5-Dihydro-1H-imidazol-2-yl)-2-hydroxy-5,6,7,8-tetrahydronaphthalen-1-yl]methane sulfonamide
AH11110A	4-Imino-1-(2-phenylphenoxy)-4-piperidinebutan-2-ol hydrochloride
BMY7378	dihydrochloride 8-[2-[4-(2-methoxyphenyl)-1-piperozyn]-8-azaspiro (4,5) decone-7,9-dione
$CaCl_2$	Calcium chloride
cAMP	Adenosine 3'-5' cyclic monophosphate

CEC	Chloroethylclonidine
CHO	Chinese hamster ovary
CLSM	Confocal laser scanning microscopy
CO_2	Carbon dioxide
COS	Chinese hamster ovary
CRC	Concentration response curve
DAG	Diacylglycerol
EC	Endothelial cells
GFP	Green fluorescent protein
HEK	Human embryonic kidney
IP_3	Inositol-1,4,5-triphosphate
L-NAME	Nω-Nitro-L-arginine methyl ester
mM	Millimolar
mRNA	Messenger ribonucleic acid
NA	Noradrenaline
nM	Nanomolar
NO	Nitric oxide
NOS	Nitric oxide synthase
pA_2	affinity estimate of an antagonist derived from a Schild plot
PE	Phenylephrine

pEC_{50}	negative log of agonist concentration producing fifty percent of the maximal response, alone, or in the presence of an antagonist
PIP_2	Phosphatidylinositol 4,5-biphosphate
pK_B	Negative logarithm of the equilibrium dissociation constant
pK_i	Negative logarithm of a concentration of competing ligand in a competition assay that would occupy 50% of the receptors if no radioligand was present.
PMT	photomultiplier tube
PSS	Physiological salt solution
QAPB	Quinazoline Piperazine Borate-dipyrromethene (BODIPY FL-prazosin)
RS100 329	N-[(2-trifluoroethoxy)phenyl],N'-(3-thyminylpropyl) piperazine hydrochloride
SEM	standard error of the mean
SMC	Smooth muscle cell

Chapter 1 General Introduction

Adrenoceptors regulate the actions of the endogenous catecholamines noradrenaline (a neurotransmitter) and adrenaline (a hormone) in many physiological processes in both the central and peripheral nervous system. In the peripheral nervous system adrenoceptors mediate a variety of processes, such as vascular tone, glycogenolysis and cardiac contraction. The role of adrenoceptors in vascular tone shall be examined in this thesis.

1.1. Adrenoceptor classification

In 1905, Dale reported that adrenaline produced vasoconstriction, which resulted in a rise in blood pressure and vasodilation. These early experiments were the first to associate adrenaline with the concept of a receptor and were the initial steps in the identification of adrenoceptors. In 1948, Ahlquist studied the effects of catecholamines on physiological responses in isolated tissues and proposed that two adrenoceptor subtypes existed, which were designated alpha (α) and beta (β). This designation was based on different potency series for the catecholamines: the potency series for α-ARs was adrenaline = noradrenaline > isoproterenol, and for β-ARs was isoproterenol > adrenaline > noradrenaline. This subdivision of adrenoceptors was later confirmed when phentolamine and ergotoxine were shown to selectively antagonise α-ARs, while dichloroisoprenaline (Powell & Slater, 1958) and propranolol (Black *et al.*, 1964) blocked β-ARs. Two β-ARs subtypes were then identified and classified as β_1 and β_2 (Lands AM *et al.*, 1967;Furchgott, 1967). A study by Brown and Gillespie (1957) reporting that the α-AR antagonists dibenamine and phenoxybenzamine increased noradrenaline release by nerve stimulation, together with a study by Starke (1972), lead to the identification of pre-junctional α-ARs. The α-ARs were subsequently subdivided into subgroups based on their anatomical location: α_1-ARs were labelled post-junctional and α_2-ARs pre-junctional (Langer, 1974). An alternative classification designating α-ARs according to function was proposed, in which α_1-ARs mediated the excitatory responses, while α_2-ARs mediated inhibitory responses (Berthelsen & Pettinger, 1977). This classification was superseded by a classification based on the potency of agonists and antagonists for α-ARs (McGrath, 1982b;Bylund DB *et al.*, 1994;Hieble *et al.*, 1995). α_1-ARs could be activated by methoxamine, cirazoline or phenylephrine and inhibited by prazosin, WB4101 or corynanthine. α_2-ARs could be activated by α-methylnoradrenaline, UK-14304, B-HT920 or B-HT933 and inhibited by yohimbine, rauwolscine or idazoxan α_2-AR. It later became evident that heterogeneous subgroups existed within both the α_1-AR and α_2-AR subtypes.

The α_1-ARs were the first to be subclassified. Based on functional studies, McGrath et al. (1982a) proposed that the α_1-ARs be further subdivided on the basis of agonist selectivity. Furthermore, Morrow and Creese (1986) proposed two α_1-AR subtypes: α_{1A}-ARs and α_{1B}-ARs based on differences in affinity for WB4101 and phentolamine in radioligand binding assays. The existence of these α_1-AR subtypes was supported by subsequent studies, which identified antagonists showing selectivity for what was then considered to be the α_{1A}-AR over the α_{1B}-AR (Gross *et al.*, 1988;Minneman *et al.*, 1988).

From the late 1980s, the development of molecular cloning techniques and drugs with improved selectivity aided the subclassification of adrenoceptors. Molecular cloning techniques were used to identify four α_1-AR subtypes which were designated α_{1a}, α_{1b}, α_{1c} and α_{1d}. Uppercase and lowercase are used to designate the α_1-AR subtypes defined by pharmacological and molecular techniques, respectively. The α_{1b}-AR was the first α_1-AR cloned (Cotecchia *et al.*, 1988) and has since been shown to correspond to the pharmacologically defined α_{1B}-AR (Heible JP *et al.*, 1995b). However, the other subtypes cloned were inconsistent with those that had been characterised pharmacologically or by radioligand binding. The cloned α_{1c}-AR was thought to be a novel subtype (Schwinn *et al.*, 1990) but subsequent studies showed it was a homologue of the existing α_{1a}-AR subtype (Perez *et al.*, 1994;Rokosh *et al.*, 1994;Price *et al.*, 1994a;Pimoule *et al.*, 1995;Laz *et al.*, 1994) and was reclassified as α_{1A}-AR (Heible JP *et al.*, 1995a). It was determined that the clone initially identified as α_{1a}-AR was a novel subtype (Ford *et al.*, 1994;Perez *et al.*, 1991;Lomasney *et al.*, 1991) and was classified as the α_{1D}-AR (Bylund DB *et al.*, 1994). In addition, α_1-ARs showing low affinity for prazosin were identified and classified as α_{1L}-AR (Flavahan & Vanhoutte, 1986). It has been proposed that the α_{1L}-AR may be a different conformational state of the α_{1A}-AR (Ford *et al.*, 1998;Marti *et al.*, 2005).

The α_2-ARs were subdivided into α_{2A}-AR, α_{2B}-AR and α_{2C}-AR largely based on radioligand binding assays (Bylund *et al.*, 1988), corroborated by molecular cloning (Regan *et al.*, 1988;Bylund DB *et al.*, 1994). Molecular cloning also revealed an α_{2D}-AR subtype in rodents, which was later found to be a species homolog of the human α_{2A}-AR and is now referred to as the $\alpha_{2A/D}$-AR (Bylund DB *et al.*, 1994).

The pharmacological subdivision of the β-ARs into β_1-ARs and β_2-ARs was also verified by molecular cloning (Frielle *et al.*, 1987;Dixon *et al.*, 1986). A new subtype termed the

β_3-AR was also cloned (Arch *et al.*, 1984). In addition, the β_4-AR subtype was proposed (Bylund DB *et al.*, 1994) but was not cloned. Consequently, it is now recognised that the β_4-AR is a novel state of the β_1-AR (Granneman, 2001).

Adrenoceptors have now been characterised as three major subtypes, each containing heterogeneous subgroups: α_1-AR (α_{1A}-AR, α_{1B}-AR and α_{1D}-AR), α_2-AR (α_{2A}-AR, α_{2B}-AR and α_{2C}-AR) and β-AR (β_1-AR, β_2-AR and β_3-AR). The α_1-AR subtypes are of key interest to this thesis.

1.2. α_1-AR compounds

1.2.1. α_1-AR agonists

The catecholamine noradrenaline is classed as a non-selective adrenoceptor agonist as it activates α_1-ARs, α_2-ARs and β-ARs with similar potencies (Knepper et al., 1995). However, it has been demonstrated using radioligand binding assays that noradrenaline had 20-times higher affinity for α_{1D}-ARs compared to α_{1A}-ARs and α_{1B}-ARs (Minneman *et al.*, 1994).

Phenylephrine is a non-selective α_1-AR agonist, which can enable the α_1-AR response to be studied in isolation. It should be noted that in some studies phenylephrine was more potent for the α_{1D}-AR than the other α_1-AR subtypes (Knepper SM *et al.*, 1995;Perez *et al.*, 1991;Lomasney *et al.*, 1991;Minneman *et al.*, 1994). It has been suggested that the variations in the potency of phenylephrine may be due to differences in receptor populations in different tissues and species (Minneman *et al.*, 1994).

The development of selective compounds for the α_{1A}-AR subtype has proved more successful than for the α_{1B}-AR or α_{1D}-AR subtypes, which do not have any effective selective agonists at present. There are a limited number of α_{1A}-AR selective agonists available, including A-61603 (Knepper SM *et al.*, 1995).

The potential use of A-61603 as a potent α_{1A}-AR selective agonist was first reported by Knepper and colleagues (1995), who studied A-61603 in a variety of tissues believed to have a predominance of α_{1A}-ARs: the rat submaxillary gland (Michel *et al.*, 1989); the rat vas deferens (Honner & Docherty, 1999;Aboud *et al.*, 1993); the canine prostate (Goetz *et*

al., 1994); and the cloned bovine α_{1a}-AR (Schwinn et al., 1990). This was compared to the A-61603-induced response in α_{1B}-AR sites(cloned hamster α_{1b}-AR (Cotecchia et al., 1988)) and α_{1D}-AR sites (cloned rat α_{1d}-AR (Perez et al., 1991)). Radioligand binding suggested A-61603 had increased affinity for the α_{1A}-AR sites by 35-125-times compared to α_{1B}-AR sites and 45-150-times than the α_{1D}-AR. Similarly, radioligand binding experiments showed that A-61603 had 20 times increased affinity at the canine prostate α_{1A}-AR than the α_{1B}-AR of the rat spleen and had over 300 times higher affinity compared to the α_{1D}-AR of the rat aorta (Knepper et al., 1995). Furthermore, in functional experiments, for instance, at the rat vas deferens α_{1A}-AR indicated A-61603 was 60 times more potent than the α_{1B}-AR of the rat spleen and over 1000 times more potent than the α_{1D}-AR of the rat aorta (Knepper et al., 1995). The decreased potency of A-61603 at both α_{1B}-AR and α_{1D}-AR sites, reported by Knepper et al. (1995), has been supported by several other studies. For instance, a recent study using the mouse myocardium, which is believed to have α_{1A}-ARs and α_{1B}-ARs but no α_{1D}-ARs, the lack of response to A-61603 in the trabeculae from the α_{1A}-KO provided evidence that A-61603 did not stimulate the α_{1B}-AR (McClosskey et al., 2002). Similarly, despite producing a pressor response in the wild type (WT) mouse, A-61603 did not alter the baseline heart rate and mean arterial pressure in the α_{1A}-KO (Rokosh and Simpson, 2002), in agreement with A-61603 having minimal effect on the α_{1B}-AR and α_{1D}-AR. In addition, in the α_{1BD}-KO, where the only possible α_1-AR is the α_{1A}-AR, the pressor response to A-61603 was comparable to the WT mouse verifying selectivity for the α_{1A}-AR (Hosoda et al., 2005).

In radioligand binding studies, the affinity of A-61603, compared to phenylephrine and noradrenaline, at the α_{1A}-AR sites, revealed that A-61603 had 30-100-fold higher affinity than phenylephrine and 15-25-times higher affinity than noradrenaline (Knepper et al., 1995). The increase in affinity identified in the radioligand binding data was also observed in functional experiments, which showed that A-61603 was 160-300-fold more potent than phenylephrine and 130-200-fold more potent than noradrenaline at the α_{1A}-AR sites (Knepper *et al.*, 1995). In a study of the rat vas deferens, Honner and Docherty (1999) reported potency values for A-61603, noradrenaline and phenylephrine that support those obtained by Knepper et al. (1995). Additional functional studies also showed that A-61603 was more potent than noradrenaline and phenylephrine in various vessels where the α_{1A}-AR was considered to be dominant. For instance, in human subcutaneous resistance arteries, A-61603 demonstrated ten-fold higher potency than noradrenaline and was 54-fold more potent than phenylephrine (Jarajapu et al., 2001d).

Knepper et al. (1995) also reported that the potency of A-61603 compared to noradrenaline and phenylephrine was less substantial at the α_{1B}-AR and the α_{1D}-AR. For instance, A-61603 was only 40 times more potent than phenylephrine at α_{1B}-AR sites, compared to 160-300 at α_{1A}-AR sites, and only 30 times more potent than noradrenaline, as opposed to 130-200 times higher potency at α_{1A}-AR sites. Furthermore, at the α_{1D}-AR in rat aortic rings A-61603 was 30-fold less potent than phenylephrine and over 500-times less potent than noradrenaline. Thus, there is considerable evidence that A-61603 shows higher potency than noradrenaline and phenylephrine at α_{1A}-AR sites and lower potency at α_{1B}-AR and α_{1D}-AR sites.

There is, therefore, substantial evidence for the effectiveness of A-61603 as an α_{1A}-AR agonist. However, it should be noted that A-61603 is an imidazoline and can act through a non-adrenoceptor-mediated mechanism in some vessels (Willems *et al.*, 2001). The A-61603-induced contractile response in the carotid arteriovenous anastomes of the pig was not characterised despite the activation of α_1-ARs, α_2-ARs, 5-$HT_{1B/D}$ receptors, 5-HT_2 receptors and eicosanoid receptors being excluded.

1.2.2. α_1-AR selective antagonists

Prazosin is a non-selective α_1-AR antagonist (Hanft & Gross, 1989;Ford *et al.*, 1994). In the vast majority of studies prazosin acts as a competitive reversible antagonist. However, agonist curves with depressed maximum responses and nonparallel shifts have been reported in the rat aorta (Alosachie & Godfraind, 1988;Doggrell, 1992) and murine aorta (Yamamoto & Koike, 2001b). In addition, although being classed as a non-selective antagonist, there is evidence from IP accumulation experiments that prazosin shows some selectivity for the α_{1B}-AR and α_{1D}-AR over the α_{1A}-AR (Williams *et al.*, 1999).

WB 4101 was the first compound classed as an α_{1A}-AR selective antagonist (Morrow & Creese, 1986) and showed 20-fold selectivity for what was then termed the α_{1A}-AR over the α_{1B}-AR. However, the α_1-AR subtype referred to in this study as the α_{1A}-AR was redesignated as the α_{1D}-AR. In fact, subsequent studies have demonstrated that WB 4101 has high affinity at both the α_{1A}-AR and the α_{1D}-AR (Perez *et al.*, 1991;Schwinn *et al.*, 1995;Weinberg *et al.*, 1994). Since the identification of WB 4101, several other α_{1A}-AR selective antagonists became available, such as 5-methylurapidil (Gross *et al.*, 1988), KMD-3213 (Shibata *et al.*, 1995), RS 17053 (Ford et al., 1996), tamusolin (Foglar et al., 1995), Rec 15/2739 (Leonardi et al., 1997) and RS100 329 (Williams *et al.*, 1999). The

selectivity of 5-methylurapidil and RS100 329 has been examined in more detail for the purposes of this thesis.

5-methylurapidil has been used as an α_{1A}-AR selective compound in both radioligand binding assays (Gross *et al.*, 1988;Yoshio R *et al.*, 2001) and functional experiments (Kong *et al.*, 1994;Daniel *et al.*, 1999;Yang *et al.*, 1998;Argyle & McGrath, 2000;Perez *et al.*, 1994). 5-methylurapidil displayed approximately 100-fold higher affinity for α_{1A}-ARs in the rat hippocampus, heart and vas deferens over α_{1B}-ARs in the rat liver and spleen (Gross *et al.*, 1988). It has also been shown that 5-methylurapidil has intermediate affinity for the α_{1D}-AR (Kenny *et al.*, 1995;Perez *et al.*, 1991;Schwinn *et al.*, 1995). In the literature, in rat and mouse vessels in which the α_{1A}-AR is predominant, affinity estimates for 5-methylurapidil ranged from 8.0 to 9.2 (Daly *et al.*, 2002a;Buckner *et al.*, 1996;Gisbert *et al.*, 2003;Shibano *et al.*, 2002;Zacharia *et al.*, 2004;Kamikihara *et al.*, 2005;Lachnit *et al.*, 1997). In vessels of these rodents in which the α_{1D}-AR predominates, affinity estimates ranged from 7.5 to 8.3 (Daly *et al.*, 2002a;Kenny *et al.*, 1995;Aboud *et al.*, 1993;Buckner *et al.*, 1996;Testa *et al.*, 1997;Gisbert *et al.*, 2003). With the overlap in affinity estimates it is clear that 5-methylurapidil does not clearly differentiate the α_{1A}-AR from the α_{1D}-AR.

An alternative α_{1A}-AR selective antagonist, RS100329, has been reported to have 126-fold increased selectivity for the α_{1A}-AR over the α_{1B}-AR and 50-fold over the α_{1D}-AR in radioligand binding studies (Williams *et al.*, 1999) and has been increasingly used in recent studies. The reported affinity of RS100 329 in the mouse vas deferens, in which the α_{1A}-AR predominates was 9.6 (Cleary *et al.*, 2003), while in the rat aorta, in which the α_{1D}-predominates an affinity estimate of 7.9 was reported (Williams *et al.*, 1999).

Only one antagonist is available that is selective for the α_{1D}-AR over the α_{1A}-AR and the α_{1B}-AR. BMY 7378 has been shown to competitively antagonise α_{1D}-ARs with 100-fold higher selectivity over both the α_{1A}-AR and α_{1B}-AR (Goetz *et al.*, 1995;Saussy *et al.*, 1996). Affinity estimates ranging from 8.3 to 9.6 have been reported from vessels in the rat and mouse which are predominantly α_{1D}-AR (Daly *et al.*, 2002a;Hosoda *et al.*, 2005b;Tanoue *et al.*, 2002b;Yamamoto & Koike, 2001b). In comparison, in the rat and mouse affinity estimates for BMY 7378 in vessels where the α_{1A}-AR predominates ranged from 5.8 to 6.7 (Shibano *et al.*, 2002;Gisbert *et al.*, 2003;Lachnit *et al.*, 1997;Kamikihara *et al.*, 2005;Zacharia *et al.*, 2004). It should be noted that BMY 7378 acts as a partial agonist at the 5-HT_{1A} receptor . Furthermore, a recent study reported that at concentrations greater

than 0.3 μM BMY 7378 acted as an antagonist at the α_{2C}-AR (Cleary *et al.*, 2005). Nevertheless, BMY 7378 is widely used to identify α_{1D}-ARs (Hosoda *et al.*, 2005b;Daly *et al.*, 2002a;Tanoue *et al.*, 2002b;Yamamoto & Koike, 2001b).

There is a distinct lack of α_{1B}-AR selective antagonists. Chloroethylclonidine was initially classified as an α_{1B}-AR selective antagonist (Han *et al.*, 1987), showing approximately 5-fold higher affinity for the α_{1B}-AR over what was then considered to be the α_{1A}-AR in radioligand binding and functional experiments, and 3-fold higher affinity for the α_{1B}-AR over the α_{1D}-AR (Kenny *et al.*, 1995;Michel *et al.*, 1989;Schwinn *et al.*, 1995). However, there is substantial evidence that chloroethylclonidine alkylated all of the α_1-AR subtypes and could not be classed as an α_{1B}-AR antagonist (Perez *et al.*, 1994;Lomasney *et al.*, 1991;Schwinn *et al.*, 1990;Hirasawa *et al.*, 1997). Several other compounds have been proposed as potential α_{1B}-AR selective antagonists, based on radioligand binding studies, such as spiperone (Bylund *et al.*, 1994), respiperone (Sleight *et al.*, 1993), cyclazosin (Giardina *et al.*, 1996) and AH11110A (Saussy *et al.*, 1996). However, these compounds proved to be only moderately selective for the α_{1B}-AR over the α_{1A}-AR and α_{1D}-AR, or discrepancies were found between binding and functional studies (Stam *et al.*, 1998;Giardina *et al.*, 2003;Eltze *et al.*, 2001;Giardina *et al.*, 2003;Schwinn *et al.*, 1995).

It is clear that agonists and antagonists with clear selectivity for the individual α_1-AR subtypes are still required. Despite the current attempts to develop new compounds, the lack of subtype selective compounds hinders the pharmacological characterisation of α_1-ARs. The subtype selectivity of the compounds used will be assessed throughout the studies described in this thesis.

1.3. α_1-AR signalling

Adrenoceptors are G-protein coupled receptors, which consist of seven transmembrane spanning domains and are connected by three intracellular and three extracellular loops. The transmembrane domains are highly conserved between α_1-AR subtypes, but the C-terminus and N-terminus differ (Graham *et al.*, 1996;Faure *et al.*, 1994a). Stimulation of α_1-ARs produces cellular responses by initiating multiple signalling pathways, which can vary depending on the guanine nucleotide binding protein (G protein) that the α_1-AR subtype couples to.

The $G_{q/11}$ family is the predominant G-protein for all three α_1-AR subtypes (Wu *et al.*, 1992). Upon stimulation, the α_1-ARs couple to the $G_{q/11}$, which usually results in the activation of phospholipase C. Once activated, phospholipase C catalyses the hydrolysis of phosphatidylinositol-4,5-bisphosphate, producing the second messengers inositol-1,4,5-trisphosphate (IP_3) and diacylglycerol (DAG). IP_3 stimulates the release of intracellular calcium ($[Ca^{2+}]_i$) from internal stores and DAG activates protein kinase C. Differences in the coupling of the α_1-AR subtypes to this signalling pathway are apparent. For instance, Schwinn et al. (1991) showed that the α_{1A}-AR activates IP_3 formation more efficiently than the α_{1B}-AR. Furthermore, subsequent studies reported that the α_{1A}-AR is efficiently coupled to IP_3, while the α_{1D}-AR is poorly coupled (Schwinn *et al.*, 1995;Theroux *et al.*, 1996;Taguchi *et al.*, 1998;Gisbert *et al.*, 2000;Garcia-Sainz & Villalobos-Molina, 2004). Interestingly, this contrasts with native cells in which the α_{1D}-AR appears to be particularly well coupled relative to the α_{1A}-AR.

In addition to phospholipase C, α_1-ARs have been shown to activate phospholipase A_2 (Perez *et al.*, 1993), phospholipase D (Ruan *et al.*, 1998), voltage-dependent and independent Ca^{2+}-channels leading to Ca^{2+} influx (Minneman, 1988) and mitogen-activated protein kinase (Williams *et al.*, 1998).

1.4. α_1-AR subcellular localisation

1.4.1. Unstimulated cells

The development of antibodies specific to the α_1-AR subtypes have enabled the localisation of α_1-AR proteins to be identified. One of the first studies to use this approach was performed in unstimulated Chinese hamster ovary (COS-7) cells and reported a difference in the localisation of the α_{1A}-AR and α_{1B}-AR: a predominance of the α_{1A}-AR intracellularly and the α_{1B}-AR on the cell surface (Hirasawa *et al.*, 1997). A later study in rat-1 fibroblasts and cells cultured from the femoral and renal arteries, identified all three α_1-ARs on both the cell surface and inside the cell (Hrometz *et al.*, 1999). However, the α_{1B}-AR was most visible on the cell surface, while the localisation of the α_{1A}-AR and α_{1D}-AR was less clear. McCune et al. (2000) agreed that the α_{1B}-AR was predominantly located on the cell surface in unstimulated rat-1 fibroblasts. This study also reported that the α_{1D}-AR was mainly intracellular. A more recent study employed α_1-AR antibodies in transfected human embryonic kidney (HEK-293) cells to investigate the effect of α_1-AR

heterodimers on subcellular localisation (Uberti *et al.*, 2003). It was found that the α_{1B}-AR could dimerise with the α_{1A}-AR and α_{1D}-AR. In particular, the α_{1B}-AR/α_{1D}-AR dimer resulted in a reduction in the intracellular expression, and an increase in the cell surface expression, of the α_{1D}-AR.

Green fluorescent protein (GFP) is an autofluorescent protein that can be attached to recombinant receptors to examine receptor localisation. The use of α_1-AR-GFP-tagged receptors in COS-7 transfected cells revealed that the α_{1B}-AR was predominantly found on the cell surface and that α_{1A}-ARs were predominantly located at intracellular sites (Hirasawa *et al.*, 1997). This was in agreement with the findings of the studies using α_1-AR antibodies. However, a subsequent study using transfected HEK 293 cells reported the predominance of both the α_{1A}-AR-GFP and α_{1B}-AR-GFP on the cell surface and found that the α_{1D}-AR-GFP was intracellular (Chalothorn *et al.*, 2002). Hague *et al.*(2004a) also demonstrated that the α_{1D}-AR was mainly intracellular in HEK 293 cells, as well as in rat aortic smooth muscle cells and CHO cells. This study suggested that the limited cell surface expression of the α_{1D}-ARs-GFP in HEK 293 cells was due to a long N-terminus. This was demonstrated by a reduction in the binding site density of the α_{1A}-AR and α_{1B}-AR when the N-terminus of these subtypes was replaced with that of the α_{1D}-AR. Furthermore, the cell surface expression of the α_{1D}-AR was improved when the α_{1D}-AR N-terminus was shortened or substituted with the N-terminus of the α_{1B}-AR (Hague *et al.*, 2004a).

BODIPY fluorescent prazosin (Quinazoline Piperazine Bodipy (QAPB)) is a useful tool for the study of the subcellular localisation of α_1-ARs as it is a green fluorescent ligand with high affinity for α_1-ARs. Using QAPB in rat-1 fibroblasts transfected with the α_{1d}-AR, α_1-ARs have been detected both intracellularly and on the cell surface (Daly *et al.*, 1998). This was also demonstrated in a subsequent study in five rat basilar SMCs (McGrath *et al.*, 1999). Furthermore, in human SMCs the population of intracellular α_1-ARs detected at intracellular sites was quantified as approximately 40% of the total population of α_1-ARs (Mackenzie *et al.*, 2000). A subsequent study using QAPB in transfected COS-7 cells reported that the α_{1a}-AR was predominantly inside the cell and the α_{1b}-AR mostly localised on the cell surface, although some evidence of intracellular α_{1b}-ARs was reported (Sugawara *et al.*, 2002). This supports previous results by that group using GFP-tagged α_1-ARs (Hirasawa *et al.*, 1997). A recent study in the mouse mesenteric artery found that the α_{1A}-AR was located on both the cell surface and intracellularly

(McBride *et al.* Submitted for publication) in agreement with findings in isolated cells (Sugawara *et al.*, 2002). At present, no other studies have examined the subcellular location of α_1-ARs in whole blood vessels.

The findings of the localisation studies using α_1-AR antibodies, GFP-tagged α_1-ARs and fluorescent α_1-AR ligands are in general agreement. Collectively, they suggest that in unstimulated isolated cells the α_{1B}-AR is predominantly located on the cell surface and the α_{1A}-AR and α_{1D}-AR are predominantly located at intracellular sites. However, all three α_1-AR subtypes do appear to be present both on the cell membrane and inside the cell of most cell types.

1.4.2. Receptor cycle

The receptor cycle has been visualised using GFP-tagged receptors (Kallal & Benovic, 2000). Like other G-protein coupled receptors, α_1-ARs are synthesised in the Golgi apparatus, where they are inserted into the cell membranes of intracellular vesicles. The intracellular vesicles transport the receptors to the cell surface and the vesicles fuse with membrane. At the cell surface, the receptors can be activated by agonists to produce functional responses. Subsequently, the receptors become phosphorylated, resulting in inactivation. This is followed by internalisation, with the vesicles moving back to the perinuclear region, and recycled by dephosphorylation or degraded in lysosomes.

There is evidence from immunohistochemistry to suggest that exposure to an agonist at the cell surface can stimulate the internalisation of the receptor and translocation to the perinuclear region. The majority of evidence is provided for the α_{1B}-AR, which has been shown to internalise when exposed to noradrenaline (Fonseca *et al.*, 1995;Hague *et al.*, 2004b), phenylephrine (McCune *et al.*, 2000) or adrenaline (Hague *et al.*, 2004b). However, Chalothorn *et al.*(2002) reported that upon stimulation, the proportion of α_{1A}-ARs located intracellularly increases, but there was little evidence of the α_{1D}-AR undergoing agonist-induced internalisation. This study also found that internalisation was dependent on the stimulated receptors associating with arrestin molecules and that the agonist-stimulated internalization of the α_{1A}-AR was slower than the α_{1B}-AR. It has been suggested that the lack of evidence for the agonist-induced internalisation of the α_{1D}-AR may be due to a constitutively active α_{1D}-AR resulting in the high proportion of α_{1D}-ARs already being intracellular prior to agonist exposure (Chalothorn et al., 2003).

The fluorescent ligand QAPB has been used to study α_1-AR cycling in rat-1 fibroblasts and HEK 293 cells expressing the α_{1A}-AR (Pediani *et al.*, 2005). It was found that QAPB bound the α_{1A}-AR on the cell surface, and was internalised with the receptor. However, the potential for QAPB acting as an agonist or inverse agonist has been discounted (Pediani *et al.*, 2000). Therefore, the internalisation of QAPB bound to the α_{1A}-AR appeared to be due to spontaneous endocytosis. It was shown that the bound QAPB was transported to perinuclear regions by vesicles and could be recycled back to the cell surface. In agreement with the subcellular localisation reported in previous studies (Hirasawa *et al.*, 1997;Sugawara *et al.*, 2002), α_{1A}-ARs were predominantly intracellular, consistent with the α_{1A}-AR moving between the cell surface and perinuclear compartments. Pediani et al. (2005) also reported that the internalisation of the α_{1A}-AR relied on β-arrestins, which supports the study by Chalothorn *et al.* (2002), since there was no evidence for the uptake of QAPB in β-arrestin deficient cells but there was evidence of QAPB and β-arrestin-2-GFP being colocalised.

In addition to examining the subcellular localisation of α_1-ARs in unstimulated cells, α_1-AR antibodies, GFP-tagged receptors for the α_1-AR subtypes and α_1-AR fluorescent ligands can be used to visualise α_1-AR cycling. This evidence suggests that α_1-AR internalisation and the subsequent receptor cycling can be stimulated, by agonist binding, or can be spontaneous.

1.5. α_1-AR tissue distribution

RT-PCR, RNase protection assays and Northern blotting can be used to study mRNA expression. Northern blotting and RNase protection assays can successfully detect mRNA for α_1-AR subtypes in tissues (Garcia-Sainz *et al.*, 1994;Price *et al.*, 1994b;Price *et al.*, 1994a), while RT-PCR can identify where the α_1-AR subtypes are expressed as well as quantify the mRNA present (Scofield *et al.*, 1995). Radioligand binding is another common method to investigate receptor distribution. In contrast to Northern blotting and RNAse protection assays, radioligand binding determines the distribution of α_1-AR protein instead of mRNA.

α_1 –AR subtypes are distributed in a wide variety of tissues. The majority of evidence of α_1-AR distribution has come from rats and humans. However, in recent years α_1-AR expression has also been studied in the mouse (Cavalli et al., 1997; Alonso-Llamazares et al., 1995; Yang et al., 1998). In general, multiple subtypes are present in most tissues, but

species heterogeneity is apparent in the distribution of α_1-AR subtypes in some tissues. Therefore, an overview of the distribution of α_1-ARs in the major organs and blood vessels of humans, rats and mice is described below.

1.5.1. Organs

The balance of evidence suggests that the human heart has a predominance of α_{1A}-ARs (Price *et al.*, 1994a;Faure *et al.*, 1995), while the rat heart has high levels of both α_{1A}–AR and α_{1B}-ARs expressed (Price *et al.*, 1994a;Garcia-Sainz *et al.*, 1994;Rokosh *et al.*, 1994;Scofield *et al.*, 1995;Faure *et al.*, 1994b). Like the heart, the human liver appears to predominantly express the α_{1A}–AR (Price *et al.*, 1994a;Faure *et al.*, 1995;Garcia-Sainz *et al.*, 1994). The rat liver has high levels of α_{1B}–AR expression (Garcia-Sainz *et al.*, 1994;Price *et al.*, 1994a;Rokosh *et al.*, 1994;Scofield *et al.*, 1995;Faure *et al.*, 1994b). While homogeneous populations of α_{1B}-ARs have been identified in the mouse liver (Yang *et al.*, 1998;Deighan *et al.*, 2004). It appears that α_{1B}–ARs are expressed predominantly in the human spleen (Faure *et al.*, 1995;Price *et al.*, 1994a;Scofield *et al.*, 1995). Although a homogeneous population of α_{1B}–ARs were detected in the rat spleen (Kong *et al.*, 1994;Michel *et al.*, 1993), Faure et al. (1994b) detected high levels of α_{1D}–ARs. It has been shown that the human, rat and mouse lung have a predominance of α_{1B}–ARs (Faure *et al.*, 1995;Yang *et al.*, 1998), however, high levels of α_{1D}–ARs have also been detected in the rat lung (Faure *et al.*, 1994b). Price et al. (1994a) reported that both the human and rat kidney had predominant α_{1B}-AR expression. It has been reported that similar levels of α_{1A}–AR and α_{1B}–AR are expressed in the murine kidney (Yang *et al.*, 1998).

In general, expression of the α_1-AR subtypes in the brain is high. It appears that, in humans, the cerebellum (Price *et al.*, 1994b;Faure *et al.*, 1995) and the cerebral cortex (Price *et al.*, 1994b;Faure *et al.*, 1995) have a predominance of α_{1A}–ARs. In the rat, the cerebellum (Scofield *et al.*, 1995) has high levels of α_{1A}–ARs. There are reports that the rat cerebral cortex shows a predominance of α_{1D}–ARs (Perez *et al.*, 1991;Lomasney *et al.*, 1991), but Scofield et al. (1995) concluded that there was no dominant α_1–AR subtype expressed in the rat cerebral cortex. The murine cerebellum has a predominance of α_{1B}–ARs (Yang *et al.*, 1998;Papay *et al.*, 2004). While high levels of both the α_{1A}–AR and α_{1B}–AR have been reported in the murine cerebral cortex (Yang *et al.*, 1998;Papay *et al.*, 2006;Papay *et al.*, 2004).

These studies demonstrate that the α_1-ARs are distributed in a variety of tissues. Some differences do exist between species in the predominant α_1-AR subtype expressed in some of the organs. However, in the human, rat and mouse, the balance of evidence suggests that the expression of the α_{1A}-AR is higher than the α_{1B}-AR and α_{1D}-AR in the major organs.

1.5.2. Vascular smooth muscle

It has previously been established that all three α_1-AR subtypes are expressed in vascular smooth muscle (Miller *et al.*, 1996). However, approximately 90% of the total α_1 –AR mRNA expression in peripheral arteries appeared to be due to the α_{1A}-AR (Guarino *et al.*, 1996). Generally, expression of the α_{1A}-AR was highest, followed by the α_{1B}-AR, and the α_{1D}-AR was lowest (Piascik *et al.*, 1997). A recent study in the rat demonstrated that the α_{1D}-AR was predominant in the thoracic aorta and mesenteric artery, the α_{1A}-AR was predominant in the tail and small mesenteric artery and the expression of the α_{1B}-AR was minimal (Marti *et al.*, 2005).

Blood vessels are composed of three layers: the adventitia, media and intima. The media consists of smooth muscle cells and elastic lamina, while the adventitia is made up of fibres, fibroblasts and nerve endings, and the intima is a single layer of endothelial cells. Recently, the relative distribution of α_1-ARs in the media and adventitia of the carotid artery and the aorta in the rat has been examined. In the aorta, the media and adventitia have been shown to express all three α_1-AR subtypes (Faber *et al.*, 2001). The adventitia showed larger populations of α_{1A}-ARs and α_{1B}-ARs than the media, while α_{1D}–ARs were in larger proportions in the media than adventitia. Faber and Yang (2006) reported similar findings in the carotid artery, in which greater proportions of α_{1D}-ARs were detected in the media but the adventitia had greater proportions of α_{1A}-ARs. However, in contrast to the thoracic aorta, the carotid artery had a greater proportion of α_{1B}-ARs detected in the media than the adventitia. At present, there is no evidence of α_1-AR expression on the endothelium of rat or mouse arteries.

The differing distributions of the α_1-subtypes suggest that the roles of the α_1-AR subtypes in vasoconstriction differ. Nevertheless, the detection of the mRNA or protein cannot be taken as evidence that the α_1-AR subtype is functional or point to that function.

1.6. α_1-AR vascular function

In most mammalian species, the contraction of vascular smooth muscle is principally mediated by α_1-ARs (Guimaraes & Moura, 2001;Vargas & Gorman, 1995). Generally, a predominant α_1-AR subtype has been assigned to each blood vessel but it appears that more than one α_1-AR subtype can contribute to the contraction of a particular vessel. The α_1-AR subtype mediating the contraction of a particular vessel is often comparable between species; though differences can exist (Buscher *et al.*, 1996). For this reason, the roles of α_1-ARs in the arteries of both mice and rats are summarised below.

1.6.1. α_{1A}-AR

There is substantial evidence that α_{1A}-ARs are the predominant subtype mediating the contraction of small, innervated resistance arteries. In the mouse, these vessels include mesenteric resistance arteries and tail arteries (Daly *et al.*, 2002a;Rokosh & Simpson, 2002;Shibano *et al.*, 2002;Hedemann & Michel, 2002;Lachnit *et al.*, 1997). Similarly in rats, α_{1A}-ARs appear to be the principal mediators of contraction in the tail artery (Ibarra *et al.*, 2000) and small mesenteric arteries (Stassen *et al.*, 1998), as well as in the renal artery (Hrometz *et al.*, 1999). These findings suggested that the α_{1A}-AR is a main mediator of vascular smooth muscle contraction. There is a lack of evidence for the α_{1A}-AR being involved in the contraction of large, poorly innervated conductance arteries in the mouse (Deighan C, 2002;Daly *et al.*, 2002a) and rat (Kenny *et al.*, 1995;Buckner *et al.*, 1996). However, there is recent evidence to suggest that a minor α_{1A}-AR-mediated response may exist in the thoracic aorta of the mouse (Hosoda *et al.*, 2005b;Lazaro-Suarez *et al.*, 2006) and the rat carotid artery (Chiba & Tsukada, 2002;Naghadeh, 1996 University of Glasgow PhD Thesis.). It is clear that evidence of an α_{1A}-AR contractile response in conductance arteries is inconsistent and further investigation is required.

1.6.2. α_{1D}-AR

It appears that the predominant contractile receptor in large, non-innervated conductance arteries is the α_{1D}-AR. For instance, there is substantial evidence that in the mouse, α_{1D}-ARs regulate the contraction of the thoracic aorta, carotid artery, femoral artery, iliac artery and superior mesenteric artery (Yamamoto & Koike, 2001b;Piascik *et al.*, 1997;Hrometz *et al.*, 1999;Daly *et al.*, 2002a;Martinez L *et al.*, 1999;Tanoue *et al.*, 2002c;Ali,

2004;Deighan C, 2002;Jarajapu *et al.*, 2001a;Jarajapu *et al.*, 2001b;Lachnit *et al.*, 1997;Stassen *et al.*, 1997). Similarly α_{1D}-ARs mediate the contraction of the rat iliac artery, carotid artery, thoracic aorta, mesenteric artery, and renal artery (Hedemann J & Michel, 2002;Gisbert *et al.*, 2000;Kenny *et al.*, 1995;Buckner *et al.*, 1996). The predominance of the α_{1D}-AR in the media of conductance arteries is consistent with the evidence that it regulates the contraction of these vessels (Kenny *et al.*, 1995;Leech & Faber, 1996;Martinez L *et al.*, 1999). In addition, there is increasing evidence that the α_{1D}-AR shows constitutive activity in conductance arteries of the rat (Gisbert *et al.*, 2000;McCune *et al.*, 2000). It has been suggested that this activity may occur to prevent abrupt changes to the response when an agonist is added (Ziani *et al.*, 2002). Until recently there was no evidence for the α_{1D}-AR contributing to the contraction of small resistance arteries (Stassen *et al.*, 1998;Hedemann J & Michel, 2002). However, evidence to suggest that the α_{1D}-AR has a minor contractile role in the first order mesenteric arteries of the mouse, in addition to the predominant α_{1A}-AR, has now been reported (McBride *et al.* Submitted for publication). In addition to a dominant role in vasoconstriction, there is also evidence that the α_{1D}-AR may regulate the hypertrophic growth of the smooth muscle cells, as demonstrated in the rat aorta (Xin *et al.*, 1997).

1.6.3. α_{1B}-AR

In contrast to the α_{1A}-AR and α_{1D}-AR, there is a lack of evidence for a dominant role of the α_{1B}-AR in the contraction of any murine blood vessels. However, there is evidence that the α_{1B}-AR may contribute to the regulation of the rat mesenteric artery in addition to the α_{1D}-AR (Piascik *et al.*, 1997). Furthermore, the α_{1B}-AR may have a small contribution to contraction of the murine thoracic aorta and carotid artery (see section 1.7.1.1.). Nevertheless, it has become evident that a more prominent role of the α_{1B}-AR may be the regulation of smooth muscle cell growth (Chen *et al.*, 1995;Milano *et al.*, 1994;Vecchione *et al.*, 2002) or vascular modelling (McGrath *et al.*, 2002). Additionally, α_{1B}-ARs have been associated with the regulation of cardiac growth and contractile function (Chalothorn *et al.*, 2003), as well as the regulation of skeletal muscle venules (Leech & Faber, 1996).

There is evidence that the α_{1L}-AR mediates the contractile responses in the rabbit aorta (Muramatsu *et al.*, 1990;Oshita *et al.*, 1993), carotid artery (Muramatsu, 1991) and mesenteric artery (Muramatsu *et al.*, 1990;Van der Graaf *et al.*, 1997). However, evidence of the α_{1L}-AR in the rat is limited to the mesenteric resistance arteries (Van der Graaf *et*

al., 1996) and there is no evidence to suggest α_{1L}-ARs mediate contraction in murine arteries.

1.6.4. The murine carotid artery

To date, the availability of literature characterising the α_1-AR-mediated contractile response in the murine carotid artery is limited. In an earlier PhD thesis, Deighan (2002) characterised the α_1-AR-mediated contractile response in the mouse carotid artery, using both WT mice and the α_{1B}-KO. Based on the high potency of the selective α_{1D}-AR antagonist, BMY 7378, against the contractile response to phenylephrine, it was found that the α_{1D}-AR was the predominant contractile receptor in this vessel. An α_{1A}-AR component to the contractile response was excluded due to the low affinity of 5-methylurapidil and it was, therefore, concluded that the α_{1B}-AR was most likely to contribute to the α_1-AR contractile response, in addition to the dominant α_{1D}-AR (Deighan C, 2002). Nevertheless, no α_{1B}-AR antagonists are available, which are adequately selective over the α_{1A}-AR and α_{1D}-AR. Thus, there was no direct evidence that the α_{1B}-AR contributed to the contraction in the WT mouse. At present, the contributions of the α_{1A}-AR and α_{1B}-AR in the murine carotid artery are not fully resolved. It should be noted that the findings of Deighan (2002) have been published with some of the results from Chapter Four of this thesis (Deighan C *et al.*, 2005).

1.7. Genetically altered mice

In the last decade, the use of mice to study vascular tissues has markedly increased due to the development mice with either a deletion or overexpression of a specific gene. With the limited number of compounds selective between α_1-AR subtypes, mice with alterations to the α_1-AR genes were developed as an alternative approach to characterise α_1-ARs.

In the knockout mouse, the normal expression pattern can be disrupted, or the gene of the relevant α_1-AR subtype can be replaced with a modified gene (Rohrer & Kobilka, 1998). A knockout mouse can be utilised to study the pharmacology of a major subtype in isolation, or to study a minor subtype in the absence of the predominant subtype. Single α_1-AR knockout mice have been developed for the α_{1A}-AR (Rokosh & Simpson, 2002), α_{1B}-AR (Cavalli *et al.*, 1997) and α_{1D}-AR (Tanoue *et al.*, 2002c). For each strain, the α_1-AR gene was disrupted using homologous recombination in embryonic stem cells (O'Connell *et al.*, 2003;Tanoue *et al.*, 2002c;Cavalli *et al.*, 1997).

1.7.1.1. α_{1B}-KO

The α_{1D}-KO was the first α_1-AR knockout to be created (Cavalli *et al.*, 1997). The first exon of the α_{1B}-AR gene was replaced with a deoxyribonucleic acid cassette containing the neomycin resistance gene. The gene was then electroporated into 129Sv embryonic stem cells and microinjected into C57/Bl/6 blastocytes before being transferred to pseudopregnant females. The disrupted gene was bred into C57/Bl/6 mice creating α_{1B}-KOs and corresponding WT mice with mixed genetic backgrounds.

Cavalli et al. (1997) reported that in the α_{1B}-AR knockout, the pressor response to phenylephrine was reduced and phenylephrine was less potent in the thoracic aorta compared to WT mice. From these findings it was proposed that the α_{1B}-AR had a role in the regulation of blood pressure and that there was evidence for α_{1B}-AR mediated vasoconstriction. A later study by Daly et al. (2002a) found that the phenylephrine-induced response in the thoracic aorta, first order mesenteric artery and tail artery of the α_{1B}-KO was not reduced, while, the carotid artery of the α_{1B}-KO was more sensitive to phenylephrine. This study did not rule out the possibility of the α_{1B}-AR contributing to vasoconstriction but, in contrast to Cavalli et al. (1997), suggested that the contribution was relatively small. Deighan (2002;Deighan *et al.*, 2005) provided further evidence that the α_{1B}-AR had a minor role in vasoconstriction as the α_{1D}-AR antagonist BMY 7378 was more potent in the carotid artery of the α_{1B}-KO than the WT mouse. The findings of Hosoda et al. (2005a) were also consistent with the role of the α_{1B}-AR in vasoconstriction being minor. For instance, the potency of noradrenaline and phenylephrine was slightly reduced in the thoracic aorta but there was no change in resting blood pressure in the α_{1B}-KO compared to the WT mouse. The balance of evidence from the α_{1B}-KO suggests that the α_{1B}-AR has a minor role in vasoconstriction.

Cavalli et al. (1997) also performed radioligand binding assays and found that, in the α_{1B}-KO, α_1-AR expression was decreased in the liver, heart, kidneys and brain (Cavalli *et al.*, 1997). The presence of the α_{1B}-AR in the murine liver was confirmed by a subsequent radioligand binding study, which compared the WT mouse with the α_{1B}-KO (Deighan *et al.*, 2004). These findings are consistent with the expression of the α_{1B}-AR in these organs reported in previous studies (Yang *et al.*, 1998).

1.7.1.2. α_{1A}-KO

The α_{1A}-KO was generated by Rokosh and Simpson (2002), who replaced the entire first exon of the α_{1A}-AR gene with the *Escherichia coli* β-galactosidase gene Lac Z and the neomycin-resistance gene. Mouse 129Sv embryonic stem cells were then electroporated, selected for neomycin resistance and injected into C57/Bl/6 blastocytes. The modified gene was bred into mice with FVB/N and C57/Bl/6 backgrounds. Several generations of α_{1A}-KOs have now been back-crossed to ensure that the mice have a congenic C57/Bl/6 background, enabling the potential for phenotypic differences to be excluded (Simpson, 2006).

In the α_{1A}-KO, resting blood pressure and the pressor response to both phenylephrine and A-61603 were reduced (Rokosh & Simpson, 2002), demonstrating that the α_{1A}-AR has a prominent role in the regulation of arterial blood pressure. The Lac Z gene encodes for β-galactosidase production, therefore β-galactosidase staining was used as a marker for α_{1A}-AR expression. Thus, evidence of β-galactosidase staining was found in both the heart and kidney of α_{1A}-KO mice and radioligand binding showed that α_1-AR expression was reduced in the heart, kidney and brain (Rokosh & Simpson, 2002), supporting the expression of the α_{1A}-AR in these organs reported by Yang et al. (1998). Furthermore, evidence indicative of α_{1A}-AR expression was found in resistance arteries, including the celiac, mesenteric, hepatic, tail, femoral, iliac and renal arteries. However, in the thoracic aorta, carotid artery and the subclavian artery, the absence of β-galactosidase opposed the expression of α_{1A}-ARs. These findings are consistent with the predominance of α_{1A}-AR in resistance arteries described in earlier studies (Kong *et al.*, 1994).

1.7.1.3. α_{1D}-KO

The α_{1D}-KO was generated by Tanoue et al. (2002c), who also used targeted gene disruption. In this case the residues coding for the first 61 amino acids of the first exon of the α_{1D}-AR gene were replaced with a deoxyribonucleic acid cassette containing the neomycin resistance gene. The targeting vector containing the modified gene was then electroporated into 129Sv embryonic stem cells and microinjected into C57/Bl/6J blastocytes before being transferred to pseudopregnant females. The disrupted gene was bred into C57/Bl/6 mice creating α_{1D}-KOs and corresponding WT mice with mixed genetic backgrounds.

Tanoue et al. (2002c) found that in the α_{1D}-KO mean arterial blood pressure was reduced and the pressor response to both phenylephrine and noradrenaline was reduced. In addition, both phenylephrine and noradrenaline were less potent in the thoracic aorta of the α_{1D}-KO. It therefore appeared that the α_{1D}-AR regulated systemic arterial blood pressure by vasoconstriction (Tanoue *et al.*, 2002c). These findings were supported by Hosoda et al. (2005a) who reported that systemic blood pressure was decreased in the α_{1D}-KO and that mean arterial blood pressure was not markedly increased in response to noradrenaline. This study also found that the potency of noradrenaline and phenylephrine was decreased in the thoracic aorta. Thus, the α_{1D}-KO provides evidence for a predominant role of the α_{1D}-AR in vasoconstriction and in the maintenance of resting blood pressure. In addition, it has been shown that in the thoracic aorta of the α_{1D}-KO, the α_{1B}-AR mediates the contractile response to both noradrenaline (Hosoda *et al.*, 2005a) and phenylephrine (Ali, 2004). These studies in the α_{1D}-KO confirm a contractile role for the α_{1D}-AR, but also suggest the α_{1B}-AR does have a role in vasoconstriction.

Radioligand binding studies in the α_{1D}-KO revealed that α_1-AR binding was reduced in the cerebral cortex (Tanoue *et al.*, 2002c) suggesting that the α_{1D}-AR is present in the cerebral cortex of the WT mouse, in addition to the high levels of α_{1A}-ARs and α_{1B}-ARs detected in previous radioligand binding studies (Yang *et al.*, 1998). Tanoue et al. (2002c) also found that α_1-AR protein was absent in the thoracic aorta of the α_{1D}-KO, which provides further evidence that this α_1-AR is predominant in conductance arteries.

1.7.1.4. Double knockouts

Double knockout mice have recently been generated where only a single α_1-AR population remains. At present only the $\alpha_{1A/B}$-KO (Turnbull *et al.*, 2003;McCloskey *et al.*, 2003;O'Connell *et al.*, 2003) and $\alpha_{1B/D}$-KO (Hosoda *et al.*, 2005a;Hosoda *et al.*, 2005b) have been characterised, although studies of the $\alpha_{1A/D}$-KO and a triple $\alpha_{1A/B/D}$-KO are ongoing. The double α_1-AR knockout mice were generated by crossbreeding two of the single knockout mice.

The $\alpha_{1A/B}$-KO was generated by mating α_{1A}-KO mice with α_{1B}-KO mice (Turnbull *et al.*, 2003). As a result of the mixed genetic background of the breeding pairs, the $\alpha_{1A/B}$-KO had a mixed genetic background of 129Sv, FVB/N and C57/Bl/6. It has been shown that despite the loss of the α_{1A}-AR and α_{1B}-AR, blood pressure was unchanged in the $\alpha_{1A/B}$-KO

compared to the WT mouse (O'Connell et al., 2000), which suggests that the α_{1D}-AR has a role in the maintenance of blood pressure. However, the majority of current evidence of the $\alpha_{1A/B}$-AR double knockout mouse is limited to the heart.

The $\alpha_{1B/D}$-KO was generated by mating α_{1B}-KO mice with α_{1D}-KO mice (Hosoda *et al.*, 2005a). The α_{1B}-KO and α_{1D}-KO had the genetic background of 129Sv and C57/Bl/6, thus the $\alpha_{1B/D}$-KO had the same genetic background. In the $\alpha_{1B/D}$-KO resting blood pressure and mean arterial pressure were reduced compared to the WT mouse (Hosoda *et al.*, 2005a). Furthermore, the pressor response to noradrenaline and phenylephrine was decreased, but the pressor response to A-61603 was comparable to the WT mouse. These findings suggest that the α_{1A}-AR regulates arterial blood pressure, in agreement with the study in the α_{1A}-KO (Rokosh & Simpson, 2002). In addition, Hosoda et al. (2005a) did not observe any contractile responses to α_1-AR agonists in the thoracic aorta of the $\alpha_{1B/D}$-KO, which suggests that the α_{1A}-AR does not mediate the contractile response of this artery at all. This conclusion was also reached by Ali (2004), who failed to identify a contractile response to phenylephrine in the thoracic aorta of the $\alpha_{1B/D}$-KO. Although, a subsequent study, Hosoda et al. (2005b) acknowledged that an α_{1A}-AR-mediated contraction was present but was minimal. In the later study by Hosoda et al. (2005b) both the maximum response and sensitivity of noradrenaline was reduced in the mesenteric artery of the $\alpha_{1B/D}$-KO but was still detectable. This suggests that, in contrast to the thoracic aorta, the α_{1A}-AR does mediate vasoconstriction in the mesenteric artery. Hosoda et al. (2005a) also examined α_1-AR expression in the $\alpha_{1B/D}$-KO, using both real-time PCR and radioligand binding assays. The loss of α_{1B}-AR and α_{1D}-AR mRNA was confirmed in the brain, heart, aorta, kidney and liver, while total α_1-AR binding was reduced in the brain, heart and kidney. Furthermore, α_1-AR binding was abolished in the liver, which has been shown to express α_{1B}-ARs (Deighan *et al.*, 2004;Yang *et al.*, 1998), and similarly in the aorta, which has been shown to express α_{1D}-ARs (Hosoda *et al.*, 2005b), no α_1-AR binding was detected.

1.7.1.5. Compensatory mechanisms

It has been proposed that knocking out an α_1-AR may result in the other α_1-ARs compensating for this loss of function, such as an up-regulation of another subtype (Rohrer & Kobilka, 1998;Tanoue *et al.*, 2002c). It can be argued that, in the knockout, compensation for the loss of the receptor may occur as the animal develops. However,

pharmacologically blocking the receptor enables the mouse to develop normally. Recent studies have shown that the pressor responses to phenylephrine and noradrenaline of the α_{1D}-KO and α_{1B}-KO were reduced, implying that the remaining subtypes did not appear to compensate for the loss of an α_1-AR (Cavalli *et al.*, 1997;Daly *et al.*, 2002a;Ziani *et al.*, 2002;Rohrer & Kobilka, 1998). Furthermore, the loss of both the α_{1B}-AR and α_{1D}-AR did not appear to be compensated for in a functional study of the mesenteric artery in the $\alpha_{1B/D}$-KO (McBride *et al.* Submitted for Publication). However, a study in the mouse liver demonstrated that the normally homogeneous population of α_{1B}-ARs was replaced by the α_{1A}-AR in α_{1B}-KO (Deighan *et al.*, 2004). Furthermore, the α_{1A}-AR and α_{1B}-AR are functional in the murine heart and when either the α_{1A}-AR or α_{1B}-AR was deleted, the other subtype compensated for the loss (O'Connell *et al.*, 2003) but when both subtypes were deleted in the $\alpha_{1A/B}$-KO, the α_{1D}-AR compensated (O'Connell *et al.*, 2003;Turnbull *et al.*, 2003). In addition, despite a lack of evidence for a role of the α_{1B}-AR in the vasoconstriction of the murine thoracic aorta, there is evidence of an α_{1B}-AR-mediated contractile response in the α_{1D}-KO (Ali, 2004). It is, therefore, possible that the loss of the dominant receptor is required for a compensatory mechanism to occur.

1.7.1.6. Transgenic mice

Overexpression of an α_1-AR gene is also a valuable tool for studying α_1-AR subtypes. Transgenic mice have been generated for the α_{1A}-AR (Lin *et al.*, 2001) and α_{1B}-AR (Milano *et al.*, 1994), under the α-myosin heavy chain promoter. Mice with a constitutively active α_{1B}-AR mutation enable the α_{1B}-AR to be studied, while the other α_1-ARs remain inactivated (Milano *et al.*, 1994). This is a particularly useful tool to isolate the α_{1B}-AR response with the absence of α_{1D}-AR selective agonists. Zuscik et al. (2001) showed that mice with over-expression of the α_{1B}-AR were hypotensive but the α_1-AR mediated contractile response of the mesenteric artery was not different to the WT mouse (Zuscik *et al.*, 2001). In agreement with studies using α_1-AR knockout mice (Daly *et al.*, 2002a), this suggests that the α_{1B}-AR was not involved in vasoconstriction.

1.8. Role of the endothelium on α_1-AR-meditated contraction

It is now known that the vascular endothelium has an important role in the control of vascular tone (Angus J *et al.*, 1986;Cocks T & Angus J, 1983;Furchgott RF & Zawadzki

JV, 1980). Endothelial cells (EC) release endothelium-derived relaxing factors, such as nitric oxide (NO), prostacyclin and endothelium-derived hyperpolarizing factor (EDHF), as well as endothelium-derived contracting factors, including endothelin-1, thromboxane A_2, superoxide anions and endoperoxides (Furchgott RF & Vanhoutte, 1989). It has been shown that in large conductance arteries, NO has a major role, while the role of EDHF and prostacyclin is minimal (Shimokawa H *et al.*, 1996;Scotland RS *et al.*, 2005). Consequently, the role of NO on vascular contraction will be of particular interest to this thesis.

NO was previously known as endothelium-derived relaxing factor and was first linked to the endothelium by Furchgott and Zawadski (1980). It was demonstrated that when the endothelium was present in the rabbit aorta a relaxatory response to acetylcholine was observed, but in the absence of the endothelium acetylcholine produced contractions. Shortly after EDHF was identified as NO (Palmer *et al.*, 1987), the pathways for NO synthesis and degradation were discovered (Palmer *et al.*, 1988). NO is produced by EC from L-arginine by endothelial NO synthase (eNOS), which is a constitutive, Ca^{2+}-dependent enzyme. Once released, NO diffuses into vascular SMCs and stimulates soluable guanylate cyclase, leading to vasodilation.

The involvement of NO on vascular contraction has been widely studied. It has been shown that using a denuded preparation or inhibitors of NOS, such as L-NMMA and L-NAME (Rees *et al.*, 1990), results in an increased contractile response to α_1-AR agonists (Cocks & Angus, 1983;Kaneko & Sunano, 1993;Amerini S *et al.*, 1995). The release of NO can be constitutive or stimulated by agonists. Recently, an endothelium-dependent α_1-AR-mediated relaxatory response was reported in the rat mesenteric artery (Filippi *et al.*, 2001) and the rat carotid artery (de Andrade C *et al.*, 2006). It is, therefore, possible that α_1-AR agonists can stimulate NO release through the direct activation of endothelial α_1-ARs. Alternatively, it has been proposed that the activation of SMC α_1-ARs indirectly stimulates NO release via myoendothelial connections (Dora K, 2001). These possibilities have been described in greater detail in Chapter Seven.

1.9. Aims and objectives

With the ambiguity concerning the contractile role of the α_{1A}-AR and α_{1B}-AR in large conductance arteries, such as the carotid artery, and the potential for α_1-ARs existing on the endothelium, the main objectives of the following research were:

(i). To establish whether there is an α_{1A}-AR-mediated contractile response in the carotid artery of the WT mouse and also assess whether there is evidence of a functional α_{1B}-AR. This was achieved by using the α_{1A}-AR selective agonist A-61603 and range subtype selective antagonists, in addition to the α_1-AR non-selective agonist phenylephrine.

(ii). To determine whether an α_{1A}-AR-mediated contractile response could be identified in the carotid artery of α_1-AR knockout mice and therefore aid the characterisation of α_1-AR response in the WT mouse. This was achieved using a similar approach to (i) to isolate the α_{1A}-AR in the α_{1B}-KO, α_{1D}-KO and $\alpha_{1B/D}$-KO.

(iii). To investigate the role of NO on the vascular response to phenylephrine and A-61603 in the murine carotid artery. This was achieved by preventing NO release using the NOS inhibitor L-NAME.

(iv). To characterise the α_1-AR subtypes present in the media of the carotid artery by using subtype selective antagonists to compete with the fluorescent ligand QAPB in the WT mouse and α_1-AR knockout mice. In doing so, the distribution and cellular localisation of the α_1-AR subtypes in SMC was examined.

(v). To establish whether α_1-ARs exist on the endothelium of the murine carotid artery and to determine the α_1-AR subtypes present in EC. This was achieved using the fluorescent ligand QAPB in the WT mouse and α_1-AR knockout mice as well as subtype selective antagonists.

Chapter 2 General Methods

2.1. Mice

C57 Black mice were used as control (WT mouse) and for the breeding of colonies. Mice with a knockout of the α_{1B}-AR gene (α_{1B}-KO), α_{1D}-AR gene (α_{1D}-KO) or both ($\alpha_{1B/D}$-KO) were bred at the University of Glasgow from breeding pairs kindly provided by Professor Susanna Cotecchia (University of Lausanne, Lausanne, Switzerland; α_{1B}-KO) and Professor Gozoh Tsujimoto (National Children's Medical Research Center, Tokyo, Japan; α_{1D}-KO). α_{1BD}-KO mice were generated by cross-breeding homozygous α_{1B}-KO with homozygous α_{1D}-KO at the University of Glasgow following the same protocol as Hosoda et al. (2005a). The generation and background of the knockouts have been described in detail (α_{1B}-KO (Cavalli *et al.*, 1997;Tanoue *et al.*, 2002a); $\alpha_{1B/D}$-KO (Hosoda *et al.*, 2005a).

All mice were maintained on a 12:12-hour light/dark schedule at 22-25°C with 45-65% humidity and fed ad-libitum on a standard chow diet and provided with distilled drinking water. All mice were killed by the schedule one method of carbon dioxide overdose.

All mice used for experimental protocols were four to five-month old males weighing between 25g and 54g (wild type (26g-44g); α_{1D}-KO (25g-34g); α_{1B}-KO (31g-46g); $\alpha_{1B/D}$-KO (32g-55g)).

2.2. Common carotid artery dissection

The murine carotid artery was used for all experiments described in this thesis. The dissection of both common carotid arteries was performed with the aid of a Zeiss dissecting microscope. The skin covering the area over trachea was removed. The two lobes of the exposed thyroid gland were separated and an incision was made into the carotid sheath to reveal the trachea. Both common carotid arteries were located within the carotid sheath formed by this incision, and were medial to the internal jugular vein and vagus nerve (Figure 2.1).

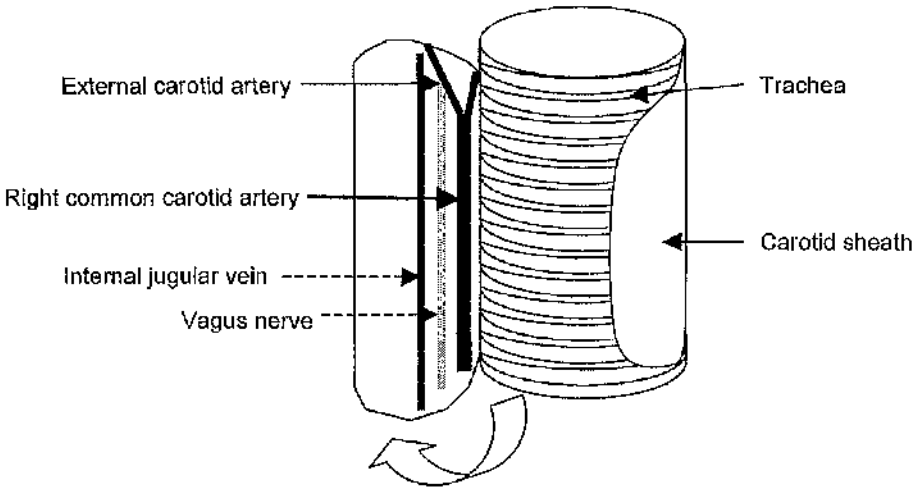

Figure 2.1. Dissection of the common carotid artery.

The left common carotid artery is a direct branch of the aorta, while the right common carotid artery is a branch of the brachiocephalic artery. The left common carotid artery was gently gripped with forceps at the branch point with external carotid to avoid damage to the vessel. The artery was dissected free from any connective tissue and was cut at both ends and placed in Petri dish with cold physiological salt solution (PSS). This was repeated for the right common carotid artery. When placed in the Petri dish, the branch point was removed and the vessels were cleaned. Care was taken to remove blood from the lumen of the artery, which has been shown to limit damage to the endothelium (Horvath *et al.*, 2005).

2.3. Myography

Wire myography was first developed by Bevan and Osher (1972) to enable small isolated vessels (<200 μm in diameter) to be studied. Mulvany and Halpern (1976) adapted this myograph design to permit isometric tension measurements to be made in vessels with a diameter as small as 100 μm. Consequently, wire myography is now a widely used *in vitro* technique. The murine carotid artery is a relatively small vessel (approximately 300 μm in diameter) and has been used for wire myography in a number of studies (Deighan C *et al.*, 2005;Daly *et al.*, 2002a;Deighan C, 2002). This experimental technique has been used for the functional experiments in Chapters Three, Four and Five.

2.3.1. The wire myograph

The wire myograph consists of four stainless steel 5ml baths (Danish MyoTech, Aarhus, Denmark) (Figure 2.2). Each bath contains two detachable stainless steel heads. One of

the heads was connected to a micrometer, to adjust the tension on the vessel, while the other head was attached to a force transducer, which measures the force in millinewtons generated by the vessel. Each bath contains fresh, gassed (95% O_2 / 5% CO_2) physiological salt solution (PSS: 119mM NaCl, 4.7mM KCl, 2.5mM $CaCl_2$, 1.2mM $MgSO_4 \cdot H_2O$, 1.2mM KH_2PO_4, 24.9mM $NaHCO_3$, and 11.1mM glucose). A Perspex lid was used to maintain the temperature within the bath and prevent any evaporation of PSS. Changes in tension were measured by the transducer head and sent to an ADI PowerLab (4/20), via the myograph interface, and the data was displayed and recorded in grams tension on a computer using Chart software. The equipment was calibrated on a regular basis using a 2g weight.

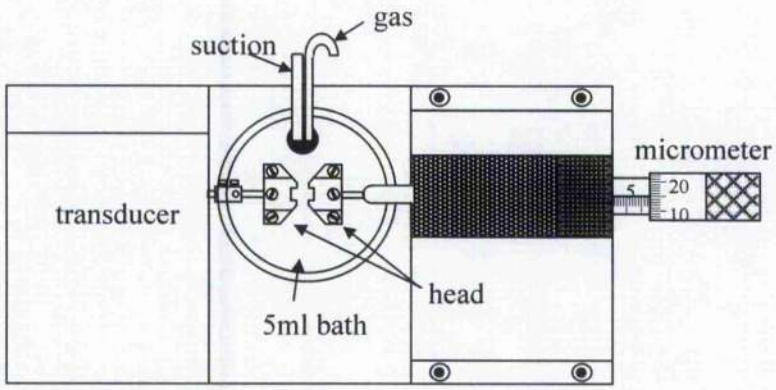

Figure 2.2. The components of a myograph bath (Morton, 2006).

2.3.2. Vessel mounting

Following dissection and cleaning, each carotid artery was cut into two 2mm sections in a Petri-dish containing fresh, cold PSS. One 40μm stainless steel wire was threaded through the lumen of the vessel, with care being taken to minimise damage to the endothelium or smooth muscle cells. The sections were then transferred to individual myograph chambers (Figure 2.3(i)). The head attached to the micrometer was positioned so that the wire was trapped in between the two heads (Figure 2.3(ii)). The wire was attached to the transducer head by both ends of the wire being screwed in place (Figure 2.3(iii)). The heads were then separated and a second wire threaded through the lumen of the artery (Figure 2.3(iv)), trapped between the two heads (Figure 2.3(v)) and secured to the micrometer head (Figure 2.3(vi)). The heads were opened until the wires were just touching and the position of the wires was adjusted to ensure that they were parallel.

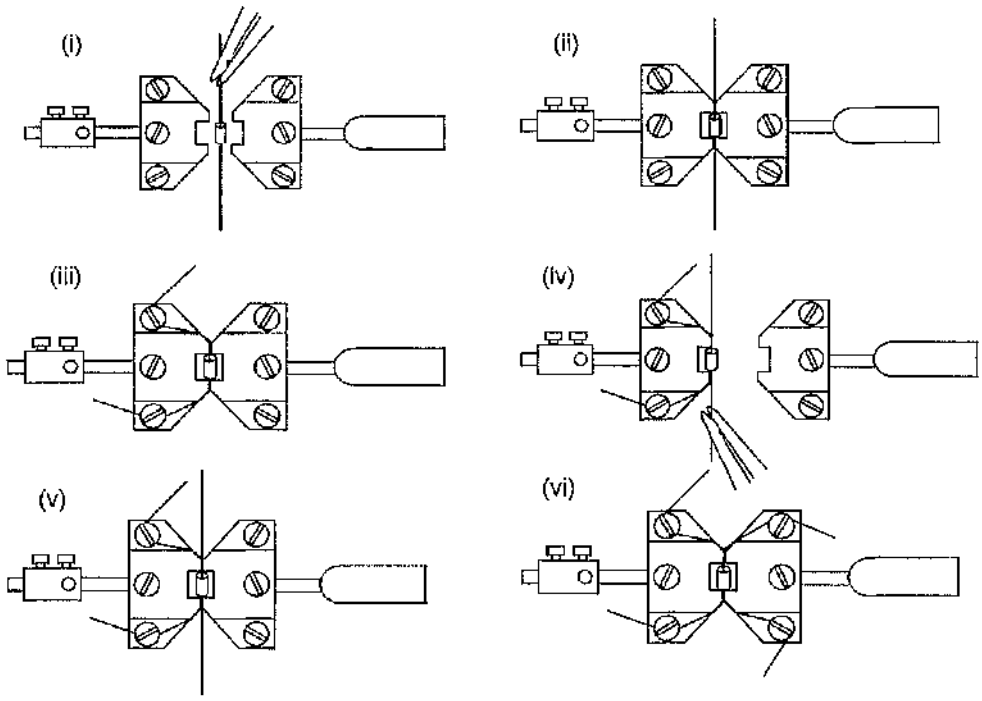

Figure 2.3. Vessel mounting procedure: (i) after being threaded through the lumen of the vessel, the wire was held between the two heads in the myograph bath; (ii) the head attached to the micrometer was positioned so that the wire was trapped between the heads; (iii) both ends of the wire were attached to the transducer head with small screws; (iv) the heads were separated and a second wire was threaded through the lumen of the artery; (v) the second wire was trapped between the two heads; (vi) both ends of the second wire were secured to the micrometer head by screws. Diagram from Morton (2006).

2.3.3. Equilibration period

The PSS in each bath was replaced immediately after vessel mounting and the myograph heated to 37°C with the vessels being allowed to acclimatise over a 30 minute period. Following this equilibration period, the arteries were set to a resting tension of 0.25g, which was determined in a previous study by a series of length tension experiments (Deighan C, 2002). The vessels were then equilibrated at this resting tension for a further 45 minutes, with washes every 15 minutes. The tension was readjusted to ensure that each vessel was at the desired resting tension at the end of this period.

2.3.4. Wake-up procedure

To ensure that the vessels were functional following dissection and mounting, the vessels were exposed to three additions of a submaximal concentration of an agonist. Depending on the experimental protocol either phenylephrine 10 μM, A-61603 10 μM or 5-HT 1 μM was selected for the wake-up procedure. Once the response had reached a plateau the vessels were washed four times with PSS and rested for 10 minutes between additions. On

the third contraction to the agonist, the ability of 3 μM acetylcholine (ACh) to relax the vessels was tested. Only vessels where at least 30% relaxation occurred in response to ACh were used for the experimental protocol. The vessels were then washed with PSS and allowed to rest for 30 minutes.

2.3.5. Experimental protocols

2.3.5.1. Agonist comparison

Cumulative concentration response curves (CRC) to an agonist were produced using half-log increments. The agonists used to construct CRCs were: phenylephrine (1 nM – 0.1 mM); A-61603 (1 nM – 0.1 mM) or 5-HT (1nM – 30μM). When a maximum response was achieved, the vessels were washed with PSS at five-minute intervals until resting tone resumed.

2.3.5.2. Antagonist affinity

In Chapters Three and Four, the affinity of α_1-AR antagonists against an agonist response was estimated. Prior to a second CRC, the vessels were incubated with an antagonist for 30 minutes. The antagonists tested during the studies were: the non-selective α_1-AR antagonist prazosin (1 nM, 10 nM, 0.1 μM) (Hanft & Gross, 1989;Ford *et al.*, 1994) the α_{1A}-AR selective antagonists 5-methylurapidil (10 nM, 0.1 μM, 0.3 μM, 1 μM) (Gross *et al.*, 1988) and RS100329 (1 nM, 10 nM, 0.1 μM) (Williams *et al.*, 1999); the α_{1D}-AR selective antagonist BMY7378 (1 nM, 10 nM, 0.1 μM) (Goetz *et al.*, 1995) and the α_2-AR antagonist rauwolscine (Perry & U'Prichard, 1981;Weitzell *et al.*, 1979). A second CRC was produced in the presence of an antagonist, or in the absence of an antagonist acting as a time control.

In chapter six, the effect of L-NAME (Rees *et al.*, 1990) on the responses to phenylephrine and A-61603 (Knepper *et al.*, 1995) was tested. Following the first CRC, vessels were incubated with L-NAME 0.1mM for 40 minutes, before a second CRC was produced.

2.3.6. Statistical analysis

All statistical analysis was performed using Graph Pad Prism (Version 4) and Microsoft Excel. Tests for statistical significance were performed on individual curves rather than

mean data for improved accuracy. For all data analysis, statistical significance was established as $p < 0.05$.

2.3.6.1. Agonist responses

The raw data from the agonist responses were expressed as means ± SEM in grams tension. The maximum responses (or greatest response recorded within the concentration range used) were calculated for each agonist and compared using one-way ANOVA, followed by a Bonferroni's post test. CRCs were compared using a two-way-ANOVA with a Bonferroni's post-test.

The percentage of the maximum response to the agonist was calculated for individual data sets using the maximum response of individual control CRC and pEC_{50} values were calculated for each agonist in each strain of mice. The pEC_{50} is defined as the negative logarithm of the concentration of agonist that produces half of the maximum response. Therefore, when a maximum response to an agonist was not obtained within the concentration range used a pEC_{50} could not be determined. pEC_{50} values were compared using one-way ANOVA, followed by a Bonferroni's post test.

Nonlinear regression was performed to fit sigmoidal-curves (variable slope) on mean data of responses in grams and percentage of the maximum response, using the equation:

$$Y = \text{Bottom} + \frac{(\text{Top} - \text{Bottom})}{1 + 10^{(\text{Hillslope}(\log EC_{50} - X))}}$$

Where Bottom is the minimum value for Y in the absence of agonist, Top is the maximum value for Y at a high concentration of agonist, Hill slope is the steepness of the concentration-response curve, X is the logarithm of the molecular concentration of the agonist and Y is the response.

The analysis described above was also performed on the agonist responses in the absence and presence of L-NAME.

2.3.6.2. Antagonist data

The agonist CRCs in the presence of an antagonist were expressed as means ± SEM in grams tension or as a percentage of the maximum response of the first CRC. The maximum responses, Hill slopes and pEC_{50} values of the agonist response in the presence

of an antagonist were calculated and compared using either a Student's t-test or one-way ANOVA, followed by a Bonferroni's post test.

The agonist concentration ratios were determined from the ratio of the EC_{50} of the agonist in the presence and absence of the antagonist. Concentration ratios were used for Schild analysis where the log of the antagonist concentration was plotted against log (DR-1). The pA_2 is defined as the negative logarithm of the molar concentration of an antagonist which reduces the effect of a dose of an agonist to that of half the dose. Following linear regression, the pA_2 was identified from the X-intercept of the Schild plot. A Schild slope not significantly different from unity indicated that an antagonist was acting competitively.

When a single concentration of antagonist had no effect or significantly reduced the maximum response, it was not appropriate to apply Schild analysis. A pK_B is the negative logarithm of the dissociation equilibrium constant for an antagonist (K_B) and can be defined as the concentration of drug that occupies fifty percent of available receptors. A pK_B was calculated from the effective concentrations of antagonist using the equation: $pK_B = \log (DR-1) - \log[B]$. Where [B] is the concentration of antagonist.

2.4. Confocal microscopy

The confocal microscope was developed from the conventional light microscope by Minsky in 1955. The aim was to produce sharp images of thin cross sections, which had not been possible with conventional microscopy. The basic confocal microscope system has been improved upon over the years and confocal laser scanning microscopy (CLSM) is now a widely used technique. Several confocal studies have been performed on cells (Sugawara *et al.*, 2002;Daly *et al.*, 2002b;Deighan *et al.*, 2004;Mackenzie *et al.*, 2000) but recently this technique has been applied to whole vessels (Boumaza *et al.*, 2001;Daly *et al.*, 2002b;Coats *et al.*, 2003;McBride *et al.* Submitted for Publication).

2.4.1. The confocal microscope

The confocal microscope consists of a photomultiplier tube (PMT), a detector pinhole, a source pinhole, a dichroic mirror and an objective (Figure 2.4.).

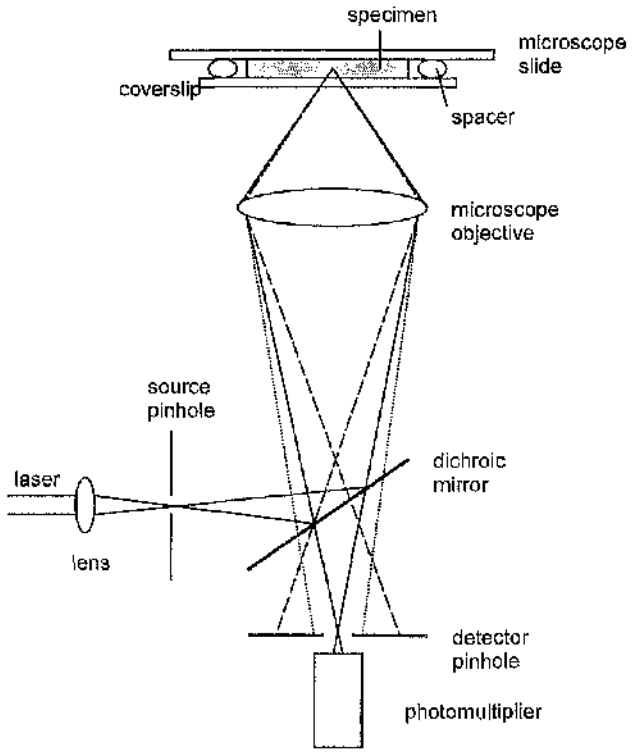

Figure 2.4. The confocal microscope. (Adapted from Figure 1, Stelzer (1995).

An excitation light from a laser is focused into the source pinhole and the dichroic mirror reflects the light from the source and passes it through the objective to the sample. The excitation light fills a converging cone as it is focused through the specimen to the object plane, and all the excitation light passes out through a similar diverging cone. The fluorescent light from the fluorophore in the specimen is emitted in all directions. Light from the specimen passes through both the objective and dichroic mirrors and is focused into the detector pinhole, then measured by the PMT. The detector pinhole ensures that only light from the in-focus planes reach the PMT, and prevents the light scattered from out-of-focus planes reaching the PMT, so that the image produced is of a single plane. An image is built up from individual pixels using a computer with imaging software to visualise a complete image.

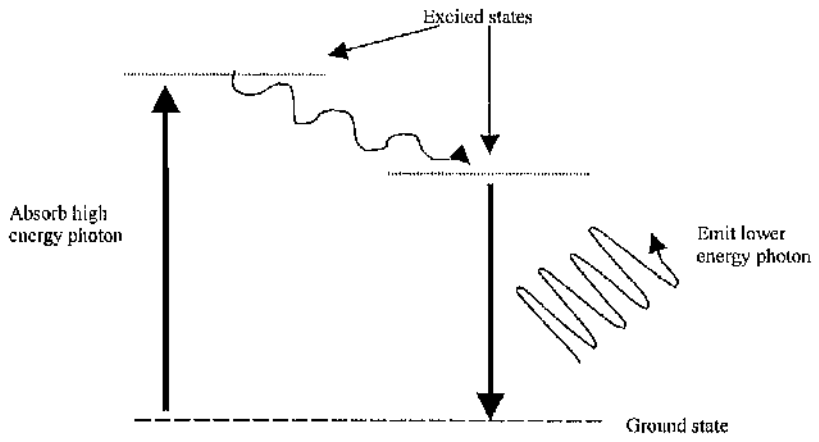

Figure 2.5. Fluorescence generation. (Figure 1 Semwogerere & Weeks (2005).

Fluorescence occurs when a molecule absorbs light, resulting in the emission of light of a different colour (Figure 2.5). The lowest energy state of a molecule is the ground state. When stimulated, the molecule absorbs a photon of light, resulting in an increase in energy and an electron jumps to a higher energy state. The molecule disperses some of the absorbed energy and the electron drops to a lower energy state. The remaining energy is lost by the molecule emitting a photon of light with a longer wavelength and the electron drops back to the ground state.

In Chapters Six and Seven, CLSM was used to examine the distribution of α_1-AR subtypes in the murine carotid artery using QAPB, a green fluorescent analogue of prazosin (nonselective α_1-AR antagonist). A radioligand binding study, comparing specific antibodies to QAPB in rat fibroblasts, has shown that QAPB has 10-fold lower affinity than prazosin; but like prazosin, is not selective between α_1-AR subtypes (Daly *et al.*, 1998;Mackenzie *et al.*, 2000). However, there is evidence that QAPB can bind α_2-ARs with moderate to low affinity (McGrath & Daly, 2005). Generally, QAPB fluoresces only when bound (Daly *et al.*, 1998;Mackenzie *et al.*, 2000). Thus, when bound to the α_1-ARs in the carotid artery a fluorescent signal was generated by excitation of QAPB with a laser.

2.4.2. Determination of incubation conditions

A series of experiments was carried out to determine the optimum conditions for vessel incubation. The fluorescence and binding of 1μM QAPB, 0.1μM and 10nM QAPB were compared to assess the quality of QAPB binding at the lower concentrations (<1 μM), which are believed to be more specific to α_1-ARs (Daly *et al.*, 1998). Despite concentrations below 10nM being used successfully in studies on cells, in the intact carotid artery binding of QAPB 10nM was poor. QAPB 0.1μM was selected for use for further experiments.

The most appropriate method of preparing the carotid artery for imaging was also established. The whole vessel; cross-sectional rings of carotid artery; and vessels which had been sliced longitudinally and opened out (Miquel RM *et al.*, 2005), were trialled. In the whole vessels, it was difficult to focus into the smooth muscle layers and endothelium due to the thick elastic wall of the carotid artery. In another attempt to use the whole intact vessel, the carotid artery was turned 'inside out' exposing the endothelium and stretching the elastic lamina. This preparation enabled the vessels to be imaged from the endothelium through to the media; however, severe endothelial cell damage occurred. In unfixed tissue damage was inflicted by slicing the cross-sectional rings, thus the use of this preparation was also discontinued. The open preparation was selected for use in the experimental protocols as it allowed imaging of the endothelium and smooth muscle cells with minimum damage. The live tissue was most appropriate for use in this study as the physiological processes for binding QAPB were preserved. Nevertheless, certain additional obstacles can arise from using a live tissue: the tissue is susceptible to damage due to changes in pH, temperature, oxidation, and glucose levels; and movements in the tissue can cause difficulties in focusing (Terasaki & Dailey, 1995). These factors were limited as much as practically possible for the duration of the experimentation.

In an attempt to keep incubation conditions as physiological as possible, initial experiments were carried out where the unfixed tissue was incubated in a water bath at 37°C. However, when heated, the calcium in the PSS precipitated out of solution and the physiological pH was lost. As the total volume of the incubation solution was 200 μl it was not practical to continually bubble with 95% O_2/5% CO_2, which would have buffered the solution to maintain pH. Instead freshly bubbled PSS solutions were replaced every 30 minutes for the duration of the incubation period; however the problem still occurred at this temperature. A buffer that was not dependent on pH, such as HEPES, could have been used in the incubation solutions instead of PSS; however, as the confocal study would be

examined in conjunction with the myography data, the use of PSS was continued. Thus, the incubations were performed at room temperature (21°C) and the solutions were changed every 30 minutes, which ensured the pH did not change during the incubation period. In addition to preventing the calcium precipitating out of solution, replacing the PSS also kept the living vessel supplied with glucose.

Once the concentration of QAPB, tissue preparation and temperature had been selected, vessels were imaged at a series of time-points (30 min, 60 min, 90 min, 120 min and 180 min) in order to determine the optimum incubation time for 0.1 μM QAPB, which was found to be 120 minutes.

2.4.3. Incubations used for experimental protocol

5mm segments of carotid artery were incubated at room temperature with 0.1μM QAPB, in a PSS solution at room temperature for 60 minutes. Incubating the vessels with QAPB 0.1 μM prior to the addition of the selective antagonists ensured that QAPB binding was established and the antagonist competed with QAPB for α_1-AR binding sites during the co-incubation reaching equilibrium. The arteries were then incubated for a further 60 minutes with a 0.1μM QAPB/PSS solution containing selected antagonist(s): prazosin 0.1 μM, (non-selective α_1-AR antagonist); RS100329 0.1 μM, (α_{1A}-AR selective antagonist); 5-methylurapidil 1 μM (α_{1A}-AR selective antagonist); BMY7378 0.1 μM (α_{1D}-AR selective antagonist); both BMY 7378 0.1 μM and RS100329 0.1 μM; or rauwolscine 0.1 μM (α_2-AR antagonist). The concentrations of antagonist were based on the competitor's affinity at the α_1-AR subtypes, so that they would act with ten-times greater affinity than QAPB 0.1 μM. The affinity estimates were based on the pK_i values obtained in a radioligand binding study (Mackenzie *et al.*, 2000). The antagonist concentrations used in functional experiments were also taken into consideration when selecting the concentrations used to compete with QAPB in confocal microscopy experiments. The same antagonists were used for CLSM studies of both the smooth muscle (Chapter Six) and endothelium (Chapter Seven).

Two sets of control vessels were used during the full incubation period: (i) controls for autofluorescence, which were incubated in PSS only, and (ii) QAPB control segments, which were incubated in a QAPB/PSS solution in the absence of antagonists. Throughout the incubation period all solutions were replaced every 30 minutes to ensure the pH of the solution and glucose levels were maintained.

A series of experiments was carried out where the nuclear dye Syto 61 was co-incubated with QAPB 0.1 μM. The vessel was incubated with a 0.1 μM QAPB/PSS solution for 30 minutes, followed by a 90 minute co-incubation of QAPB 0.1 μM and Syto 61 1 μM, at room temperature, with solutions being replaced every 30 minutes.

2.4.4. Slide mounting

At the end of the incubation period each carotid artery segment was sliced open with a single-edged razor blade and laid flat on a microscope slide with the endothelial side up (Miquel RM *et al.*, 2005) (Figure 2.6).

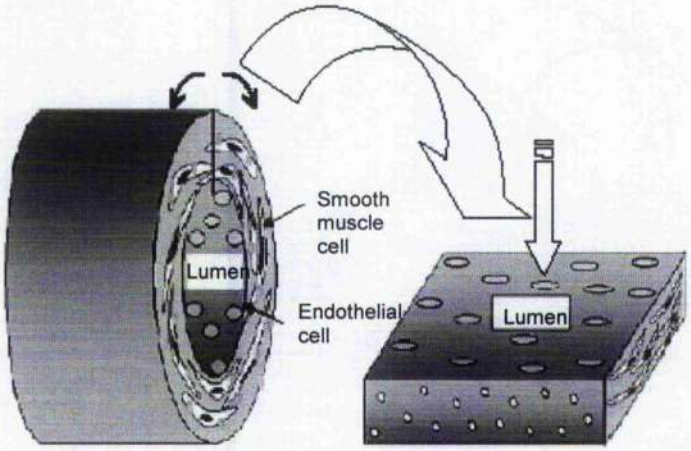

Figure 2.6. Vessel preparation (Miquel RM *et al.*, 2005)

A small well was formed on the microscope slide using grease, which was filled with the solution that the vessel was incubated in. A coverslip thickness 1.5, suitable for the x40 objective, was placed on top creating a seal. This closed chamber prevented loss of mounting media and stabilised the temperature during imaging.

2.4.5. Imaging

Initially, the specimen was viewed through the microscope eyepiece and the microscope (Nikon Eclipse TE300) used conventionally to focus on the specimen. Once focussed, the view was changed from the microscope eyepiece to the computer. The scanning settings for the confocal microscope were selected (see below) and an exploratory scan started, enabling the focus on the specimen to be finely adjusted under the objective, prior to data being recorded. It should be noted that prior to experimentation the objective was cleaned

to remove any dust particles and a glass rod was used to drop oil onto the objective to prevent air bubbles forming in the immersion oil.

All arteries were visualised using the Bio-Rad Radiance 2100 Confocal Laser Scanning System. An argon-ion laser with an excitation wavelength of 488nm with an emission filter of 515nm was used for QAPB and a x40 oil immersion objective (NA 0.75) was used for all experiments. Two different settings were used to record images. For images recorded at zoom three, a laser intensity of 40; a gain of 12; offset 0.0; and pinhole setting of 1.4 were selected. For images recorded at zoom eight, a laser intensity of 20; gain 22; offset 0.0; and pinhole setting of 2.4 were chosen. At a higher magnitude, the rate at which photobleaching occurs is higher as the excitation light is focused over a smaller area, which increases the local intensity. To limit photobleaching at the high zoom setting, the laser intensity was reduced and the gain and exit pinhole size were also increased to increase the brightness. This increased the signal reaching the PMT at the lower laser intensity. The standard scan speed of 500 lines per second was used for all experiments. An image size of 512 x 512 pixels produced a field size of 289µm x 289µm.

During the co-staining experiments the settings for QAPB were as described above, while a red diode, with an excitation/emission wavelength of 628/645nm, was used for Syto 61. At a zoom of three, laser intensity was set to 30, with a gain of 12, offset 0.0 and an optimal pinhole of 1.4.

Each vessel was imaged from the internal elastic lamina through to the media, between the bands of elastic lamina (Figure 2.7). A minimum of three images was collected from random areas of the vessel. Care was taken not to image close to where the vessel had been cut. Each experiment was repeated four times for each strain of mice.

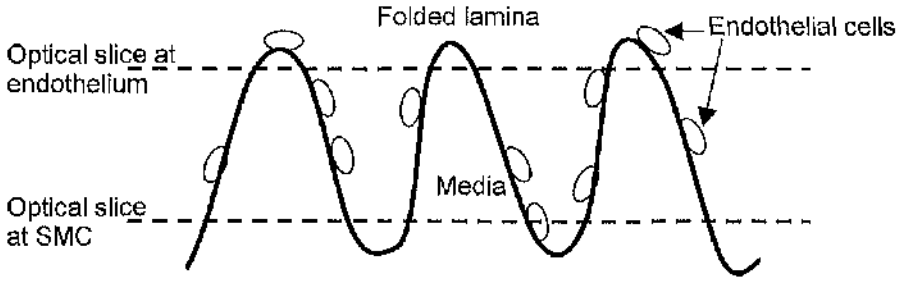

Figure 2.7. Illustration of imaging of open vessels.

Kalman (5 frames) was used to record individual 2D images. Averaging the data from several frames improved image quality. Z-series were also produced in stacks of 1 μm slices, starting at the last smooth muscle layer in focus and ending at the internal elastic lamina, producing a stack of approximately 30 μm.

2.4.6. *Image analysis*

8-bit images were produced and displayed spatially as pixels, where each pixel represents an intensity value between 0 (black) and 255 (white) from the Gray scale. Following image capture, Metamorph software (version 4) was used to analyse the 2D images collected at zoom eight to exclude any autofluorescence from the elastic lamina. Image histogram statistics were produced for each image to obtain the number of pixels at each intensity. The number of pixels was then used to calculate the total fluorescence at each intensity and the mean of replicate experiments was displayed in a histogram plot of fluorescence against intensity. Region statistics were used to generate integrated (total) intensity for each image and the mean data plotted in bar charts. Integrated intensity for QAPB was compared between all four strains of mice using one-way ANOVA. Integrated intensity of QAPB in presence of the selected antagonists was compared to QAPB alone using one-way ANOVA.

3D images were produced from a 3D projection of the stack of "optical sections". Autofluorescence from elastic lamina can mask the fluorescence from QAPB when bound to receptors. As the fluorescence from the elastic lamina obstructed the visualisation of smooth muscle cells, a series of adjacent planes was selected from the stack and used to create the 3D projection.

The images produced from the colocalisation experiments with QAPB and Syto 61 were overlaid. Thus, the localisation of QAPB binding was directly compared with the nuclear binding of Syto 61.

2.5. Drugs and Solutions used

Physiological salt solution (PSS) composition (in mM): 119 NaCl, 4.7 KCl, 1.2 $MgSO_4.H_2O$, 1.2 KH_2PO_4, 24.9 $NaHCO_3$, 2.5 $CaCl_2$, and 11.1 glucose.

The following stock solutions were made from crystalline form using distilled water (unless otherwise stated). All drug stock solutions used were prepared and diluted (1:10) in

distilled water to give the concentrations used for experimental protocols (unless otherwise stated).

2.5.1. Agonist

Phenylephrine (*(R)-(-)-1-(3-Hydroxyphenyl)-2-methylaminoethanol*): 100mM [SIGMA]

A61603 (*N-[5-(4,5-Dihydro-1H-imidazol-2-yl)-2-hydroxy-5,6,7,8-tetrahydronaphthalen-1-yl]methanesulfonamide*): 100mM [TOCRIS]

5-hydroxytryptamine (*3-[2-Aminoethyl]-5-hydroxyindole*): 10mM [SIGMA]

Acetylcholine: 10mM [SIGMA]

2.5.2. Antagonists

Prazosin (*1-(4-Amino-6, 7-dimethoxy-2-quinazolinyl)-4-(2-furanylcarbonyl)piperazine*): 1mM [SIGMA]

5-methylurapidil (*5-Methyl-6[[3-[4-(2-methoxyphenyl)-1-piperazinyl]propyl]amino]-1,3-dimethyluracil*): 100µM [SIGMA]

RS100-329 *(N-[(2-trifluoroethoxy)phenyl],N'-(3-thyminylpropyl) piperazine hydrochloride)*: 1mM [Roche]

BMY 7378 (*8-[2-[4-(2-Methoxyphenyl)-1-piperazinyl]ethyl]-8-azaspiro[4.5]decane-7,9-dione*): 1mM [Research Biochemicals]

Rauwolscine (*17α-Hydroxy-20α-yohimban-16β-carboxylic acid methyl ester*): 100µM [Research Biochemicals]

L-NAME (N_{ω}-*Nitro-L-arginine methyl ester*): 100mM fresh daily [SIGMA]

QAPB (BODIPY FL-Prazosin or Quinazoline Piperazine Bodipy). 0.1mM in DSMO [Molecular Probes]. Diluted in freshly bubbled PSS to the required concentration. Photosensitive so prepared in a dark room and vials protected with aluminium foil.

Syto 61: 0.1mM, in DMSO [Molecular Probes]. Diluted in freshly bubbled PSS to the required concentration.

Chapter Three

Characterisation of the WT mouse

3.1. Introduction

To date, the availability of literature characterising the contractile response in the mouse carotid artery is limited. For this reason the pharmacology of the rat carotid artery and other mouse conductance arteries, such as the thoracic aorta, can provide an insight into the situation in the mouse carotid artery.

3.1.1. Mouse carotid artery

Deighan (2002) was the first *in vitro* study to determine the adrenoceptors mediating the contraction of the mouse carotid artery. Based on the contractile responses to the α_1-AR non-selective agonist, phenylephrine, it was reported that the dominant contractile response was mediated by α_1-ARs. Furthermore, the lack of response to the α_2-AR agonist, UK14304, and the β-AR agonist, isoprenaline, ruled out α_2-AR- or β-AR-mediated contractions. The study characterised the phenylephrine-induced response using selective antagonists and concluded that the α_{1D}-AR was the predominant α_1-AR subtype due to the affinity of the selective α_{1D}-AR antagonist, BMY 7378. However, the Schild slope produced in the presence of BMY 7378 was shallow, raising the possibility that more than one subtype was contributing to the contractile response. The low potency of 5-methylurapidil against the phenylephrine-induced response failed to reveal any α_{1A}-AR component to the contraction. By a process of elimination it was concluded that the α_{1B}-AR was most likely to mediate the secondary α_1-AR contractile response (Deighan C, 2002;Daly *et al.*, 2002a;Deighan *et al.*, 2005). However, no α_{1B}-AR antagonists are available that are adequately selective over the α_{1A}-AR and α_{1D}-AR. Thus, there was no direct evidence that the α_{1B}-AR contributed to the contraction of the carotid artery in the WT mouse.

3.1.2. Rat carotid artery

In contrast to the mouse carotid artery, the rat carotid artery has been widely used. It has been demonstrated that the α_{1D}-AR is the predominant subtype, based on the potency of BMY 7378 (Villalobos-Molina & Ibarra, 1996;Chiba & Tsukada, 2002;Martinez L *et al.*, 1999). For instance, Villalobos-Molina & Ibarra (1996) reported a high pA_2 of 8.66 for BMY 7378 against the contractile response to methoxamine in normotensive Wistar Kyoto rats. In addition, the high affinity values obtained for 5-methylurapidil (pA_2 9.1), WB4101 (pA_2 10.7) and BMY 7378 (pA_2 9.2) suggested that both the α_{1A}-AR and α_{1D}-AR mediate

the contractile response to noradrenaline in the rat carotid artery (Naghadeh, 1996). This was supported by Chiba and Tsukada (2002) who reported that both WB4101 and BMY 7378 inhibited changes in perfusion pressure in response to noradrenaline and phenylephrine, but no evidence of an α_{1D}-AR response was found. De Oliveria et al. (1998) reported that the phenylephrine-induced response in the rat carotid artery was mediated by the α_{1A}-AR, but also reported an α_{1B}-AR-mediated component. However, this was based on the use of chloroethylclonidine, which does not show convincing selectivity for the α_{1B}-AR (Perez *et al.*, 1994;Lomasney *et al.*, 1991;Schwinn *et al.*, 1990;Hirasawa *et al.*, 1997). Furthermore, de Oliveria et al. (1998) concluded that there was no evidence of an α_{1D}-AR response. However, it has been shown that their key antagonist WB4101 also has high affinity for the α_{1D}-AR and the analysis was carried out without the use of the α_{1D}-AR selective antagonist. Nevertheless, the balance of evidence from studies in the rat carotid artery suggests that the predominant subtype is the α_{1D}-AR, with a contribution from the α_{1A}-AR and/or α_{1B}-AR. This compares with the evidence obtained in the mouse carotid artery to date (Deighan C, 2002;Daly *et al.*, 2002a;Deighan *et al.*, 2005).

3.1.3. Mouse aorta

Studies in the mouse carotid artery and thoracic aorta suggest that the pharmacological profile of these conductance arteries is similar. For instance, it has been established that the α_{1D}-AR has a main contractile function and there are several reports that the α_{1B}-AR may have a minor contractile role in the aorta of the WT mouse (Daly *et al.*, 2002a;Piascik & Perez, 2001;Garcia-Sainz *et al.*, 1999;Yamamoto & Koike, 2001b;Yamamoto & Koike, 2001a;Hosoda *et al.*, 2005a;Hosoda *et al.*, 2005b;Yamamoto & Koike, 2001b). However, the role of the α_{1A}-AR and α_{1B}-AR is unclear in this vessel (Tanoue *et al.*, 2002c;Yamamoto & Koike, 2001b;Tanaka *et al.*, 2004;Hosoda *et al.*, 2005b;Ali, 2004;Hosoda *et al.*, 2005a). Interestingly, like the thoracic aorta the upper abdominal aorta is predominantly α_{1D}-AR-mediated, but a change in α_1-AR subtypes occurs in the lower abdominal aorta, which is predominantly α_{1A}-AR-mediated (Yamamoto & Koike, 2001a). Thus, the α_1-AR population in the thoracic aorta may be unique, with a contractile response that is mediated by the α_{1D}-AR and α_{1B}-AR changing down the length of the aorta.

3.1.4. Aims

It is clear from the studies in the conductance arteries of both mouse and rat that the α_{1D}-AR is the predominant contractile α_1-AR subtype. However, assessing the functional roles of the other α_1-AR subtypes is complex. In the absence of selective α_{1B}-AR compounds, the current study used the α_{1A}-AR selective agonist A-61603 in an attempt to isolate an α_{1A}-AR response. The aims of the study were:

- To compare the A-61603-induced response with the contractile response to phenylephrine in the mouse carotid artery.
- To use α_{1A}-AR selective antagonists to further investigate the phenylephrine-induced response.
- To characterise the A-61603-induced response to ascertain whether an α_{1A}-AR component to contraction exists in the mouse carotid artery.

3.2. Methods

The dissection, vessel mounting and acclimatisation period are described in detail in Chapter Two. In brief, four-five-month old male WT mice (C57 Black; 26g-44g) were killed by carbon dioxide overdose and both common carotid arteries were dissected. Following cleaning, vessels were mounted in a four-chamber wire myograph containing gassed (95% O_2 / 5% CO_2) and heated (37°C) PSS. Vessels were allowed to acclimatise for 30 minutes before a resting tension of 0.25g was added to each vessel and a further 45 minutes acclimatisation period prior to the start of the experimental protocol.

3.2.1. Characterisation of phenylephrine-induced response

A wake-up protocol for phenylephrine was performed as described in Chapter Two. The vessels were washed with PSS and allowed to rest for 30 minutes. CRCs to phenylephrine (1 nM – 0.1 mM) were produced using half-log increments. Prior to the second CRC, vessels were incubated for 30 minutes with the α_{1A}-AR selective antagonist RS100329 (1 nM, 10 nM, 0.1 μM). A second phenylephrine CRC was then produced in the presence of the antagonist or in the absence of an antagonist acting as a time control.

3.2.2. Characterisation of A-61603-induced response

A wake-up protocol for A-61603 was performed as described in Chapter Two. A CRC to A-61603 (1 nM – 0.1 mM) was constructed in half log increments. Vessels were incubated for 30 minutes with the α_{1A}-AR selective antagonists 5-methylurapidil (10 nM, 0.1 μM, 0.3 μM, 1 μM) and RS100 329 (1 nM, 10 nM, 0.1 μM); or the α_{1D}-AR selective antagonist BMY7378 (1 nM, 10 nM, 0.1 μM). A second CRC was produced in the presence of an antagonist, or in the absence of an antagonist acting as a time control.

3.2.3. Statistical analysis

Data were expressed as means ± standard error in grams tension and percentage of the maximum response of the control CRC. The maximum responses obtained, pEC_{50} values of the agonist response in the absence or presence of an antagonist were compared using either a Student's t-test or one-way ANOVA, followed by a Bonferroni's post test. CRCs were compared using two-way-ANOVA with a Bonferroni post-test. Nonlinear regression was performed to fit sigmoidal-curves (variable slope) on mean data of responses in grams and percentage of the maximum response of the control CRC. Linear regression was performed to obtain the pA_2 which was identified from the X-intercept of the Schild plot. When a single concentration of antagonist had no effect, or the antagonist caused the maximum response obtained to be significantly reduced compared to the control CRC, a pK_B was calculated from the remaining concentrations of antagonist.

3.3. Results

3.3.1. Comparison of phenylephrine and A-61603 response

Phenylephrine produced concentration-dependent contractions in the WT mouse (Figure 3.1; Table 3.1). No significant differences were observed between the maximum response obtained or pEC_{50} values of the phenylephrine control and the phenylephrine time control.

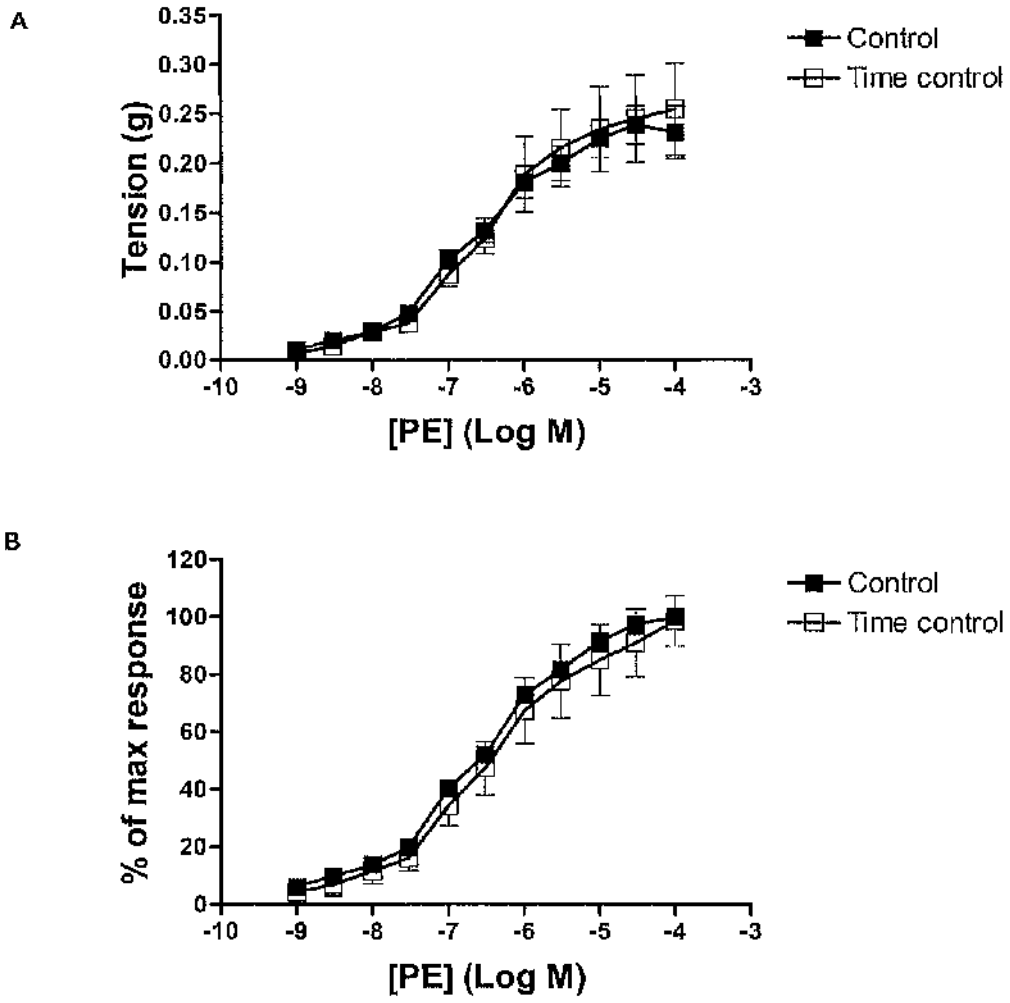

Figure 3.1. WT mouse: Phenylephrine CRCs in the carotid artery (n=7) expressed as mean ± S.E. in (A) grams tension and (B) percentage of maximum response of the control CRC.

Table 3.1. Comparison of phenylephrine CRCs in the WT mouse.

Agonist	n	pEC_{50}	Maximum response (g)	Hill slope (95% CI)
PE control	7	6.6±0.05	0.27±0.03	0.6 (0.5-0.7)
PE time control	7	6.7±0.05^{+}	0.25±0.05^{+}	0.7 (0.5-0.9)$^{+}$

$^{+}$ **p>0.05 compared to PE control (Student's t-test).**

A-61603 produced concentration-dependent contractions in the WT mouse (Figure 3.2; Table 3.2). No significant differences were observed between the maximum response obtained or pEC_{50} values of the A-61603 control and the A-61603 time control.

A

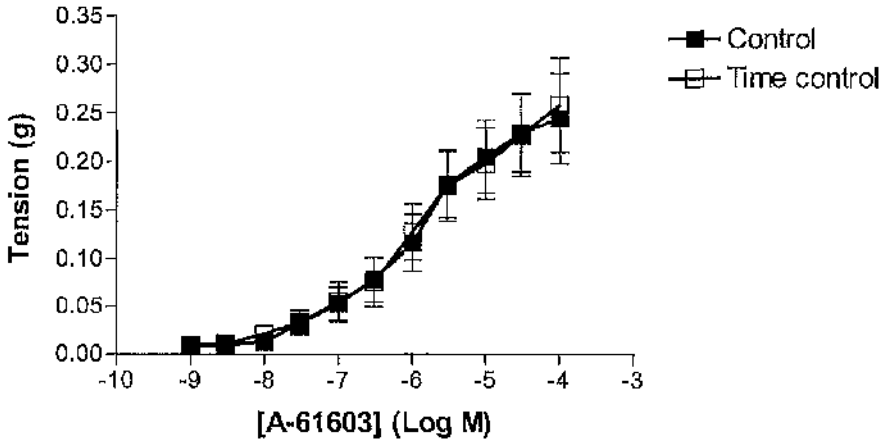

B

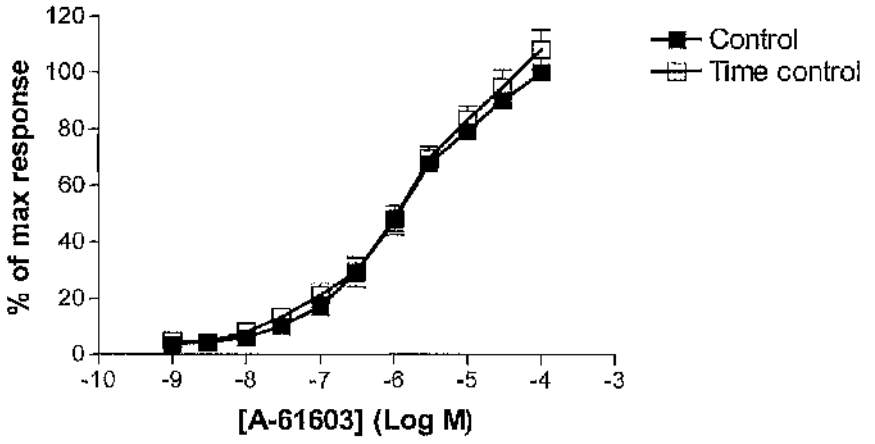

Figure 3.2. WT mouse: A-61603 CRC in the carotid artery (n=10) expressed as mean ± S.E. in (A) grams tension and (B) percentage of maximum response of the control CRC.

Table 3.2. Comparison of A-61603 CRCs in the WT mouse.

Agonist	n	pEC_{50}	Maximum response (g)	Hill slope (95% CI)
A-61603 control	10	6.0±0.06	0.28±0.02	0.7 (0.5-0.9)
A-61603 time control	10	6.0±0.03[+]	0.28±0.05[+]	0.7 (0.4-0.9)[+]

[+] p>0.05 compared to A-61603 control (Student's t-test).

No significant difference was observed in the maximum response recorded between the phenylephrine control and A-61603 control, but sensitivity to phenylephrine was significantly higher than A-61603 (Figure 3.3; Table 3.3).

A

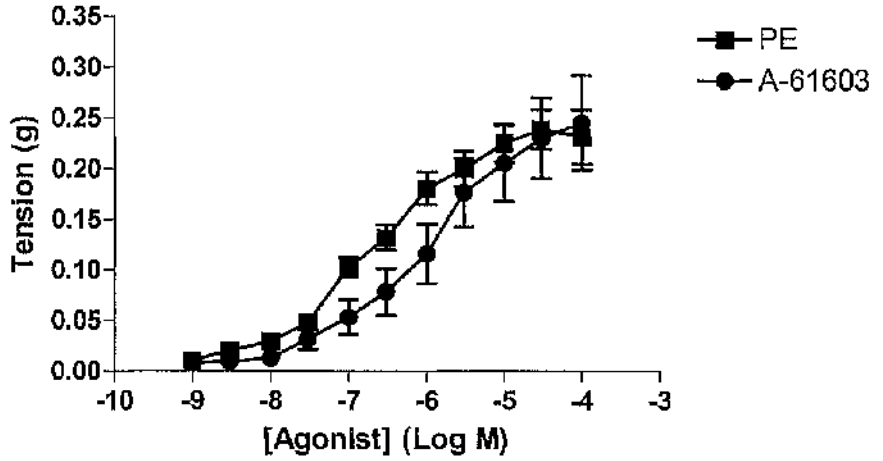

B

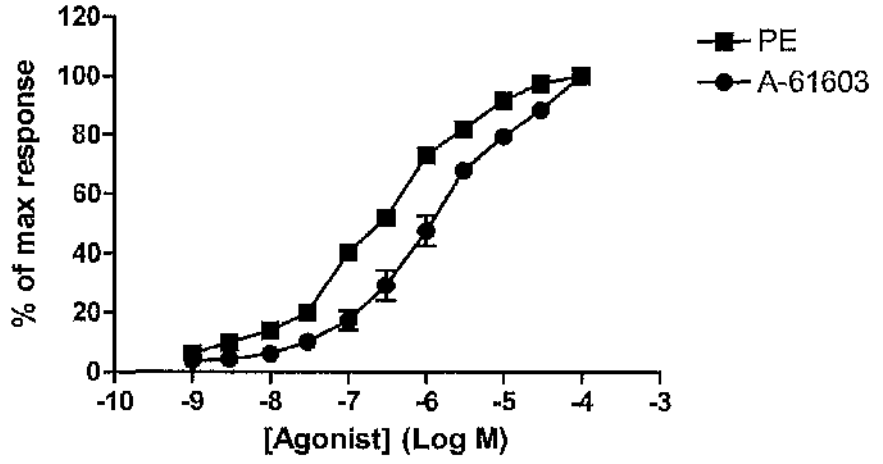

Figure 3.3. WT mouse: Comparison of control CRCs to phenylephrine (n=7) and A-61603 (n=10) in the carotid artery expressed in grams mean ± S.E.

Table 3.3. Comparison of control CRCs to phenylephrine and A-61603 in the WT mouse.

Agonist	n	pEC_{50}	Maximum response (g)	Hill slope (95% CI)
PE control	7	6.6±0.05	0.27±0.03	0.6 (0.5-0.7)
A-61603 control	10	6.0±0.03*	0.28±0.05+	0.7 (0.4-0.9)+

+ p>0.05; * p<0.05 compared to PE control (Student's t-test).

3.3.2. Antagonist data

3.3.2.1. Phenylephrine-induced response

Deighan (2002;Deighan *et al.*, 2005) calculated affinity estimates for prazosin, BMY 7378 and 5-methylurapidil against the phenylephrine-induced response. These values have been included in Table 3.8 for completeness.

RS100 329

RS100 329 produced a rightward displacement of the phenylephrine response at 0.1 μM (Figure 3.4; Table 3.4), enabling a pK_B of 7.9 to be calculated at this concentration.

A

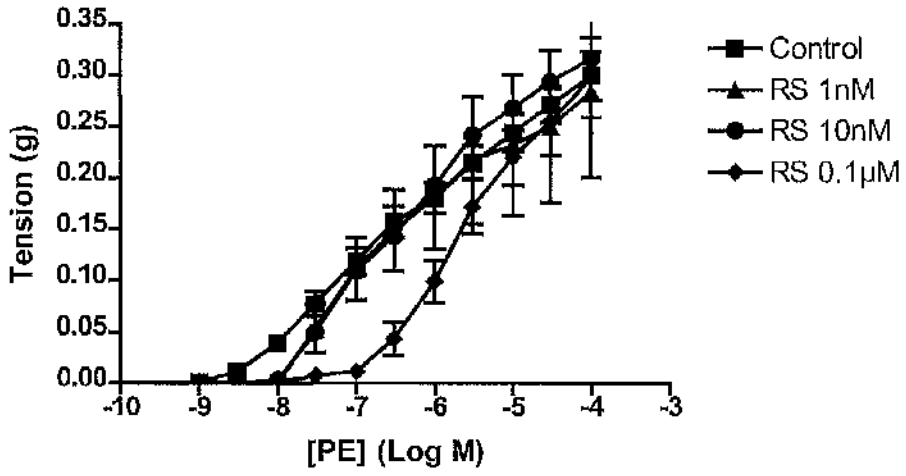

B

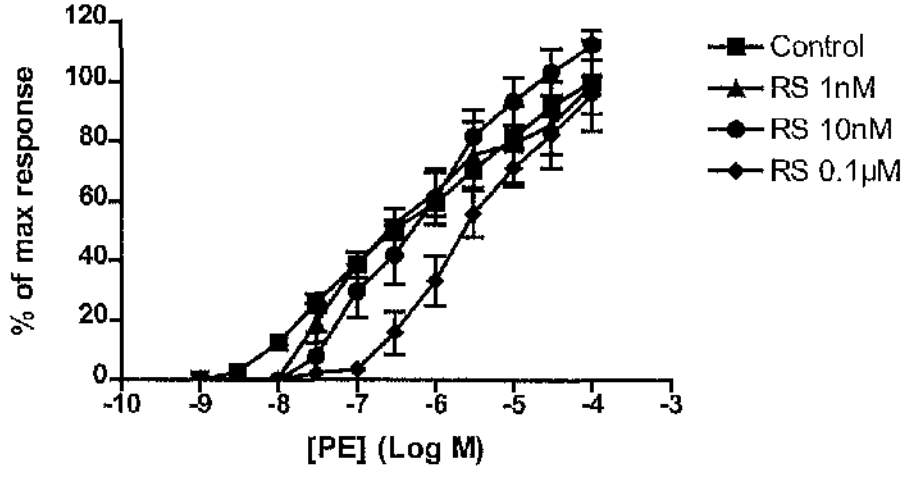

Figure 3.4. WT mouse: Phenylephrine CRCs in the presence of RS100 329 (n=6) expressed as mean ± S.E. in (A) grams tension and (B) percentage of maximum response of the control CRC.

Table 3.4. Phenylephrine CRCs in the presence of RS100 329 in the WT mouse

Agonist	n	pEC_{50}	Maximum response (g)	Hill slope (95% CI)
PE control	8	6.5±0.13	0.30±0.02	0.5 (0.5-0.6)
RS100 329 1nM	6	$6.7\pm0.07^{+}$	$0.28\pm0.08^{+}$	$0.7\ (0.6\text{-}0.9)^{+}$
RS100 329 10nM	6	$6.6\pm.26^{+}$	$0.32\pm0.04^{+}$	$0.7\ (0.6\text{-}0.8)^{+}$
RS100 329 0.1μM	6	$5.6\pm0.22^{*}$	$0.30\pm0.04^{+}$	$0.9\ (0.6\text{-}1.2)^{+}$

$^{+}p>0.05$; $^{*}p<0.05$ compared to PE control (one-way ANOVA, Bonferroni's post test).

3.3.2.2. A-61603-induced response

BMY 7378

The CRC produced in the presence of BMY 10 nM was biphasic. Only the highest concentration of BMY7378 used (0.1μM) produced a significant rightward displacement of the A-61603 CRC (Figure 3.5; Table 3.5), enabling a pK_B of 8.3 to be calculated at this concentration.

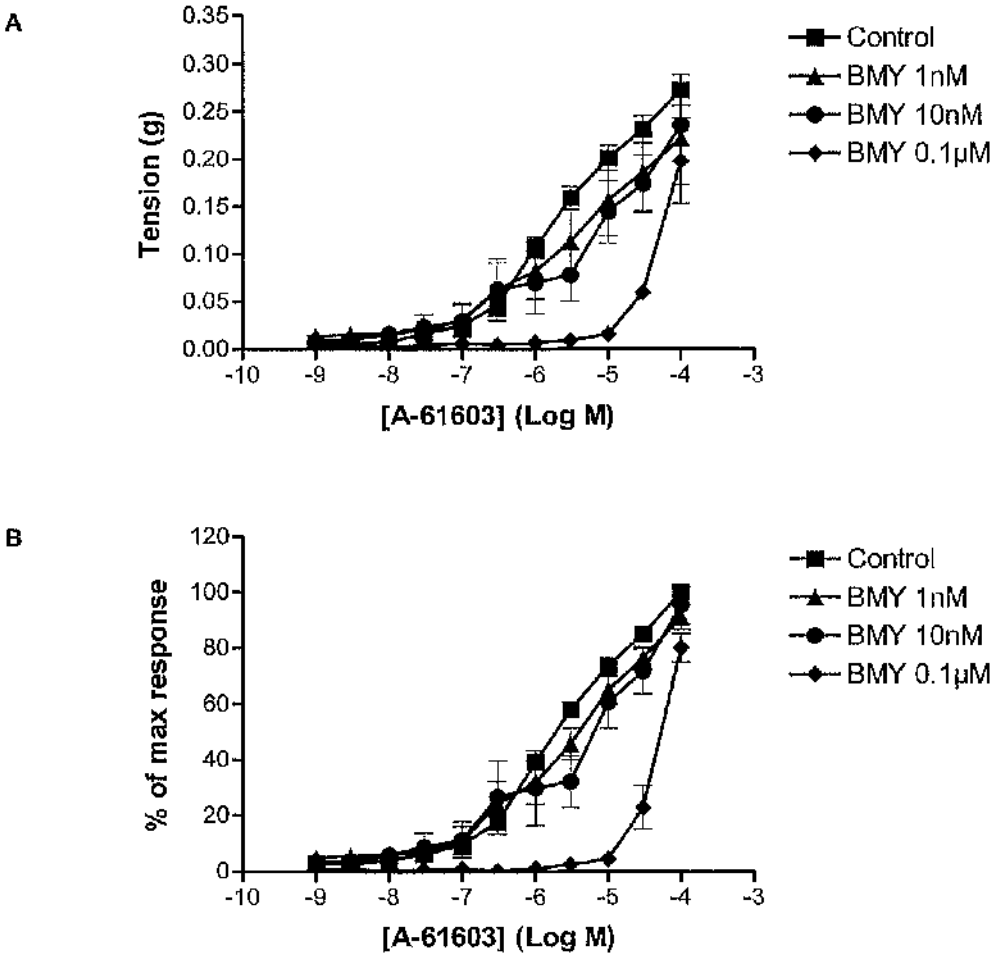

Figure 3.5. WT mouse: A-61603 CRCs in the presence of BMY 7378 (n=6) expressed as mean ± S.E. in (A) grams tension and (B) percentage of maximum response of the control CRC.

Table 3.5. A-61603 CRCs in the presence of BMY 7378 in the WT mouse.

Agonist	n	pEC_{50}	Maximum response (g)	Hill slope (95% CI)
A-61603 control	6	5.7±0.05	0.27±0.02	0.7 (0.6-0.9)
BMY 7378 1nM	6	5.3±0.18^{+}	0.22±0.05^{+}	0.6 (0.3-0.9)$^{+}$
BMY 7378 10nM	6	5.4±0.41^{+}	0.24±0.04^{+}	0.6 (0.4-0.7)$^{+}$
BMY 7378 0.1µM	6	4.3±0.04*	0.22±0.04^{+}	0.8 (0.3-1.3)$^{+}$

$^{+}$ p>0.05; *p<0.05 compared to A-61603 control (one-way ANOVA, Bonferroni's post test).

5-methylurapidil

5-Methylurapidil caused a rightward displacement of the A-61603 CRC (Figure 3.6; Table 3.6). A pA_2 value of 8.3 was calculated with a slope of 1.0 (0.6-1.3), indicating competitive antagonism.

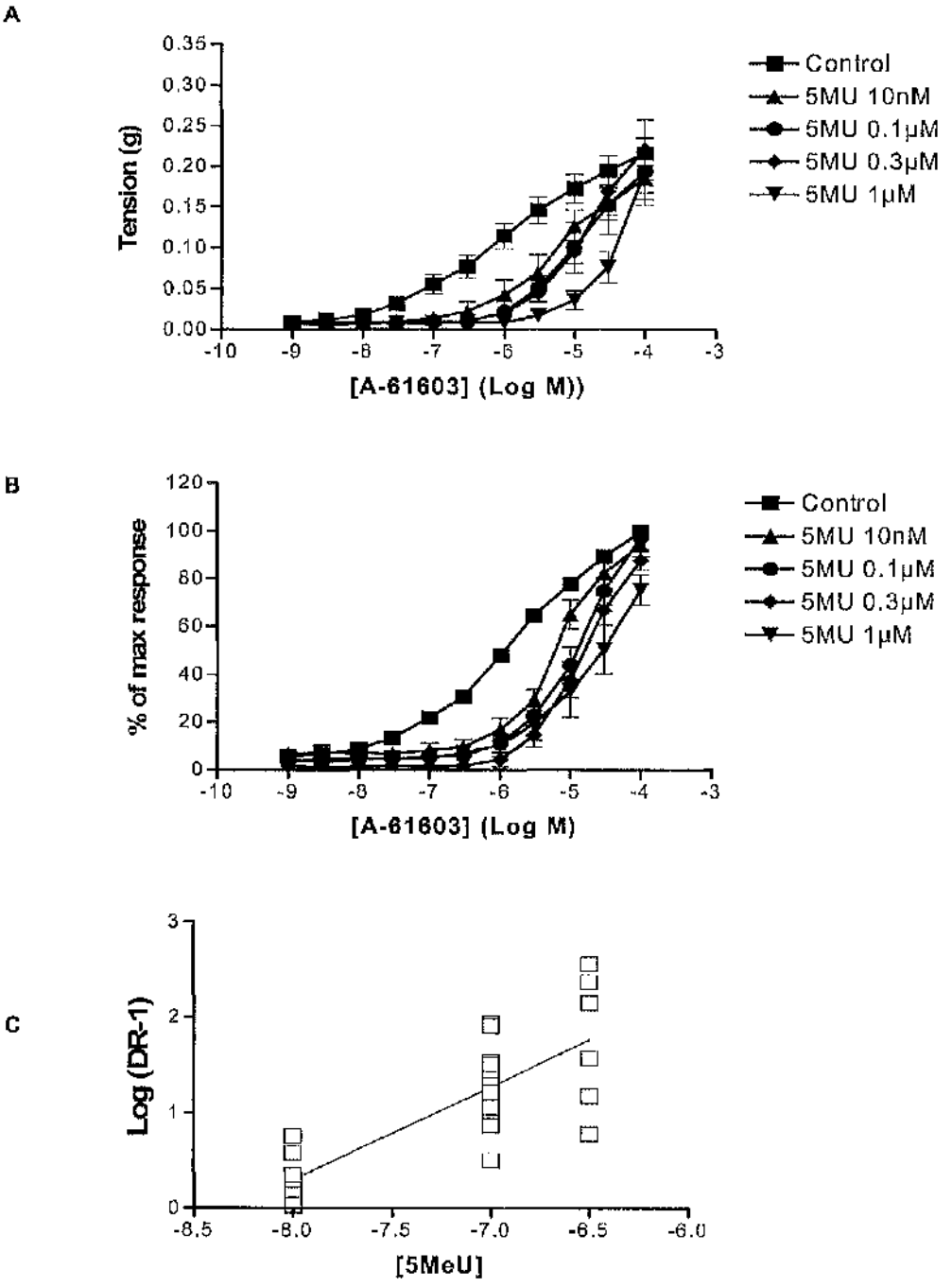

Figure 3.6. WT mouse: A-61603 CRCs in the presence of 5-methylurapidil (n=6) expressed as mean ± S.E. in (A) grams tension, (B) percentage of maximum response of the control CRC and (C) Schild plot for 5-methylurapidil.

Table 3.6. A-61603 CRCs in the presence of 5-methylurapidil in the WT mouse.

Agonist	n	pEC_{50}	Maximum response (g)	Hill slope (95% CI)
A-61603 control	10	6.0±0.08	0.22±0.02	0.9 (0.8-1.1)
5-MeU 10nM	7	5.2±0.05*	0.18±0.03+	1.1 (0.5-1.6)+
5-MeU 0.1μM	6	4.9±0.11*	0.19±0.04+	1.0 (0.7-1.4)+
5-MeU 0.3μM	6	4.8±0.18*	0.22±0.04+	1.3 (0.7-1.9)+
5-MeU 1μM	6	4.9±0.23*	0.19+-0.03+	1.2 (0.5-2.0)+

+ p>0.05; *p<0.05 compared to A-61603 control (one-way ANOVA, Bonferroni's post test).

RS100 329

RS100 329 10nM and 0.1 μM shifted the A-61603 CRC to the right (Figure 3.8; Table 3.8). Due to the lack of effect of the lowest concentration of RS100329 (1nM), and a significant reduction in the maximum response recorded for phenylephrine in the presence of RS100-329 0.1 μM a pK_B of 8.7 was calculated for RS100 329 10nM.

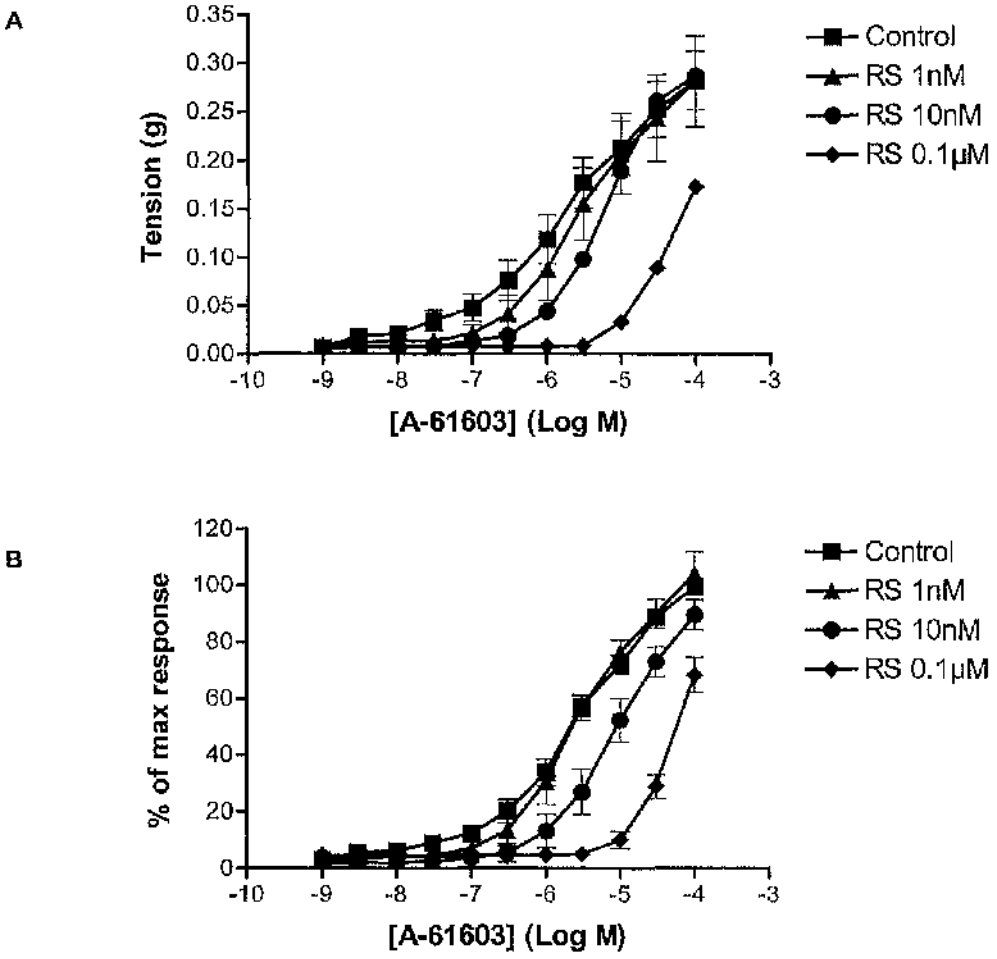

Figure 3.7. WT mouse: A-61603 CRCs in the presence of RS100 329 (n=7) expressed as mean ± S.E. in (A) grams tension and (B) percentage of maximum response of the control CRC.

Table 3.7. A-61603 CRCs in the presence and absence of RS100 329 in the WT mouse.

Agonist	n	pEC_{50}	Maximum response (g)	Hill slope (95% CI)
A-61603 control	8	5.8±0.11	0.28±0.03	0.9 (0.6-1.2)
RS100 329 1nM	7	5.7±0.12^{+}	0.28±0.05^{+}	0.8 (0.6-1.0)$^{+}$
RS100 329 10nM	8	5.3±0.14*	0.29±0.04^{+}	1.0 (0.9-1.1)$^{+}$
RS100 329 0.1µM	8	N.D.	0.17±0.03*	1.2 (0.4-1.9)$^{+}$

$^{+}$ p>0.05; *p<0.05 compared to A-61603 control (one-way ANOVA, Bonferroni's post test).

Table 3.8. Affinity estimates of selective α_1-AR antagonists for phenylephrine and A-61603

	Prazosin		5MeU		RS100-329		BMY7378	
Agonist	pA_2 /pK_B	Slope. (95% CI)	pA_2 /pK_B	Slope (95% CI)	pA_2 /pK_B	Slope (95% CI)	pA_2 /pK_B	Slope (95% CI)
PE	9.6*	0.9 (0.8-1.1)	7.5*	1.1 (0.7-1.5)	7.9	-	8.3*	-
A-61603	-	-	8.3	1.0 (0.6-1.3)	8.7	-	8.3	-

*** Denotes data from Deighan, University of Glasgow PhD Thesis (2002).**

3.4. Discussion

The present study set out to further characterise the α_1-AR-mediated contractile response in the murine carotid artery by determining whether an α_{1A}-AR response existed. Due to α_1-AR heterogeneity, the characterisation of the α_1-AR-mediated contractile response in the WT mouse is complex. In an attempt to isolate an α_{1A}-AR response in the WT mouse, A-61603, an agonist with reported selectivity for the α_{1A}-AR (Knepper SM *et al.*, 1995)(see Chapter One) was employed, in addition to the non-selective α_1-AR agonist phenylephrine.

3.4.1. Agonist responses

Both phenylephrine and A-61603 produced concentration-dependent contractions with no differences being observed between the control and time control, validating the use of these agonists for further analysis.

The maximum response recorded for phenylephrine and A-61603 were not significantly different. Phenylephrine has been shown to be 30-times more potent than A-61603 in the rat aorta (Knepper SM *et al.*, 1995), in which the α_{1D}-AR is predominant and there is no evidence of an α_{1A}-AR response (Buckner *et al.*, 1996;Kenny *et al.*, 1995;Aboud *et al.*, 1993). Like the rat aorta, the mouse carotid artery is predominantly α_{1D}-AR-mediated. However, in the mouse carotid artery the potency for phenylephrine was only 4-fold higher than A-61603. This raises the possibility that the α_{1A}-AR may contribute to the contractile response in the carotid artery. Nevertheless, this is markedly different from observations from tissues that are predominately α_{1A}-AR (rat submaxillary gland (Michel *et al.*, 1989), rat vas deferens (Honner V & Docherty, 1999;Aboud *et al.*, 1993), canine prostate (Goetz *et al.*, 1994), in which A-61603 was at least 160-fold more potent than phenylephrine

(Knepper SM *et al.*, 1995). Overall, the agonist responses alone provide further evidence in support of the α_{1D}-AR being the predominant α_1-AR in the mouse carotid artery and highlights that an α_{1A}-AR-mediated response may exist.

3.4.2. α_{1D}-AR antagonism

The pK_B of 8.3 for BMY 7378 versus A-61603 is similar to that against phenylephrine and is in line with published values at the α_{1D}-AR, so implicates the involvement of the α_{1D}-AR in the A-61603 response. However, the α_{1D}-AR selectivity of BMY 7378 may be lost at 0.1 μM and it is plausible that BMY 7378 was acting on the α_{1A}-AR. Furthermore, a biphasic A-61603 CRC was observed with BMY 7378 10nM, highlighting the possible involvement of two subtypes in the A-61603 response: a low concentration effect resistant to BMY 7378 10 nM and a high concentration response that is susceptible to this concentration of BMY 7378. In the previous study of the WT mouse carotid artery, BMY7378 antagonised the phenylephrine-induced response only at the highest concentration used (0.1 μM) (Deighan C, 2002;Deighan *et al.*, 2005) but at this concentration a pK_B of 8.3 was produced. This pK_B was taken to be indicative of an α_{1D}-AR-mediated response as it was consistent with published affinity estimates for BMY 7378 at this subtype. In a recent study from our laboratory, Ali (2004) showed that neither A-61603 nor phenylephrine produced a contraction in the $\alpha_{1B/D}$-KO thoracic aorta arguing against an α_{1A}-AR in that artery. However, it was also reported that phenylephrine but not A-61603 was potent and efficacious in the α_{1D}-KO, suggesting that phenylephrine, but not A-61603, acts on the α_{1B}-AR as well as the α_{1D}-AR in the aorta. This absence of α_{1B}-AR potency for A-61603 in the aorta suggests that the two components observed in the present study arise from the α_{1D}-AR and the α_{1A}-AR.

3.4.3. α_{1A}-AR antagonism

In the current study, 5-methylurapidil acted with higher affinity against A-61603 than that reported for phenylephrine, producing a pA_2 of 8.3, compared with 7.5 versus phenylephrine (Deighan C, 2002;Deighan *et al.*, 2005). According to the potency values from the literature, 8.3 is indicative of an α_{1A}-AR-mediated response (See Chapter One). In contrast, in the previous study the low potency of 5-methylurapidil against the phenylephrine-induced response was used to argue against an α_{1A}-AR component to the contraction and it was concluded that the α_{1B}-AR was most likely to contribute to the α_1-

AR contractile response to phenylephrine, in addition to the dominant α_{1D}-AR (Deighan C, 2002;Deighan *et al.*, 2005). In the thoracic aorta of the WT mouse a relatively low pK_B of 7.7 was produced for 5-methylurapidil against the phenylephrine-induced response (Ali, 2004). This affinity estimate is similar to that obtained for 5-methylurapidil against the phenylephrine-induced response in the study by Deighan (2002;Deighan *et al.*, 2005) and does not support a functional role for the α_{1A}-AR. However, an earlier study in the WT mouse aorta Daly et al. (2002a) reported that 5-methylurapidil antagonised the phenylephrine-induced response producing the higher pA_2 of 8.3. Despite acknowledging that the α_{1A}-AR may be involved in the response, it was again concluded that the α_{1B}-AR contributed to the contractile response in addition to the α_{1D}-AR. In the first order mesenteric artery of the mouse, in which the α_{1A}-AR predominates, a pK_B of 8.9 was produced for 5-methylurapidil against the A-61603-induced response (McBride *et al.* Submitted for Publication). This higher pK_B in the mesenteric artery may reflect the involvement of the α_{1D}-AR in the A-61603-induced response in the carotid artery. Nevertheless, the relatively high pA_2 of 8.3 obtained in the present study versus A-61603 is more consistent with 5-methylurapidil acting at the α_{1A}-AR rather than the α_{1B}-AR or α_{1D}-AR.

The α_{1A}-AR selective antagonist, RS100329 was used in the current study to consolidate the 5-methylurapidil data. RS100329 0.1 μM competitively antagonised the phenylephrine response producing a pK_B of 7.9. As the same affinity estimate value was obtained against the noradrenaline-induced response in the rat aorta (Williams *et al.*, 1999), which is believed to be mediated by the α_{1D}-AR, it seemed likely that this highest concentration of RS100329 was antagonising the action of phenylephrine at the α_{1D}-AR. A shallow Hill slope was obtained for the phenylephrine-induced response but in the presence of 0.1 μM RS100329, a steeper Hill slope, not significantly different from 1.0, was produced. This suggests that the phenylephrine-induced response is mediated by the α_{1D}-AR and another receptor. RS100329 antagonised the A-61603-induced response with higher affinity (pK_B 8.7), which is closer to affinity estimates in α_{1A}-AR tissues such as the human lower urinary tract (9.2) and rabbit bladder neck (9.2) reported by Williams et al. (1999). The high affinity of RS100329 against the A-61603-induced response provides evidence that the α_{1A}-AR is involved in the contractile response in the mouse carotid artery, reinforcing the less clear-cut 5-methylurapidil data. It is apparent that both an α_{1A}-AR and α_{1D}-AR-mediated response exists in the mouse carotid artery.

3.4.4. Comparison with aorta

The aorta and carotid artery are considered to share similar pharmacological properties with the major contractile α_1-AR of both being the α_{1D}-AR (Daly *et al.*, 2002a;Piascik & Perez, 2001;Garcia-Sainz *et al.*, 1999;Yamamoto & Koike, 2001b;Yamamoto & Koike, 2001a;Hosoda *et al.*, 2005a;Hosoda *et al.*, 2005b;Yamamoto & Koike, 2001b;Deighan C, 2002;Deighan *et al.*, 2005). However, there is no evidence of an α_{1A}-AR-mediated response in the thoracic aorta of the WT mouse. Thus, the α_{1A}-AR-mediated response in the carotid artery, described in the present study, may be a difference that exists between these vessels. Like the thoracic aorta, the upper abdominal aorta is α_{1D}-AR-mediated, but the lower abdominal aorta is α_{1A}-AR-mediated (Yamamoto & Koike, 2001a). This evidence of regional variations in the α_1-AR subtypes in the same vessel suggests that, despite being considered pharmacologically similar, differences between the minor subtypes in the thoracic aorta and the carotid artery are entirely plausible. Furthermore, differences exist in the α_1-AR subtypes present in the branches of the aorta. For instance, this study has shown that the carotid artery is predominantly α_{1D}-AR-mediated, with a contribution from the α_{1A}-AR, while the iliac artery, a branch of the lower abdominal aorta is predominantly α_{1A}-AR-mediated (Shibano *et al.*, 2002). It is plausible that as the distance from the aortic arch increases the predominance of the α_{1D}-AR may decrease, while the predominance of the α_{1A}-AR may increase.

3.4.5. Comparison with rat

In addition to supporting evidence of the α_{1D}-AR being predominant, the current study has provided evidence indicative of the α_{1A}-AR having a functional role in the mouse carotid artery. The rat carotid artery has been more commonly studied and provides an insight to the mouse. The balance of evidence suggests that in the rat carotid artery the α_{1D}-AR is also the dominant α_1-AR (Villalobos-Molina & Ibarra, 1996;Martinez L *et al.*, 1999). The findings of the present study are similar to two studies in the rat carotid artery where both an α_{1A}-AR and α_{1D}-AR response was identified but no involvement from the α_{1B}-AR was detected (Chiba & Tsukada, 2002;Naghadeh, 1996). However, there are still some discrepancies over the role of the α_{1B}-AR in the rat carotid artery (de Oliveria *et al.*, 1998) and an α_{1B}-AR-mediated response cannot be ruled out at present. The possible contribution of the α_{1B}-AR in the rat carotid artery raises the possibility that this α_1-AR may contribute to the contractile response in the mouse carotid artery.

3.4.6. Conclusion

Without a doubt, the characterisation of α_1-AR subtypes in vessels with α_1-AR heterogeneity is restricted by the availability of agonists and antagonists and a definite conclusion cannot be reached about the contribution of the α_{1A}-AR and α_{1B}-AR in the WT mouse. Fortunately, knockout mice of the α_1-AR subtypes are available and have been used in Chapter Three to provide an insight into the situation in the WT mouse.

Chapter Four

Characterisation of the α_1-AR knockout mice

4.1. Introduction

Chapter Three has shown that the pharmacological analysis of the α_1-AR subtypes is complex in the WT mouse, especially due to the limited numbers of selective agonists and antagonists. Consequently, mouse strains with single and double knockout of the α_1-AR subtypes have been developed and have been employed to assess α_1-AR contractility.

4.1.1 α_1-AR knockout mice

The α_{1B}-KO was the first α_1-AR knockout mouse to be generated. Cavalli et al. (1997) reported that the efficacy of phenylephrine was reduced in the thoracic aorta of the α_{1B}-KO compared to the WT mouse, suggesting that the α_{1B}-AR has a role in vasoconstriction. A later study by Daly et al. (2002a) found that, in contrast to Cavalli et al. (1997), the efficacy of phenylephrine in the aorta was not significantly different to the WT mouse. However, this study found that the α_{1D}-AR was the major α_1-AR subtype in the aorta and carotid artery, while the α_{1A}-AR was dominant in the first order mesenteric artery and tail artery. This study lent support to the conclusion of Cavalli et al. (1997) that the α_{1B}-AR was involved in vasoconstriction, since some quantitative pharmacological differences existed in the α_{1B}-KO, but added that this role was minor.

In the α_{1D}-KO the contractile response in the aorta was markedly decreased in comparison with the WT mouse, providing evidence that the α_{1D}-AR regulates vasoconstriction (Tanoue *et al.*, 2002c). The findings of two further studies (Ali, 2004;Yamamoto & Koike, 2001b), supported both Tanoue et al. (2002a) and Daly et al. (2002a), as it was reported that the main contractile α_1-AR in the mouse aorta was the α_{1D}-AR. In addition, an α_{1B}-AR-mediated contractile response to phenylephrine was present in the α_{1D}-KO (Ali, 2004).

The α_{1A}-KO revealed that the α_{1A}-AR has a functional role in the maintenance of arterial blood pressure (Rokosh & Simpson, 2002) but, to date, *in vitro* studies have not been performed in this mouse. Similarly, there has not been an *in vitro* study of the vascular responses in the α_{1AB}-KO (O'Connell *et al.*, 2003).

In a recent study comparing α_1-AR-mediated responses in the thoracic aorta of the $\alpha_{1B/D}$-KO, Hosoda et al. (2005a) reported that contractile responses to phenylephrine and noradrenaline were reduced in the $\alpha_{1B/D}$-KO, as well as the α_{1B}-KO and α_{1D}-KO. In

particular, the $\alpha_{1B/D}$-KO showed the response to noradrenaline or phenylephrine was abolished. Thus, it was concluded that the α_{1D}-AR was the predominant α_1-AR in the aorta, with a small contribution from the α_{1B}-AR, which was consistent with the findings of the earlier studies in the single knockouts (Ali, 2004;Daly *et al.*, 2002a;Tanoue *et al.*, 2002c). In a subsequent study, Hosoda et al. (2005b) characterised the noradrenaline-induced response in the thoracic aorta and mesenteric artery of the $\alpha_{1B/D}$-KO and compared this to the single knockouts of the α_{1B}-AR and α_{1D}-AR. In the thoracic aorta of the $\alpha_{1B/D}$-KO, the noradrenaline-induced response was almost abolished but was still detectable indicating that the role of the α_{1A}-AR in the regulation of the thoracic aorta was minimal.

4.1.2. Carotid artery

Deighan (2002) undertook a detailed study of the carotid artery in the α_{1B}-KO, in which a functional role of the α_{1A}-AR was excluded due to the low affinity of 5-methylurapidil against the phenylephrine-induced response. BMY 7378 antagonised the phenylephrine response with high potency, which implicated that the α_{1D}-AR mediated the contractile response in the α_{1B}-KO. In addition, Deighan (2002) presented evidence indicative of α_1-AR heterogeneity in the WT mouse carotid artery, raising the possibility that the α_{1B}-AR may contribute to the contractile response in the WT mouse.

4.1.3. Aims

While several research groups have examined the contractile α_1-ARs in the aorta and resistance arteries in the α_1-AR knockout mice, a comparative study of the carotid artery in the α_{1D}-KO, $\alpha_{1B/D}$-KO or $\alpha_{1A/B}$-KO has not been performed. Furthermore, the α_{1D}-AR has been characterised as the predominant α_1-AR in the mouse carotid artery, but the roles of the α_{1A}-AR and α_{1B}-AR have not been resolved. The α_{1D}-KO thus provides an opportunity to identify and study the other α_1-AR subtypes.

The aims of the current study were:

- To characterise the phenylephrine-induced response in the α_{1D}-KO carotid artery, enabling its profile to be studied when only the α_{1A}-AR and α_{1B}-AR can be present.

- To characterise the A-61603-induced response in the carotid artery of the $\alpha_{1B/D}$-KO in order to study its profile when only the α_{1A}-AR can be present.

- To isolate an α_{1A}-AR-mediated response in the carotid artery of the α_{1D}-KO, using the α_{1A}-AR selective agonist A-61603, and then determine whether the α_{1A}-AR and/or α_{1B}-AR are functional using selective antagonists.

- To determine whether the contractile response in the carotid artery of the α_{1B}-KO has an α_{1A}-AR-mediated component.

- To carry out preliminary experiments in the α_{1AB}-KO, in which only α_{1D}-ARs can be present.

- To compare the findings in the knockouts with the WT mouse in order to further assess the subtype profile of the WT mouse in light of the findings in the knockout mice.

4.2. Methods

The dissection, vessel mounting and acclimatisation period are described in detail in Chapter Two. In brief, four-five-month old male knockout mice (α_{1B}-KO (31-46g); α_{1D}-KO (25-34g); $\alpha_{1B/D}$-KO (32-54g); α_{1AB}-KO (29-31g)) were killed by carbon dioxide overdose and both common carotid arteries were dissected. Following cleaning, vessels were mounted in a four-chamber wire myograph containing gassed (95% O_2 / 5% CO_2) and heated (37°C) PSS. Vessels were allowed to acclimatise for 30 minutes before a resting tension of 0.25g was added to each vessel and a further 45 minutes acclimatisation period prior to the start of the experimental protocol.

4.2.1. Comparison of agonist responses in the double knockouts

In the $\alpha_{1A/B}$-KO and $\alpha_{1B/D}$-KO, the contractile response to phenylephrine, A-61603 and 5-HT were compared. A wake-up protocol for phenylephrine was performed as described in Chapter Two. Following further PSS washes and ten minute rest period, a 5-HT wake-up protocol was also performed. Then the vessels were washed with PSS and allowed to rest for 30 minutes. CRCs to phenylephrine (1 nM – 0.1 mM), A-61603 (1 nM – 0.1 mM) and 5-HT (1 nM – 30 μM) were produced using half-log increments.

4.2.2. Characterisation of phenylephrine-induced response

In the α_{1D}-KO, the phenylephrine-induced response was characterised. A phenylephrine wake-up protocol was performed as described in Chapter Two. Then the vessels were washed with PSS and allowed to rest for 30 minutes. CRCs to phenylephrine (1 nM – 0.1 mM) were produced using half-log increments. Prior to the second CRC, vessels were incubated for 30 minutes with: the non-selective α_1-AR antagonist prazosin (0.1 nM, 1 nM, 10 nM); α_{1A}-AR selective antagonists 5-methylurapidil (10nM, 0.1 μM, 0.3 μM, 1 μM) and RS100 329 (1 nM, 10 nM, 0.1 μM); or α_{1D}-AR selective antagonist BMY 7378 (1nM, 10 nM, 0.1 μM). A second phenylephrine CRC was then produced in the presence of the antagonist or in the absence of an antagonist acting as a time control.

Following the same protocol, prazosin (10 nM) was tested against the phenylephrine-induced response in the $\alpha_{1B/D}$-KO, while BMY 7378 (10 nM) was tested against the phenylephrine-induced response in the $\alpha_{1A/B}$-KO.

4.2.3. Characterisation of A-61603-induced response

A wake-up protocol for A-61603 was performed as described in Chapter Two. Following washing with PSS and a 30 minute rest period the first CRC to A-61603 (1 nM 0.1 mM) was constructed in half-log increments. Prior to the second CRC the vessels were incubated for 30 minutes with an antagonist. The non-selective α_1-AR antagonist prazosin (1 nM, 10 nM, 0.1 μM) was used against the A-61603 CRC in the α_{1D}-KO and $\alpha_{1B/D}$-KO. The α_{1A}-AR selective antagonists 5-methylurapidil (10 nM, 0.1 μM, 0.3 μM, 1 μM) and RS100 329 (1 nM, 10 nM, 0.1 μM), as well as the α_{1D}-AR selective antagonist BMY 7378 (1 nM, 10 nM, 0.1 μM), were tested in the α_{1B}-KO and α_{1D}-KO. RS100 329 (10 nM) and BMY 7378 (10 nM) were tested against the A-61603-induced response in both double knockouts, while 5-methylurapidil (0.1 μM) and the α_2-AR antagonist rauwolscine (10 nM) were also used in the $\alpha_{1B/D}$-KO. A second CRC was produced in the presence of an antagonist, or in the absence of an antagonist acting as a time control.

4.2.4. Statistical analysis

Data were expressed as means ± standard error in grams tension and percentage of the maximum response of the control CRC. The maximum responses recorded, pEC_{50} values of the agonist response in the absence or presence of an antagonist were compared using

either a Student's t-test or one-way ANOVA, followed by a Bonferroni's post test. CRCs were compared using two-way-ANOVA with a Bonferroni post-test. Nonlinear regression was performed to fit sigmoidal-curves (variable slope) on mean data of responses in grams and percentage of the maximum response of the control CRC. Linear regression was performed to determine the pA_2 from the X-intercept of the Schild plot. When a single concentration of antagonist had no effect, or there was a significant reduction in the maximum response obtained, a pK_B was calculated from the remaining concentration(s) of antagonist.

4.3. Results

4.3.1. Agonist responses

4.3.1.1. $\alpha_{1A/B}$ -KO

In the α_{1AB}-KO, the agonist responses to phenylephrine (α_1-AR non selective agonist), A-61603 (α_{1A}-AR selective agonist) and 5-HT were compared (Figure 4.1; Table 4.1). Concentration-dependent contractions were produced in response to both phenylephrine and 5-HT. However, contractions to A-61603 were produced only at high concentrations.

Table 4.1. Comparison of agonist responses in $\alpha_{1A/B}$-KO.

Agonist	n	pEC_{50}	Maximum response (g)	Hill slope (95% CI)
PE control	3	7.6±0.11	0.23±0.03	1.4 (1.3-1.4)
A-61603 control	3	$5.5\pm0.17^{***}$	$0.10\pm0.02^{**}$	$1.2\ (1.2\text{-}1.3)^{+}$
5-HT control	3	$7.1\pm0.02^{+}$	$0.21\pm0.02^{+}$	$2.5\ (1.1\text{-}3.9)^{+}$

$^{+}p>0.05$, $^{**}p<0.01$, $^{***}p<0.001$ compared to PE control (one-way ANOVA, Bonferroni's post test).

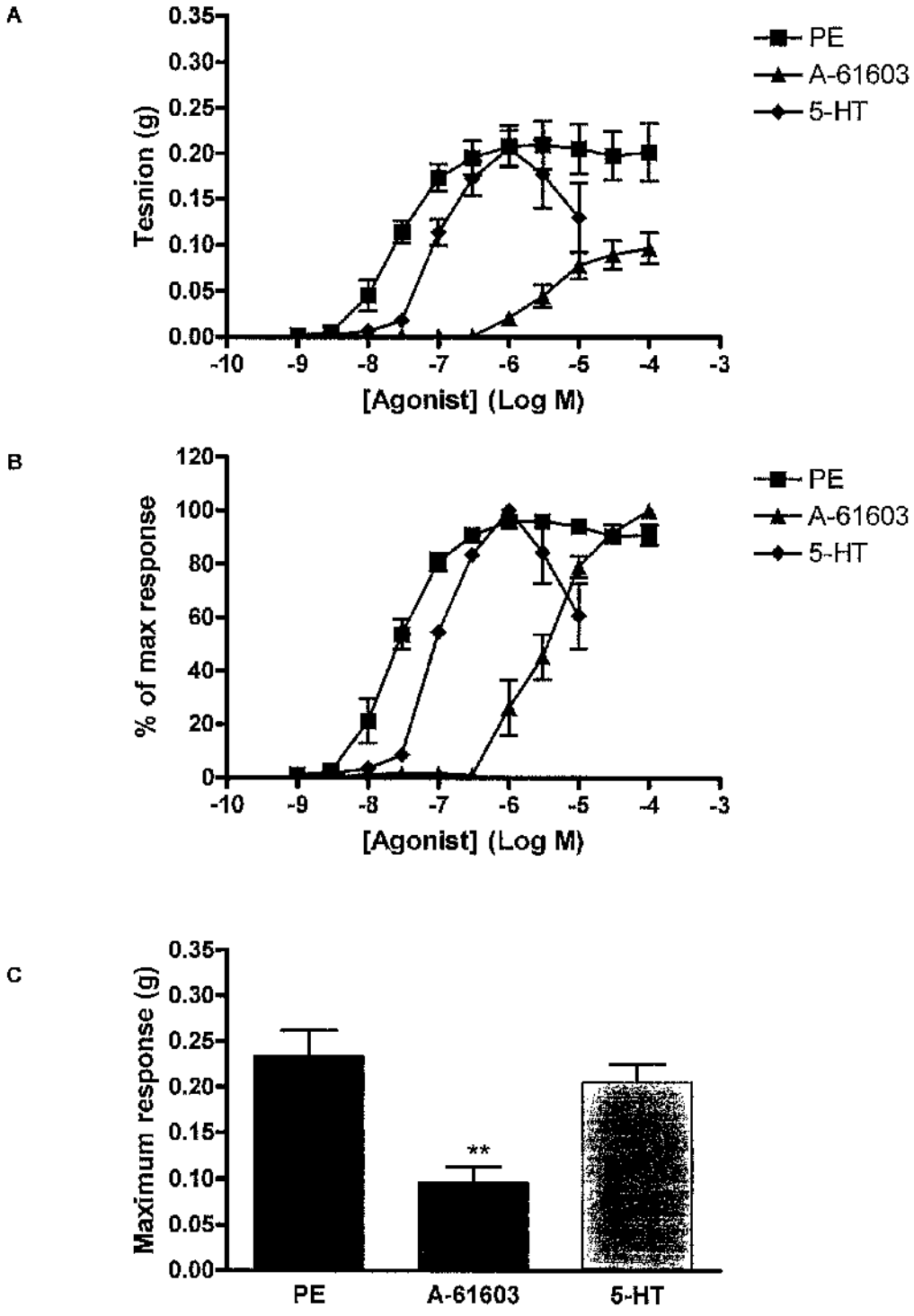

Figure 4.1. $\alpha_{1A/B}$**-KO: Comparison of agonist responses expressed as means ± S.E. in (A) grams force and (B) percentage of maximum response of the control CRC (n=3). (C) Comparison of maximum response obtained in grams tension ± S.E. ** p<0.01 compared to PE control.**

4.3.1.2. $\alpha_{1B/D}$-KO

In the $\alpha_{1B/D}$-KO, contractions to phenylephrine were produced only at high concentrations (Figure 4.2; Table 4.2). Concentration-dependent contractions to A-61603 (Figure 4.3; Table 4.3) and 5-HT (Figure 4.4; Table 4.4) were observed. The responses in the $\alpha_{1B/D}$-KO varied between agonists (Figure 4.5; Table 4.5) and the potency series differed markedly from the $\alpha_{1A/B}$-KO (Figure 4.1; Table 4.1).

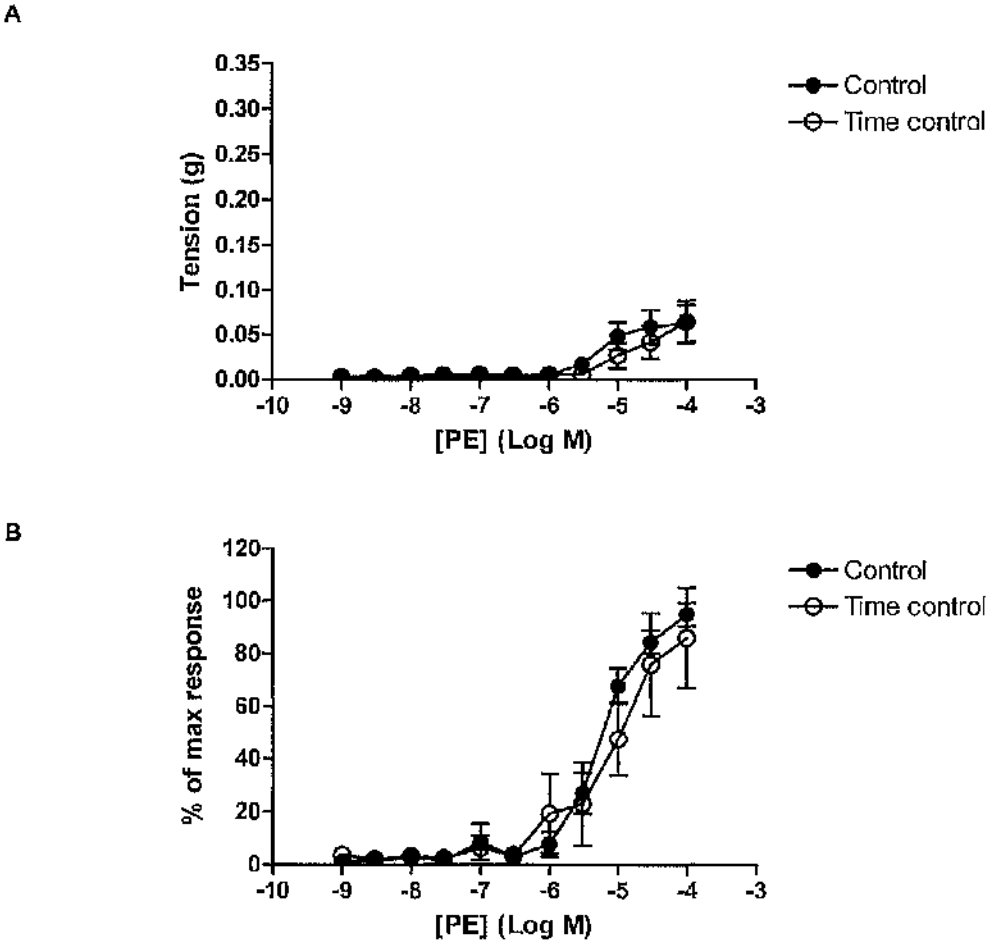

Figure 4.2. $\alpha_{1B/D}$-KO: Comparison of the phenylephrine control and time control CRCs expressed as means ± S.E. In (A) grams force and (B) percentage of maximum response of the control CRC (n≥7).

Table 4.2. Comparison of phenylephrine control and time control in $\alpha_{1B/D}$-KO.

Agonist	n	pEC_{50}	Maximum response (g)	Hill slope (95% CI)
PE control	8	5.2±0.04	0.06 ±0.02	1.3 (1.1-1.5)
PE time control	7	5.0±0.07^{+}	0.06 ±0.02^{+}	1.1 (1.0-1.3)$^{+}$

$^{+}$ **p>0.05 compared to phenylephrine control (Student's t-test).**

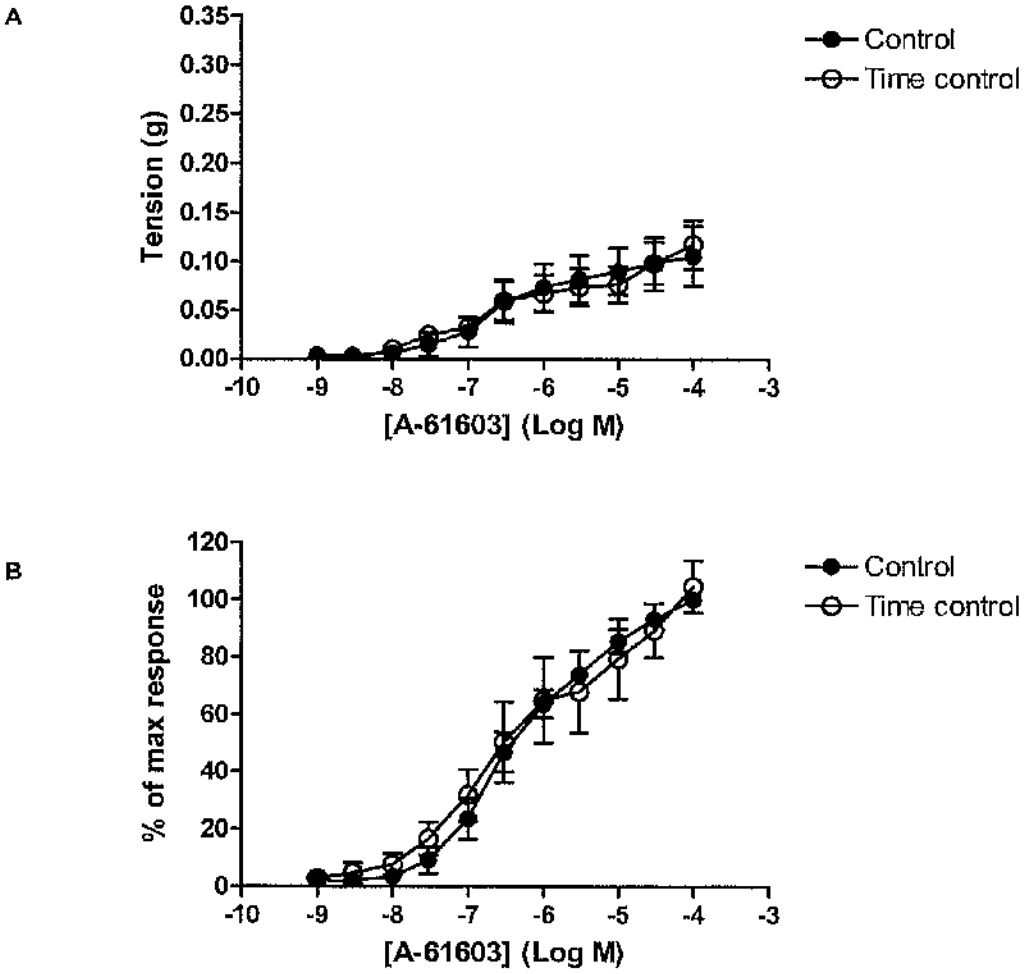

Figure 4.3. $\alpha_{1B/D}$**-KO: CRC to A-61603 for control and time control expressed as means ± S.E. in (A) grams force and (B) percentage of maximum response of the control CRC (n=7).**

Table 4.3. Comparison of A-61603 control and time control in $\alpha_{1B/D}$**-KO.**

Agonist	n	pEC_{50}	Maximum response (g)	Hill slope (95% CI)
A-61603 control	7	6.6±0.07	0.10 ±0.03	0.6 (0.5-0.7)
A-61603 time control	7	6.5±0.22^{+}	0.10±0.03^{+}	0.6 (0.5-0.7)$^{+}$

$^{+}$ **p>0.05 compared to A-61603 control (Student's t-test).**

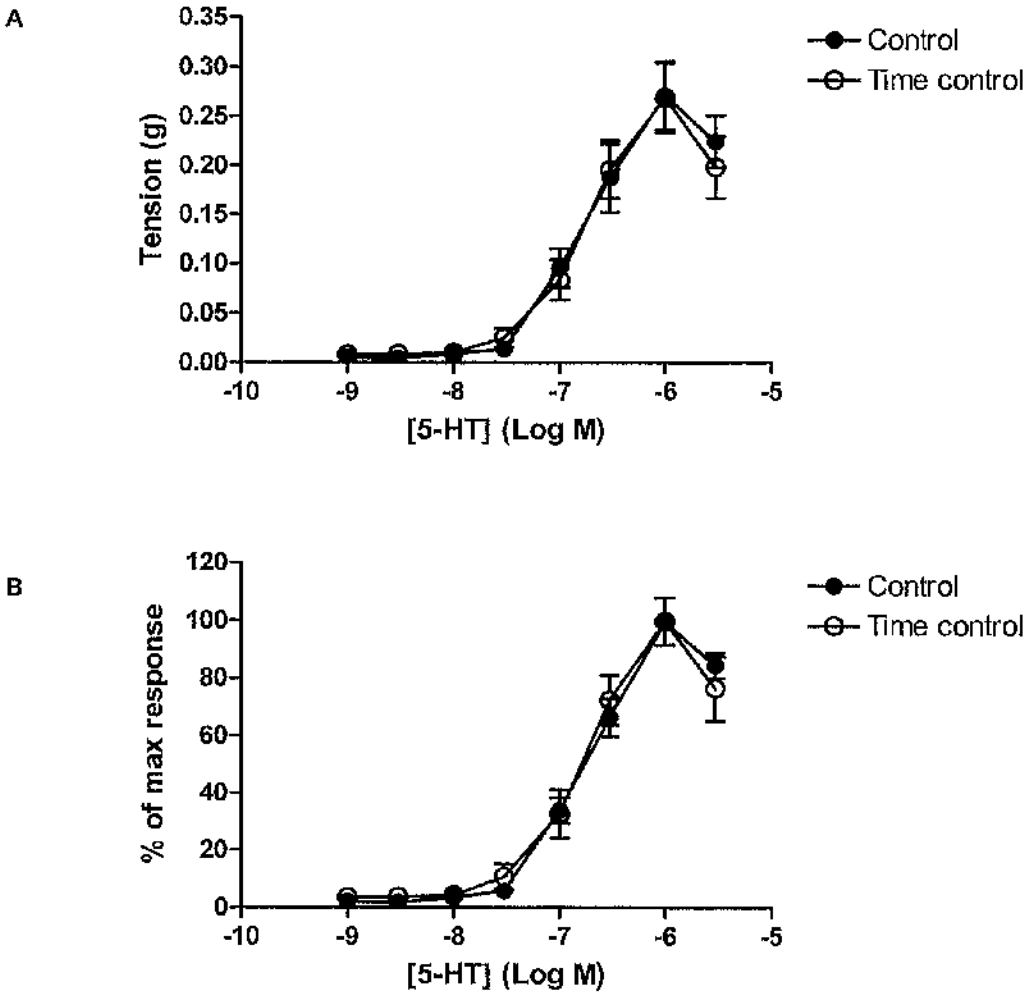

Figure 4.4. $\alpha_{1B/D}$**-KO: Comparison of 5-HT control and time control expressed as means ± S.E in (A) grams force and (B) percentage of maximum response of the control CRC. (n=7).**

Table 4.4. Comparison of 5-HT control and time control in $\alpha_{1B/D}$**-KO.**

Agonist	n	pEC_{50}	Maximum response (g)	Hill slope (95% CI)
5-HT control	7	6.8±0.07	0.26±0.03	1.4 (1.3-1.4)
5-HT time control	7	6.8±0.12^{+}	0.27±0.04^{+}	1.3 (1.2-1.4)$^{+}$

$^{+}$**p>0.05 compared to 5-HT control (Student's t-test).**

A

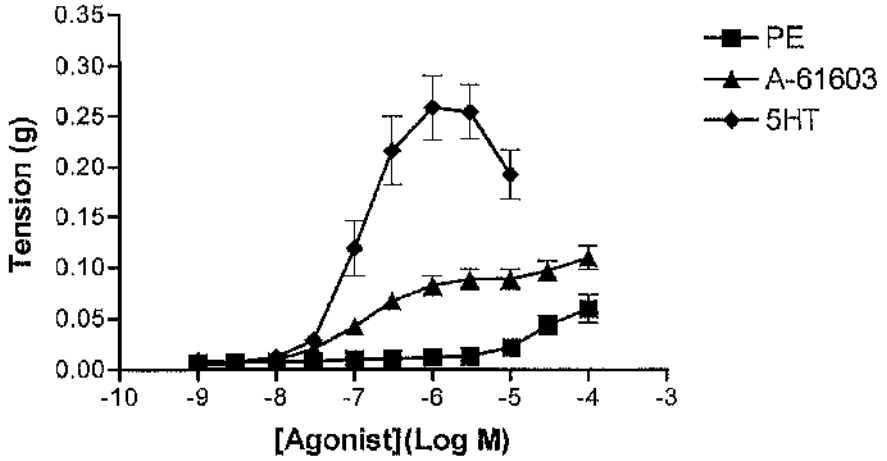

B

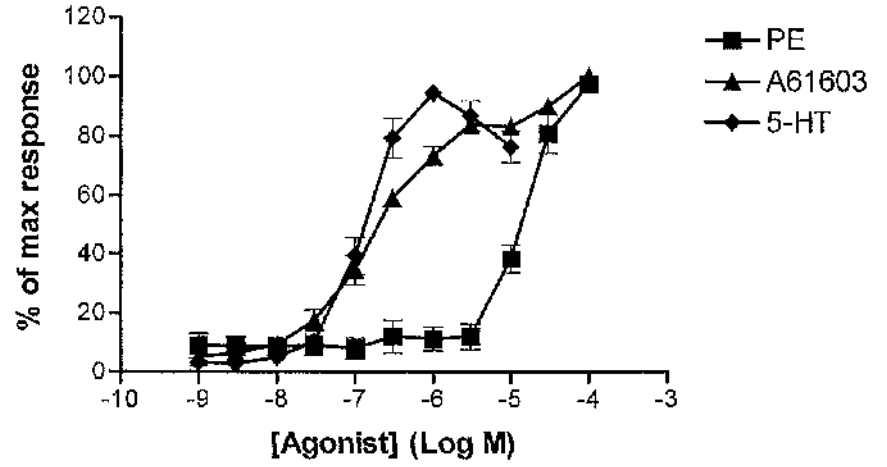

C

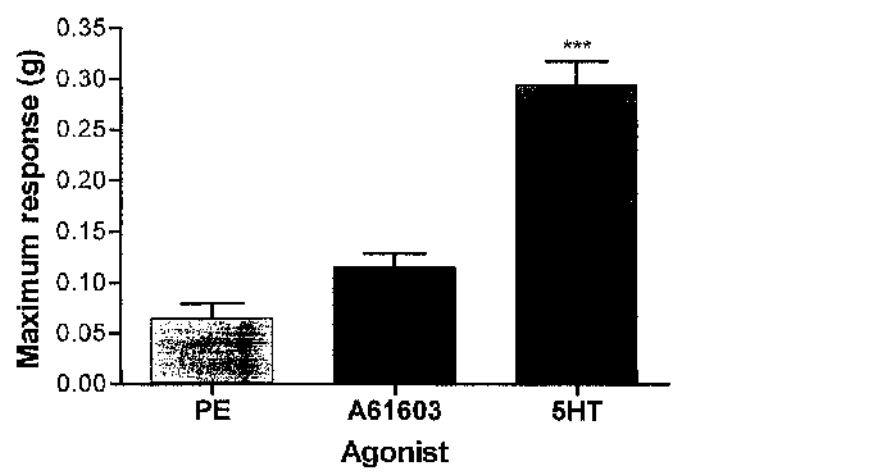

Figure 4.5. $\alpha_{1B/D}$**-KO: Comparison of agonist responses expressed as means ± S.E in (A) grams force and (B) percentage of maximum response of the control CRC (n≥10). (C) Comparison of maximum response obtained in grams tension ± S.E. *** p<0.001 compared to PE control.**

Table 4.5. Comparison of agonist responses in the $\alpha_{1B/D}$-KO.

Agonist	n	pEC_{50}	Maximum response (g)	Hill slope (95% CI)
PE control	8	5.2±0.04	0.06 ±0.02	1.3 (1.1-1.5)
A-61603 control	7	6.6±0.07***	0.10 ±0.03^{+}	0.6 (0.5-0.7)*
5-HT control	7	6.8±0.07***	0.26±0.03***	1.4 (1.3-1.4)$^{-}$

$^{+}$p>0.05, * p<0.05, *** p<0.001 compared to PE control (one-way ANOVA, Bonferroni's post test).

4.3.1.3. α_{1D}-KO

In the α_{1D}-KO, reproducible concentration-dependent contractions were obtained in response to phenylephrine (Figure 4.6; Table 4.6) and A-61603 (Figure 4.7; Table 4.7). For both agonists no differences in the maximum response obtained or sensitivity were observed.

A

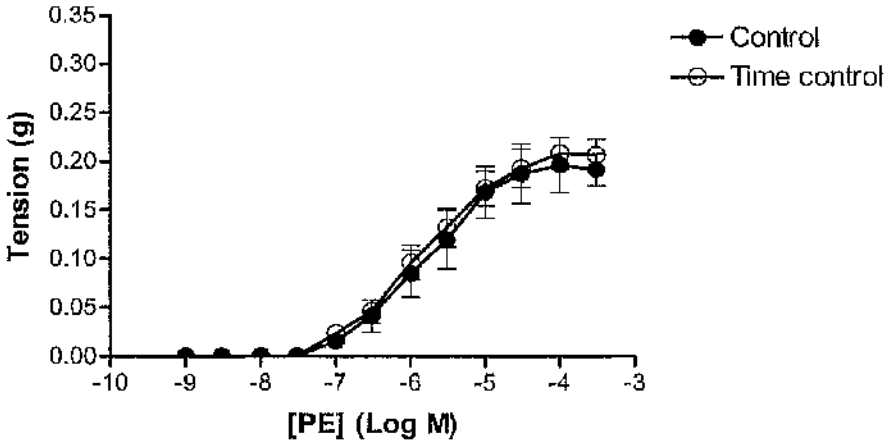

B

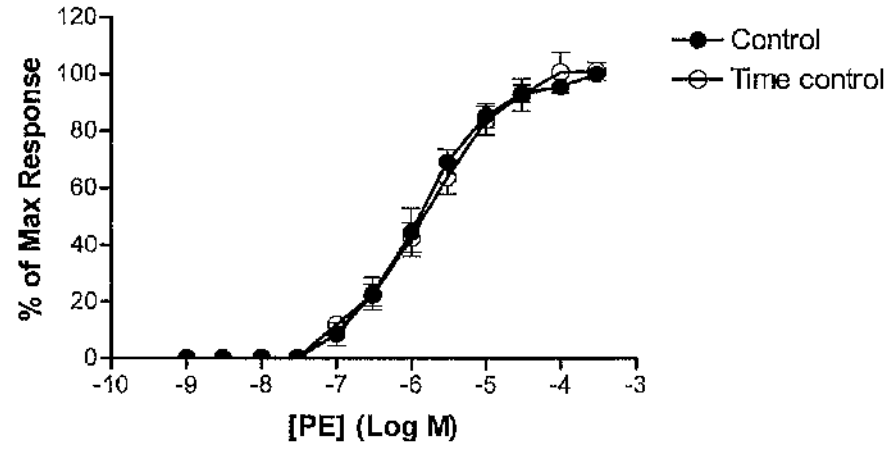

Figure 4.6. α_{1D}-KO: CRC to phenylephrine control and time control expressed as means ± S.E. in (A) grams force and (B) percentage of maximum response of the control CRC (n=12).

Table 4.6. Comparison of phenylephrine control and time control in α_{1D}-KO.

Agonist	n	pEC_{50}	Maximum response (g)	Hill slope (95% CI)
PE control	12	5.6±0.06	0.22±0.02	0.9 (0.7-1.2)
PE time control	12	5.6±0.13^{+}	0.21±0.02^{+}	0.8 (0.7-0.9)$^{+}$

$^{+}$ **p>0.05 compared to phenylephrine control (Student's t-test).**

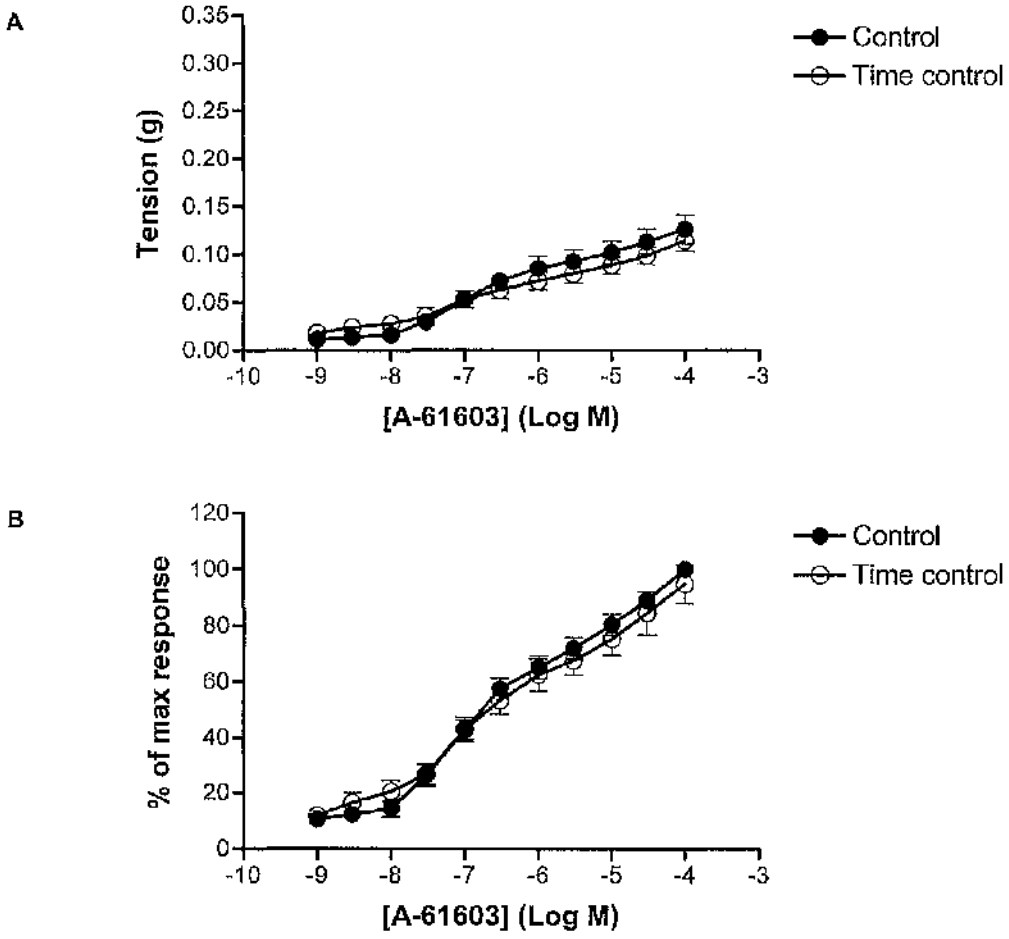

Figure 4.7. α_{1D}**-KO: CRC to A-61603 for control and time control expressed as means ± S.E. in (A) grams force and (B) percentage of maximum response of the control CRC (n=10).**

Table 4.7. Comparison of A-61603 control and time control in α_{1D}**-KO.**

Agonist	n	pEC_{50}	Maximum response (g)	Hill slope (95% CI)
A-61603 control	10	6.9±0.06	0.13±0.01	0.5 (0.4-0.7)
A-61603 time control	10	6.9±0.17^{+}	0.11±0.01^{+}	0.3 (0.3-0.3)$^{+}$

+ p>0.05 compared to A-61603 control (Student's t-test).

4.3.1.4. α_{1B}-KO

In the α_{1B}-KO, concentration-dependent contractions were produced to phenylephrine (Figure 4.8; Table 4.8) and A-61603 (Figure 4.9; Table 4.9). For both agonists no differences in the maximum response obtained or sensitivity were observed.

A

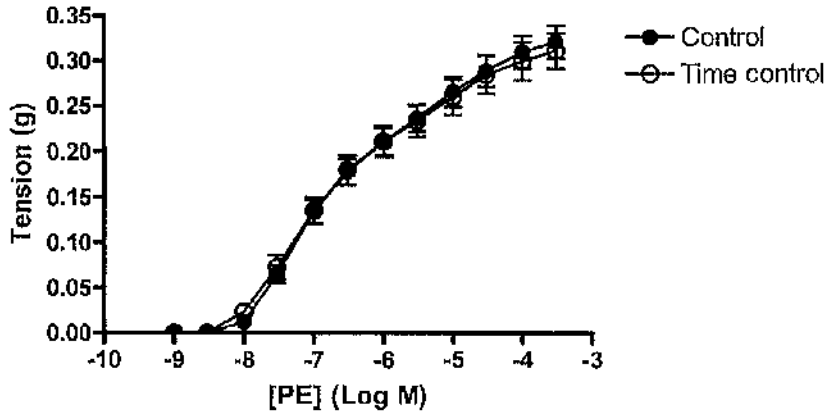

B

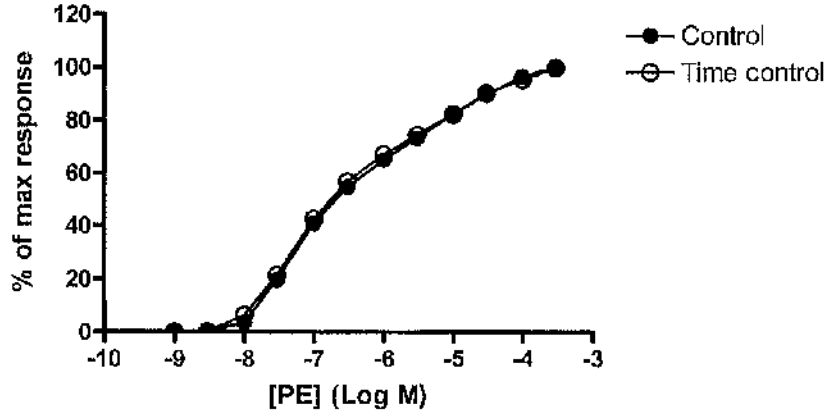

Figure 4.8. α_{1B}-KO: CRC to phenylephrine for control and time control expressed as means ± S.E. in (A) grams force and (B) percentage of maximum response of the control CRC (n=9).

Table 4.8. Comparison of phenylephrine control and time control in α_{1B}-KO.

Agonist	n	pEC_{50}	Maximum response (g)	Hill slope (95% CI)
PE control	9	6.9±0.09	0.32 ±0.02	0.6 (0.5-0.6)
PE time control	9	6.9±0.10[+]	0.31±0.02[+]	0.6 (0.5-0.6)[+]

[+] **p>0.05 compared to phenylephrine control (Student's t-test).**

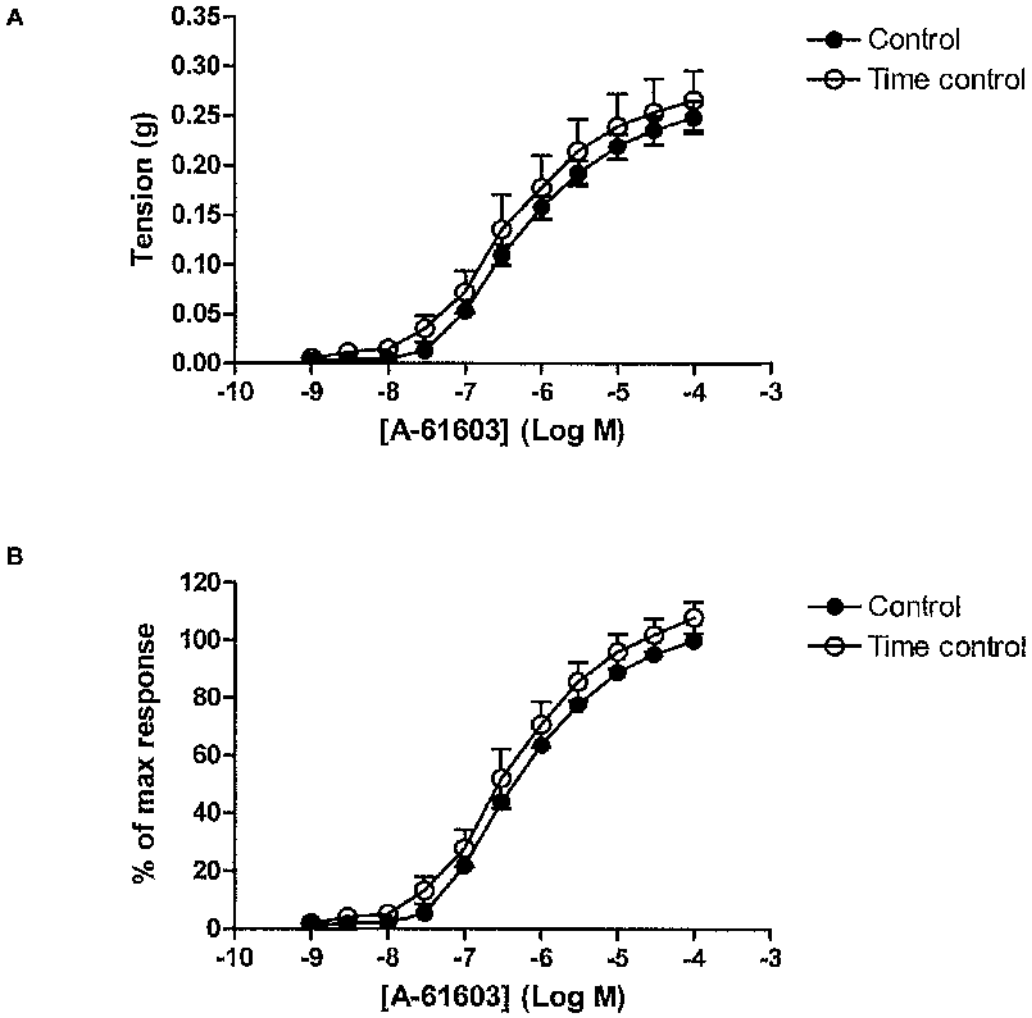

Figure 4.9. α_{1B}-KO: CRC to A-61603 for control and time control expressed as means ± S.E. in (A) grams force and (B) percentage of maximum response of the control CRC (n=7).

Table 4.9. Comparison of A-61603 control and time control in α_{1D}-KO.

Agonist	n	pEC_{50}	Maximum response (g)	Hill slope (95% CI)
A-61603 control	7	6.6±0.11	0.25 ±0.01	0.8(0.7-0.8)
A-61603 time control	7	6.7±0.21^{+}	0.27±0.03^{+}	0.7 (0.7-0.7)$^{+}$

$^{+}$ p>0.05 compared to A-61603 control (Student's t-test).

4.3.1.5. Comparison of agonist responses in WT mouse and knockouts

Phenylephrine-induced response

Phenylephrine produced concentration-dependent contractions in all mouse strains with the exception of the $\alpha_{1B/D}$-KO, where contractions were produced only in response to high concentrations of the agonist (Figure 4.10, Table 4.10). Compared to the WT mouse the maximum response obtained to phenylephrine was not significantly different in the α_{1B}-KO and $\alpha_{1A/B}$-KO but was reduced in the α_{1D}-KO. The phenylephrine-induced response was significantly smaller in the $\alpha_{1B/D}$-KO than in the other four strains of mice. The $\alpha_{1A/B}$-KO showed the highest sensitivity to phenylephrine followed by the α_{1B}-KO and the WT mouse with the α_{1D}-KO and the $\alpha_{1B/D}$-KO showing significantly lower sensitivity.

Table 4.10. Comparison of phenylephrine response in the WT mouse and knockouts.

Mouse	n	pEC_{50}	Maximum response (g)	Hill slope (95% CI)
WT	7	6.6±0.05	0.27±0.03	0.6 (0.5-0.7)
α_{1B}-KO	9	6.9±0.10^{+}	0.32±0.02^{+}	0.6 (0.5-0.6)$^{+}$
α_{1D}-KO	12	5.6±0.06***	0.22±0.02**	0.9 (0.7-1.2)$^{+}$
$\alpha_{1B/D}$-KO	8	5.0±0.07***	0.06 ±0.02***	1.3 (1.1-1.5)***
$\alpha_{1A/B}$-KO	3	7.6±0.11***	0.23±0.03^{+}	1.4 (1.3-1.4)***

$^{+}$ p>0.05, ** p<0.01, *** p<0.001 compared to WT mouse (one-way ANOVA, Bonferroni's post test).

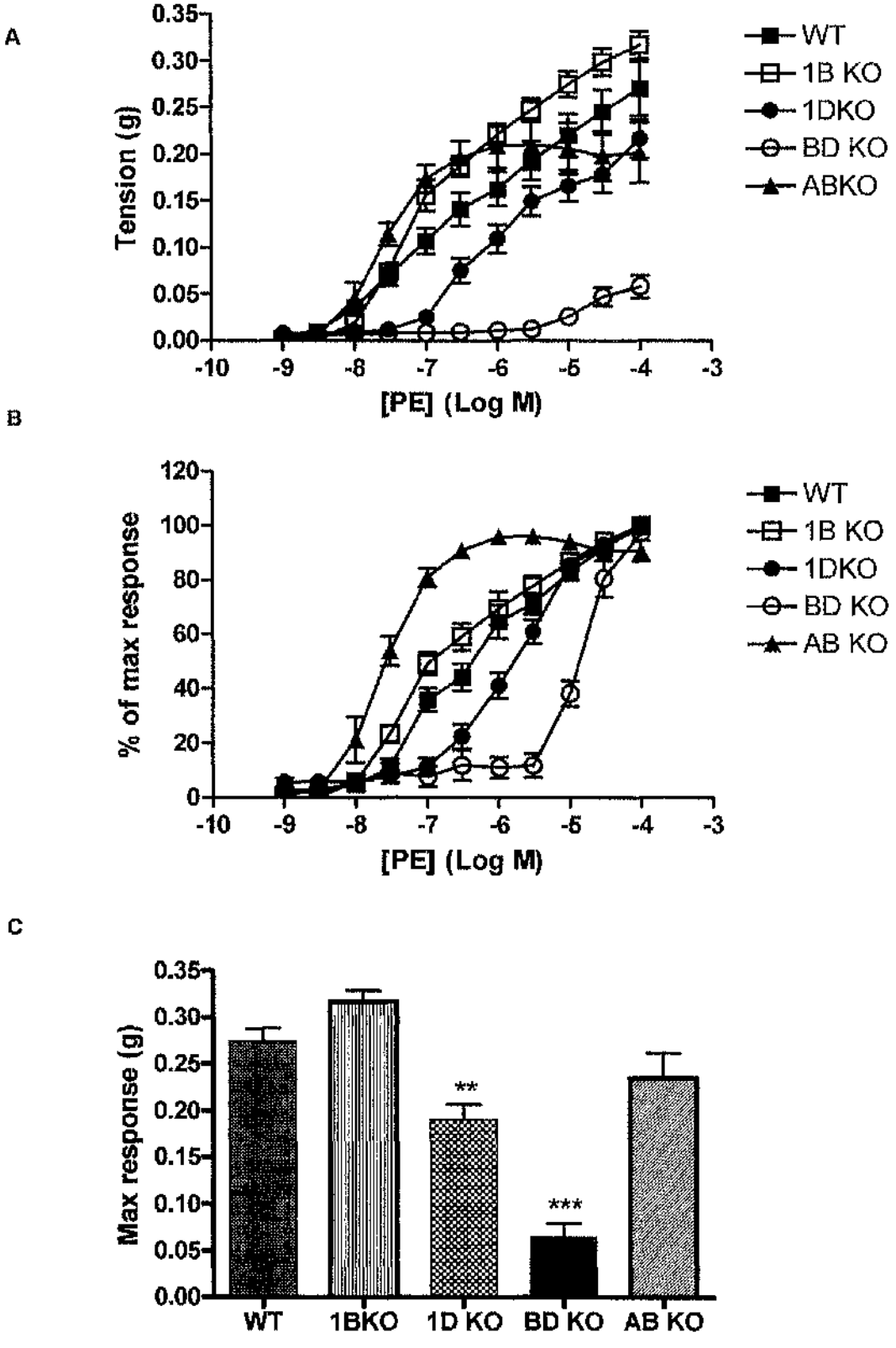

Figure 4.10. Comparison WT mouse and knockouts: phenylephrine response expressed as mean ± S.E. in (A) grams tension and (B) percentage of maximum response of the control CRC (n≥10, with exception of $\alpha_{1A/B}$-KO (n=3)). (C) Comparison of maximum response obtained to phenylephrine in grams tension ± S.E. ** p<0.01 and *** p<0.001.

A-61603-induced response

A-61603 produced concentration-dependent contractions in all strains of mice, with the exception of the $\alpha_{1A/B}$-KO, in which contractions were produced only at high concentrations of the agonist (Figure 4.11; Table 4.11). The maximum responses recorded for A-61603 were not significantly different in the WT mouse and α_{1B}-KO. Similarly, the maximum responses obtained to A-61603 were not significantly different in the α_{1D}-KO, $\alpha_{1B/D}$-KO and $\alpha_{1A/B}$-KO, however, the efficacy in these strains was significantly reduced compared to the WT mouse and α_{1B}-KO. Compared to the WT mouse the sensitivity to A-61603 was not significantly different in the $\alpha_{1A/B}$-KO but sensitivity was significantly higher in the α_{1B}-KO, α_{1D}-KO and $\alpha_{1B/D}$-KO.

Table 4.11. Comparison of the A-61603 response in the WT mouse and knockouts.

Mouse	n	pEC_{50}	Maximum response (g)	Hill slope (95% CI)
WT	10	6.0±0.06	0.28±0.02	0.7 (0.5-0.9)
α_{1B}-KO	7	6.6±0.11***	0.25 ±0.01^{+}	0.8(0.7-0.8)$^{+}$
α_{1D}-KO	10	6.9±0.06***	0.13±0.01***	0.5 (0.4-0.7)$^{+}$
$\alpha_{1B/D}$-KO	7	6.6±0.07***	0.10 ±0.03***	0.6 (0.5-0.7)$^{+}$
$\alpha_{1A/B}$-KO	3	5.5±0.17^{+}	0.10±0.02***	1.2 (1.2-1.3)**

$^{+}$ p>0.05, ** p<0.01, *** p<0.001 compared to WT mouse (one-way ANOVA, Bonferroni's post test).

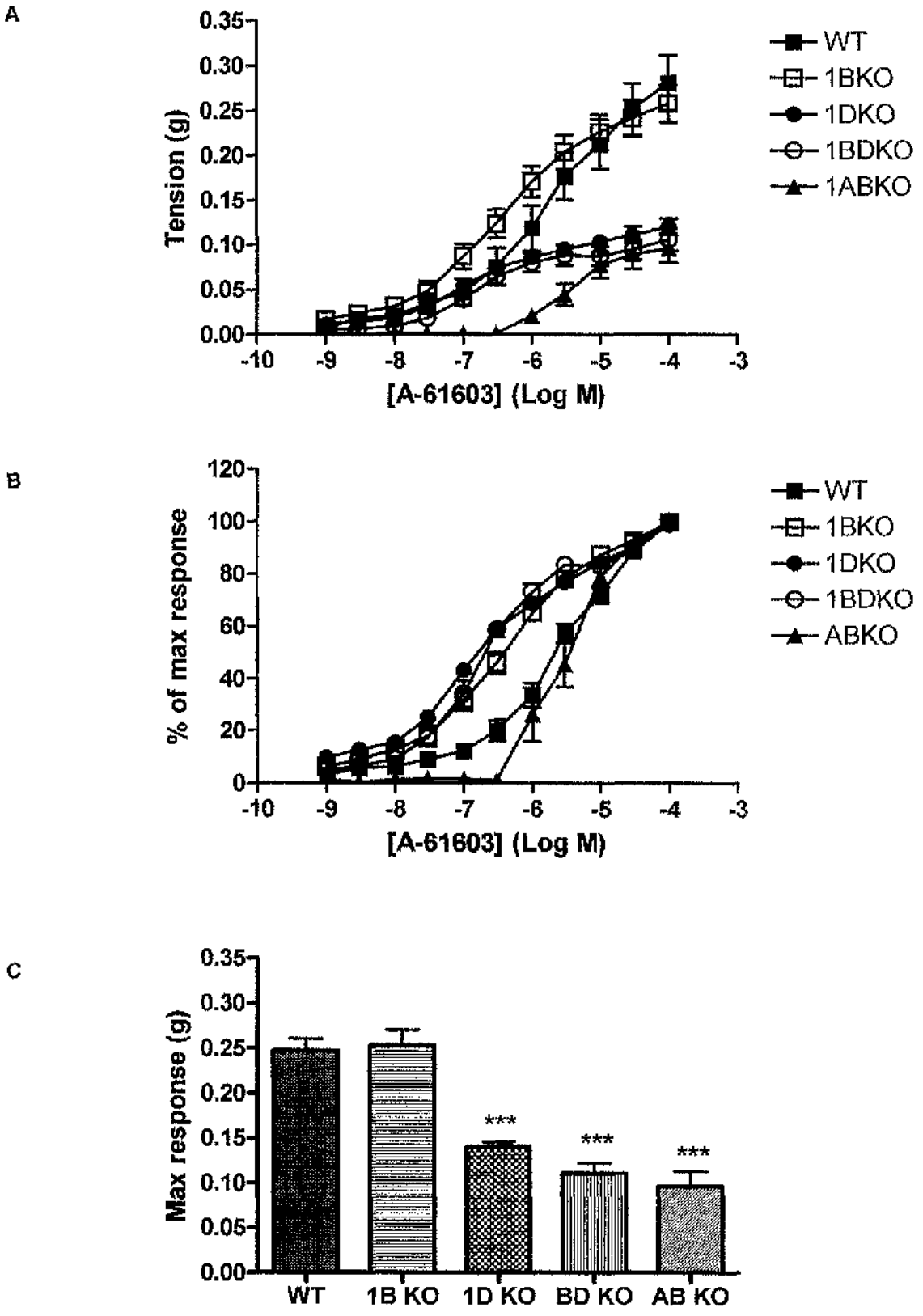

Figure 4.11. Comparison of WT mouse and knockouts: A-61603 response expressed as mean ± S.E. in (A) grams tension and (B) percentage of maximum response of the control CRC. (C) Comparison of maximum response obtained to A-61603 in grams tension ± S.E. (n≥10, with exception of $\alpha_{1A/B}$-KO (n=3)) *** p<0.001.

4.3.2. Antagonist data

4.3.2.1. Phenylephrine-induced response

Deighan (2002;Deighan *et al.*, 2005) obtained affinity estimates for prazosin, BMY 7378 and 5-methylurapidil against the phenylephrine-induced response. These values have been included in Table 4.32. for completeness.

Prazosin

Prazosin potently antagonised the phenylephrine-induced response in the $\alpha_{1B/D}$-KO (Figure 4.12; Table 4.12). Compared to the control CRC, the maximum response to phenylephrine was significantly reduced in the presence of prazosin 10 nM, therefore, it was not possible to calculate a pEC_{50} or a pK_B.

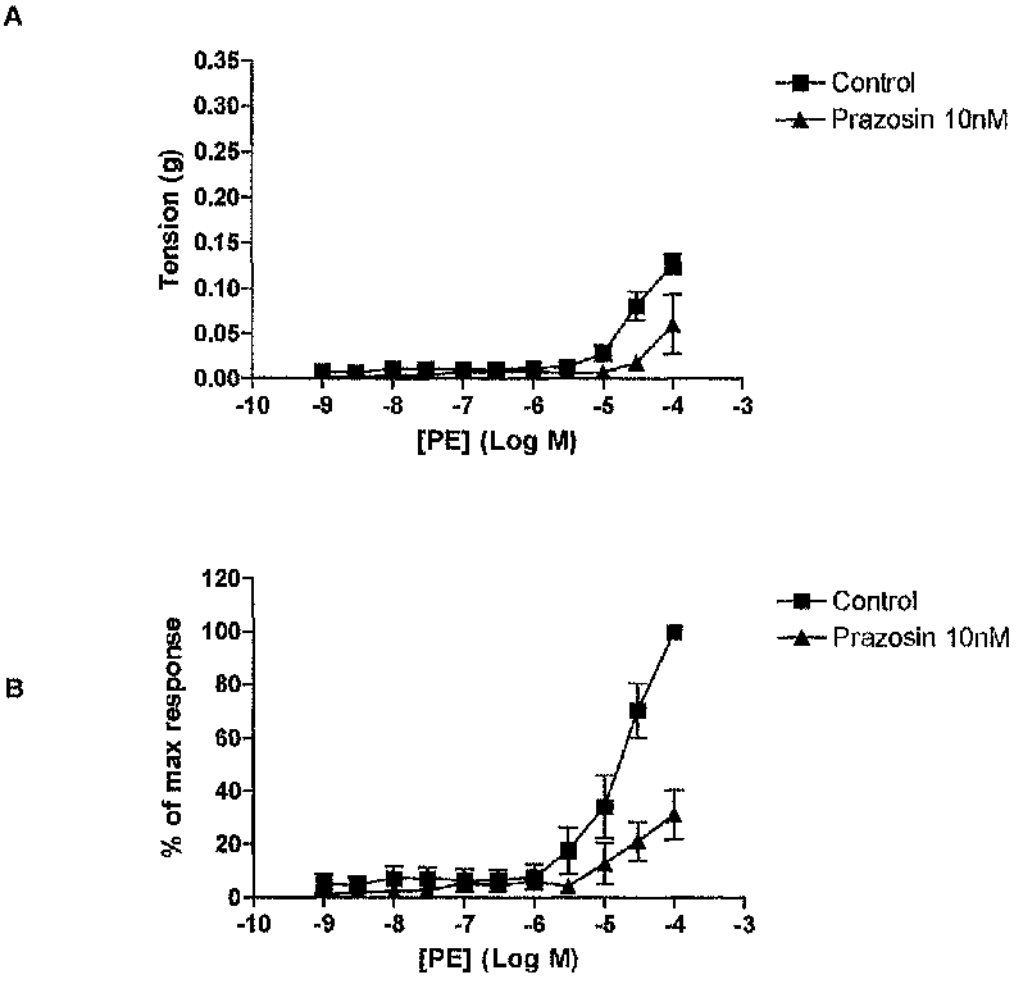

Figure 4.12. α_{1BD}-KO: CRC to phenylephrine in the presence of prazosin expressed as means ± S.E. in (A) grams tension and (B) percentage of maximum response of the control CRC (n=6).

Table 4.12. Phenylephrine response in presence of prazosin in $\alpha_{1B/D}$-KO.

Agonist	n	pEC_{50}	Maximum response (g)	Hill slope (95% CI)
PE control	6	4.8	0.13±0.01	1.2 (1.1-1.3)
Prazosin 10nM	6	N.D.	0.06±0.03***	0.9 (0.3-1.5)*

* p>0.05, *** p=0.001 compared to PE control (Student's t-test).

In the α_{1D}-KO, the phenylephrine-induced response was potently antagonised by prazosin (Figure 4.13; Table 4.13). The size of the response to phenylephrine was significantly reduced in the presence of prazosin 1 nM and 10 nM, therefore pEC_{50} values could not be calculated. A pK_B of 10.6 was calculated at prazosin 0.1nM.

A

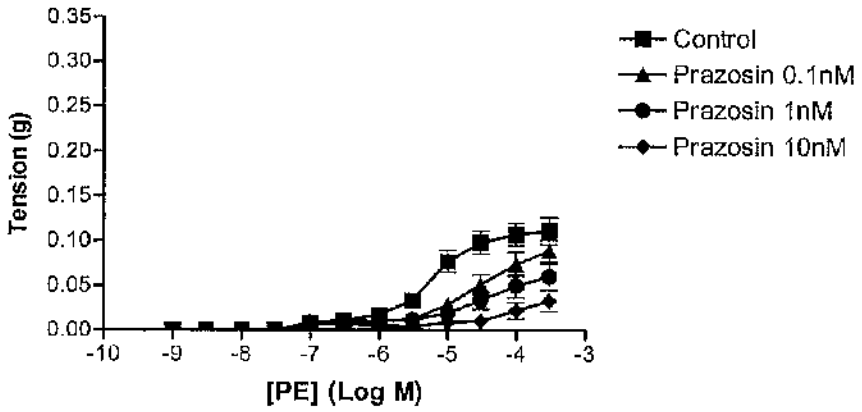

B

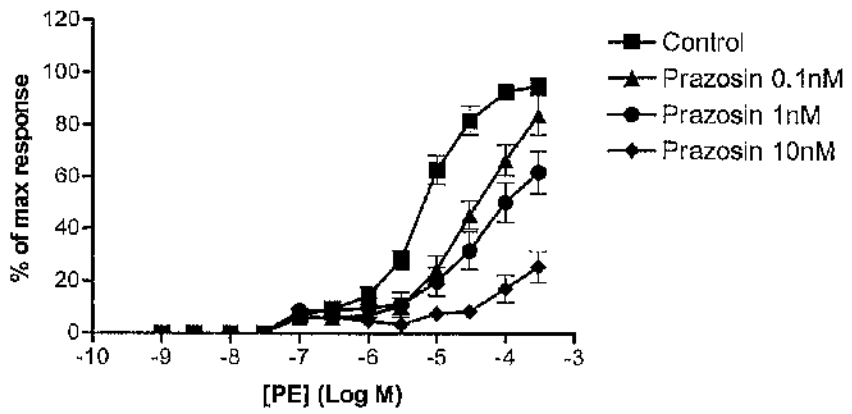

Figure 4.13. α_{1D}-KO: CRC to phenylephrine in the presence of prazosin expressed as means ± S.E. in (A) grams tension and (B) percentage of maximum response of the control CRC (n≥7).

Table 4.13. Phenylephrine response in presence of prazosin in α_{1D}-KO.

Agonist	n	pEC_{50}	Maximum response (g)	Hill slope (95% CI)
PE control	11	5.1±0.07	0.12±0.02	1.1 (0.8-1.3)
Prazosin 0.1nM	7	4.5±0.11***	0.09±0.01**	0.8 (0.5-1.1)$^{+}$
Prazosin 1nM	7	N.D.	0.07±0.01***	0.6 (0.3-0.9)$^{+}$
Prazosin 10nM	8	N.D.	0.04±0.01***	0.6 (0.1-1.0)$^{+}$

$^{+}$ p>0.05, ** p<0.01, *** p<0.001 compared to PE control (one-way ANOVA, Bonferroni's post test).

5-methylurapidil

5-methylurapidil acted competitively against phenylephrine in the α_{1D}-KO (Figure 4.14; Table 4.14). Schild regression analysis was performed for 5-methylurapidil against phenylephrine and produced a pA_2 of 8.1, with a slope of 0.8 (0.4-1.3).

Table 4.14. Phenylephrine response in presence of 5-methylurapidil in α_{1D}-KO.

Agonist	n	pEC_{50}	Maximum response (g)	Hill slope (95% CI)
PE control	7	5.6±0.18	0.19±0.05	1.4 (1.2-1.6)
5-MeU 0.1 µM	7	5.1±0.14*	0.19±0.02^{+}	1.0 (0.5-1.7)$^{+}$
5-MeU 0.3 µM	7	4.7±0.25*	0.15±0.03^{+}	1.3 (1.2-1.4)$^{+}$
5-MeU 1 µM	7	4.6±0.12*	0.15±0.02^{+}	1.3 (1.2-1.4)$^{+}$

$^{+}$p>0.05, * p<0.05 compared to PE control (one-way ANOVA, Bonferroni's post test).

A

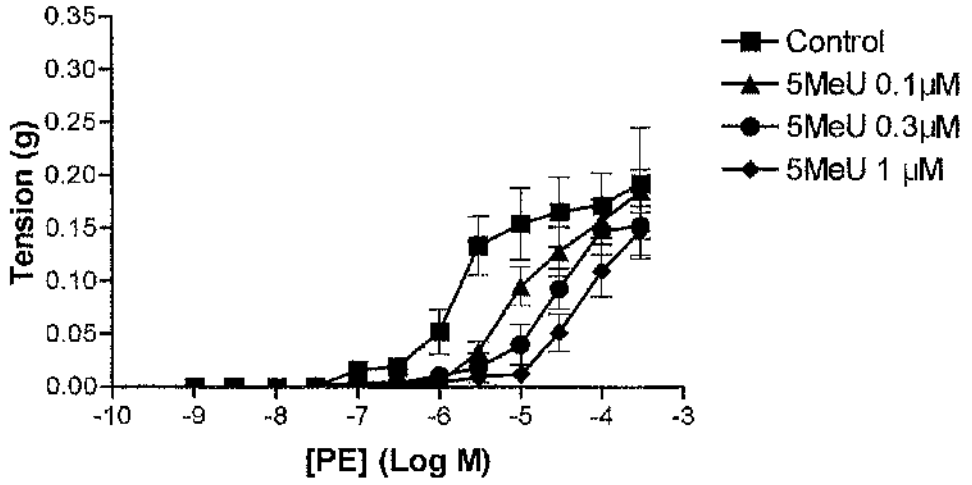

B

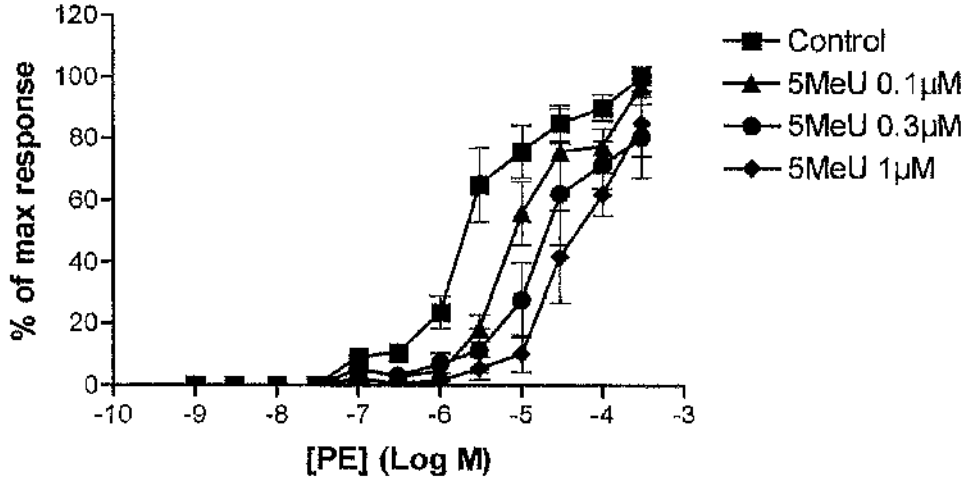

C

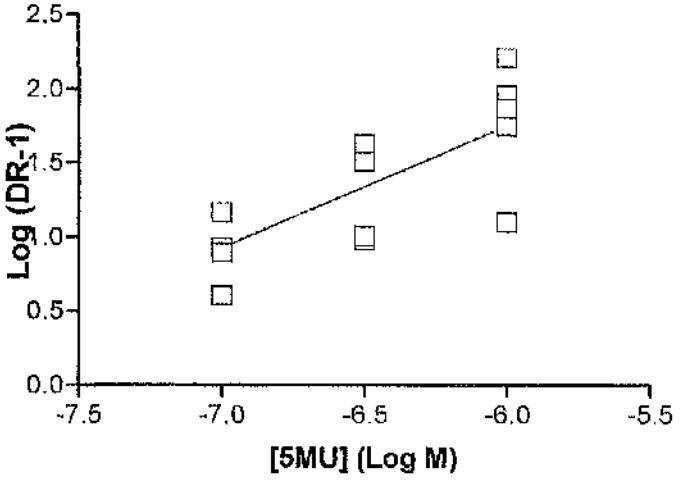

Figure 4.14. α_{1D}-KO: CRC to phenylephrine in the presence of 5-methylurapidil expressed as means ± S.E. in (A) grams tension and (B) percentage of maximum response of the control CRC (n=7).

RS100 329

In the α_{1D}-KO the phenylephrine-induced response was antagonised by RS100 329 10nM and 0.1 μM (Figure 4.15; Table 4.15). In the presence of RS100 329 0.1 μM a maximum response was not obtained at the highest concentration of phenylephrine used, therefore a pEC_{50} was not calculated. A pK_B of 9.1 was calculated at RS100 329 10 nM.

A

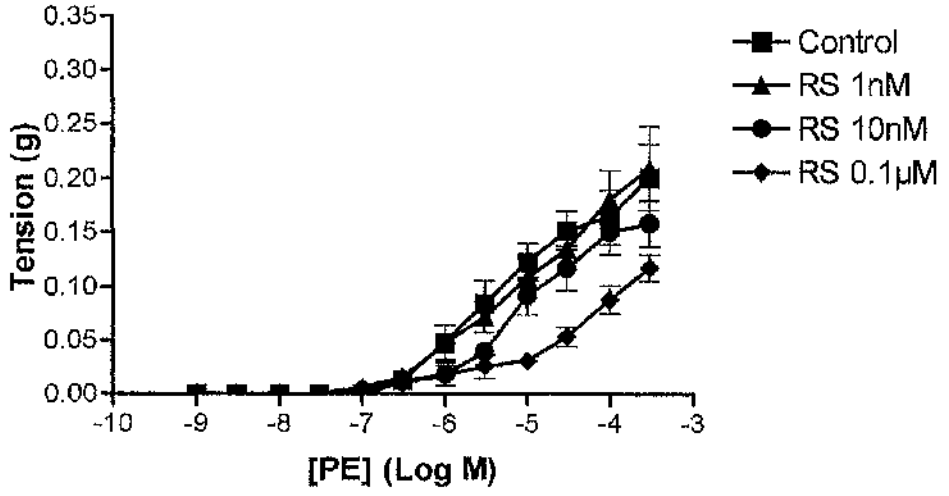

B

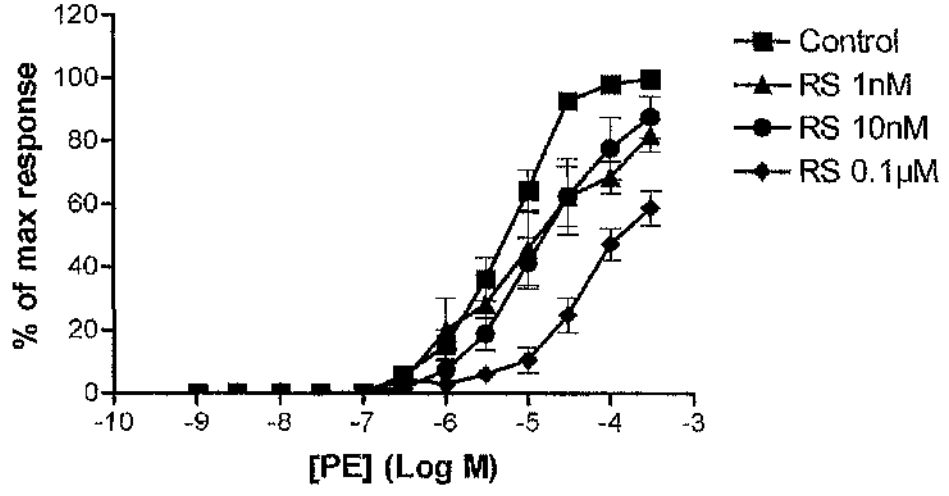

Figure 4.15. α_{1D}-KO: CRC to phenylephrine in the presence of RS100 329 expressed as means ± S.E. in (A) grams tension and (B) percentage of maximum response of the control CRC (n≥7).

Table 4.15. Phenylephrine response in presence of RS100 329 in α_{1D}-KO.

Agonist	n	pEC_{50}	Maximum response (g)	Hill slope (95% CI)
PE control	8	5.4±0.09	0.20±0.03	1.2 (0.8-1.5)
RS100 329 1nM	8	4.7±0.29^{+}	0.21±0.04^{+}	0.9 (0.7-1.2)$^{+}$
RS100 329 10nM	6	4.6±0.16*	0.16±0.02^{+}	1.3 (1.1-1.5)$^{+}$
RS100 329 0.1 μM	8	N.D.	0.12±0.01*	0.8 (0.5-1.2)$^{+}$

$^{+}$p>0.05, * p<0.05 compared to PE control (one-way ANOVA, Bonferroni's post test).

BMY 7378

In the $\alpha_{1A/B}$-KO, BMY 7378 10 nM caused a rightward displacement of the phenylephrine-induced response (Figure 4.16; Table 4.16). A pK_B of 9.0 was calculated for BMY 7378 10 nM against the phenylephrine-induced response.

A

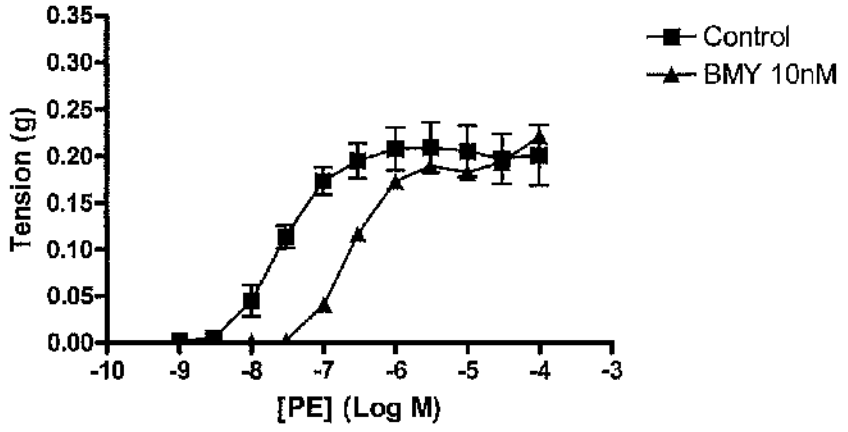

B

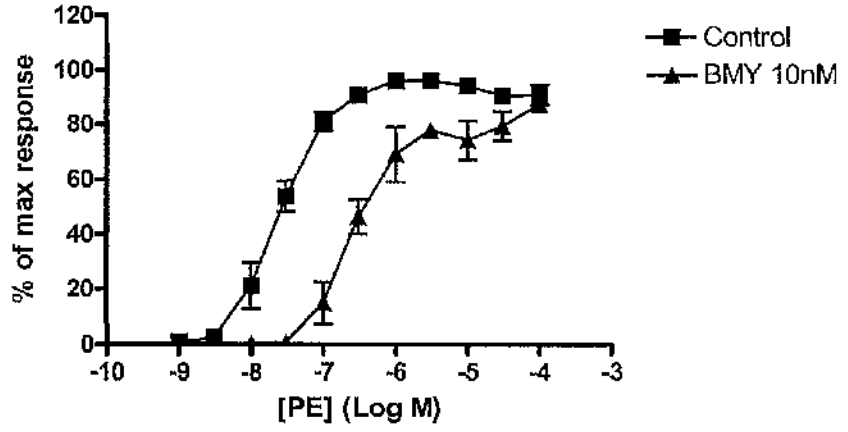

Figure 4.16. $\alpha_{1A/B}$**-KO: CRC to phenylephrine in the presence of BMY 7378 expressed as means ± S.E. in (A) grams tension and (B) percentage of maximum response of the control CRC (n=3).**

Table 4.16. Phenylephrine response in presence of BMY 7378 in $\alpha_{1A/B}$**-KO.**

Agonist	n	pEC_{50}	Maximum response (g)	Hill slope (95% CI)
PE control	3	7.6±0.11	0.23±0.03	1.4 (1.3-1.4)
BMY 7378 10nM	3	6.4±0.14***	0.22±0.03+	1.5 (1.2-1.7)+

+ p>0.05, *** p<0.001 compared to PE control (Student's t-test).

In the α_{1D}-KO a rightward shift in the phenylephrine CRC was observed in the presence of BMY 7378 0.1 μM (Figure 4.17; Table 4.17). A pK_B of 7.0 was calculated for BMY 7378 at 0.1 μM.

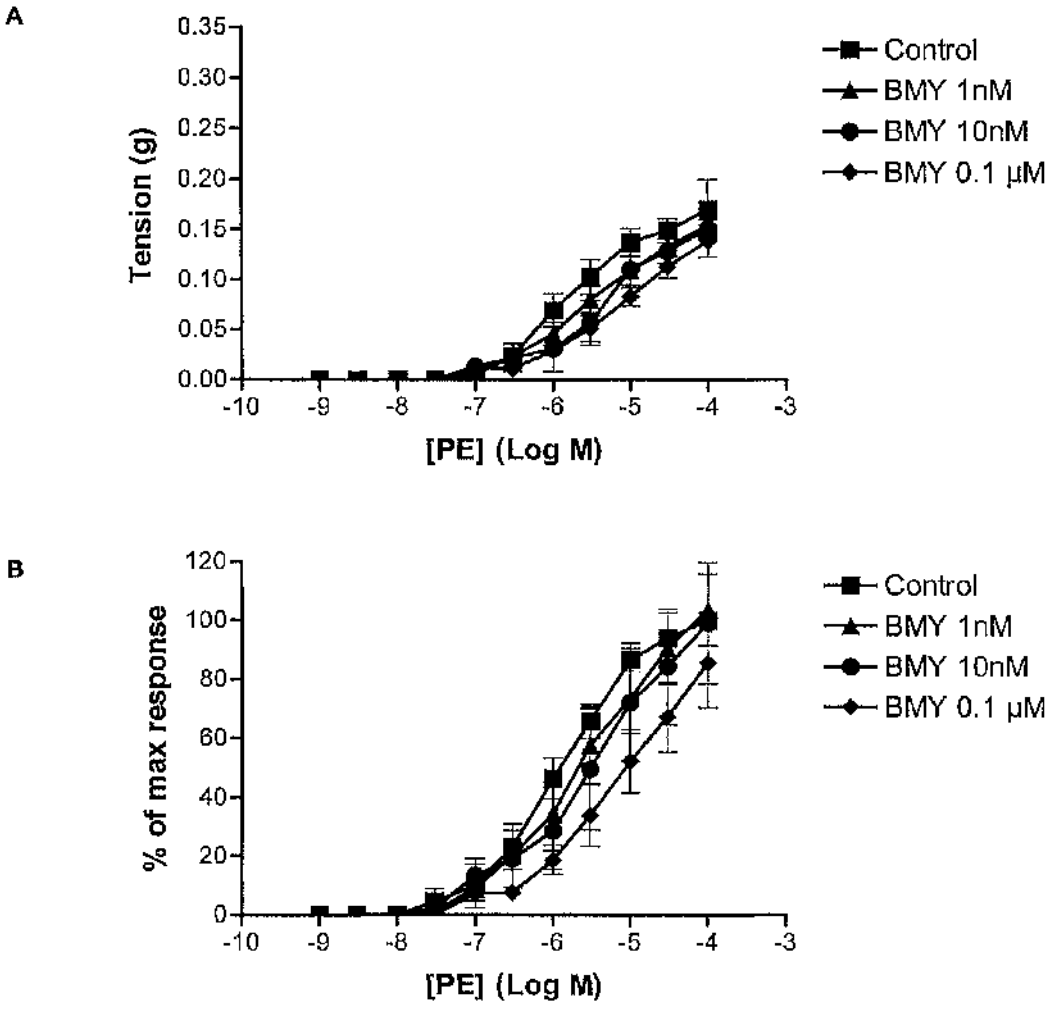

Figure 4.17. α_{1D}**-KO: CRC to phenylephrine in the presence of BMY 7378 expressed as means ± S.E. in (A) grams tension and (B) percentage of maximum response of the control CRC (n≥6).**

Table 4.17. Phenylephrine response in presence of BMY 7378 in α_{1D}**-KO.**

Agonist	n	pEC_{50}	Maximum response (g)	Hill slope (95% CI)
PE control	8	6.0±0.17	0.17±0.03	0.9 (0.9-1.0)
BMY 7378 1nM	7	$5.6\pm0.32^{+}$	$0.15\pm0.01^{+}$	$0.7\ (0.6\text{-}0.7)^{+}$
BMY 7378 10nM	6	$5.6\pm0.49^{+}$	$0.15\pm0.01^{+}$	$0.8\ (0.6\text{-}0.7)^{+}$
BMY 7378 0.1µM	7	$4.8\pm0.23^{**}$	$0.14\pm0.02^{+}$	$0.7\ (0.6\text{-}0.7)^{+}$

$^{+}$ p>0.05, **p<0.01 compared to PE control (one-way ANOVA, Bonferroni's post test).

4.3.2.2. A-61603-induced response

Prazosin

In the $\alpha_{1B/D}$-KO prazosin 10nM antagonised the A-61603-induced response (Figure 4.18; Table 4.18) producing a pK_B of 9.1.

A

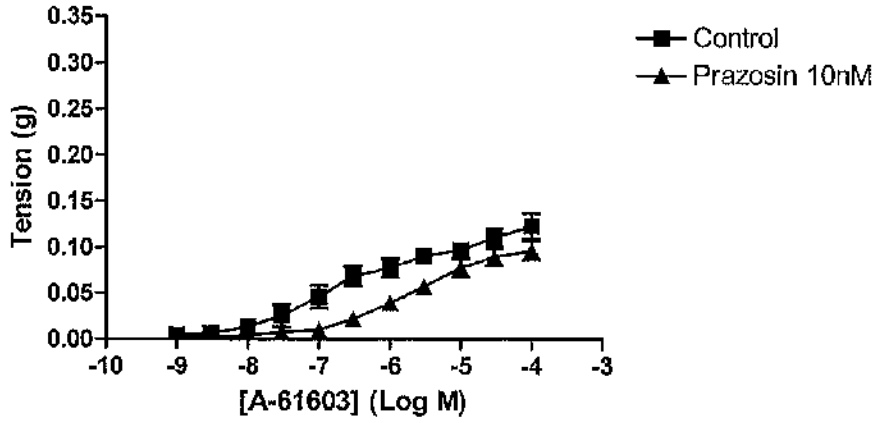

B

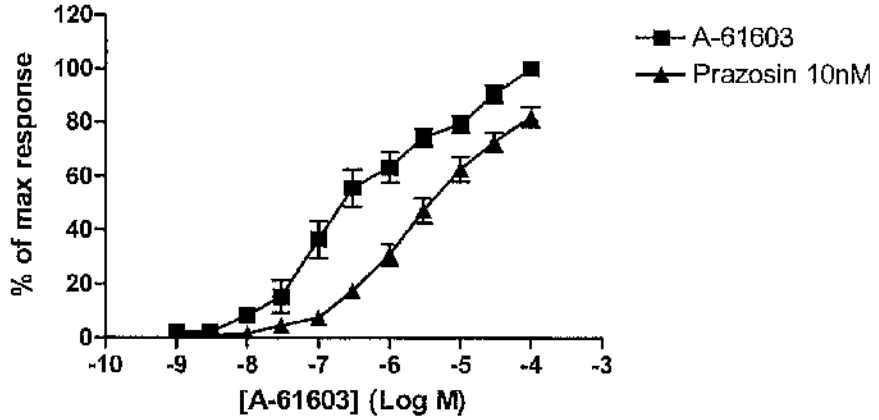

Figure 4.18. α_{1BD}-KO: CRC to A-61603 in the presence of prazosin expressed as means ± S.E. in (A) grams tension and (B) percentage of maximum response of the control CRC (n=6).

Table 4.18. A-61603 response in presence of prazosin in α_{1BD}-KO.

Agonist	n	pEC_{50}	Maximum response (g)	Hill slope (95% CI)
A-61603 control	6	6.6±0.23	0.12±0.01	0.5 (0.3-0.5)
Prazosin 10nM	6	5.4±0.11**	0.10±0.01+	0.5 (0.2-0.8)

+p>0.05, p<0.01 compared to the A-61603 control (Student's t-test).

A rightward shift in the A-61603 CRC was produced by prazosin 10nM and 0.1 μM in the α_{1D}-KO (Figure 4.19; Table 4.19) enabling a pK_B of 8.9 to be calculated.

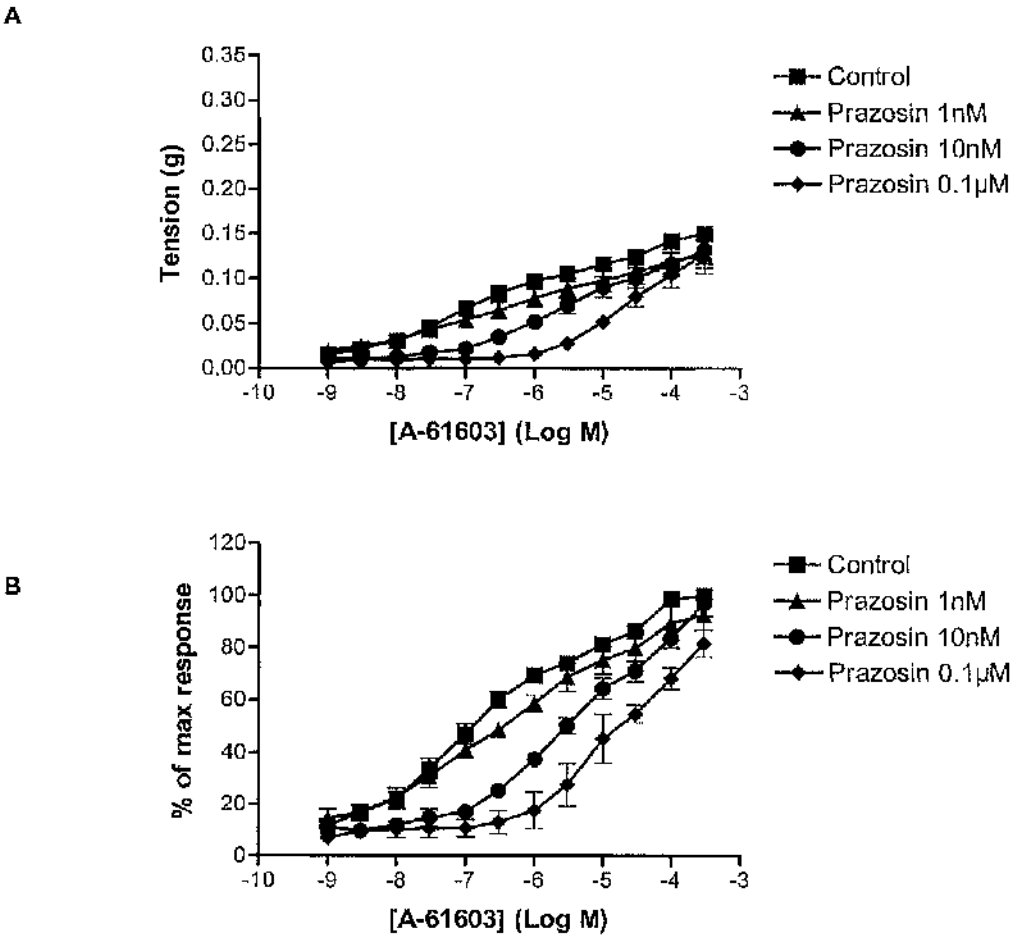

Figure 4.19. α_{1D}-KO: CRC to A-61603 in the presence of prazosin expressed as means ± S.E. in (A) grams tension and (B) percentage of maximum response of the control CRC (n≥7).

Table 4.19. A-61603 response in presence of prazosin in α_{1D}-KO.

Agonist	n	pEC_{50}	Maximum response (g)	Hill slope (95% CI)
A-61603 control	8	7.0±0.15	0.15±0.01	0.5 (0.5-0.6)
Prazosin 1nM	8	6.4±0.14^{+}	0.13±0.02^{+}	0.3 (0.2-0.4)$^{+}$
Prazosin 10nM	7	5.6±0.16**	0.13±0.02^{+}	0.4 (0.2-0.6)$^{+}$
Prazosin 0.1 μM	7	5.1±0.35***	0.13±0.02^{+}	0.5 (0.1-0.9)$^{+}$

$^{+}$ p>0.05, ** p<0.01, *** p<0.001 compared to A-61603 control (one-way ANOVA, Bonferroni's post test).

Rauwolscine

In the $\alpha_{1B/D}$-KO rauwolscine 10nM did not produce a rightward shift in the A-61603-induced response (Figure 4.20; Table 4.20).

A

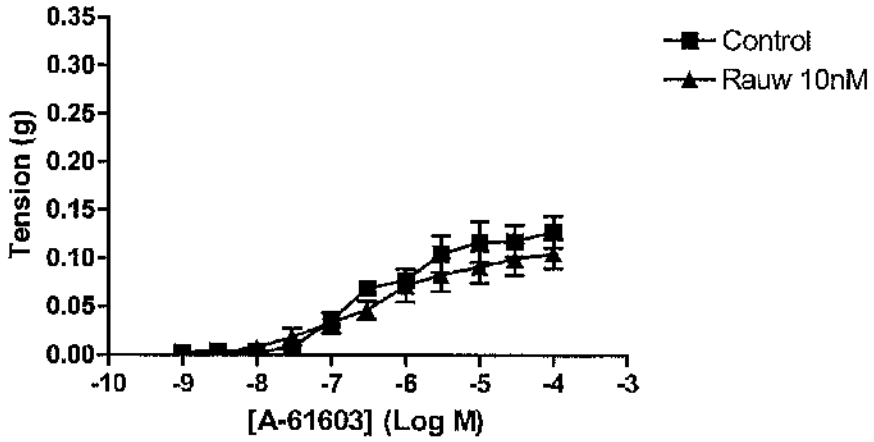

B

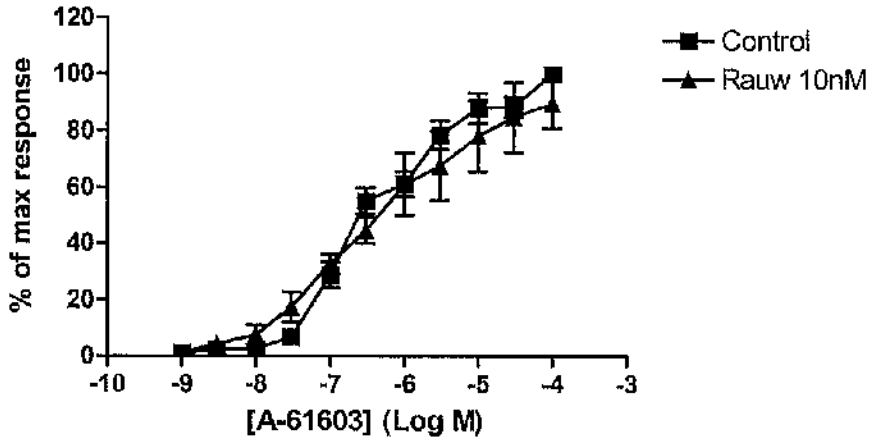

Figure 4.20. α_{1BD}-KO: CRC to A-61603 in the presence of rauwolscine expressed as means ± S.E. in (A) grams tension and (B) percentage of maximum response of the control CRC (n=6).

Table 4.20. A-61603 response in presence of rauwolscine in α_{1BD}-KO.

Agonist	n	pEC_{50}	Maximum response (g)	Hill slope (95% CI)
A-61603 control	6	6.5±0.14	0.13±0.02	0.9 (0.6-1.2)
Rauwolscine 10nM	6	6.2±0.24^{+}	0.11±0.02^{+}	0.8 (0.5-1.2)$^{+}$

$^{+}$p>0.05 compared to A-61603 control (Student's t-test).

5-methylurapidil

In the $\alpha_{1B/D}$-KO, 5-methylurapidil caused a rightward displacement of the A-61603 CRC (Figure 4.21; Table 4.21), producing a pK_B of 8.3.

A

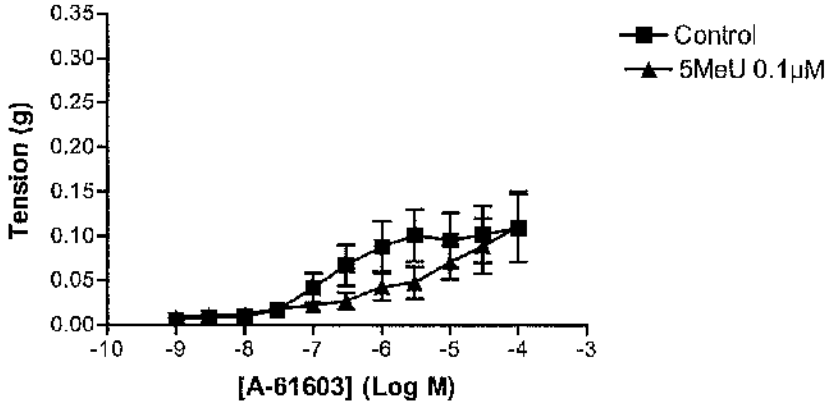

B

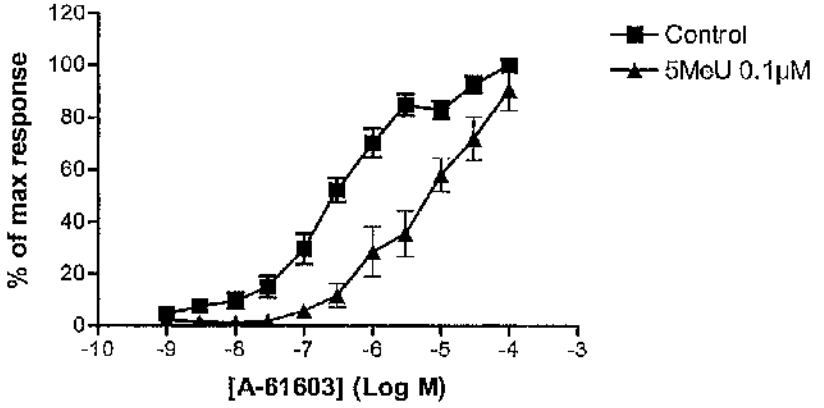

Figure 4.21. α_{1BD}-KO: CRC to A-61603 in the presence of 5-methylurapidil expressed as means ± S.E. In (A) grams tension and (B) percentage of maximum response of the control CRC (n≥7).

Table 4.21. A-61603 response in presence of 5-methylurapidil in α_{1BD}-KO.

Agonist	n	pEC_{50}	Maximum response (g)	Hill slope (95% CI)
A-61603 control	8	6.5±0.13	0.11±0.04	0.8 (0.5-1.1)
5-MeU 0.1 µM	7	5.4±0.20**	0.11±0.04+	0.6 (0.1-1.1)+

+ p>0.05, ** p<0.01 compared to the A-61603 control (Student's t-test).

Increasing concentrations of 5-Methylurapidil produced rightward shifts in the A-61603 CRC in the α_{1D}-KO (Figure 4.22; Table 4.17). A pA_2 of 9.2 with a slope of 0.7 (0.4-1.0) was calculated for 5-methylurapidil in the α_{1D}-KO.

A

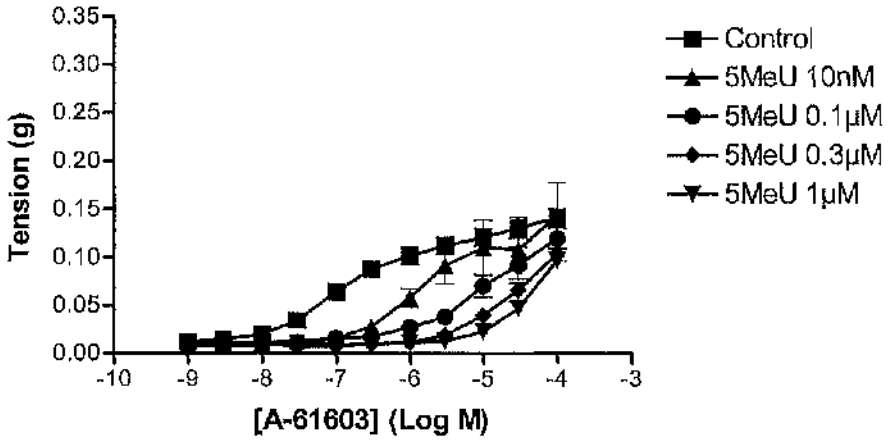

B

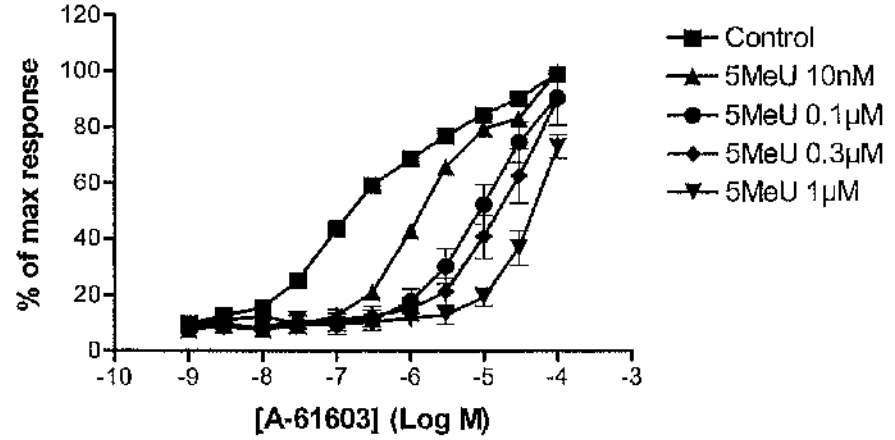

C

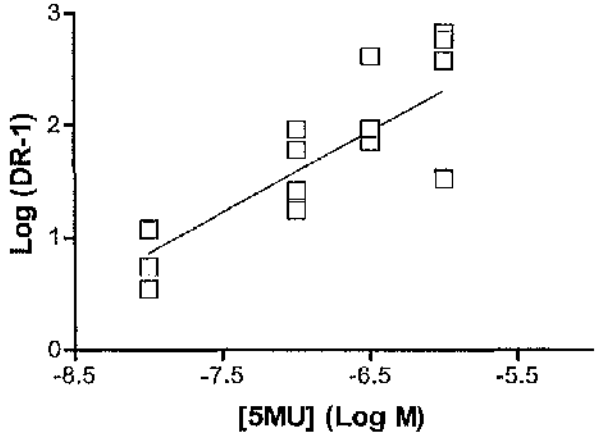

Figure 4.22. α_{1D}-KO: A-61603 CRC in the presence of 5-methylurapidil expressed as means ± S.E. in (A) grams tension and (B) percentage of maximum response of the control CRC (n≥6).

Table 4.22. A-61603 response in presence of 5-methylurapidil in α_{1D}-KO

Agonist	n	pEC_{50}	Maximum response (g)	Hill slope (95% CI)
A-61603 control	10	6.7±0.08	0.14±0.01	0.6 (0.5-0.6)$^{+}$
5-MeU 10nM	6	5.8±0.12***	0.14±0.03^{+}	0.8 (0.7-1.0)$^{+}$
5-MeU 0.1 µM	6	5.1±0.12***	0.12±0.02^{+}	0.7 (0.7-0.8)$^{+}$
5-MeU 0.3 µM	6	5.1±0.12***	0.10±0.01^{+}	0.9 (0.8-1.0)$^{+}$
5-MeU 1 µM	6	4.5±0.06***	0.10±0.02^{+}	0.9 (0.7-1.1)$^{+}$

$^{+}$ p>0.05, *** p<0.001 compared to the A-61603 control (one-way ANOVA, Bonferroni's post test).

In the presence of increasing concentrations of 5-Methylurapidil, a rightward displacement of the A-61603 CRC was observed in the α_{1B}-KO (Figure 4.23; Table 4.23). A pA_2 of 8.1 was produced, with a slope of 1.1 (0.6-1.6), indicating competitive antagonism.

Table 4.23. A-61603 response in presence of 5-methylurapidil in α_{1B}-KO.

Agonist	n	pEC_{50}	Maximum response (g)	Hill slope (95% CI)
A-61603 control	10	6.7±0.14	0.28±0.02	0.8 (0.5-1.2)
5-MeU 10nM	6	6.2±0.16^{+}	0.32±0.02^{+}	0.8 (0.3-1.4)$^{+}$
5-MeU 0.1 µM	6	5.2±0.20***	0.27±0.05^{+}	0.8 (0.4-1.2)$^{+}$
5-MeU 0.3 µM	6	4.9±0.29***	0.28±0.07^{+}	1.2 (1.0-1.3)$^{+}$
5-MeU 1 µM	6	4.2±0.20***	0.23±0.04^{+}	1.1 (0.3-1.8)$^{+}$

$^{+}$ p>0.05, *** p<0.001 compared to A-61603 control (one-way ANOVA, Bonferroni's post test).

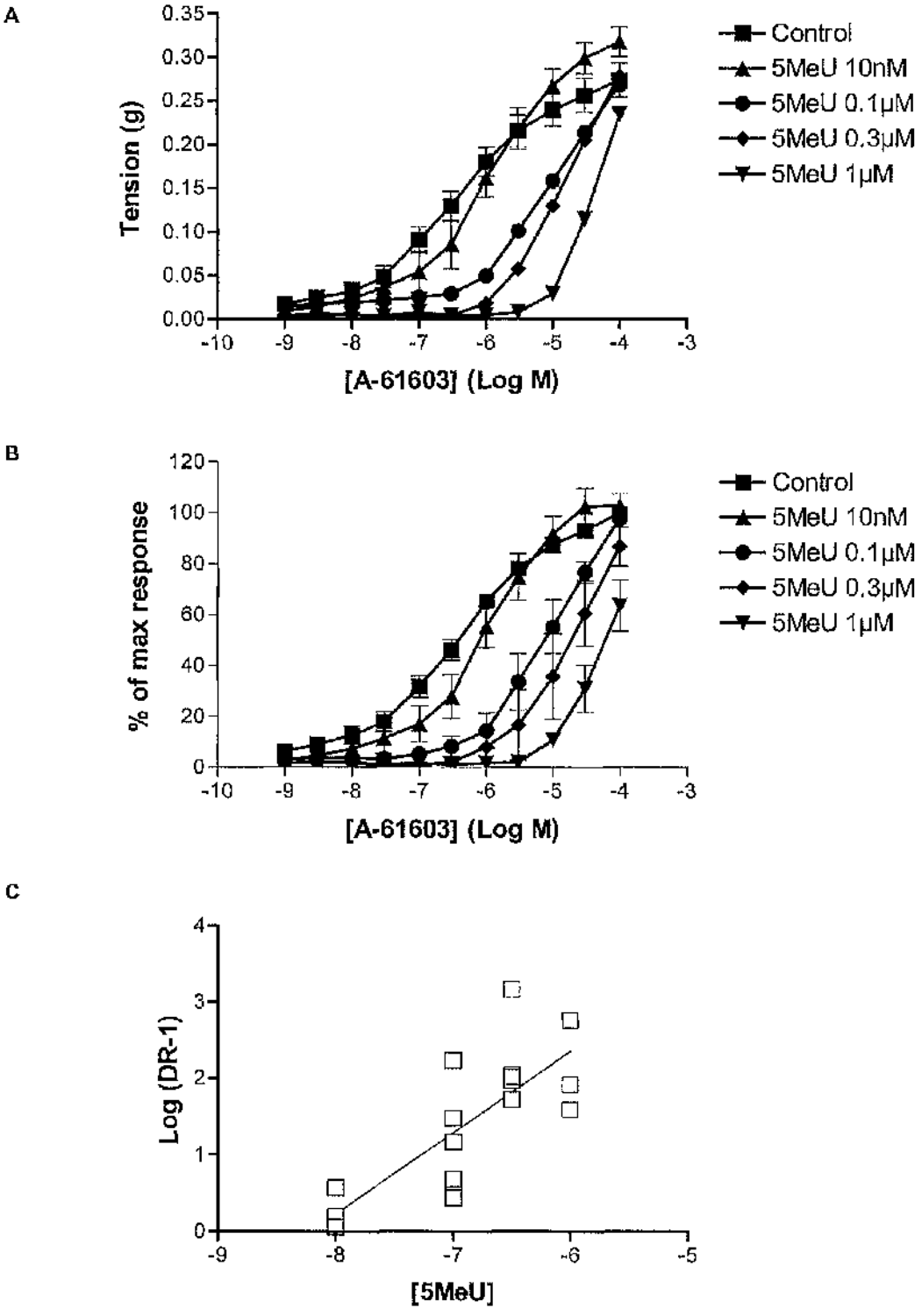

Figure 4.23. α_{1B}**-KO: CRC to A-61603 in the presence of 5-methylurapidil expressed as means ± S.E. in (A) grams tension and (B) percentage of maximum response of the control CRC (n≥6).**

RS100 329

RS100 329 10 nM did not antagonise the A-61603-induced response in the $\alpha_{1A/B}$-KO (Figure 4.24; Table 4.24).

A

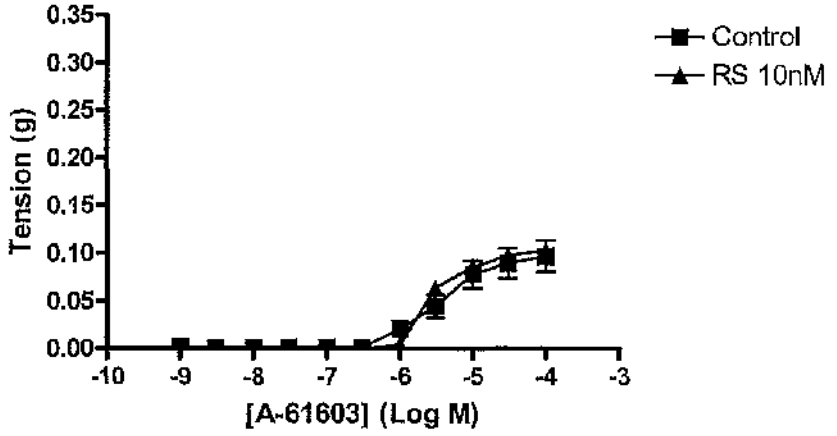

B

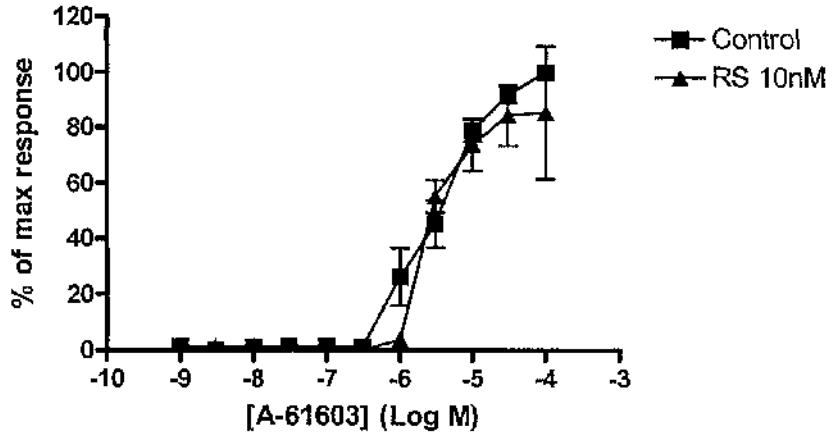

Figure 4.24. $\alpha_{1A/B}$-KO: CRC to A-61603 in the presence of RS100 329 expressed as means ± S.E. in (A) grams tension and (B) percentage of maximum response of the control CRC (n=2).

Table 4.24. A-61603 response in presence of RS100 329 in $\alpha_{1A/B}$-KO.

Agonist	n	pEC_{50}	Maximum response (g)	Hill slope (95% CI)
A-61603 control	2	5.5±0.17	0.10±0.02	1.2 (1.2-1.3)
RS100 329 10nM	2	5.6±0.05^{+}	0.10±0.05^{+}	3.0 (2.1-3.9)*

$^{+}$ p>0.05, *p<0.05 compared to A-61603 control (Student's t-test).

In the $\alpha_{1B/D}$-KO RS100-329 10nM caused a rightward shift in the A-61603 response (Figure 4.25; Table 4.25). A maximum response was not obtained at the highest concentration of A-61603 used, therefore, a pK_B could not be estimated.

A

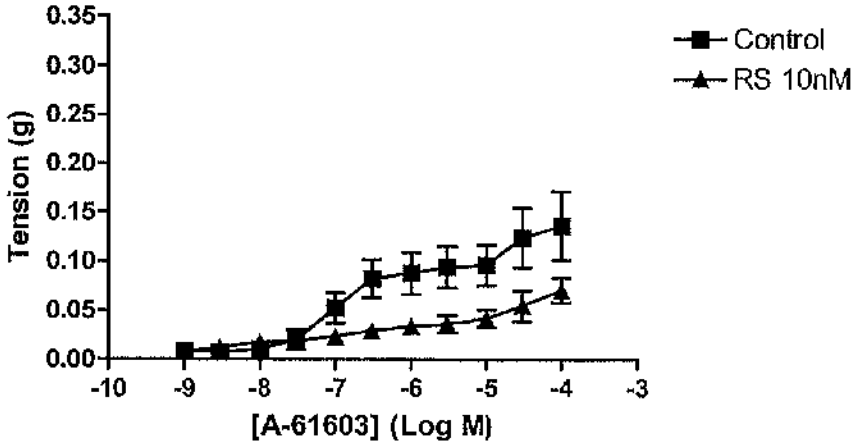

B

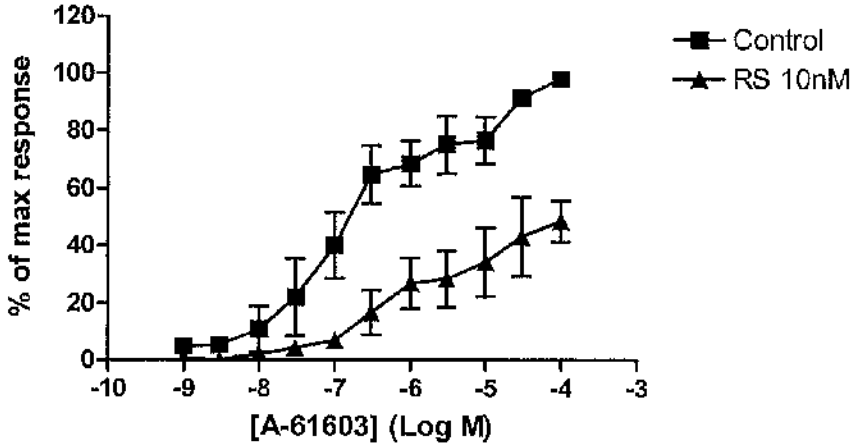

Figure 4.25. α_{1BD}-KO: CRC to A-61603 in the presence of RS100 329 expressed as means ± S.E. in (A) grams tension and (B) percentage of maximum response of the control CRC (n=6).

Table 4.25. A-61603 response in presence of RS100 329 in α_{1BD}-KO.

Agonist	n	pEC_{50}	Maximum response (g)	Hill slope (95% CI)
A-61603 control	6	6.6±0.42	0.14±0.04	0.8 (0.2-1.6)
RS100 329 10nM	6	N.D.	0.07±0.01*	0.6 (0.2-1.2)+

+ p>0.05, * p<0.05 compared to A-61603 response (Student's t-test).

In the α_{1D}-KO, increasing concentrations of RS100 329 caused rightward displacements of the A-61603 CRC (Figure 4.26; Table 4.26). At RS100 329 0.1 μM, a maximum response to A-61603 was not obtained, therefore, a pK_B of 10.0 was calculated at RS100 329 1nM and 10nM.

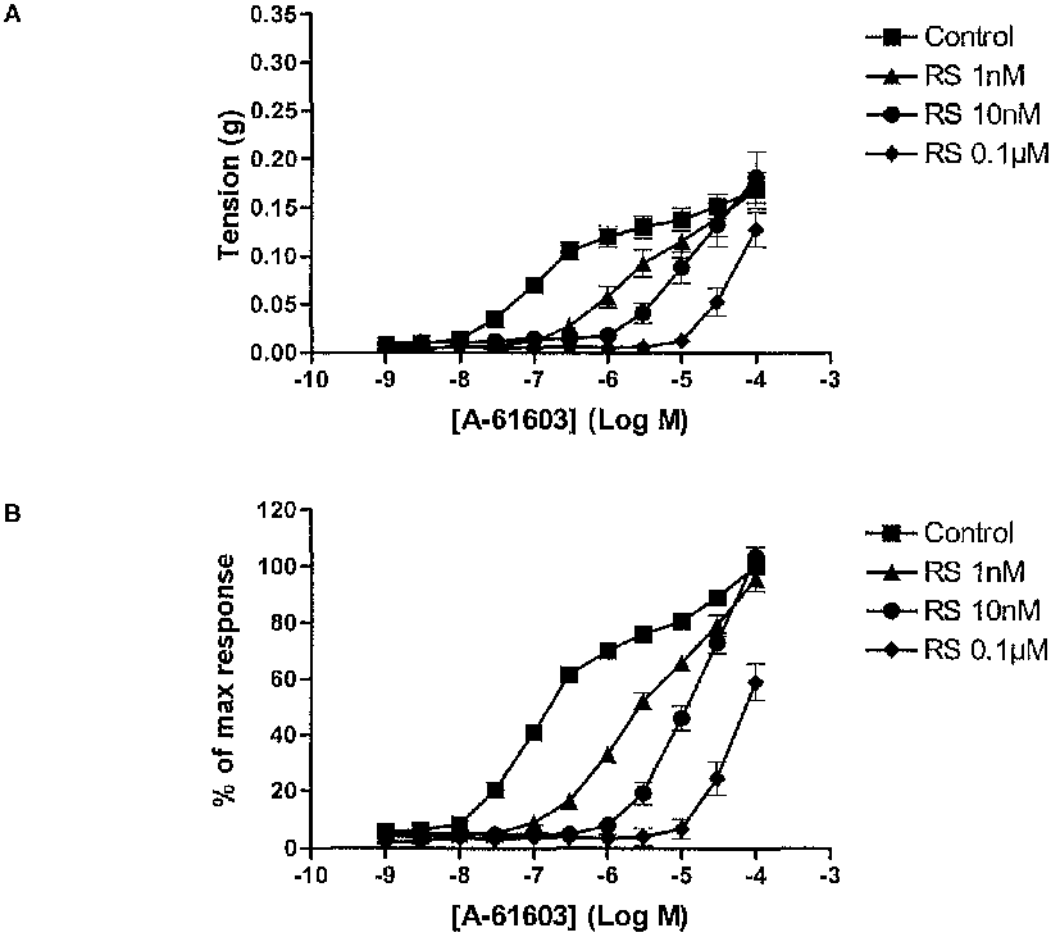

Figure 4.26. α_{1D}-KO: CRC to A-61603 in the presence of RS100 329 expressed as means ± S.E. In (A) grams tension and (B) percentage of maximum response of the control CRC (n=7).

Table 4.26. A-61603 response in presence of RS100 329 in α_{1D}-KO.

Agonist	n	pEC_{50}	Maximum response (g)	Hill slope (95% CI)
A-61603 control	10	6.8±0.07	0.17±0.01	0.8 (0.5-1.0)
RS100 329 1nM	7	5.6±0.09***	0.17±0.02+	0.6 (0.5-0.7)+
RS100 329 10nM	7	5.0±0.07***	0.18±0.03+	0.8 (0.3-1.2)+
RS100 329 0.1 μM	7	N.D.	0.13±0.02*	1.3 (1.1-1.6)+

+p>0.05, * p<0.05, *** p<0.01 compared to A-61603 control (one-way ANOVA, Bonferroni's post test).

In the α_{1B}-KO, the presence of RS100 329 10 nM and 0.1 μM produced a significant rightward displacement of A-61603 CRC (Figure 4.27; Table 4.27), enabling a pK_B of 8.5 to be produced. With RS100 329 0.1 μM a biphasic CRC was produced.

A

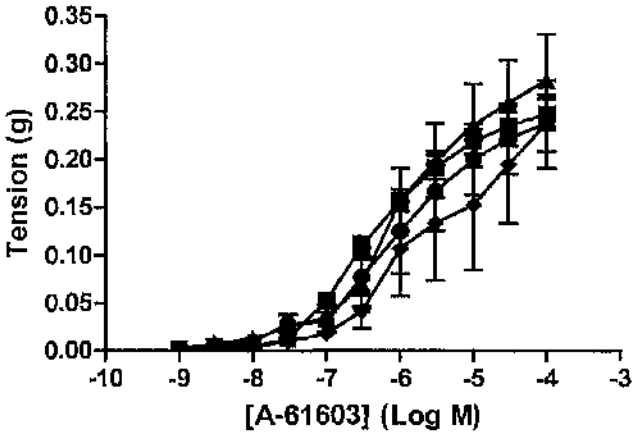

B

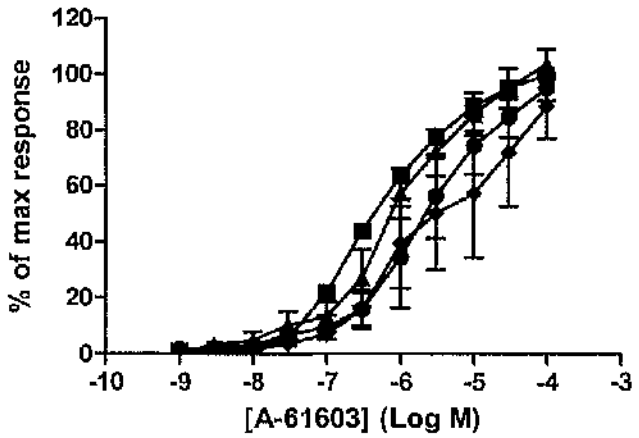

Figure 4.27. α_{1B}-KO: CRC to A-61603 in the presence of RS100 329 expressed as means ± S.E. in (A) grams tension and (B) percentage of maximum response of the control CRC (n≥6).

Table 4.27. A-61603 response in presence of RS100 329 in α_{1B}-KO.

Agonist	n	pEC_{50}	Maximum response (g)	Hill slope (95% CI)
A-61603 control	10	6.4±0.05	0.25±0.02	0.8 (0.7-0.8)
RS100 329 1nM	6	6.0±0.23^{+}	0.28±0.05^{+}	0.8 (0.8-0.9)$^{+}$
RS100 329 10nM	6	5.8±0.71	0.24±0.03^{+}	1.0 (0.8-1.3)$^{+}$
RS100 329 0.1 μM	6	5.7±0.37	0.25±0.04^{+}	1.0 (0.5-1.9)$^{+}$

$^{+}$ p>0.05; * p<0.05 compared to A-61603 control (one-way ANOVA, Bonferroni's post test).

BMY 7378

In the $\alpha_{1A/B}$-KO, BMY 7378 10 nM produced a rightward shift to the A-61603 CRC (Figure 4.28; Table 4.28), enabling a pK_B of 9.1 to be obtained.

A

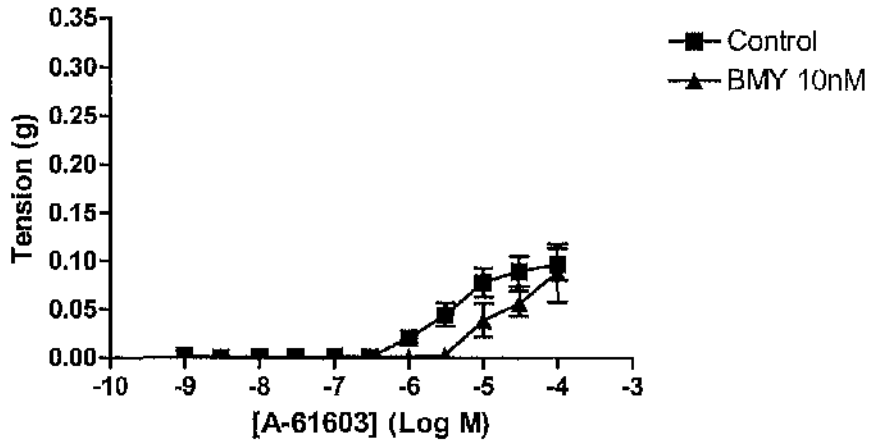

B

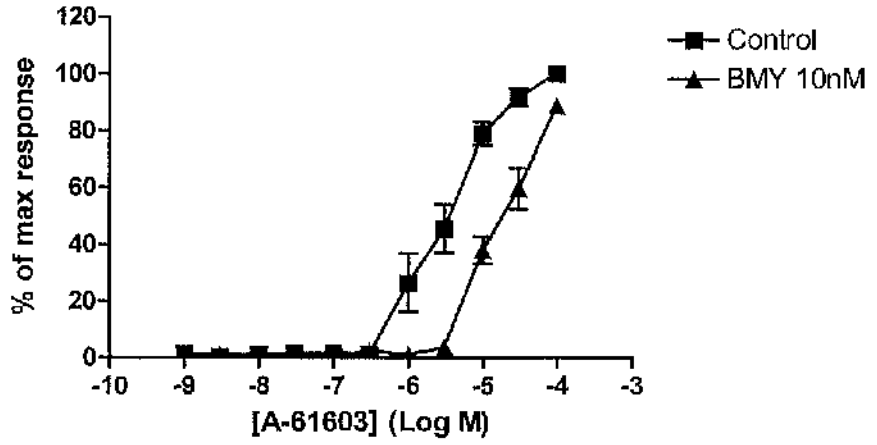

Figure 4.28. $\alpha_{1A/B}$-KO: CRC to A-61603 in the presence of BMY 7378 expressed as means ± S.E. in (A) grams tension and (B) percentage of maximum response of the control CRC (n=2).

Table 4.28. A-61603 response in presence of BMY 7378 in $\alpha_{1A/B}$-KO.

Agonist	n	pEC_{50}	Maximum response (g)	Hill slope (95% CI)
A-61603 control	2	5.5±0.17	0.10±0.02	1.2 (1.2-1.3)
BMY 7378 10nM	2	4.7±0.06*	0.09±0.03^{+}	1.2 (0.8-1.5)$^{+}$

$^{+}$ p>0.05, * p<0.05 compared to A-61603 control (Student's t-test).

In the $\alpha_{1B/D}$-KO, BMY 7378 failed to produce a significant shift in the A-61603 response (Figure 4.29; Table 4.29).

A

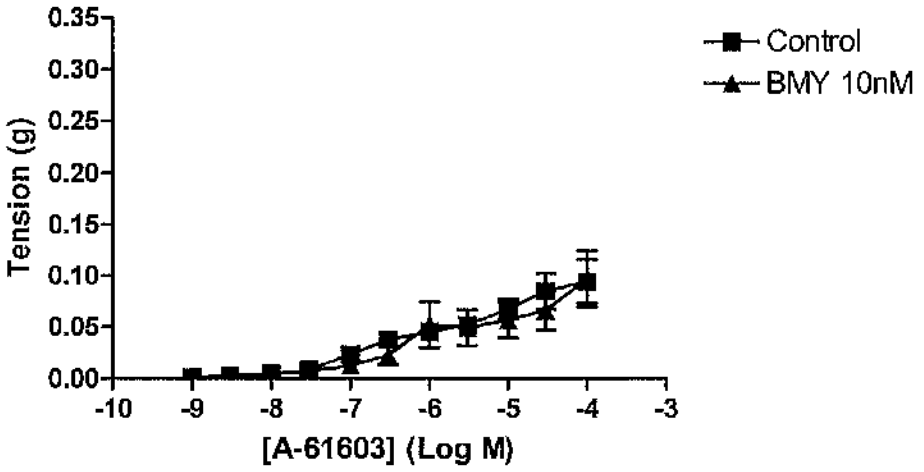

B

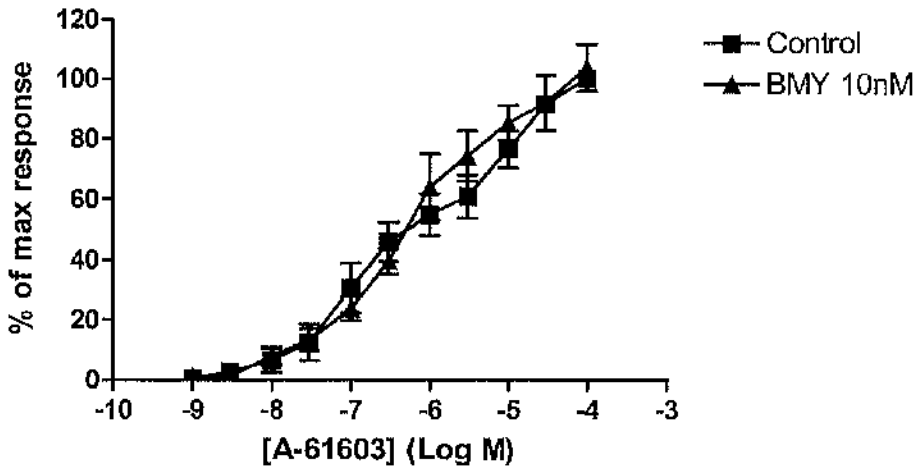

Figure 4.29. α_{1BD}-KO: CRC to A-61603 in the presence of BMY 7378 expressed as means ± S.E. in (A) grams tension and (B) percentage of maximum response of the control CRC (n=6).

Table 4.29. A-61603 response in presence of BMY 7378 in α_{1BD}-KO.

Agonist	n	pEC_{50}	Maximum response (g)	Hill slope (95% CI)
A-61603 control	6	6.2±0.33	0.09±0.02	0.4 (0.4-0.5)
BMY 7378 10nM	6	6.1±0.16[+]	0.10±0.03[+]	0.5 (0.4-0.6)[+]

[+]p>0.05 compared to A-61603 control (Student's t-test).

Increasing concentrations of BMY 7378 did not antagonise the A-61603 CRC in the α_{1D}-KO (Figure 4.30; Table 4.30).

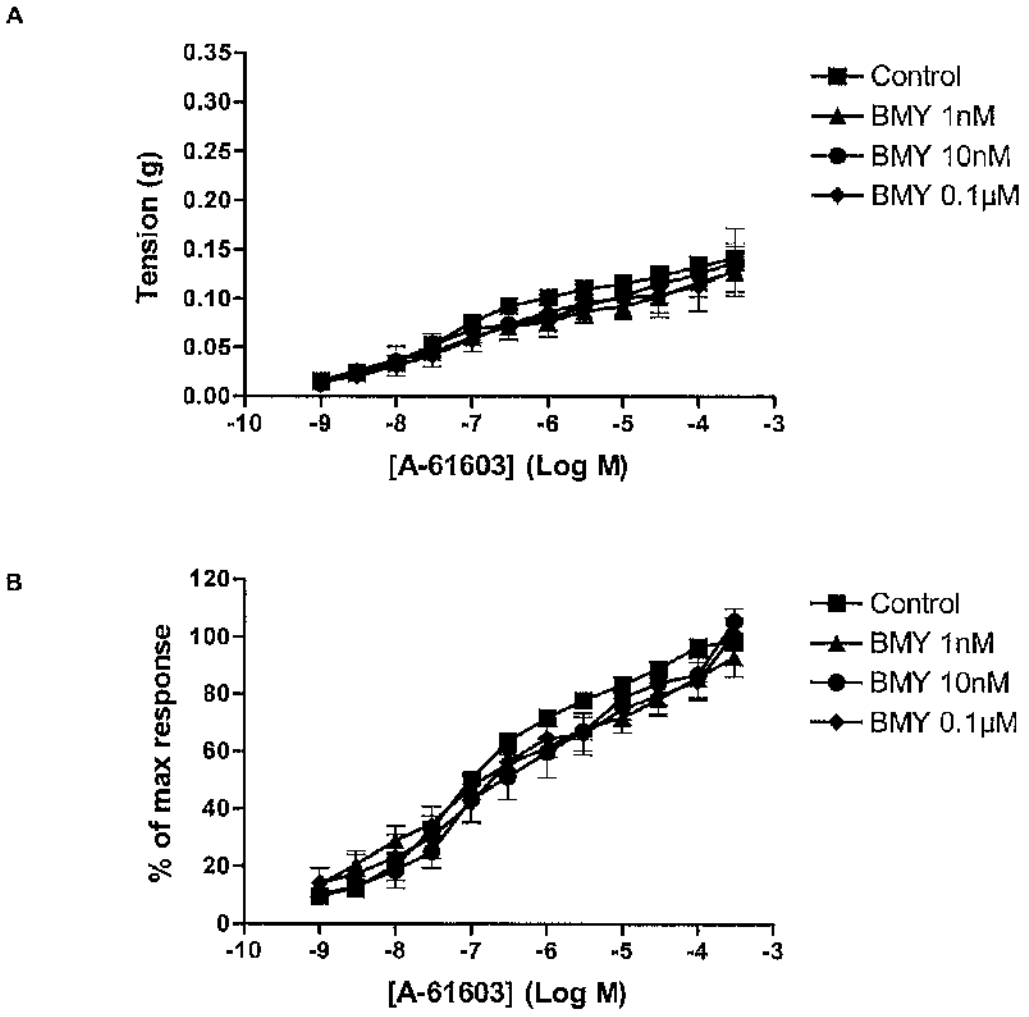

Figure 4.30. α_{1D}-KO: CRC to A-61603 in the presence of BMY 7378 expressed as means ± S.E. in (A) grams tension and (B) percentage of maximum response of the control CRC (n≥6).

Table 4.30. A-61603 response in presence of BMY 7378 in α_{1D}-KO.

Agonist	n	pEC_{50}	Maximum response (g)	Hill slope (95% CI)
A-61603 control	10	7.1±0.13	0.14±0.01	0.4 (0.4-0.5)
BMY 7378 1nM	6	6.8±0.26^{+}	0.13±0.02^{+}	0.3 (0.2-0.3)$^{+}$
BMY 7378 10nM	6	6.5±0.40^{+}	0.14±0.03^{+}	0.3 (0.3-0.3)$^{+}$
BMY 7378 0.1 µM	7	6.5±0.15^{+}	0.13±0.03^{+}	0.3 (0.2-0.3)$^{+}$

$^{+}$ p>0.05 compared to A-61603 control (one-way ANOVA, Bonferroni's post test).

In the α_{1B}-KO, BMY 7378 did not cause a rightward shift in the A-61603 CRC (Figure 4.31; Table 4.31).

A

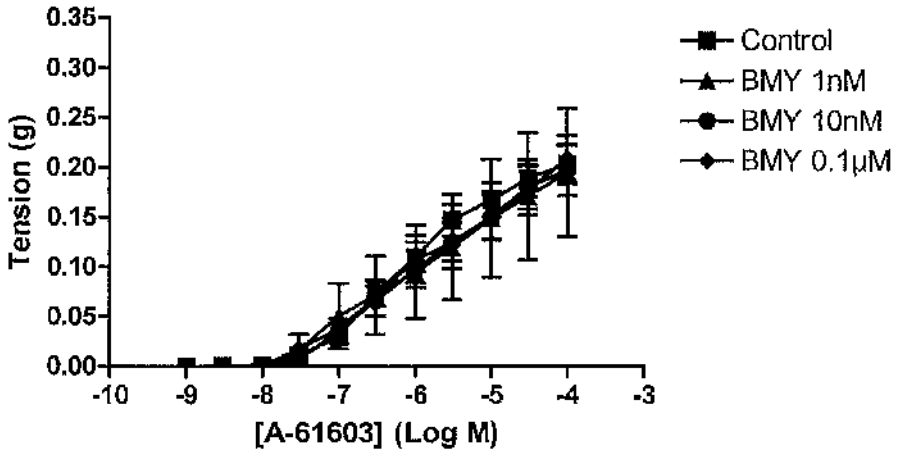

B

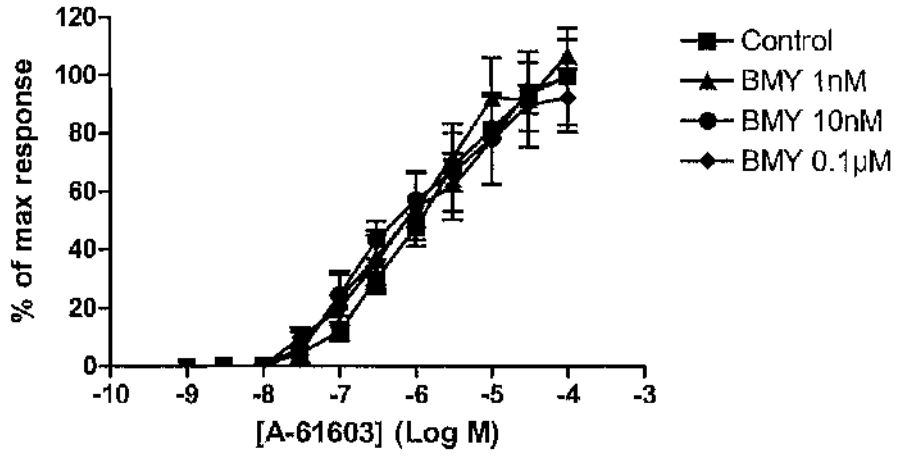

Figure 4.31. α_{1B}-KO: CRC to A-61603 in the presence of BMY 7378 expressed as means ± S.E. in (A) grams tension and (B) percentage of maximum response of the control CRC (n≥6).

Table 4.31. A-61603 response in presence of BMY 7378 in α_{1B}-KO.

Agonist	n	pEC_{50}	Maximum response (g)	Hill slope (95% CI)
A-61603 control	8	6.2±0.10	0.20±0.02	0.9 (0.7-1.1)
BMY 7378 1nM	6	6.2±0.33^{+}	0.19±0.07^{+}	0.6 (0.5-0.8)$^{+}$
BMY 7378 10nM	6	6.1±0.24^{+}	0.20±0.03^{+}	0.7 (0.6-0.8)$^{+}$
BMY 7378 0.1 μM	6	5.8±0.37^{+}	0.21±0.02^{+}	0.6 (0.3-0.9)$^{+}$

$^{+}$ p>0.05 compared to A-61603 control (one-way ANOVA, Bonferroni's post test)

Table 4.40. Summary of affinity estimates for antagonists against phenylephrine response for knockout mice.

	Prazosin		5MeU		RS100-329		BMY 7378	
	pA_2 /pK_B	Slope	pA_2 /pK_B	Slope	pA_2 /pK_B	Slope	pA_2 /pK_B	Slope
α_{1B}-KO	10.3*	0.9 (0.7-1.2)	7.6*	1.1 (0.8-1.5)	-	-	9.6*	0.7(0.5-0.8)
α_{1D}-KO	10.6	-	8.1	0.8 (0.4-1.3)	9.1	-	7.0	-
α_{1BD}-KO	N.D.	-	-	-	-	-	-	-
$\alpha_{1A/B}$-KO	-	-	-	-	-	-	9.0	-

*Denotes data from (Deighan C, 2002)

Table 4.41. Summary of affinity estimates for antagonists against A-61603 response for knockout mice.

	Prazosin		5MeU		RS100-329		BMY 7378	
	pA_2 /pK_B	Slope	pA_2 /pK_B	Slope	pA_2 /pK_B	Slope	pA_2 /pK_B	Slope
α_{1B}-KO	-	-	8.1	1.1(0.6-1.6)	8.6	-	No shift	-
α_{1D}-KO	8.9	-	9.2	0.7(0.4-1.0)	10.0	-	No shift	-
α_{1BD}-KO	9.1	-	8.3	-	Non-competitive block	-	No shift	-
$\alpha_{1A/B}$-KO	-	-	-	-	No shift	-	9.1 (n=2)	-

4.4. Discussion

In the present study single and double knockouts of the α_1-AR subtypes were employed to provide a valuable insight into the function of the α_1-AR subtypes mediating the contractile response in the carotid artery of the WT mouse.

4.4.1. α_1-AR characterisation in the $\alpha_{1A/B}$-KO

Preliminary experiments were performed in the $\alpha_{1A/B}$-KO in order to gauge the α_1-AR-mediated contractile response in this mouse. The α_{1D}-AR is the only possible α_1-AR subtype in the $\alpha_{1A/B}$-KO and this mouse provided the opportunity to assess the actions of the agonists and antagonists used throughout this study solely at the α_{1D}-AR. It should be noted that no time controls for either phenylephrine or A-61603 were obtained in the $\alpha_{1A/B}$-KO due to the preliminary nature of the experiments in this strain. The phenylephrine-induced response was potent producing a large maximum response. In contrast, a contractile response was observed only at high concentrations of A-61603 and the response showed reduced efficacy compared to phenylephrine. The responses to the α_1-AR agonists were compared with 5-HT to assess the contractile capability of the carotid artery in this mouse via a non-adrenergic mechanism. The contractile response to 5-HT was comparable to that reported in the WT mouse and single knockouts (Deighan C, 2002;Deighan *et al.*, 2005). It is, therefore, apparent that the reduction in the contractile response to A-61603 was due to the loss of the two α_1-AR subtypes, and not due to an overall reduction in the ability of the carotid artery to contract. From these early results, it was clear that phenylephrine does show some selectivity for the α_{1D}-AR over the α_{1A}-AR and α_{1B}-AR, supporting the findings of Knepper et al. (1995). Furthermore, high concentrations of A-61603 produced a contractile response. This suggests that A-61603 does have an action on the α_{1D}-AR, but has reduced sensitivity and efficacy at this α_1-AR subtype compared to the α_{1A}-AR, which supports the findings of Knepper and colleagues (1995;Meyer *et al.*, 1996). However, as a study of the pig carotid vasculature reported that A-61603 can act via a non-adrenergic mechanism (Willems et al., 2001), further pharmacological analysis of the A-61603 contractile response was required.

BMY 7378 acted potently against phenylephrine (pA_2 9.0) and A-61603 (pA_2 of 9.1). This is consistent with published affinity values for the α_{1D}-AR (see Chapter One.), confirming that the α_{1D}-AR was functional in this mouse. Furthermore, this confirms that A-61603

also acts on the α_{1D}-AR. RS100 329 10 nM did not have an effect on the A-61603 CRC, indicating that RS100 329 has very low affinity for the α_{1D}-AR. It has been reported that A-61603 acted through a non-adrenoceptor-mediated mechanism in the carotid arteriovenous anastomes of the pig (Willems *et al.*, 2001). Therefore, the possibility that the A-61603-induced response in the $\alpha_{1A/B}$-KO is mediated by a non-adrenergic pathway does require further investigation. However, based on the evidence obtained in the $\alpha_{1A/B}$-KO at present the A-61603-induced response does appear to be α_1-AR-mediated.

4.4.2. α_1-AR characterisation in the $\alpha_{1B/D}$-KO

In the $\alpha_{1B/D}$-KO, the α_{1A}-AR is the only possible α_1-AR subtype. In the $\alpha_{1B/D}$-KO the phenylephrine and A-61603 time controls were reproducible, validating their use for further pharmacological analysis. Phenylephrine showed lower sensitivity and efficacy, compared to A-61603, which contrasts with the $\alpha_{1A/B}$-KO and is consistent with phenylephrine being less potent at the α_{1A}-AR, while the reverse holds for A-61603. This, together with the agonist data in the $\alpha_{1A/B}$-KO, provides good evidence that A-61603 is selective for the α_{1A}-AR over the α_{1D}-AR and that phenylephrine has some selectivity for the α_{1D}-AR over the α_{1A}-AR, which has been reported previously (Knepper SM *et al.*, 1995;Meyer *et al.*, 1996). The responses to phenylephrine and A-61603 were compared to a contractile response mediated through a non-adrenergic mechanism: 5-HT. The 5-HT CRCs were comparable to that reported in the WT mouse and single knockouts (Deighan C, 2002;Deighan *et al.*, 2005), suggesting that the reduction in the contractile response to phenylephrine was due to the loss of two α_1-AR subtypes and not due to an overall reduction in the contractility of the carotid artery.

Prazosin acted with such high affinity against the contractile response to phenylephrine that the agonist response was almost completely abolished by a low concentration. This phenomenon was also reported by Hosoda et al. (2005b) for the noradrenaline-induced response in the $\alpha_{1B/D}$-KO in the thoracic aorta. Nevertheless, prazosin potently and competitively antagonised the A-61603-induced response in $\alpha_{1B/D}$-KO (pK_B 9.1), indicating that the A-61603 response was α_1-AR-mediated. This was further supported by rauwolscine not having an effect on the A-61603 contractile response, opposing the possibility that the A-61603-induced response could be α_2-AR-mediated. The lack of effect of BMY 7378 10nM on the A-61603 CRC suggested that BMY 7378 has very low affinity for the α_{1A}-AR. This is supported by the low pA_2 of 6.5 obtained against the

phenylephrine-induced response in the first order mesenteric artery of the mouse, which is predominantly α_{1A}-AR-mediated (McBride *et al.* Submitted for publication). The pK_B of 8.3 for 5-methylurapidil against the A-61603 response was lower than expected considering that the α_{1A}-AR was the only α_1-AR subtype present. However, RS100 329 was particularly potent in the $\alpha_{1B/D}$-KO, where the contractile response to A-61603 was almost completely abolished. These findings suggest that the α_{1A}-AR does mediate the contractile response to phenylephrine and A-61603 in the $\alpha_{1B/D}$-KO.

4.4.3. The α_{1D}-KO

The α_{1D}-KO provides an opportunity to study the α_1-AR subtypes in the mouse carotid artery in the absence of the predominant contractile α_1-AR. Potentially either the α_{1A}-AR or α_{1B}-AR, or both of these α_1-AR subtypes, could regulate the contractile response in the α_{1D}-KO. The time controls for both phenylephrine and A-61603 were reproducible, validating the use of these α_1-AR agonists for further pharmacological analysis. In the α_{1D}-KO phenylephrine showed reduced sensitivity and efficacy, which can be accounted for by the loss of the α_{1D}-AR. The efficacy of A-61603 was reduced in the α_{1D}-KO suggesting that the α_{1D}-AR may mediate a component of the A-61603 response.

Prazosin acted with high affinity against the phenylephrine-induced response in the α_{1D}-KO, producing a high pK_B (10.6) comparable to that obtained by Deighan (2002;Deighan *et al.*, 2005) in the α_{1B}-KO (pA_2 10.3). However, in the α_{1D}-KO, the presence of prazosin caused nonparallel shifts and depressed the maximum response obtained to phenylephrine suggesting non-competitive antagonism. Deighan (2002) demonstrated that prazosin acted competitively against phenylephrine in the WT mouse and α_{1B}-KO. It, therefore, appears that the difference in the nature of antagonism by prazosin is due to the absence of the α_{1D}-AR. Prazosin has been reported to act non-competitively against both phenylephrine and noradrenaline in the intact rat aorta, but competitively in the absence of the endothelium (Alosachie & Godfraind, 1988). Thus, the endothelium may account for the non-competitive action of prazosin against phenylephrine in the α_{1D}-KO and $\alpha_{1B/D}$-KO. Further experiments to establish whether prazosin acts competitively in the α_{1D}-KO and $\alpha_{1B/D}$-KO in the absence of the endothelium would confirm this hypothesis.

Prazosin antagonised the A-61603-induced response (pK_B 8.9) with lower affinity than the phenylephrine response but does still indicate a high affinity site, suggesting the response is α_1-AR-mediated. As prazosin acted competitively against A-61603, this also suggests that the non-competitive nature of prazosin against phenylephrine is related to the α_{1D}-AR.

Only the highest concentration of BMY 7378 (0.1 μM) antagonised the phenylephrine response. Thus, a low pK_B of 7.0 was produced, which confirms that the α_{1D}-AR is absent. The lack of effect of BMY 7378 10 nM on the A-61603 CRC suggested that this antagonist did not have an action at either the α_{1A}-AR or α_{1B}-AR. In the α_{1D}-KO the high affinity of 5-methylurapidil against both phenylephrine (pA_2 8.1) and A-61603 (pA_2 9.2) suggested that the responses were α_{1A}-AR-mediated. The affinity estimates for RS100 329 against the A-61603-induced response in the α_{1D}-KO (pK_B 10.0) was higher than the phenylephrine response (pK_B 9.1). Both of these affinity estimates are consistent with RS100 329 acting at the α_{1A}-AR. These affinity estimates for both selective α_{1A}-AR antagonists are comparable to that obtained in the first order mesenteric artery of the WT mouse in which 5-methylurapidil showed higher affinity against phenylephrine (pK_B 8.3) than A-61603 (pK_B 8.9) and RS100 329 produced a high pK_B of 10.1 (McBride *et al.* Submitted for publication). In the present study, the lower affinity against the phenylephrine-induced response may reflect that phenylephrine, but not A-61603, is acting on the α_{1B}-AR. The findings suggest that the contractile response in the α_{1D}-KO is α_{1A}-AR-mediated, but an α_{1B}-AR response may also exist.

4.4.4. The α_{1B}-KO

In the α_{1B}-KO, where the α_{1D}-AR is present, the α_{1A}-AR could potentially contribute to contraction. In the absence of any antagonists with suitable selectivity for the α_{1B}-AR, the α_{1B}-KO can be used as a substitute. In the α_{1B}-KO the phenylephrine and A-61603 time controls were reproducible, validating the use of these agonists for further pharmacological analysis. Both the phenylephrine-induced response and A-61603-induced response were potent, with large maximum responses being produced.

In the earlier study, BMY 7378 acted with high affinity (pK_B 9.6) against the phenylephrine-induced response in the α_{1B}-KO (Deighan C, 2002;Deighan *et al.*, 2005), indicative of a α_{1D}-AR-mediated response. BMY 7378 did not antagonise the A-61603-induced response, implying that the α_{1A}-AR was mediating the response to A-61603, not the α_{1D}-AR. Against phenylephrine, the estimated affinity for 5-methylurapidil reported

by Deighan (2002) for the α_{1B}-KO (pA_2 7.6) was more indicative of an α_{1D}-AR-mediated response. When tested against A-61603, 5-methylurapidil showed higher affinity (pA_2 8.1), but this still did not clearly differentiate whether this was due to an α_{1A}-AR- or α_{1D}-AR-mediated response. A pK_B of 8.6 was obtained for RS100 329 against A-61603, which is intermediate to the reported affinity of RS100 329 at the α_{1A}-AR and the α_{1D}-AR. The lower potency of the selective α_{1A}-AR antagonists in the α_{1B}-KO may be due to the dominant contractile response of the α_{1D}-AR masking the α_{1A}-AR-mediated response. Collectively, these findings suggest that in the α_{1B}-KO the α_{1D}-AR is the predominant contractile α_1-AR, although an α_{1A}-AR-mediated response does appear to exist.

4.4.5. Comparison with the WT mouse

The data obtained from the WT mouse (Chapter Three) suggested that the α_{1A}-AR may have a functional role in the carotid artery. This was compared to the data obtained in the single knockouts (α_{1B}-KO and α_{1D}-KO) and double knockouts ($\alpha_{1A/B}$-KO and $\alpha_{1B/D}$-KO) to highlight the functional α_1-AR subtypes in the WT mouse.

It has been shown that phenylephrine has approximately ten-fold higher affinity at the α_{1D}-AR than the α_{1A}-AR and α_{1B}-AR (Knepper et al., 1995), which is reflected in a higher efficacy, and is a plausible reason for the decreased potency of phenylephrine in the α_{1D}-KO and $\alpha_{1B/D}$-KO. This was emphasised in the $\alpha_{1A/B}$-KO, where in the absence of the other α_1-AR subtypes, sensitivity to phenylephrine was higher than in any other strain of mouse. The maximum response obtained to phenylephrine in the $\alpha_{1A/B}$-KO was not statistically different to that observed in the WT mouse suggesting that the phenylephrine-induced response was predominantly mediated by the α_{1D}-AR. However, an additional component to the contractions at high concentrations of phenylephrine was observed in the WT mouse, presumably due to the α_{1A}-AR and/or α_{1B}-AR. This trend was also observed in the α_{1B}-KO, indicating that this secondary contractile α_1-AR was α_{1A}-AR-mediated. However, comparison of the agonist responses in the knockout mice with the WT mouse suggested that the phenylephrine-induced response may be mediated by all three α_1-AR subtypes. Further evidence to suggest that an α_{1B}-AR-mediated component to the phenylephrine response existed was revealed by comparison of the phenylephrine-induced response in the α_{1D}-KO and $\alpha_{1B/D}$-KO.

Comparison of the A-61603-induced response demonstrated that the maximum response obtained to A-61603 in the α_{1D}-KO, α_{1BD}-KO and $\alpha_{1A/B}$-KO was much lower than in the α_{1B}-KO and WT mouse. The reduced efficacy in the α_{1D}-KO could suggest that there was a non-α_{1A}-AR component to the A-61603-induced response, which was present in the α_{1B}-KO, but eliminated in the α_{1D}-KO. Therefore, at high concentrations A-61603 may have some action on the α_{1D}-AR. This was supported by contractions to A-61603 being observed only at high concentrations in the $\alpha_{1A/B}$-KO. The potency of A-61603 was unchanged between strains of mice, with the exception of the $\alpha_{1A/B}$-KO, in which sensitivity to A-61603 was markedly reduced. This supports A-61603 having higher efficacy at the α_{1A}-AR than the α_{1B}-AR and α_{1D}-AR.

The α_1-AR responses in the $\alpha_{1B/D}$-KO were more variable than the α_{1D}-KO. A recent study reported that the α_{1B}-AR was involved in regulating the cell surface expression of the α_{1D}-AR (Hague *et al.*, 2004b). It is, therefore, possible that the α_{1B}-AR has some regulatory role in mouse carotid artery, which would explain the difference in contraction between the α_{1D}-KO and $\alpha_{1B/D}$-KO. Alternatively, the α_{1B}-AR may have a minor contractile role as suggested by Daly et al. (2002a). However, it seemed that if the A-61603-induced response in the $\alpha_{1A/B}$-KO was combined with the response in the $\alpha_{1B/D}$-KO the overall response would be equivalent to the response in the WT mouse, indicating that the α_{1A}-AR and the α_{1D}-AR, but not the α_{1B}-AR, mediate the A-61603 response in the WT mouse.

In all knockouts where prazosin was tested, it antagonised the phenylephrine CRC, which suggests that the phenylephrine response was α_1-AR-mediated. However, there is evidence from IP accumulation experiments that prazosin shows some selectivity for α_{1B}-ARs and α_{1D}-ARs over α_{1A}-ARs (Williams et al., 1999). The affinity estimates do indicate a high affinity site, suggesting that the responses were α_1-AR-mediated. This was further supported by rauwolscine not having an effect on the A-61603 contractile response in the $\alpha_{1B/D}$-KO. In the absence of a suitably selective α_{1B}-AR antagonist the identification of an α_{1B}-AR-mediated contraction is difficult. However, in the α_{1D}-KO phenylephrine was more potent and had greater efficacy than in the $\alpha_{1B/D}$-KO, which may indicate a contractile role for the α_{1B}-AR.

In the WT mouse, BMY 7378 antagonised the A-61603 response only at the highest concentration used (pK_B 8.3). In all four knockouts the A-61603 response was unaffected by BMY 7378 0.1 μM, therefore, a pK_B of at least 7.0 would be expected in the knockouts.

It is unclear at present why BMY 7378 0.1 μM had an effect against A-61603 in the WT mouse but not in the α_{1B}-KO, in which the A-61603-induced response was expected to contain an α_{1D}-AR-mediated component. Since BMY 7378 did not affect the A-61603-induced response in the α_{1B}-KO, α_{1D}-KO and $\alpha_{1B/D}$-KO, it seems plausible that A-61603 has little or no action at the α_{1B}-AR.

In the WT mouse, affinity estimates of 7.5 for 5-methylurapidil (Deighan C, 2002) and 7.9 RS100 329 were obtained against the phenylephrine-induced response, which did not suggest an α_{1A}-AR-mediated response. Both 5-methylurapidil and RS100 329 showed higher affinity against the phenylephrine response in the α_{1D}-KO (5-methylurapidil pA_2 8.1, RS100 329 pK_B 9.1) compared to the WT mouse and α_{1B}-KO (5-methylurapidil pA_2 7.6 (Deighan C, 2002;Deighan *et al.*, 2005)). This suggests that, when present, the α_{1D}-AR has influenced the affinity estimates of the α_{1A}-AR selective compounds. RS100 329 antagonised the A-61603-induced response with higher affinity than the phenylephrine response in the WT mouse (pA_2 8.7). In the knockouts (excluding $\alpha_{1A/B}$-KO), both 5-methylurapidil (α_{1B}-KO pA_2 8.1; α_{1D}-KO pA_2 9.2; $\alpha_{1B/D}$-KO pK_B 8.3) and RS100 329 (α_{1B}-KO pK_B 8.6; α_{1D}-KO 10.0; $\alpha_{1B/D}$-KO non-competitive block) acted with high affinity against A-61603. This was higher than that obtained against the phenylephrine-induced response, supporting observations from the WT mouse. In the $\alpha_{1A/B}$-KO, contractions were produced in response to high concentrations of A-61603, which is indicative of an α_{1D}-AR-mediated component to the A-61603 response or a non-adrenergic effect. Thus, A-61603 appears to have some action on the α_{1D}-AR and binding to this lower affinity site would account for the affinity estimates of the α_{1A}-AR selective antagonists being lower in the WT mouse and α_{1B}-KO, where the α_{1D}-AR is present. Taken together, this data suggests that an α_{1A}-AR response does exist in the mouse carotid artery but is influenced by the dominant α_{1D}-AR.

This study demonstrates that the α_{1A}-AR is functional in the mouse carotid artery. The α_{1D}-AR is the predominant contractile α_1-AR in this vessel, but the α_{1A}-AR does contribute to the contractile response. The α_{1A}-AR-mediated response in the α_{1D}-KO has been published (Deighan *et al.*, 2005). However, at the time of publication it was unclear whether the α_{1A}-AR had been upregulated in the α_{1D}-KO to compensate for the loss of the main contractile receptor. The evidence suggests that the α_{1A}-AR is functional in the WT mouse, and the α_{1A}-AR in the knockout mice is not due to a compensatory upregulation. This agrees with Hosoda et al. (2005b), who did not observe any compensation for the loss

of α_1-AR subtypes in either the contractile responses or mRNA expression in both the α_{1D}-KO and $\alpha_{1B/D}$-KO.

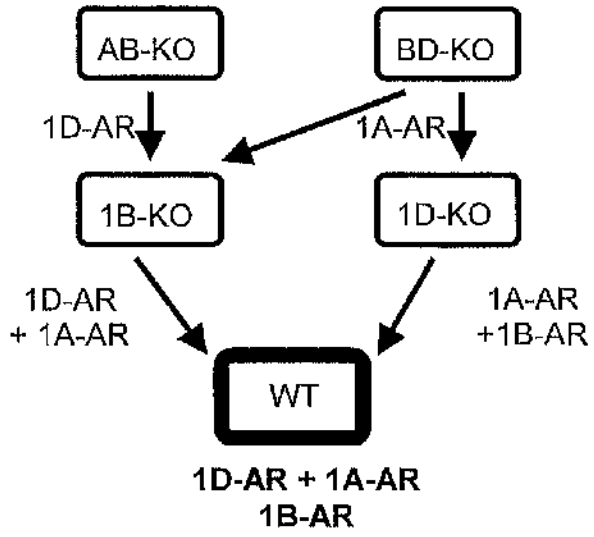

Figure 4.30: Summary of findings in the knockout mice leading to conclusion in WT mouse.

4.4.6. α_{1A}-ARs in the mouse carotid

This is the first study to report the existence of the α_{1A}-AR in the mouse carotid artery. In a study using β-galactosidase staining to identify α_{1A}-AR expression Rokosh and Simpson (2002) did not find any evidence of α_{1A}-AR in the carotid artery. Furthermore, in the only previous functional studies, the contribution of the α_{1A}-AR to contraction in the mouse carotid artery was excluded due to the low affinity estimate calculated for 5-methylurapidil (Deighan C, 2002;Daly *et al.*, 2002a). However, in these studies, 5-methylurapidil was tested only against the phenylephrine-induced response. The present study has shown that phenylephrine has some selectivity for the α_{1D}-AR, which appears to mask the α_{1A}-AR-mediated response.

Evidence for heterogeneity of α_1-AR subtypes in the mouse carotid artery has been previously reported (Deighan C, 2002): a shallow Schild slope was produced for BMY 7378 against phenylephrine in the WT mouse, but a standard Schild slope was obtained in the α_{1B}-KO. This does imply that the α_{1B}-AR may also contribute to the contractile response in the WT mouse. The current study demonstrated that comparison of the phenylephrine-induced response in the knockout mice with the WT mouse revealed an α_{1B}-AR-mediated component to contraction may exist. When considered with the findings of

Deighan (2002), it is possible that all three α_1-AR subtypes contribute to the contractile response to phenylephrine in the carotid artery of the WT mouse.

4.4.7. Conclusion

The utilisation of α_1-AR knockout mice enabled the contractile response in the mouse carotid artery to be studied in the absence of the dominant contractile receptor. The investigation of the α_{1A}-AR in the present study was enhanced by the use of the α_{1A}-AR selective agonist A-61603 and α_1-AR knockout mice. Evidence of an α_{1A}-AR-mediated contractile response was identified in all knockout mice (excluding the $\alpha_{1A/B}$-KO) and an α_{1B}-AR-mediated response appears to exist in the α_{1D}-KO. Thus, all three α_1-AR subtypes are involved in the contractile response in the WT mouse.

Chapter Five

The effect of NO on α_1-AR-mediated contraction

5.1. Introduction

NO is an endothelium derived relaxing factor, which is synthesized from L-arginine by the constitutive enzyme eNOS. The release of NO can be occur under basal conditions (Martin *et al.*, 1986) or following agonist stimulation (Vanhoutte & Miller, 1989), which may occur through a direct or indirect action on ECs. There is also evidence to suggest that the release of NO can occur in response to the contraction of a vessel (Amerini S *et al.*, 1995). Regardless of the mechanism, once released, NO diffuses to vascular SMC where it stimulates soluble guanylate cyclase to release cyclic guanosine monophosphate. This second messenger leads to a decrease in smooth muscle tone, thereby modulating the contractile response.

5.1.1. Spontaneous NO release

Early evidence of spontaneous NO release was reported by Martin et al. (1986). This study demonstrated that in the denuded rat aorta the sensitivity to phenylephrine, noradrenaline, clonidine (selective α_2-AR agonist) and 5-HT was increased compared to intact vessels. In addition, in precontracted vessels in which the endothelium was intact no relaxations were observed in response to the α-AR agonists. These findings suggested that NO release was spontaneous and not in response to agonist stimulation. Subsequent studies have also demonstrated that basal NO release occurs in the rat aorta. For instance, at resting tone L-NAME has been shown to produce a contractile response indicating that NO was being released constitutively (Shimokawa H *et al.*, 1996). NO also appears to be released basally in the mouse aorta, as the 5-HT contractile response was attenuated by L-NAME in a concentration-independent manner (Ali, 2004).

5.1.2. NO release via indirect stimulation

It has been proposed that NO release from the endothelium is indirectly triggered by the agonist-induced vasoconstriction (Dora K, 2001) (Figure 5.1 A). When α_1-ARs in the SMC are activated $[Ca^{2+}]_i$ is released and may diffuse to EC through myoendothelial gap junctions, increasing $[Ca^{2+}]_i$ in EC. eNOS would be activated by this increase in $[Ca^{2+}]_i$ and, therefore, increase the release of NO from ECs. In this way, the agonist activation of SMCs regulates contraction by causing the release of relaxatory substances from the endothelium. It has been proposed that NO is released through the indirect stimulation of EC in the mesenteric artery of the rat (Dora *et al.*, 2000). It was shown that the

phenylephrine-induced response was significantly increased by L-NAME, but the lack of effect of phenylephrine on isolated EC opposed the stimulation of α_1-AR on the endothelium. The findings of this study have been supported by the identification of myoendothelial gap junctions in this vessel (Dora, 2001;Gonzalez Unpublished observations).

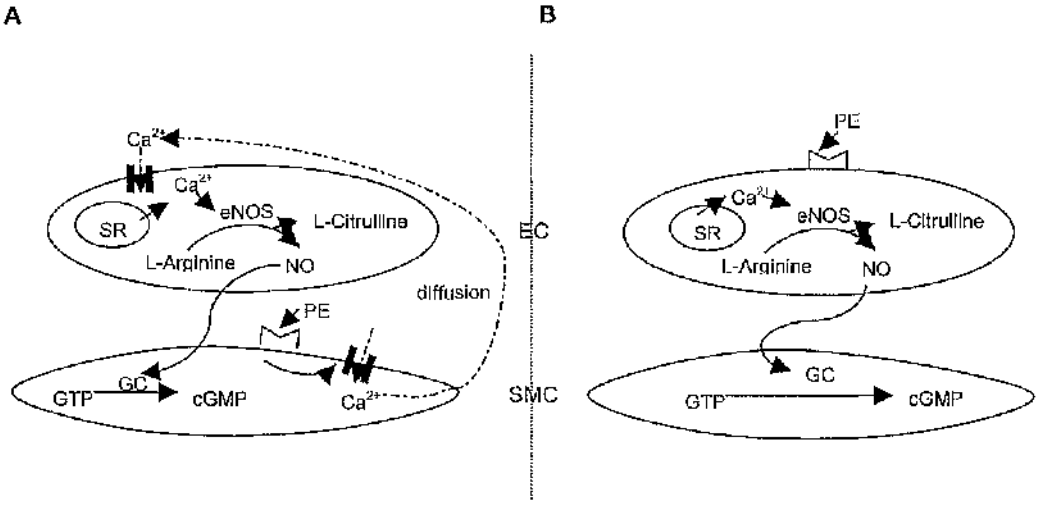

Figure 5.1. Mechanisms of NO release from EC. (A) Indirect via the stimulation of α_1-AR on SMC causing an increase in $[Ca^{2+}]_i$ and diffusion of Ca^{2+} to EC. (B) Direct through the stimulation α_1-AR on EC. In both cases the increase in $[Ca^{2+}]_i$ in the EC activates eNOS, which produces NO from L-Arginine. NO then activates GC in SMC resulting in vascular relaxation. (adapted from Figure 1. Gornik and Creager (2004)).

5.1.3. NO release via direct stimulation

It is plausible that the release of NO from EC may be triggered by the direct agonist stimulation of receptors on the endothelium (Figure 5.1 B). In general, NO release, and the resultant vasodilation, is often associated with the stimulation of endothelial α_2-ARs (Vanhoutte & Miller, 1989;Malekzadeh Shafaroudi M *et al.*, 2005). However, functional evidence of endothelial α_1-ARs is increasingly being reported. Zschauer et al. (1997) reported the first evidence to implicate α_1-ARs on the endothelium. In the rabbit bronchial arteries with an intact endothelium both L-NAME and indomethacin (a cyclooxygenase inhibitor) increased sensitivity to noradrenaline, indicating that NO and a prostanoid were being released and were suppressing vasoconstriction. In denuded arteries, sensitivity to phenylephrine and UK 14,304 (an α_2-AR agonist) was increased suggesting that both α_1-ARs and α_2-ARs may be involved in the release of the endothelium-derived relaxing factors. Furthermore, in vessels with an intact endothelium, L-NAME markedly

potentiated the contractile response to phenylephrine. The direct agonist stimulation of α_1-ARs on the endothelium, triggering NO release, could account for these findings.

Further evidence that the direct stimulation of α_1-AR on the endothelium leads to a relaxatory response was reported by Filippi et al. (2001). In the perfused rat mesenteric vascular bed, subnanomolar concentrations of phenylephrine and noradrenaline produced relaxations, which were followed by a sustained contraction at higher agonist concentrations. In denuded vessels, no relaxations to the α_1-AR agonists were observed. Therefore, the relaxant responses mediated by α_1-ARs appear to be a result of the direct stimulation of receptors on the endothelium. Although, the α_{1A}-AR selective antagonist had no effect, the relaxant response was inhibited by the α_{1D}-AR selective antagonist BMY 7378. It is, therefore, apparent that in the rat mesenteric vascular bed the response to phenylephrine involved an α_1-AR-mediated contractile response in SMC and a relaxatory response through the stimulation of α_{1D}-ARs in ECs.

In a recent study a phenylephrine-induced relaxatory response was observed at subnanomolar concentrations in the rat carotid artery (de Andrade C *et al.*, 2006). In the absence of the endothelium, or in the presence of L-NAME, the relaxations to phenylephrine were not observed. This indicates that phenylephrine was stimulating an endothelium-dependent release of NO. Furthermore, prazosin and BMY 7378, but not yohimbine (α_2-AR antagonist), inhibited the relaxations. These findings suggest that the phenylephrine-induced relaxatory response in the rat carotid artery was induced by the stimulation of α_1-ARs on endothelium, triggering NO release. In agreement with Filippi et al. (2001), the α_1-ARs on the endothelium appeared to be predominantly α_{1D}-ARs.

In addition, in a fluorescent ligand binding study investigating α_2-ARs in the thoracic aorta, binding to ECs was inhibited by prazosin (Malekzadeh Shafaroudi M *et al.*, 2005). This study in our laboratory provided preliminary evidence that α_1-ARs may exist on the endothelium.

5.1.4. Conduit arteries

Previous studies have shown that EDHF is less important in conductance arteries than resistance arteries (Shimokawa H *et al.*, 1996;Scotland RS *et al.*, 2005). Furthermore, NO production by ECs is highest at the aortic arch and becomes low at the abdominal aorta (Balbatun *et al.*, 2003). These findings imply that NO is likely to be an important

endothelial factor in the mouse carotid artery. Consequently, the role of NO in the contraction of the mouse carotid artery was investigated in this chapter.

Several studies in rat and mouse aortae have revealed NO release from ECs as a result of stimulation with noradrenaline (Kaneko & Sunano, 1993;Malekzadeh Shafaroudi M *et al.*, 2005), and phenylephrine (Tabernero *et al.*, 1999;Kaneko & Sunano, 1993;Gurdal *et al.*, 2005). Although phenylephrine has been shown to result in NO release in the rat carotid artery (de Andrade C *et al.*, 2006), the involvement of NO in relation to α_1-AR-mediated contraction has not been investigated in the mouse carotid artery.

5.1.5. Aims

The present study evaluated the role of NO on α_1-AR-mediated contraction in the carotid artery, by inhibiting the NO pathway using the L-arginine analogue L-NAME to inhibit NOS.

The aims of the present study were:

- To assess the effect of L-NAME on the basal tone of the mouse carotid artery and, in doing so, establish whether NO release in this vessel was spontaneous or stimulated.

- To investigate the effect of NO on α_1-AR-mediated contractions in the carotid artery.

5.2. Methods

The dissection, vessel mounting and acclimatisation period are described in detail in Chapter two. In brief, four-five-month old male WT mouse (C57 Black; 26g-44g), α_{1D}-KO (25-34g) and $\alpha_{1B/D}$-KO (32-54g) mice were killed by carbon dioxide overdose and both common carotid arteries were dissected. Following cleaning, vessels were mounted in a four-chamber wire myograph containing gassed (95% O_2 / 5% CO_2) and heated (37°C) PSS. Vessels were allowed to acclimatise for 30 minutes before a resting tension of 0.25g was added to each vessel and a further 45 minutes acclimatisation period prior to the start of the experimental protocol.

5.2.1. Effect of L-NAME on basal tone

The effect of L-NAME on basal tone was tested with and without prior stimulation with phenylephrine or A-61603. For the first set of experiments, without a wake-up procedure or agonist CRC, a NOS inhibitor, L-NAME 0.1 mM was added and the tone was observed for 40 minutes. This observation time was used as it would be used as the incubation time for L-NAME in subsequent experiments. For the second set of experiments, the wake-up procedure was performed for phenylephrine or A-61603 as described in Chapter Two. Following CRCs to phenylephrine (1 nM – 0.1 mM) or A-61603 (1 nM – 0.1 mM), vessels were washed with PSS and rested over a period of 30 minutes. L-NAME 0.1 mM was added and the tone was observed for 40 minutes.

5.2.2. The effect of L-NAME on the response to α_1-AR agonists

After performing the wake-up procedure (as described in Chapter Two), CRCs to phenylephrine (1 nM – 0.1 mM) or A-61603 (1 nM – 0.1 mM) were produced using half-log increments. Prior to the second CRC, vessels were incubated for 40 minutes with L-NAME 0.1mM. At the end of the protocol acetylcholine 3 μM was added to test whether the relaxation of the vessel had been inhibited. A second CRC to phenylephrine or A-61603 was produced in the absence of L-NAME, acting as a time control.

5.2.3. Statistical analysis

Data were expressed as means ± standard error in grams tension and percentage of the maximum response of the control CRC. A Student's t-test or one-way ANOVA, followed by a Bonferroni's post test was used to compare the maximum responses, pEC_{50} values of the agonist response in the absence or presence of either L-NAME. CRCs were compared using two-way-ANOVA with a Bonferroni post-test. Nonlinear regression was performed to fit sigmoidal-curves (variable slope) on mean data of responses in grams and percentage of the maximum response.

5.3. Results

5.3.1. Effect of L-NAME on basal tone

5.3.1.1. WT mouse

In the WT mouse, basal tone was unaltered by L-NAME when the vessels had not been previously stimulated but was significantly increased in the presence of L-NAME with prior stimulation to phenylephrine or A-61603 (Figure 5.2; Table 5.1).

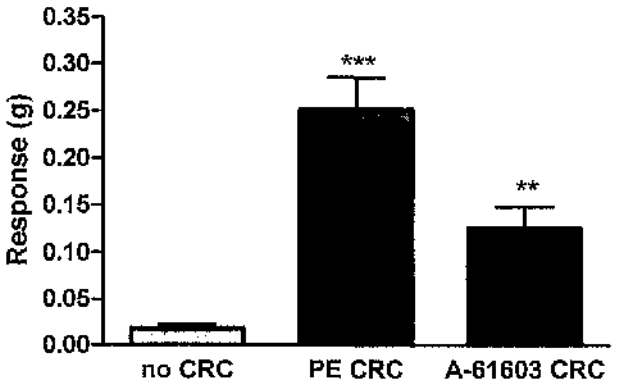

Figure 5.2. WT mouse: Effect of prior stimulation on the maximum response obtained to L-NAME 0.1mM, expressed as mean ± S.E. in grams tension (n>6). ** p<0.01, *** p<0.001 compared to maximum response without prior stimulation.

Table 5.1. Effect of prior stimulation on the maximum response to L-NAME 0.1mM in the WT mouse.

Protocol	n	Maximum response to L-NAME (g)
No CRC	6	0.02±0.004
PE CRC	8	0.25±0.03***
A-61603 CRC	7	0.13±0.02**

**** p<0.01; ***p<0.001 compared to maximum response without prior stimulation (one-way ANOVA, Bonferroni's post test).**

5.3.1.2. α_{1D}-KO

In the α_{1D}-KO, basal tone was unaltered by L-NAME when the vessels had not been previously stimulated (Figure 5.3; Table 5.2). Basal tone was not significantly increased in the presence of L-NAME with prior stimulation to phenylephrine but was significantly increased following stimulation with A-61603.

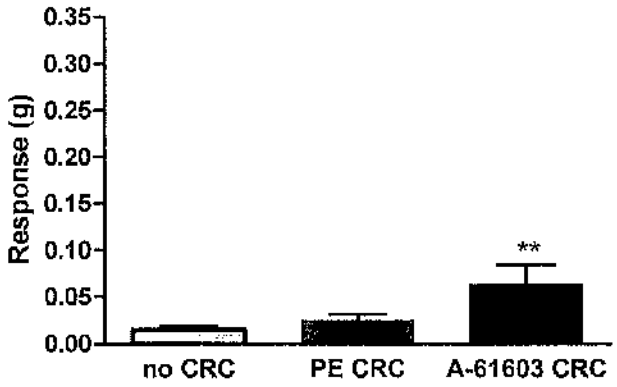

Figure 5.3. α_{1D}-KO: Effect of prior stimulation on the maximum response obtained to L-NAME 0.1 mM, expressed as mean ± S.E. in grams tension (n>5). ** p<0.01 compared to maximum response without prior stimulation.

Table 5.2. Effect of prior stimulation on the maximum response to L-NAME 0.1mM in the α_{1D}-KO.

Protocol	n	Maximum response to L-NAME (g)
No CRC	5	0.01±0.004
PE CRC	6	0.02±0.01***
A-61603 CRC	5	0.06±0.02**

****p<0.01; ***p<0.001 compared to maximum response without prior stimulation (one-way ANOVA, Bonferroni's post test).**

5.3.1.3. $\alpha_{1B/D}$-KO

In the $\alpha_{1B/D}$-KO, basal tone was unaltered by L-NAME when the vessels had not been previously stimulated (Figure 5.4; Table 5.3). A significant increase in basal tone was observed in the presence of L-NAME with prior stimulation to phenylephrine or A-61603.

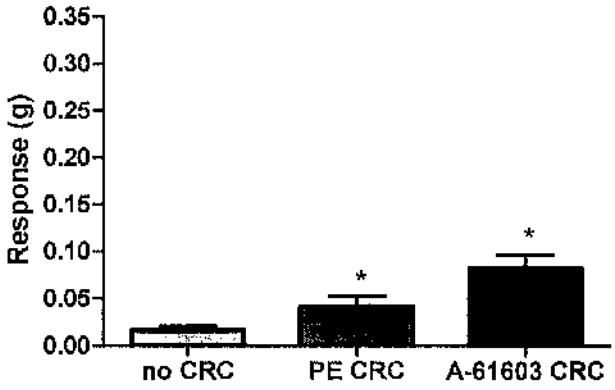

Figure 5.4. $\alpha_{1B/D}$-KO: Effect of prior stimulation on the maximum response to L-NAME 0.1mM, expressed as mean ± S.E. in grams tension (n>5). * p<0.05 compared to maximum response obtained without prior stimulation.

Table 5.3. Effect of prior stimulation on the maximum response to L-NAME 0.1mM in the $\alpha_{1B/D}$-KO.

Protocol	n	Maximum response to L-NAME (g)
No CRC	5	0.02±0.004
PE CRC	5	0.04±0.01*
A-61603 CRC	8	0.08±0.01*

***p<0.05 compared to maximum response without prior stimulation (one-way ANOVA, Bonferroni's post test).**

5.3.2. Effect of L-NAME in the WT mouse

5.3.2.1. Phenylephrine-induced response

In the WT mouse, phenylephrine produced concentration-dependent contractions in the WT mouse in the presence of L-NAME (Figure 5.5; Table 5.4). L-NAME 0.1mM significantly increased the average maximum response obtained to phenylephrine by 79% compared with the control CRC.

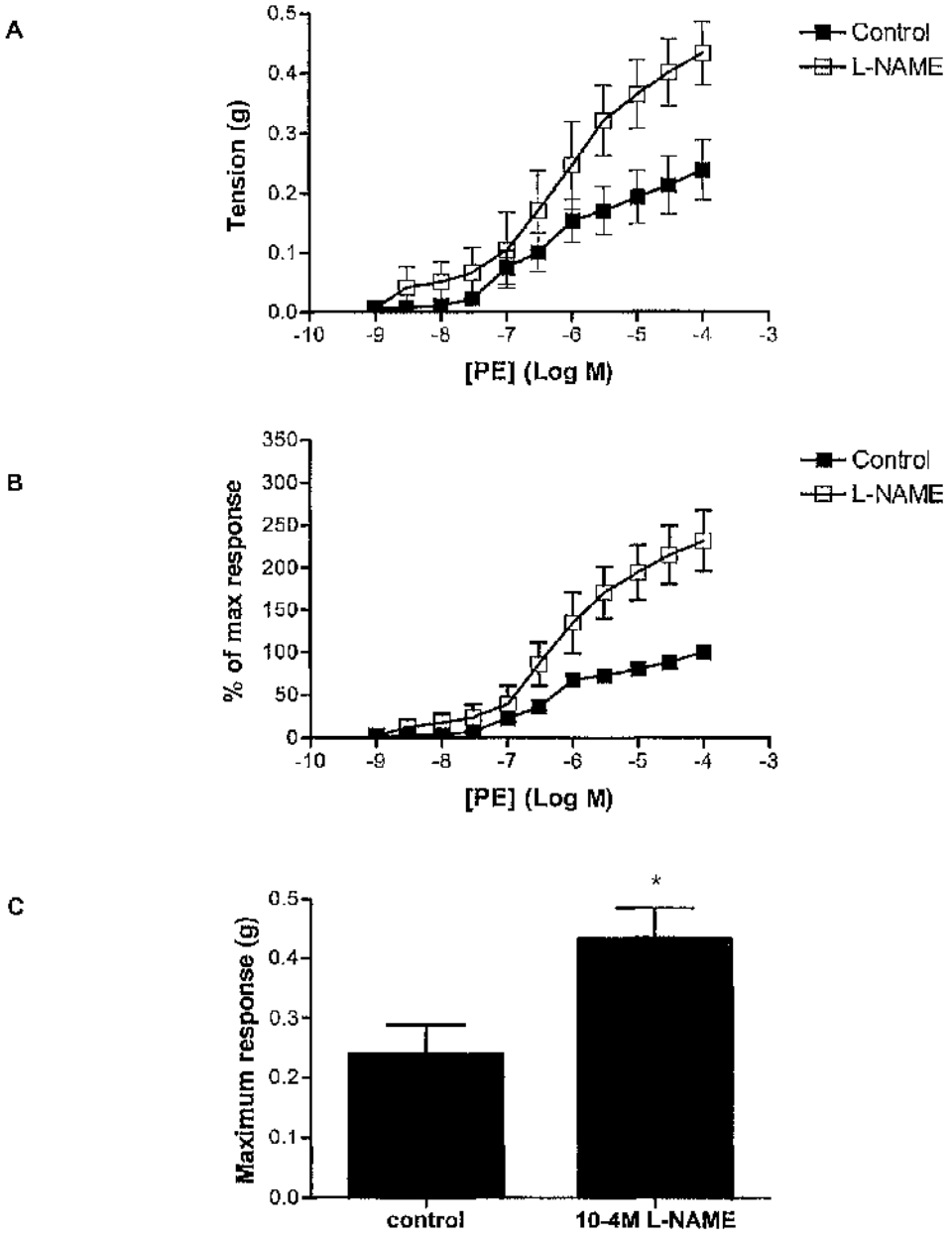

Figure 5.5. WT mouse: Effect of L-NAME on phenylephrine CRC in (A) grams tension and (B) percentage of maximum response of the control CRC. (C) Effect of L-NAME on the maximum response obtained to phenylephrine in grams tension. Data expressed as mean ± S.E. (n=7). * $p<0.05$ compared to phenylephrine control (Student's t-test).

Table 5.4. Comparison of phenylephrine CRCs in the presence of L-NAME 0.1mM in the WT mouse.

Agonist	n	pEC_{50}	Maximum response (g)	Hill slope (95% CI)
PE control	7	6.4±0.08	0.24±0.05	0.6 (0.5-0.6)
L-NAME 0.1 mM	7	$7.1\pm0.43^{+}$	$0.43\pm0.05^{*}$	$0.5\ (0.5\text{-}0.6)^{+}$

5.3.2.2. A-61603-induced response

In the presence of L-NAME 0.1mM concentration-dependent contractions to A-61603 were produced (Figure 5.6; Table 5.5). An increase of 37% in the average maximum response to A-61603 in the presence of L-NAME did not reach significance.

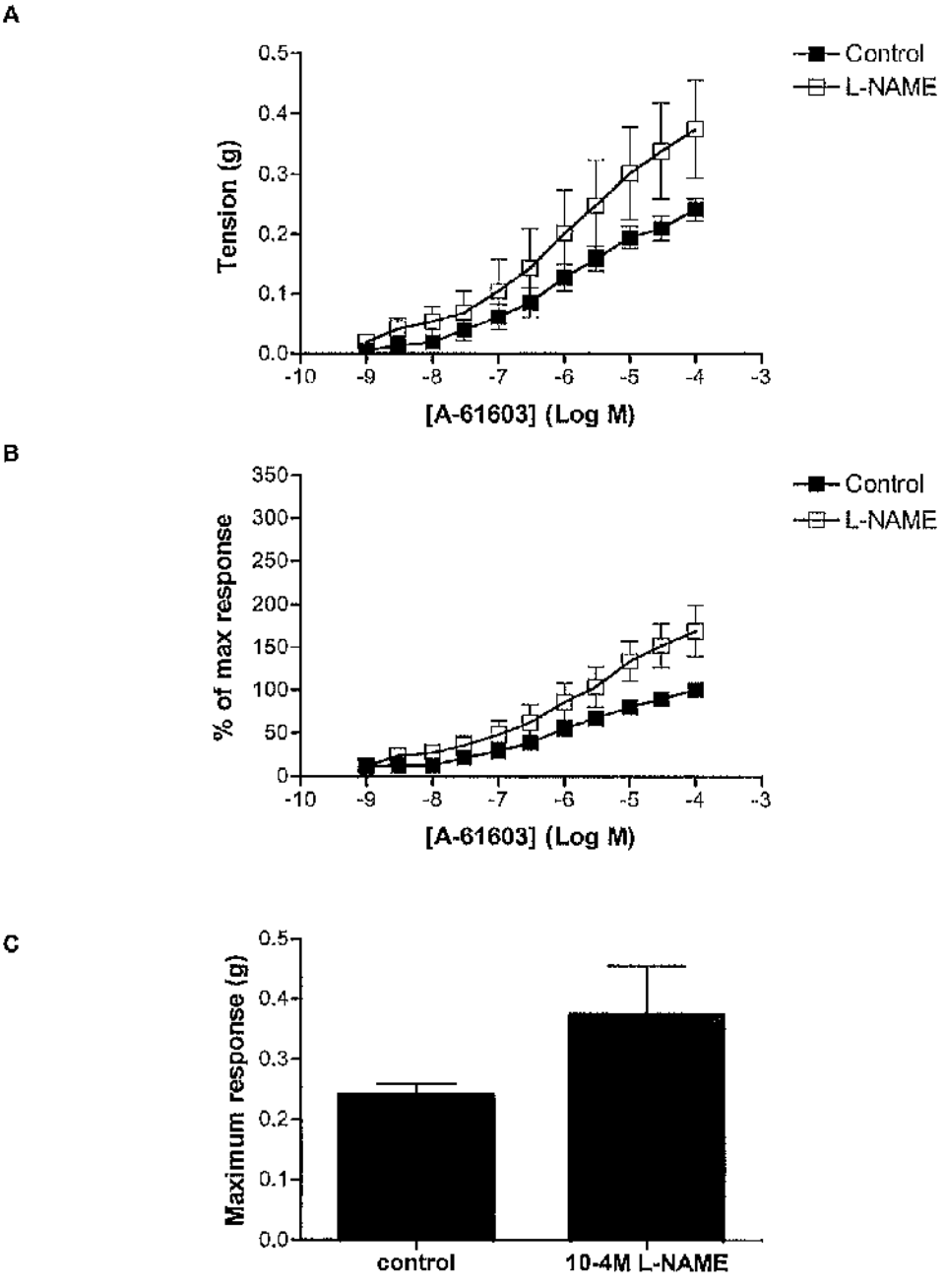

Figure 5.6. WT mouse: The effect of L-NAME on the CRC to A-61603 in (A) grams tension and (B) percentage of maximum response of the control CRC. (C) Effect of L-NAME on the maximum response obtained to A-61603 in grams tension. Data expressed as means ± S.E. (n=6).

Table 5.5. Comparison of A-61603 CRCs in the presence of L-NAME 0.1mM.

Agonist	n	pEC_{50}	Maximum response (g)	Hill slope (95% CI)
A-61603 control	6	6.1±0.14	0.24±0.02	0.4 (0.4-0.5)
L-NAME 0.1 mM	6	6.8±0.41^{+}	0.38±0.08^{+}	0.4 (0.4-0.4)$^{+}$

+ p>0.05 compared to A-61603 control (Student's t-test).

5.3.3. Effect of L-NAME in the α_{1D}-KO

5.3.3.1. Phenylephrine-induced response

In the α_{1D}-KO, phenylephrine produced concentration-dependent contractions in the α_{1D}-KO in the presence of L-NAME (Figure 5.7; Table 5.6). An average increase of 60% was observed for the phenylephrine response in the presence of 0.1mM L-NAME.

Table 5.6. Comparison of phenylephrine CRCs in presence of L-NAME 0.1mM in the α_{1D}-KO.

Agonist	n	pEC_{50}	Maximum response (g)	Hill slope (95% CI)
PE control	6	5.7±0.09	0.20±0.02	1.1 (0.0-1.1)
L-NAME 0.1 mM	6	5.9±0.08^{+}	0.32±0.04**	1.0 (0.9-1.0)$^{+}$

+ p>0.05, ** p<0.01 compared to phenylephrine control (Student's t-test).

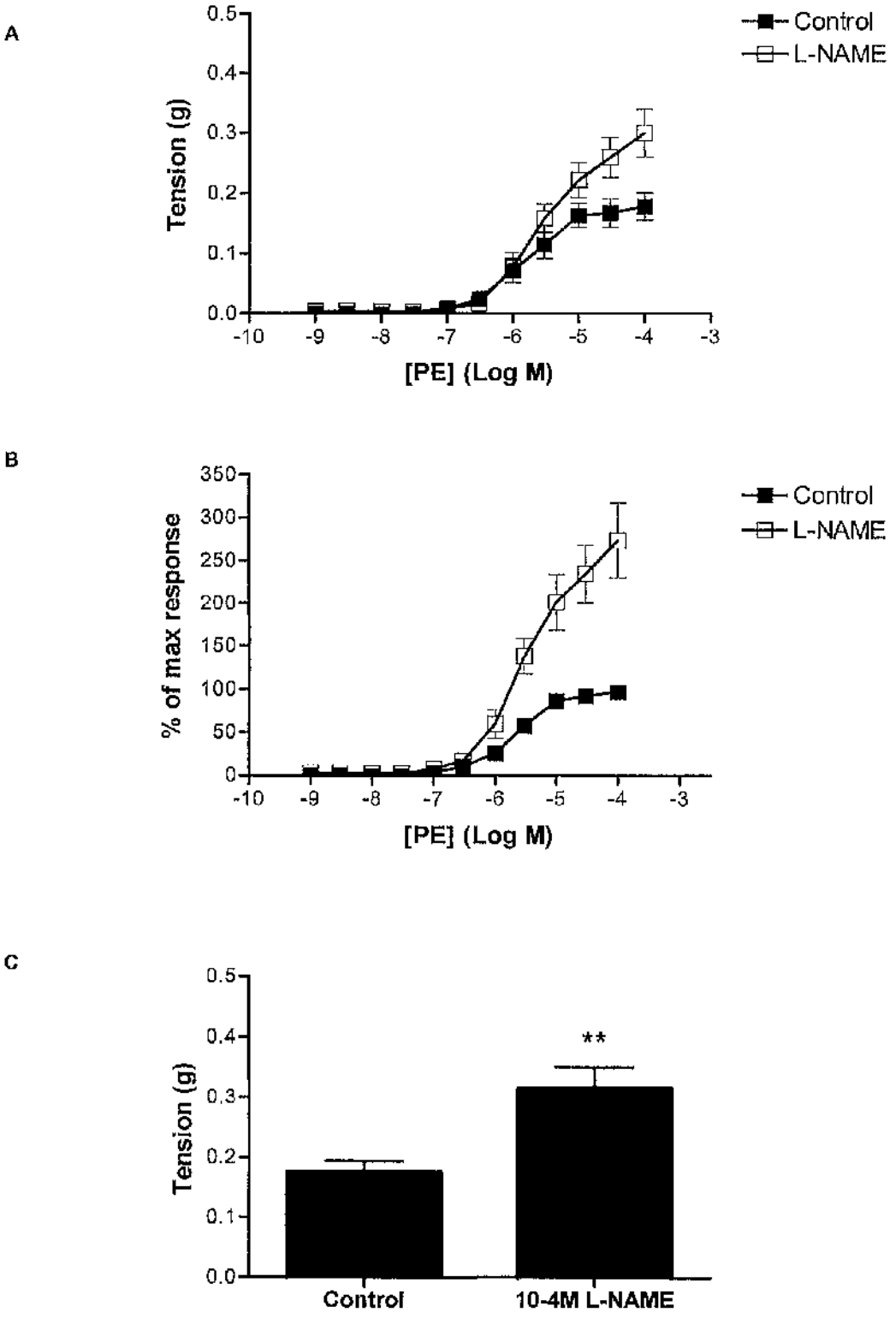

Figure 5.7. α_{1D}-KO: The effect of L-NAME on the CRC to phenylephrine in (A) grams tension and (B) percentage of maximum response of the control CRC. (C) Effect of L-NAME on the maximum response obtained to phenylephrine in grams tension. Data expressed as mean ± S.E. (n=6). ** p<0.01 compared to phenylephrine control (Student's t-test).

5.3.3.2. A-61603-induced response

Concentration-dependent contractions to A-61603 were produced in the presence of L-NAME (Figure 5.8; Table 5.7). The maximum response obtained to A-61603 was increased by 62% in the presence of 0.1mM L-NAME.

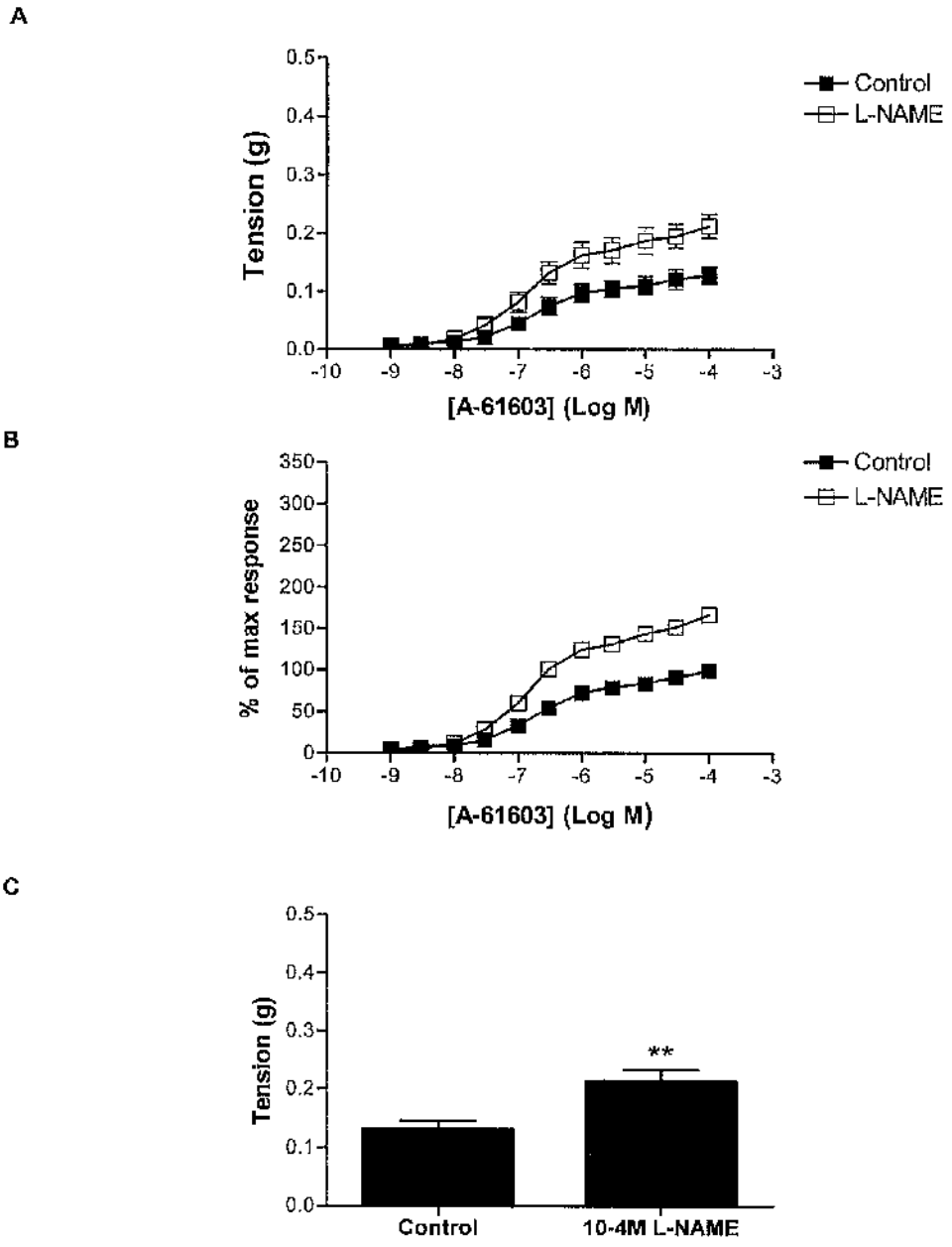

Figure 5.8. α_{1D}-KO: The effect of L-NAME on the CRC to A-61603 in (A) grams tension and (B) percentage of maximum response of the control CRC. (C) Effect of L-NAME on the maximum response obtained to A-61603 in grams tension. Data expressed as means ± S.E. (n=6). ** p<0.01 compared to phenylephrine control (Student's t-test).

Table 5.7. Comparison of A-61603 CRCs in the presence of L-NAME 0.1mM in the α_{1D}-KO.

Agonist	n	pEC_{50}	Maximum response (g)	Hill slope (95% CI)
A-61603 control	6	6.7±0.14	0.13±0.02	0.7 (0.7-0.8)
L-NAME 0.1 mM	6	7.3±0.17*	0.23±0.02***	0.7 (0.7-0.8)+

+ p>0.05, * p<0.05, *** p<0.001 compared to phenylephrine control (Student's t-test).

5.3.4. Effect of L-NAME in the $\alpha_{1B/D}$-KO

5.3.4.1. Phenylephrine-induced response

In the $\alpha_{1B/D}$-KO phenylephrine produced concentration-dependent contractions in the $\alpha_{1B/D}$-KO in the presence of L-NAME (Figure 5.9; Table 5.8). An average increase of 233% in the maximum response obtained to phenylephrine was observed in the presence of L-NAME.

Table 5.8. Comparison of phenylephrine CRCs in the presence of L-NAME 0.1mM in the $\alpha_{1B/D}$-KO.

Agonist	n	pEC_{50}	Maximum response (g)	Hill slope (95% CI)
PE control	6	5.0±0.12	0.06 ±0.01	1.1 (1.0-1.2)
L-NAME 0.1 mM	6	6.1±0.39**	0.20 ±0.06**	1.0 (0.9-1.2)+

+ p>0.05, ** p<0.01, *** p<0.001 compared to phenylephrine control (Student's t-test).

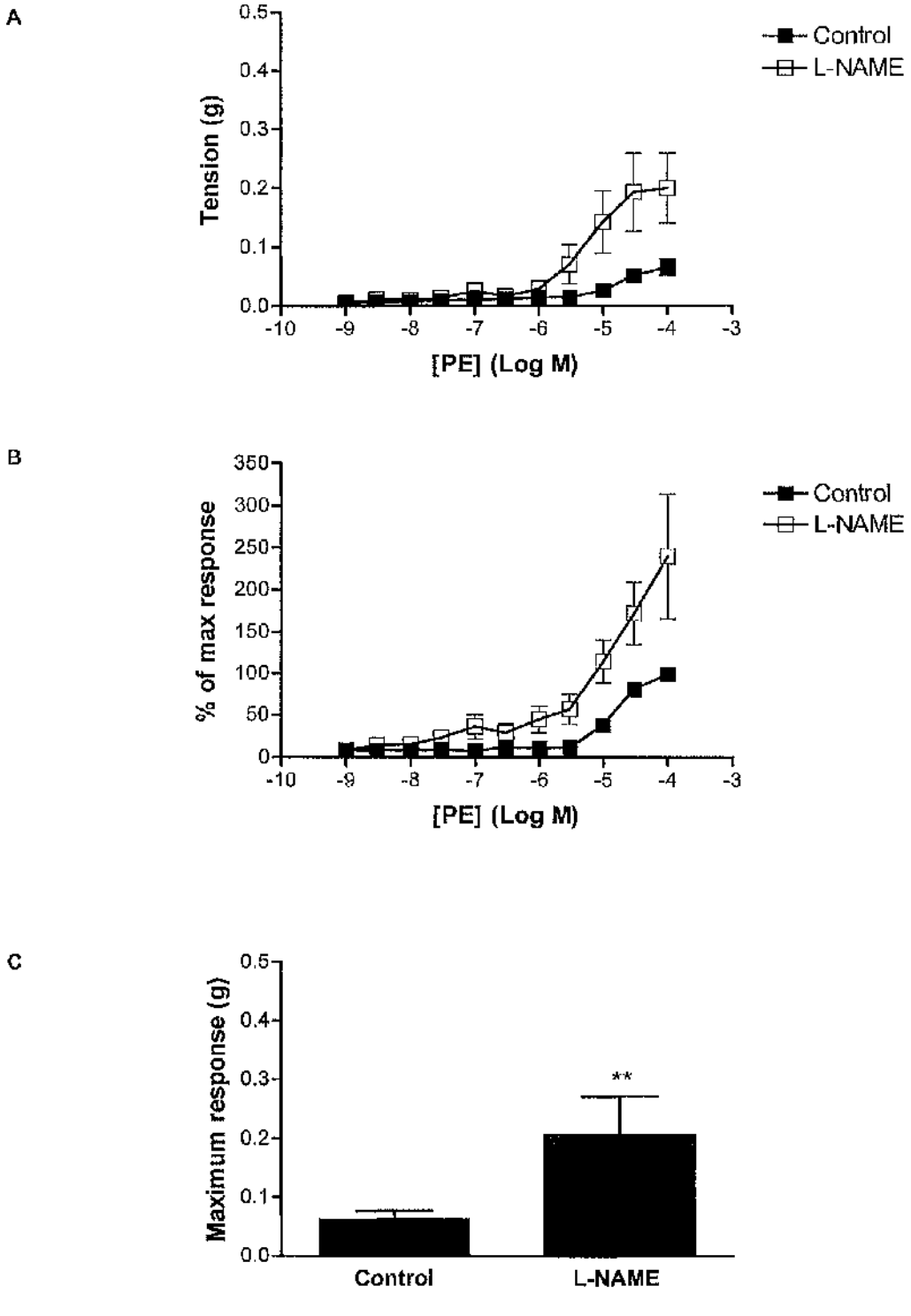

Figure 5.9. $\alpha_{1B/D}$**-KO: The effect of L-NAME on the CRC to phenylephrine in (A) grams tension and (B) percentage of maximum response of the control CRC. (C) Effect of L-NAME on maximum response obtained to phenylephrine in grams tension. Data expressed as means ± S.E. (n=6).** ** $p<0.01$ **compared to phenylephrine control (Student's t-test).**

5.3.4.2. A-61603-induced response

A-61603 produced concentration-dependent contractions in the $\alpha_{1B/D}$-KO in the presence of L-NAME (Figure 5.10; Table 5.9). The maximum response obtained for the A-61603 CRC showed an average increase of 69% in the presence of L-NAME.

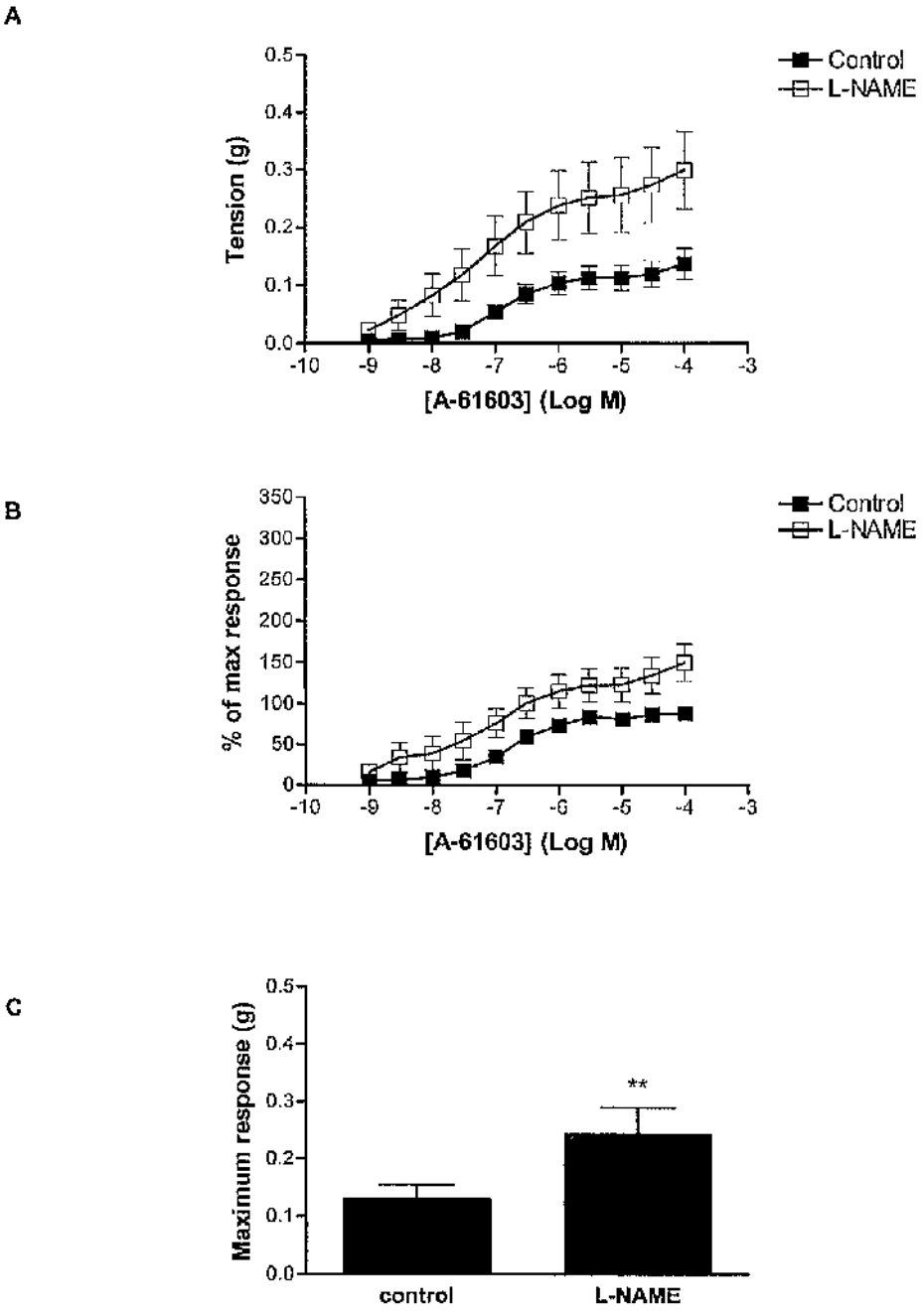

Figure 5.10. $\alpha_{1B/D}$-KO: The effect of L-NAME on the CRC to A-61603 in (A) grams tension and (B) percentage of maximum response of the control CRC. (C) Effect of L-NAME on maximum response obtained to A-61603 in grams tension. Data expressed as means ± S.E. (n=6). ** p<0.01 compared to A-61603 control (Student's t-test).

Table 5.9. Comparison of A-61603 CRCs in the presence of L-NAME 0.1mM in the $\alpha_{1B/D}$-KO.

Agonist	*n*	*pEC_{50}*	*Maximum response (g)*	*Hill slope (95% CI)*
A-61603 control	6	6.7±0.12	0.14 ±0.03	0.9 (0.7-1.0)
L-NAME 0.1 mM	6	7.6±0.38**	0.24 ±0.04**	0.8 (0.4-1.1)+

+ p>0.05, ** p<0.01 compared to A-61603 control (Student's t-test).

5.3.4.3. 5-HT-induced response

In the $\alpha_{1B/D}$- KO, 5-HT produced concentration-dependent contractions in the presence of L-NAME but the 5-HT CRC was unaffected by the presence of L-NAME (Figure 5.11; Table 5.10).

Table 5.10. Comparison of 5-HT CRCs in presence of L-NAME 0.1mM in the $\alpha_{1B/D}$-KO.

Agonist	*n*	*pEC_{50}*	*Maximum response (g)*	*Hill slope (95% CI)*
5-HT control	6	6.7±0.06	0.30±0.02	2.6 (1.7-3.5)
L-NAME 0.1 mM	6	7.0±0.14+	0.32±0.04+	2.4 (1.1-3.6)+

+ p>0.05 compared to A-61603 control (Student's t-test).

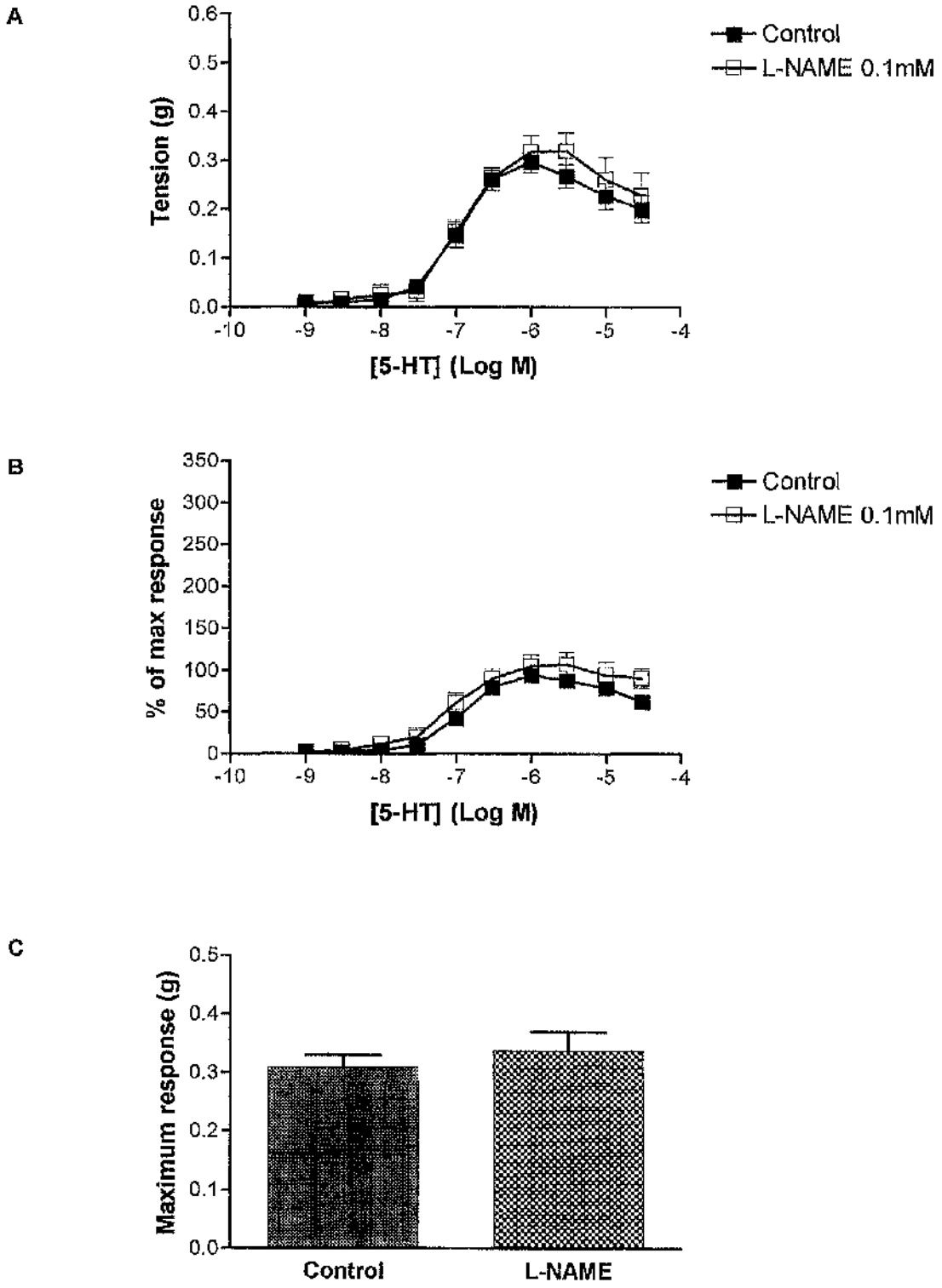

Figure 5.11. $\alpha_{1B/D}$-KO: The effect of L-NAME on the CRC to 5-HT in (A) grams tension and (B) percentage of maximum response of the control CRC. (C) Effect of L-NAME on the maximum response to 5-HT in grams tension. Data expressed as means ± S.E. (n=6).

5.3.5. Comparison of effect of L-NAME in the WT mouse and knockouts

5.3.5.1. Phenylephrine-induced response

In the presence of L-NAME, phenylephrine produced concentration-dependent contractions in the WT mouse, α_{1D}-KO and $\alpha_{1B/D}$-KO (Figure 5.12; Table 5.11). The maximum response obtained to phenylephrine was significantly higher in the WT mouse in the presence of L-NAME than the $\alpha_{1B/D}$-KO but not the α_{1D}-KO (0.32±0.04g). The pEC_{50} values for the phenylephrine-induced response in the presence of L-NAME were significantly different in the α_{1D}-KO and $\alpha_{1B/D}$- KO compared to the WT mouse.

Table 5.11. Comparison of the WT mouse, α_{1D}-KO and $\alpha_{1B/D}$-KO: the effect of L-NAME on the phenylephrine-induced response.

	phenylephrine alone			phenylephrine + L-NAME		
	pEC_{50}	Maximum response (g)	Hill slope (95% CI)	pEC_{50}	Maximum response (g)	Hill slope (95% CI)
WT mouse	6.4±0.08	0.24±0.05	0.9 (0.5-1.3)	7.1±0.43	0.43±0.05	1.0 (0.6-1.4)
α_{1D}-KO	5.6±0.06**	0.22±0.02^{-}	1.2 (0.9-1.6)$^{+}$	5.9±0.08^{+}	0.32±0.04^{+}	1.1 (0.9-1.3)$^{+}$
$\alpha_{1B/D}$-KO	4.9±0.07***	0.06 ±0.01***	1.2 (0.6-1.9)$^{+}$	6.1±0.39^{+}	0.20 ±0.06*	0.8 (0.3-1.8)$^{+}$

$^{+}$p>0.05, * p<0.05, ** p<0.01, *** p<0.001 compared to WT mouse (one-way ANOVA, Bonferroni's post test).

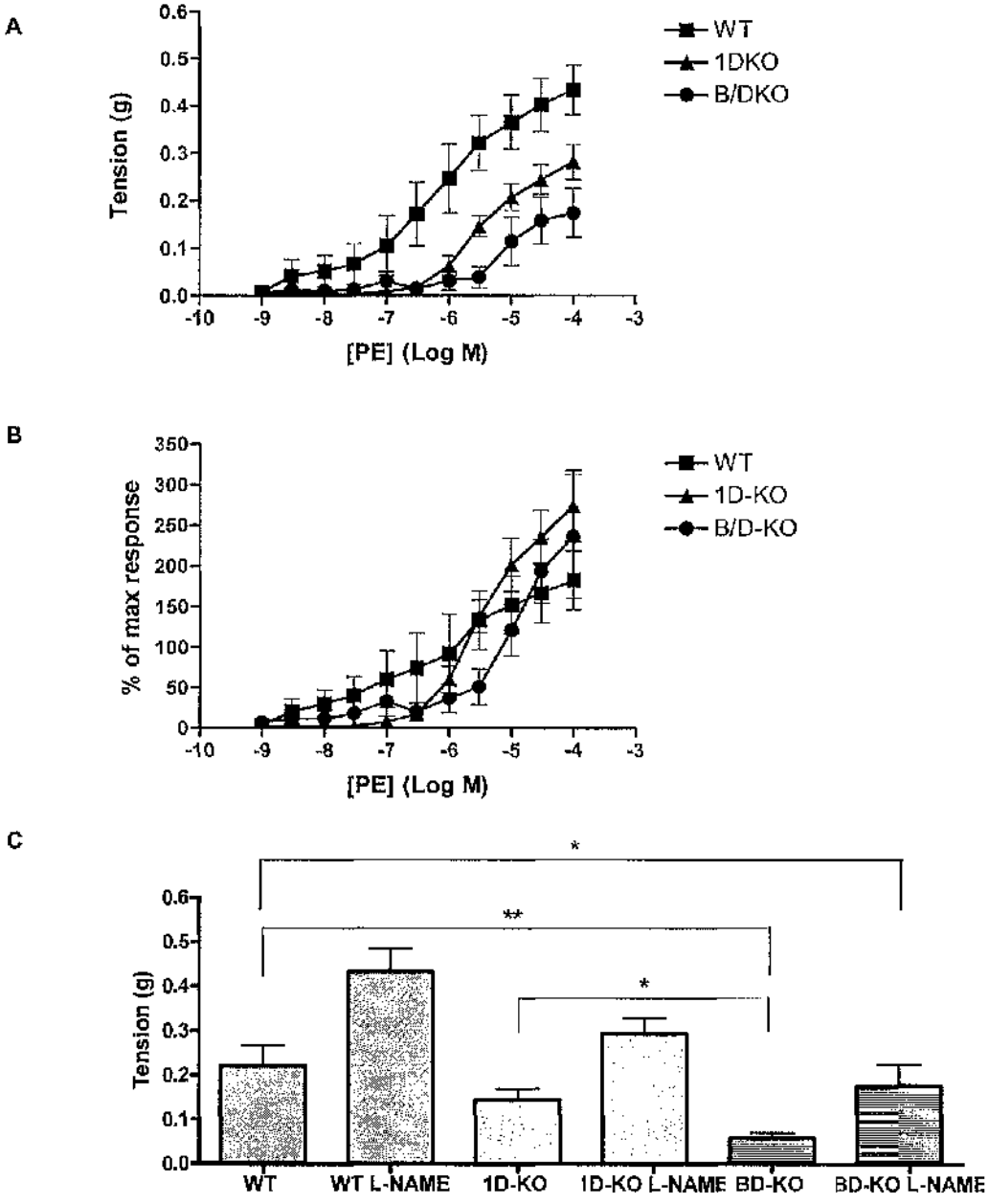

Figure 5.12. Comparison of the WT mouse, α_{1D}-KO and $\alpha_{1B/D}$-KO: the effect of L-NAME on CRCs to phenylephrine in (A) grams tension and (B) percentage of maximum response of the control CRC. (C) Effect of L-NAME on the maximum response obtained to phenylephrine in grams tension. Data expressed as means ± S.E. (n>6). * p<0.05, ** p<0.01 (one-way ANOVA, Bonferroni's post test).

5.3.5.2. A-61603-induced response

In the presence of L-NAME, concentration-dependent contractions to A-61603 were observed in all three strains of mice (Figure 5.13; Table 5.12). No significant differences were observed between strains.

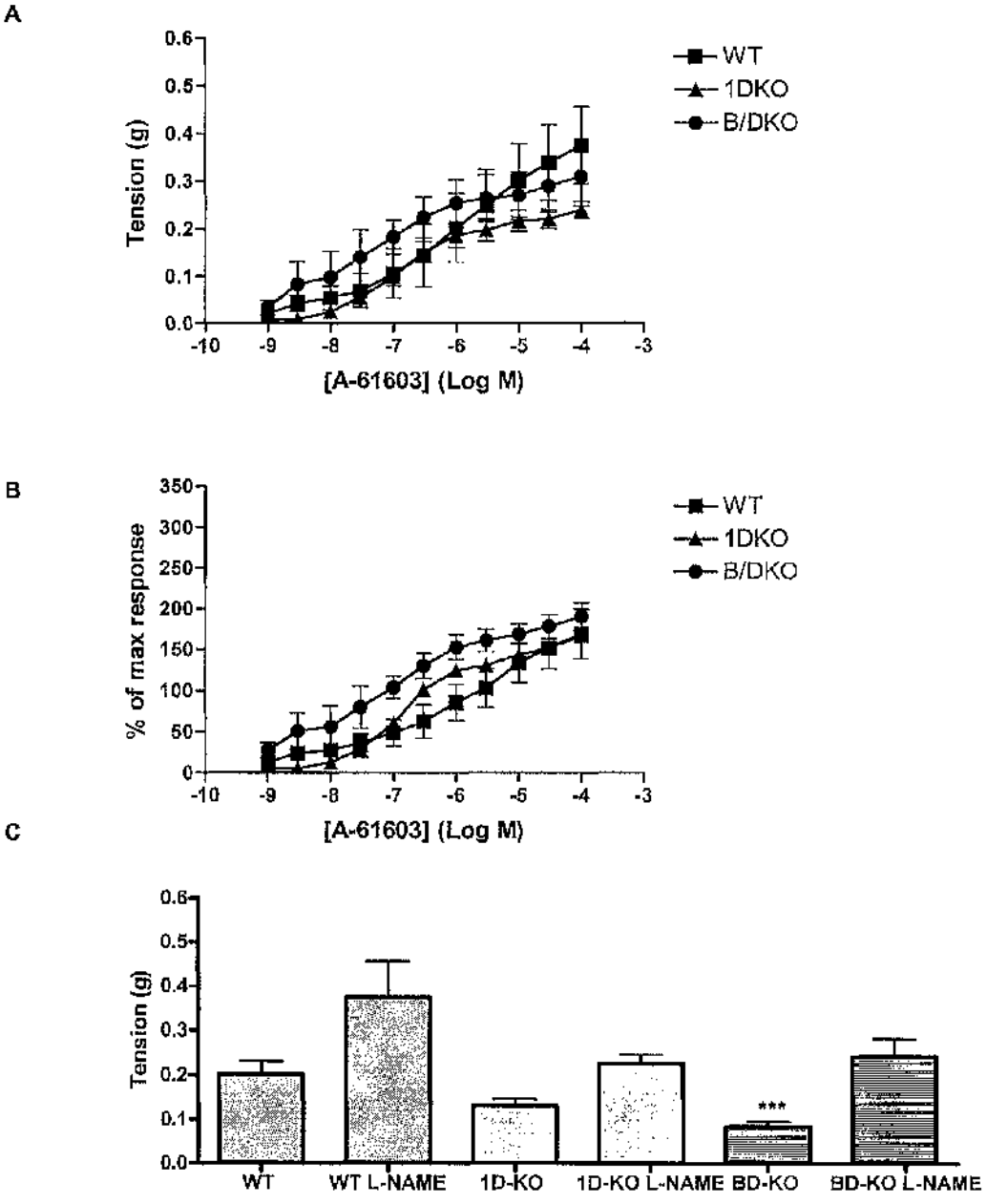

Figure 5.13. Comparison of the WT mouse, α_{1D}-KO and $\alpha_{1B/D}$-KO: the effect of L-NAME on CRCs to A-61603 in in (A) grams tension and (B) percentage of maximum response of the control CRC. (C) Effect of L-NAME on the maximum response obtained to phenylephrine in grams tension expressed as means ± S.E. (n>6). *** p<0.01 compared to WT mouse (one-way ANOVA, Bonferroni's post test).

Table 5.12. Comparison of the WT mouse, α_{1D}-KO and $\alpha_{1B/D}$-KO: the effect of L-NAME on the A-61603-induced response.

	A-61603 alone			A-61603 + L-NAME		
	pEC_{50}	Maximum response (g)	Hill slope (95% CI)	pEC_{50}	Maximum response (g)	Hill slope (95% CI)
WT mouse	6.0±0.06	0.27±0.05	0.6 (0.3-0.9)	6.8±0.41	0.38±0.08	0.5 (0.2-0.7)
α_{1D}-KO	$6.9\pm0.06^{\#\#\#}$	$0.14\pm0.01^{*}$	$0.6\ (0.2\text{-}0.9)^{+}$	$7.3\pm0.17^{+}$	$0.23\pm0.02^{+}$	$0.7\ (0.3\text{-}1.2)^{-}$
$\alpha_{1B/D}$-KO	$6.7\pm0.07^{\#\#\#}$	$0.13\pm0.01^{*}$	$0.9\ (0.7\text{-}1.1)^{+}$	$7.6\pm0.38^{+}$	$0.24\pm0.04^{+}$	$0.8\ (0.4\text{-}1.1)^{+}$

$^{+}$ p>0.05, * p<0.05, *** p<0.001 compared to WT mouse (one-way ANOVA, Bonferroni's post test).

5.4. Discussion

In the present study it was confirmed that NO had a functional role in the mouse carotid artery. The role of NO was further investigated by determining whether NO release was spontaneous, stimulated by α_1-AR agonists indirectly through the activation of SMC α_1-ARs, or through the direct stimulation of α-ARs on the endothelium.

5.4.1. Spontaneous NO release

To assess whether NO was released constitutively, the direct effect of L-NAME on basal tone was investigated. No increase in basal tone was observed in response to L-NAME in the absence of prior α_1-AR stimulation in any of the mouse strains. If spontaneous myogenic tone is suppressed by basal NO release, inhibition of NO results in an increase in tone (Rees *et al.*, 1990). Therefore, this possibility can be ruled out. It is possible that NO was being released spontaneously but did not have an effect in the mouse carotid artery, therefore, no increase was observed. Alternatively, it is possible that spontaneous NO release was simply not occurring in this vessel. From this data, neither scenario could be excluded. However, this was clarified with the subsequent experiments.

5.4.2. Stimulated NO release

5.4.2.1. Effect of L-NAME on basal tone

In order to determine whether NO release was stimulated by α_1-AR activation the effect of L-NAME with prior exposure to phenylephrine and A-61603 was investigated. In vessels which had been previously stimulated by the α_1-AR agonists, contractions were observed in response to L-NAME. Firstly, this confirms that NO release was occurring in the mouse carotid artery. Secondly, this increase in tone, indicates that NO release was stimulated by α_1-AR activation, rather than spontaneous NO release. It is possible that the increase in tone was due to the α_1-AR agonists activating SMC contraction and it was the contraction that caused NO release. However, this study has demonstrated that the 5-HT CRC was not affected by L-NAME (See section 5.4.2.2.), which opposes the possibility that the contraction itself was causing NO release. Alternatively, the agonist may have still been available to activate the receptors and, therefore, cause both contraction, through the stimulation of α_1-ARs on SMC, and relaxation, through the activation of endothelial receptors. It appears that NO release was suppressing contraction, which was removed in the presence of L-NAME and resulted in an increase in tone. This suggests that NO was released in response to α_1-AR stimulation. The findings of the present study were consistent with previous studies showing α_1-AR stimulation resulted in NO release (Filippi *et al.*, 2001;Tabernero & Vila, 1995;Gurdal *et al.*, 2005;Kaneko & Sunano, 1993;Zschauer A *et al.*, 1997).

5.4.2.2. Effect of NO on α_1-AR contractility

The effect of L-NAME on α_1-AR-mediated contractility was assessed, using both phenylephrine and A-61603. The increase in contraction and/or sensitivity to phenylephrine and A-61603 in the presence of L-NAME is indicative of NO modulating the agonist-induced contraction. In all mouse strains, the effect of L-NAME observed was greater at higher concentrations of both phenylephrine and A-61603. This suggests that the observations were not due to the constitutive release of NO, suggested in section 5.4.1. Rather, it seems that the influence of NO increases with concentration of agonist, which is consistent with the effect being induced by the agonist.

To establish whether NO release could be stimulated by a non adrenoceptor-mediated pathway, the 5-HT contractile response was investigated with and without L-NAME in the $\alpha_{1B/D}$-KO. There is evidence that NO can modulate the contractile response to 5-HT in some arteries. For instance, an earlier study in the bovine pulmonary artery, MacLean et al. (1994) demonstrated that the 5-HT contractile response was potentiated by L-NAME. Furthermore, a recent study in the mouse aorta Ali (2004) reported that while the maximum response to 5-HT was unchanged, an increase in sensitivity was observed in the presence of L-NAME. However, in the present study, L-NAME did not affect the maximum response or sensitivity of 5-HT, suggesting that NO does not modulate the contractile response to 5-HT in the mouse carotid artery. This evidence rules out the possibility that an increase in vascular tone caused NO release, as reported by Amerini et al. (1995) in the rat mesenteric vascular bed. Furthermore, the lack of effect of L-NAME provides further evidence that there is no spontaneous NO release in the murine carotid artery and suggests that NO release is in response to α_1-AR activation.

5.4.2.3. Mechanism of stimulated release

The effects of NO on the phenylephrine and A-61603 contractile response described in this chapter, suggest an α_1-AR induced release of NO. NO release may result from either from the activation of α_1-ARs on smooth muscle, which signal to the endothelium through myo-endothelial junctions (Dora K, 2001), or the direct activation of α_1-ARs on the endothelium. Myoendothelial gap junctions have been identified in small arteries, such as the rat mesenteric artery (Dora K, 2001;Gonzalez Unpublished observations). Spagnoli et al. (1982) identified myoendothelial gap junctions in the carotid artery of the rabbit, demonstrating that they are not restricted to small arteries. However, to date there is no further evidence of myoendothelial gap junctions, either from the literature or from visualisation studies in the carotid artery within our laboratory. Without positive evidence for the existence of myoendothelial gap junctions in the mouse carotid artery it cannot be concluded that NO release results from the activation of SMC α_1-ARs and has an indirect action on the endothelium.

There is no functional evidence that NO is released through the direct activation of endothelial α_1-ARs in the present study. However, increasingly, evidence of α_1-ARs on the endothelium is being reported in several blood vessels (Boer *et al.*, 1999;Filippi *et al.*, 2001;Zschauer A *et al.*, 1997;Tuttle & Falcone, 2001). For instance, Boer et al. (1999) reported that in response to α_1-AR agonists, an endothelium-dependent relaxation occurred

in pulmonary arteries, which was mediated by NO. Furthermore, an earlier study in the rat mesenteric vascular bed showed that an endothelium-dependent relaxation occurred in response to phenylephrine. This relaxation was blocked by the selective α_{1D}-AR antagonist BMY 7378, indicative of endothelial α_{1D}-ARs (Filippi *et al.*, 2001). Furthermore, preliminary evidence from a fluorescent ligand binding in our laboratory suggested that α_1-ARs may exist on the endothelium. This has been further investigated in Chapter Seven. Thus, the direct stimulation of α_1-ARs on the endothelium could result in NO release in the mouse carotid artery.

5.4.3. Physiological relevance

It has been suggested that the relaxation resulting from NO prevents arteries becoming over contracted, thus ensuring blood flow is maintained (Tuttle & Falcone, 2001;Gurdal *et al.*, 2005). The findings in this chapter indicate that the response to α_1-AR agonists consists of contraction and relaxation. When stimulated by an α_1-AR agonist, α_1-ARs on the smooth muscle contract and NO release is stimulated to suppress the contractile response. This balance of contraction and relaxation would ensure blood flow was maintained during α_1-AR-mediated contraction, which is crucial as the carotid artery supplies the brain.

5.4.4. Relevance to α_1-AR subtypes in the mouse carotid artery

Phenylephrine-induced response

The maximum response to phenylephrine was markedly increased in the presence of all mouse strains: an increase of 79%, 60% and 233% was observed in the WT mouse, α_{1D}-KO and $\alpha_{1B/D}$-KO, respectively. The greater difference in maximum response and increased sensitivity to phenylephrine with L-NAME in the $\alpha_{1B/D}$-KO appears to be due to the poor contractile response in the phenylephrine control. It is possible that due to the reduction in contractile α_1-ARs, NO may be suppressing the phenylephrine response to a greater extent in the $\alpha_{1B/D}$-KO. This is consistent with an overall improvement in the contractile response to phenylephrine when NO release is inhibited in the $\alpha_{1B/D}$-KO. With the effect of NO removed, the maximum response to phenylephrine was greater in the WT mouse than both knockouts, which corresponds to the phenylephrine control data (Chapter Three). Similarly, in the presence of L-NAME, sensitivity to phenylephrine is approximately 10-fold higher in the WT mouse than the knockouts, which

is similar to findings in the absence of L-NAME (Chapter Four). Thus, whether in the absence or presence of NO, the magnitude of the phenylephrine-induced response is dependent on the presence of the α_{1D}-AR.

Filippi et al. (2001) demonstrated that α_{1D}-ARs exist in the endothelium of rat mesenteric arteries. It was reported that phenylephrine acted on α_{1D}-ARs on both smooth muscle cells and ECs producing contraction and relaxation, which resulted in the overall size of contraction being reduced. It is possible that a similar situation exists in the mouse carotid artery. If α_{1D}-ARs were present on the endothelium of the carotid artery this could account for the greater increase in contractile response in the presence of L-NAME: the α_1-AR-mediated relaxation would be greater in the WT mouse than in the α_{1D}-KO. Thus, in the presence of L-NAME the loss of relaxation would be more substantial, in addition to the contraction by the α_{1D}-AR in the smooth muscle cells.

A-61603-induced response

In the presence of L-NAME, the maximum response to A-61603 was increased by 58% in the WT mouse, 77% in the α_{1D}-KO and 71% in the $\alpha_{1B/D}$-KO. In agreement with control data (Chapters Three and Four), the A-61603 contractile response was greater in the WT mouse than the knockouts. This can be explained by the presence of the α_{1D}-AR, which is appears to contribute to the A-61603 contractile response in WT mouse. Sensitivity to A-61603 was increased by L-NAME in both the α_{1D}-KO and $\alpha_{1B/D}$-KO. In the presence of L-NAME, no major difference in sensitivity to A-61603 was observed between strains. This contrasts with control data for A-61603 in which the WT mouse showed significantly reduced sensitivity. This suggests that NO is holding back the contractile response to A-61603 in the WT mouse, which is removed in the presence of L-NAME. In addition, the increase in tone observed in the presence of L-NAME following stimulation with A-61603 suggests that α_{1A}-ARs may exist on the endothelium.

5.4.5. Conclusion

In summary, NO release appears to be triggered by the direct stimulation of α_1-ARs most likely on the endothelium of the mouse carotid artery. Once released NO suppresses the α_1-AR-mediated contractile response.

Chapter Six

α_1-AR Distribution in the media of the mouse carotid artery

6.1. Introduction

6.1.1. α_1-AR subcellular distribution

QAPB is a fluorescent ligand with high affinity for α_1-ARs and, therefore, can be used to study the distribution of α_1-ARs in cells and tissues. QAPB has been used in several visualisation studies to examine the cellular distribution of α_1-ARs in isolated cells (Daly *et al.*, 1998;Mackenzie *et al.*, 2000;McGrath *et al.*, 1999;Deighan *et al.*, 2004). Firstly, the existence of both diffuse and clustered binding of α_1-ARs at intracellular sites was reported in transfected rat-1 fibroblasts (Daly *et al.*, 1998) and SMCs from the rat basilar artery (McGrath *et al.*, 1999). Further investigation revealed that α_1-ARs were present on the cell membrane as well as at intracellular sites in live human SMCs (Mackenzie *et al.*, 2000). In contrast a recent study in mouse hepatocytes demonstrated that the total α_1-AR population was intracellular (Deighan *et al.*, 2004). Clearly, differences in the location of α_1-ARs within the cell exist and may vary between cell types.

The subcellular distribution of α_1-ARs has also been examined visually using fluorescent antibodies and green fluorescent protein-tagged receptors in COS-7 transfected cells (Hirasawa *et al.*, 1997). This study found that α_{1A}-ARs were predominantly located at intracellular sites, while the α_{1B}-AR was predominantly found on the cell surface. Subsequent studies in transfected rat fibroblasts (McCune *et al.*, 2000) and transfected COS-7 cells (Sugawara *et al.*, 2002) also showed that the cell surface was the principal location of α_{1B}-ARs, however, some intracellular α_{1B}-ARs were detected. Furthermore, Sugawara et al. (2002) identified punctate intracellular fluorescence in COS-7 cells transfected with α_{1A}-ARs, which also confirms the findings of the previous study by this group (Hirasawa *et al.*, 1997). In addition, McCune et al. (2000) went on to show that following the activation of the α_{1B}-AR by an agonist the receptor internalised. Furthermore, fibroblasts expressing α_{1D}-ARs showed that the α_{1D}-AR was predominantly located in perinuclear regions, although some α_{1D}-ARs were detected on the cell surface (McCune *et al.*, 2000). Thus, collectively these studies have provided evidence that in isolated cells the α_{1B}-AR is predominantly located on the cell surface and the α_{1A}-AR and α_{1D}-AR are predominantly located at intracellular sites.

It was recently proposed that the α_1-AR subtypes can form dimers (Hague *et al.*, 2004b;Uberti *et al.*, 2003). Using transfected HEK 293 cells Uberti et al. (2003)

demonstrated that homodimers could be formed by the three α_1-AR subtypes, while heterodimers could only be formed between the α_{1A}-AR and α_{1B}-AR or the α_{1B}-AR and the α_{1D}-AR. Both the homodimers and heterodimers appeared to be expressed on the cell surface (Uberti *et al.*, 2003). Both binding site density and protein expression of the α_{1A}-AR and α_{1D}-AR was increased when dimerised with the α_{1B}-AR, implying that the α_{1B}-AR had a functional role in cellular expression. Furthermore, the cell surface expression of the α_{1D}-AR was markedly increased when this subtype was coexpressed with the α_{1B}-AR (Uberti *et al.*, 2003) and the α_{1D}-AR was predominantly located on the cell surface rather than at intracellular sites(Hague *et al.*, 2004b). This also implies that the α_{1B}-AR regulates the expression of the α_{1D}-AR.

6.1.2. QAPB binding in intact vessels

Recently, two studies have used QAPB to examine α_1-ARs in whole vessels. The first study to examine the α_1-AR distribution visually compared the amount of QAPB binding in the fixed aorta of the α_{1B}-KO and α_{1D}-KO with the WT mouse (Miquel RM *et al.*, 2005). This study reported that fluorescence to QAPB was similar in the WT mouse and α_{1B}-KO but reduced in the α_{1D}-KO. It was concluded that the total number of α_1-AR binding sites was reduced in the α_{1D}-KO, which was consistent with the smaller contractile response in this mouse. However, the main purpose of the study was to develop a method to quantitatively analyse the amount of fluorescence in images produced by confocal microscopy, therefore this study did not further investigate the α_1-AR subtypes present in each mouse strain nor did it concentrate on the tissue or subcellular distribution of fluorescence.

The second study examined the QAPB binding amount and distribution in unfixed mesenteric arteries of the WT mouse and $\alpha_{1B/D}$-KO to determine whether the distribution of the predominant contractile α_1-AR subtype, the α_{1A}-AR, was influenced by the α_{1B}-AR or α_{1D}-AR (McBride *et al.* Submitted for publication). It was found that the α_{1A}-AR was located on both the cell surface and inside the cell in punctate compartments and that the distribution of the QAPB binding in the $\alpha_{1B/D}$-KO was similar to the WT mouse. This suggests that the location of the α_{1A}-AR was the same whether or not the subtypes were present. However, in the absence of the α_{1B}-AR and α_{1D}-AR a reduction in the intensity of fluorescence was observed. This study demonstrated that the subcellular distribution of α_1-ARs could be examined *in situ* successfully. These two studies have shown that

valuable information about the amount and distribution of α_1-ARs can be obtained from the use of QAPB.

In the present study QAPB was used in conjunction with selective α-AR antagonists to undertake a detailed study of the distribution of α_1-ARs in SMCs of the carotid artery *in situ*. In addition, single and double knockouts of α_{1B}-AR, α_{1D}-AR were employed to assess the effect of the loss of an α_1-AR subtype on distribution. Thus, the aims of the present study were:

- To develop a protocol to examine the distribution of α_1-ARs in the media of the carotid artery.
- To compare the tissue distribution of α_1-ARs in the smooth muscle layers of the carotid artery of the WT mouse and α_1-AR knockout mice.
- To subtype the α_1-ARs in the smooth muscle layers of the carotid artery of the WT mouse and α_1-AR knockout mice.
- To examine the subcellular distribution of α_1-ARs in SMCs of the WT mouse and α_1-AR knockout mice.

6.2. Methods

6.2.1. Determination of incubation conditions

A series of experiments was carried out in the WT mouse to determine the optimum conditions for vessel incubation, which has been described in detail in Chapter Two. In brief, QAPB (1 nM, 10 nM, and 0.1 μM) was tested against the phenylephrine-induced contractile response to assess whether the α_1-AR-mediated functional response was antagonised. The fluorescence and binding of QAPB 1μM, 0.1μM and 10nM were compared to assess the quality of QAPB binding at the different concentrations.

The most appropriate method of preparing the carotid artery for imaging was also established. The whole vessel; cross-sectional rings of carotid artery; and 'opened out' vessels (Miquel RM *et al.*, 2005) were all considered. Unfixed vessels were used in this study to preserve the physiological processes for binding QAPB. Changes in pH,

temperature, oxidation, and glucose levels were limited as much as practically possible for the duration of the experimentation (as described in Chapter Two).

Once the concentration of QAPB, tissue preparation and temperature had been selected, vessels were imaged at a series of time-points (30 min, 60 min, 90 min, 120 min and 180 min) in order to determine the optimum incubation time for 0.1 μM QAPB, which was found to be 120 minutes.

6.2.2. Experimental protocol

This protocol has been described in detail in Chapter Two. In brief, 5mm segments of carotid artery were incubated at room temperature with 0.1μM QAPB, in a PSS solution at room temperature for 120 minutes. Two sets of control vessels were used during the incubation period: (i) controls for autofluorescence, which were incubated in PSS only, and (ii) QAPB control segments, which were incubated in a QAPB/PSS solution in the absence of antagonists. Throughout the incubation period all solutions were replaced every 30 minutes to ensure the pH of the solution and glucose levels were maintained.

A series of experiments was carried out where the vessel was incubated with a 0.1 μM QAPB/PSS solution for 30 minutes, followed by a 90 minute co-incubation with either a QAPB 0.1 μM / PSS solution or a QAPB 0.1 μM / PSS solution containing a subtype selective antagonist. The nonfluorescent antagonists used for the protocol were: prazosin 0.1 μM, (non-selective α_1-AR antagonist); RS100329 0.1 μM, (α_{1A}-AR selective antagonist); 5-methylurapidil 1 μM (α_{1A}-AR selective antagonist); BMY7378 0.1 μM (α_{1D}-AR selective antagonist); both BMY 7378 0.1 μM and RS100329 0.1 μM; or rauwolscine 0.1 μM (α_2-AR antagonist). Incubations were performed at room temperature (21°C) and solutions were replaced every 30 minutes.

At the end of the incubation period each carotid artery segment was sliced open with a single-edged razor blade and laid flat on a microscope slide with the endothelial side up (Miquel RM *et al.*, 2005) and coverslip (thickness 1.5) on top.

All arteries were visualised using the Bio-Rad Radiance 2100 Confocal Laser Scanning System. An argon-ion laser with an excitation wavelength of 488nm with an emission filter of 515nm was used for QAPB and a x40 oil immersion objective (NA 0.75) was used for all experiments. Two different settings were used to record images. For images

recorded at zoom three a laser intensity of 40, a gain of 12, offset 0.0 and pinhole setting of 1.4 was selected. While for images recorded at zoom eight a laser intensity of 20, gain 22, offset 0.0 and pinhole setting of 2.4 was used. The standard scan speed of 500 lps was used for all experiments. An image size of 515 x 512 pixels produced a field size of 289µm x 289µm.

During the co-staining experiments the settings for QAPB were as described above, while a red diode, with an excitation/emission wavelength of 628/645nm, was used for Syto 61. At a zoom of three, laser intensity was set to 30, with a gain of 12, offset 0.0 and an optimal pinhole of 1.4.

Open vessels were imaged from the internal elastic lamina through to the media. At least three images of the vessel were collected at random areas. Each experiment was repeated four times for each strain of mouse.

Kalman (5 frames) was used to record individual 2D images. Z-series were produced in stacks of 1µM slices, starting at the last smooth muscle layer in focus and ending at the internal elastic lamina, producing a stack of approximately 30µm.

6.2.3. Image analysis

Following image capture, the images produced from the colocalisation experiments with QAPB and Syto 61 were overlaid using Lasersharpe software. Thus, the distribution of QAPB binding was directly compared with the nuclear binding of Syto 61.

To ensure that the analysis was performed on images showing only SMCs the images collected at zoom eight were used for analysis using Metamorph software (version 4). Region statistics were generated for each image. Integrated intensity for QAPB was compared between all four strains of mice using one-way ANOVA. Integrated intensity of QAPB in presence of the selected antagonists was compared to QAPB alone using one-way ANOVA and Bonferroni's post test. For individual images the number of pixels at each intensity was obtained from image histogram statistics and used to calculate the total fluorescence at each intensity level. Mean data was displayed in histogram plots of fluorescence against intensity. These plots quantified the observations made by eye and indicated how much fluorescence originated from bright or dim pixels.

6.3. Results

6.3.1. Protocol development

6.3.1.1. Vessel preparation: Whole intact vessel

When imaging the whole intact vessel, it was difficult to focus into the smooth muscle layers and endothelium due to the thick elastic wall of the carotid artery. Consequently, an alternative approach was attempted in which the vessel was turned inside out to expose the endothelium and stretch the elastic lamina. This preparation did enable the vessels to be imaged from the endothelium through to the media but unfortunately this approach resulted in severe damage to both the endothelium and the smooth muscle. Furthermore, it proved difficult to focus the microscope on the SMCs due to movement of the vessel wall. The use of this preparation was not continued.

Cross-sectional rings

Cross-sectional rings can be easily sliced from fixed vessels. However, fresh tissue was used instead of fixed to enable the physiological processes for the ligand binding to be preserved. In the unfixed tissue slicing the cross-sectional rings caused unavoidable damage to the vessels.

Open vessel

The approach using an opened-out vessel enabled the vessel to be imaged from the endothelium through to the smooth muscle layers. This preparation was relatively easy to carry out and caused minimal damage to the vessel. Thus, the open vessel preparation was selected for use in the main experimental protocol.

6.3.1.2. Determination of optimal QAPB concentration

Functional antagonism: The CRC to phenylephrine in the presence of QAPB 1 nM (maximum response obtained 0.26±0.02g; pEC_{50} 6.7±0.15) was not significantly different ($p>0.05$, one-way ANOVA, Bonferroni's post test) to the phenylephrine control (maximum response obtained 0.21±0.06g; pEC_{50} 6.6±0.05). The maximum response obtained to phenylephrine was not significantly different ($p>0.05$, one-way ANOVA, Bonferroni's post test) in the presence of QAPB 10 nM (0.25±0.05g) or 0.1 μM

(0.17±0.02g). A rightward displacement of the phenylephrine CRC ($p<0.01$, one-way ANOVA, Bonferroni's post test) was observed in the presence of QAPB 10 nM (pEC_{50} 5.7±0.35) and 0.1 μM (pEC_{50} 5.1±0.27). A mean pK_B of 9.0 was obtained for QAPB.

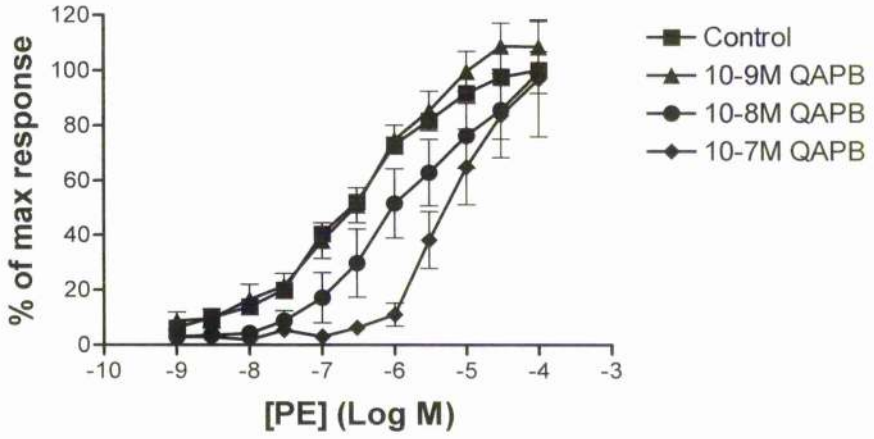

Figure 6.1. CRC to phenylephrine in the presence of QAPB expressed as percentage of the control CRC maximum as mean±S.E (n=6).

Binding: Using a standard incubation time of 120 minutes fluorescence progressively increased with increasing concentrations of QAPB (Figure 6.2). Evidence of QAPB binding was observed at 10 nM but binding was generally not intense with SMCs poorly defined. SMCs were clearly defined following incubation with QAPB 0.1 μM. With QAPB 1 μM SMCs were clearly defined and fluoresced brightly, however, some images showed evidence of saturation at this concentration. It was decided to use QAPB 0.1 μM for the experimental protocol as both the definition of the SMCs and fluorescence were sufficient at this concentration and the lower concentration is advantageous for using competitors to its binding.

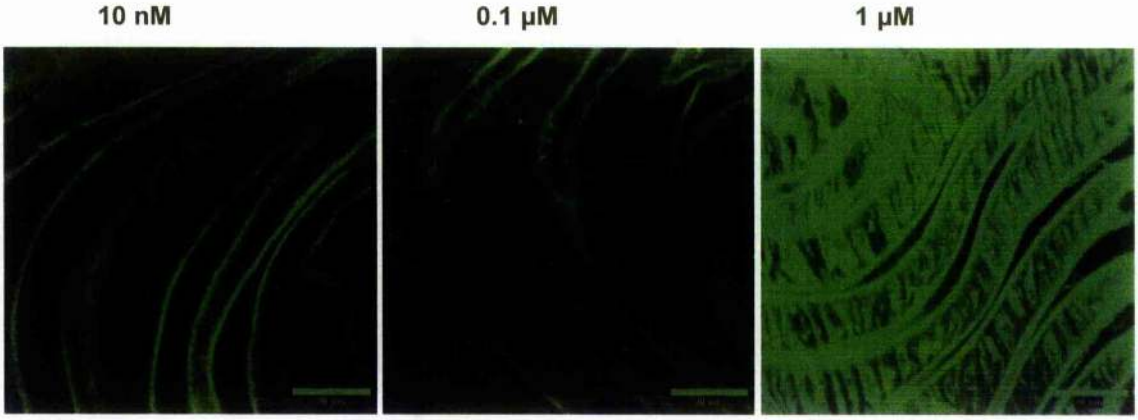

Figure 6.2 Determination of QAPB concentration in the WT mouse. Imaging settings: zoom three, laser 40, gain 12, iris 1.4.

6.3.1.3. QAPB incubation time

Over the duration of the incubation period binding to QAPB 0.1 μM increased (Figure 6.3). At zero minutes and 30 minutes only autofluorescence from the elastic lamina was visible. QAPB binding was detected at 60 minutes, which increased further at 90 minutes. Good evidence of QAPB binding was observed at both 120 minutes and 180 minutes, where SMCs were clearly defined. There was little difference between the QAPB staining at these two time points, which indicated that equilibrium had been reached. The shorter incubation time of 120 minutes was selected for use in the experimental protocol.

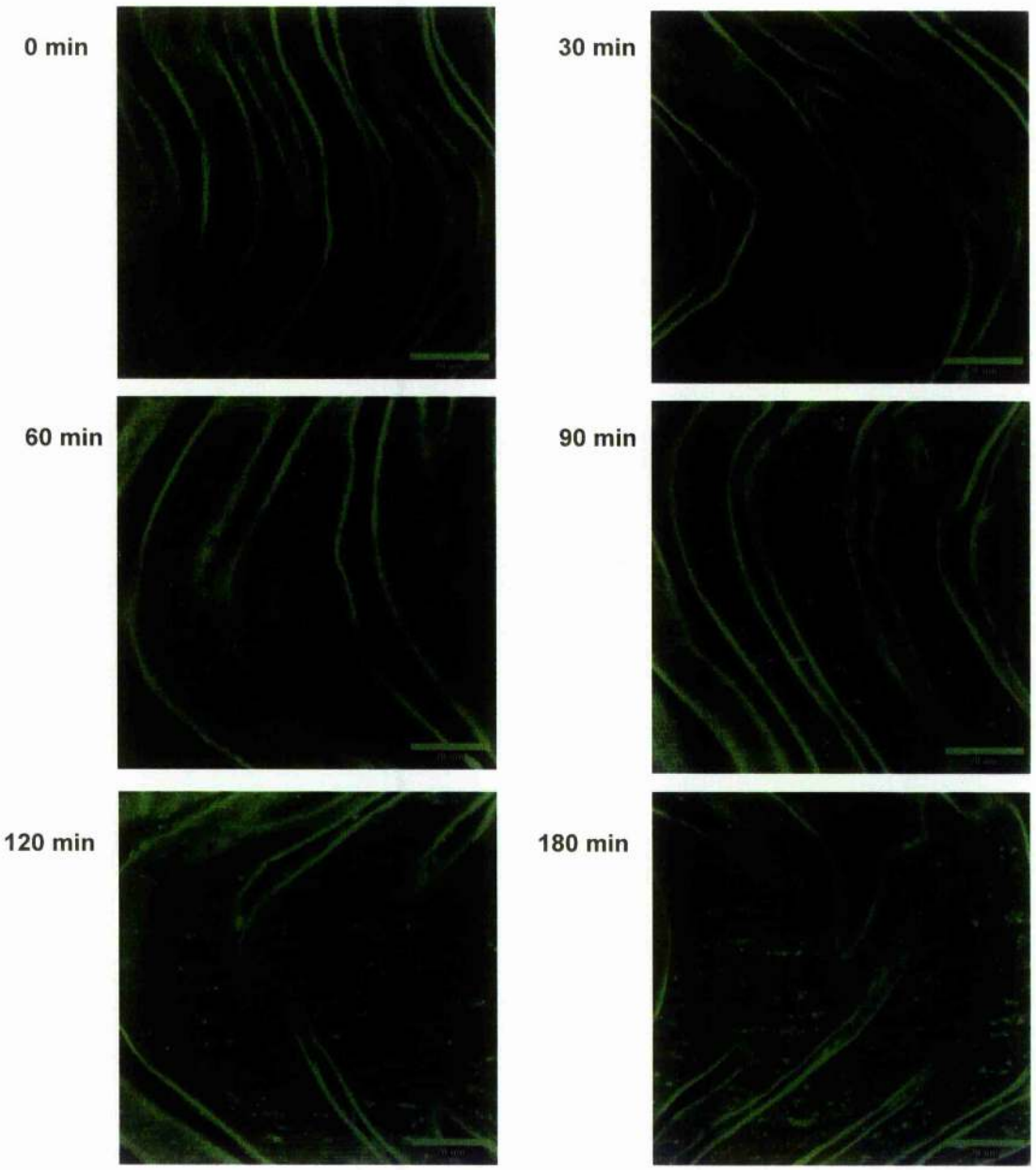

Figure 6.3. QAPB incubation times in WT mouse. Imaging settings: zoom three, laser 40, gain 12, iris 1.4.

6.3.2. QAPB binding distribution

6.3.2.1. Controls

In the absence of QAPB, only autofluorescence from the elastic lamina was visualised and there was no evidence of fluorescence from the media in any of the mouse strains (Figure 6.4).

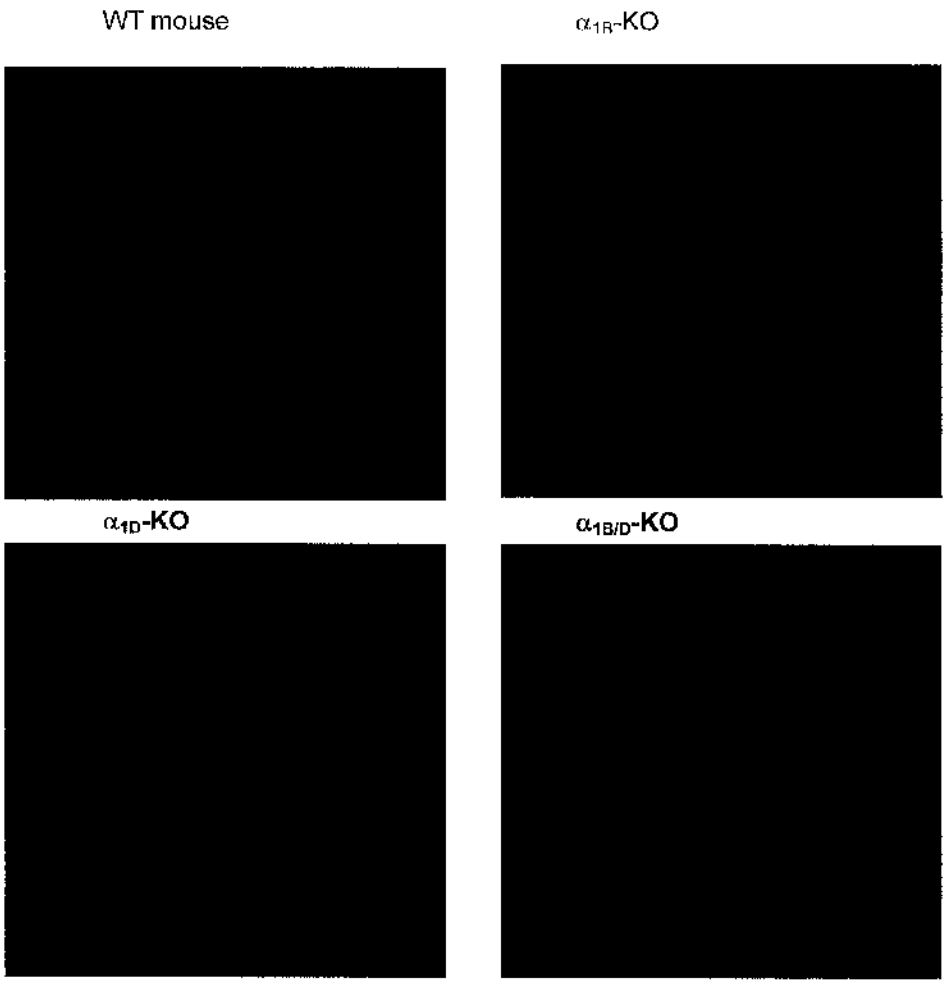

Figure 6.4. Low power view of SMCs in WT and knockout mice in the absence of QAPB. Imaging settings: zoom three, laser 40, gain 12, iris 1.4.

6.3.2.2. WT mouse

QAPB binding was evenly distributed throughout the WT mouse vessels (Figure 6.5). SMCs were clearly defined and fluoresced brightly. QAPB bound to both the cell surface and intracellular compartments (Figure 6.6). Intracellularly, evidence of both perinuclear binding and punctate binding was observed. There was no evidence of QAPB binding to nuclear sites.

6.3.2.3. α_{1B}-KO

SMCs were clearly defined by QAPB binding and fluoresced brightly in the α_{1B}-KO (Figure 6.5). QAPB binding to SMCs appeared evenly distributed throughout the vessel. In addition to QAPB binding on the cell membrane, perinuclear and punctate binding were observed inside the cell (Figure 6.6). In general, QAPB binding in the α_{1B}-KO resembled that observed in the WT mouse, except that visual observations suggested that punctate binding was increased in the α_{1B}-KO.

6.3.2.4. α_{1D}-KO

QAPB binding to SMCs in the α_{1D}-KO was variable. In some regions QAPB binding was markedly reduced and SMCs were less defined, while in other regions SMCs were clearly identified (Figure 6.5). Furthermore, the amount of fluorescence varied between individual cells. An overall reduction in SMCs stained with QAPB was evident compared to the WT mouse. The cells that QAPB bound showed both cell surface and perinuclear binding, and there was evidence of punctate binding in cells (Figure 6.6).

6.3.2.5. $\alpha_{1B/D}$-KO

In the $\alpha_{1B/D}$-KO QAPB binding to SMCs was variable. Overall, QAPB binding was markedly reduced but still detectable (Figure 6.5). Fluorescence varied between individual SMCs. Most SMCs were less defined with limited cell surface and perinuclear binding. However, most cells stained with QAPB showed evidence of punctate binding (Figure 6.6).

At a zoom setting of three, QAPB binding to SMCs was observed between the grooves formed by the elastic lamina. At a zoom setting of eight, QAPB binding to SMCs to be imaged in greater detail due to the less exciting power and, therefore, a more sensitive detection. Furthermore, at this setting quantitative analysis could be performed in the absence of elastic lamina.

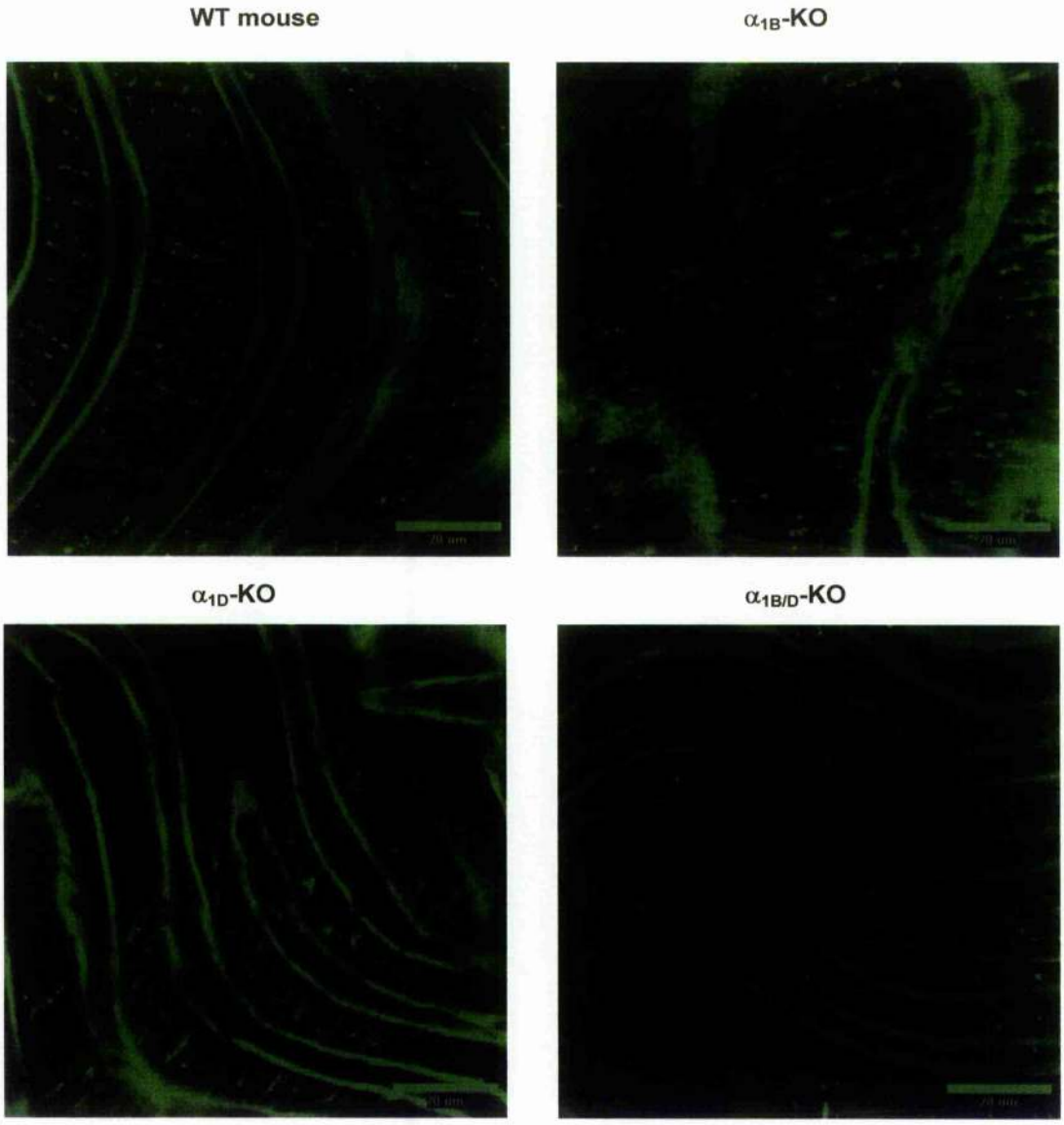

Figure 6.5. Low power view of SMCs in WT and knockout mice: QAPB binding. Imaging settings: zoom three, laser 40, gain 12, iris 1.4.

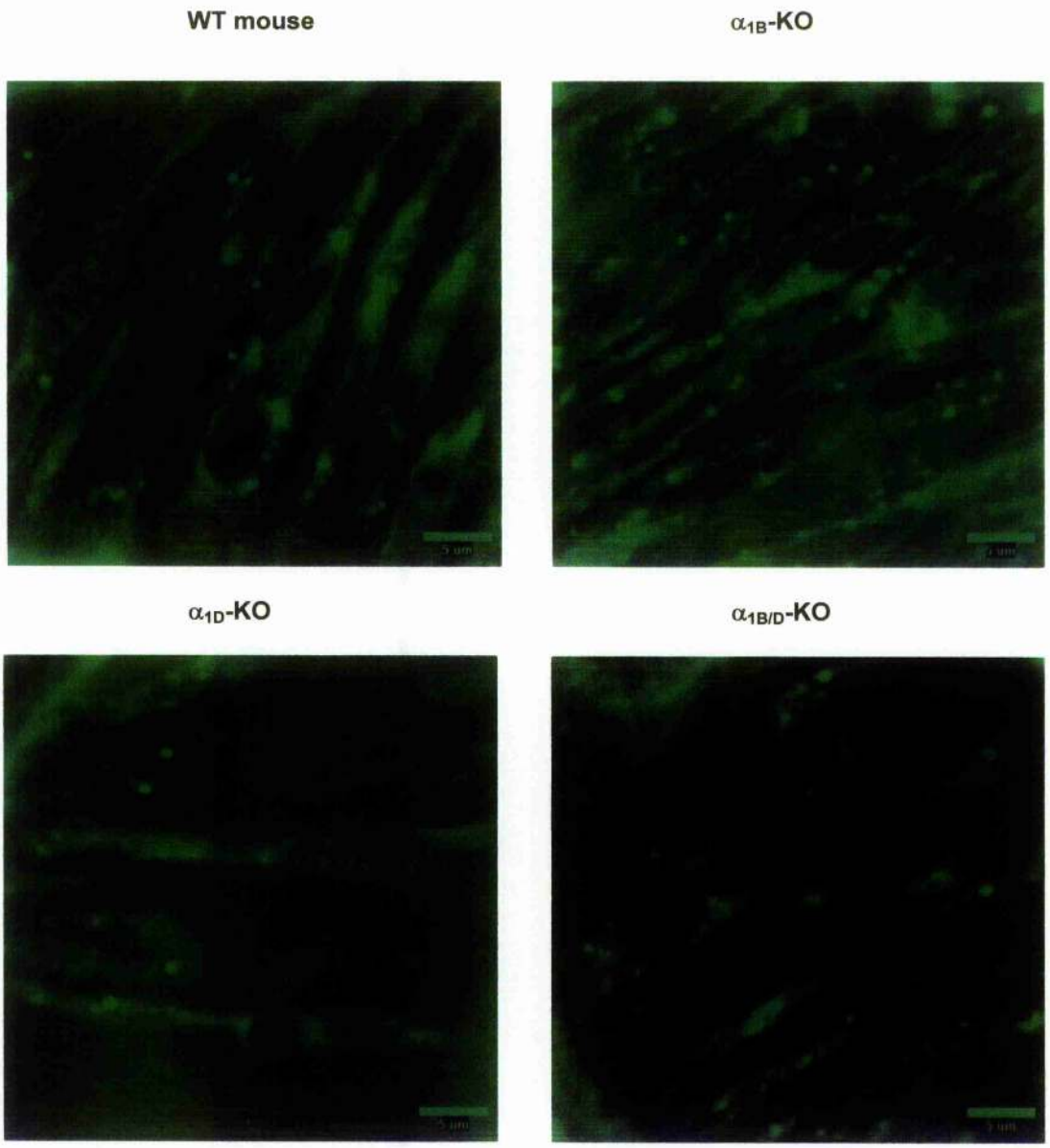

Figure 6.6. High power view of SMCs in WT and knockout mice: QAPB binding. Imaging settings: zoom eight, laser 20, gain 22, iris 2.4.

6.3.3. Comparison of QAPB intensity

Analysis of total amount of fluorescence: Fluorescence was reduced in the knockout mice compared to the WT mouse. This was shown by the leftward displacement of the histograms for the knockout mice, where the majority of fluorescence resulted from pixels of low intensity (Figure 6.7), and the significant decrease in total intensity in the knockouts compared to the WT mouse (Figure 6.8; Table 6.1).

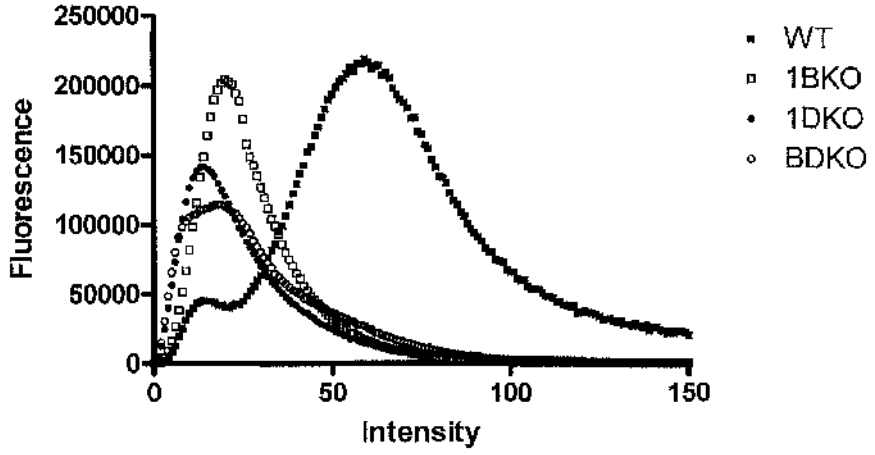

Figure 6.7. Comparison of integrated intensity to QAPB in the WT mouse and knockout mice expressed as mean ± S.E. (n=7).

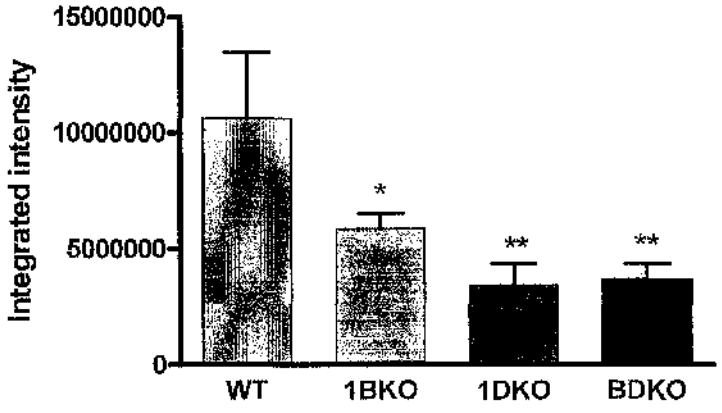

Figure 6.8. Fluorescence against Intensity to QAPB in the WT and knockout mice expressed as mean ± S.E. (n=7).

Table 6.1. Integrated Intensity to QAPB in the WT mouse and knockout mice

Mouse Strain	Integrated Intensity	% reduction
WT mouse	$1.06x10^7 \pm 2.9x10^6$	-
α_{1B}-KO	$5.84x10^6 \pm 6.6x10^5$ *	45%
α_{1D}-KO	$3.43x10^6 \pm 9.3x10^5$ **	68%
$\alpha_{1B/D}$-KO	$3.68x10^6 \pm 6.8x10^5$ **	65%

*p<0.05; **p<0.01 compared to WT mouse (one-way ANOVA, Bonferroni's post test).

6.3.4. Pharmacological characterisation of QAPB binding to SMCs

6.3.4.1. WT mouse

No binding to QAPB was observed in the presence of prazosin (Figure 6.9; 6.10). A leftward shift in the histogram (Figure 6.11) and a significant reduction in integrated intensity (Figure 6.14; Table 6.2) demonstrated that prazosin caused a decrease in number high intensity pixels and, therefore, total fluorescence.

In the presence of rauwolscine no changes to QAPB binding were observed (Figure 6.9; 6.10). The histogram produced for QAPB fluorescence in the presence of rauwolscine indicated that fluorescence was slightly decreased at low intensity pixels and increased at pixel intensities of 50 to 100 (Figure 6.11) but no significant difference in integrated intensity was observed compared to the QAPB control (Figure 6.14; Table 6.2).

QAPB binding appeared markedly reduced but not abolished by BMY 7378 and variations in binding between individual SMCs were observed (Figure 6.9; 6.10). Fluorescence at high intensity pixels was reduced, as demonstrated by the leftward displacement of the histogram (Figure 6.12) and the significant reduction in integrated intensity (Figure 6.14; Table 6.2).

Despite an apparent reduction in QAPB binding to SMCs in the presence of RS100 329, both cell surface and intracellular staining remained (Figure 6.9; 6.10). A reduction in fluorescence to QAPB was detected at pixels of intensities of approximately 40 and above (Figure 6.12) and integrated intensity was significantly reduced (Figure 6.14; Table 6.2) in the presence of RS100 329.

A reduction in fluorescence to QAPB occurred in the presence of 5-methylurapidil with SMCs being less defined (Figure 6.9; 6.10). There was less evidence of cell surface and perinuclear binding to QAPB with 5-methylurapidil. However, punctate binding in intracellular compartments was still frequently observed. The histogram indicated that fluorescence was reduced at pixels of intensities of approximately 100 and above (Figure 6.13) and a significant reduction in integrated intensity was detected (Figure 6.14; Table 6.2).

With the combination of BMY 7378 and RS100 329 QAPB binding appeared markedly reduced but was still observed (Figure 6.9; 6.10). The definition of individual SMCs was lost in the presence of these antagonists. In the presence of the combination of BMY 7378 and RS100 329 fluorescence was markedly reduced (Figure 6.12). The combination of BMY 7378 and RS100 329 resulted in a significantly reduced integrated intensity (Figure 6.14; Table 6.2).

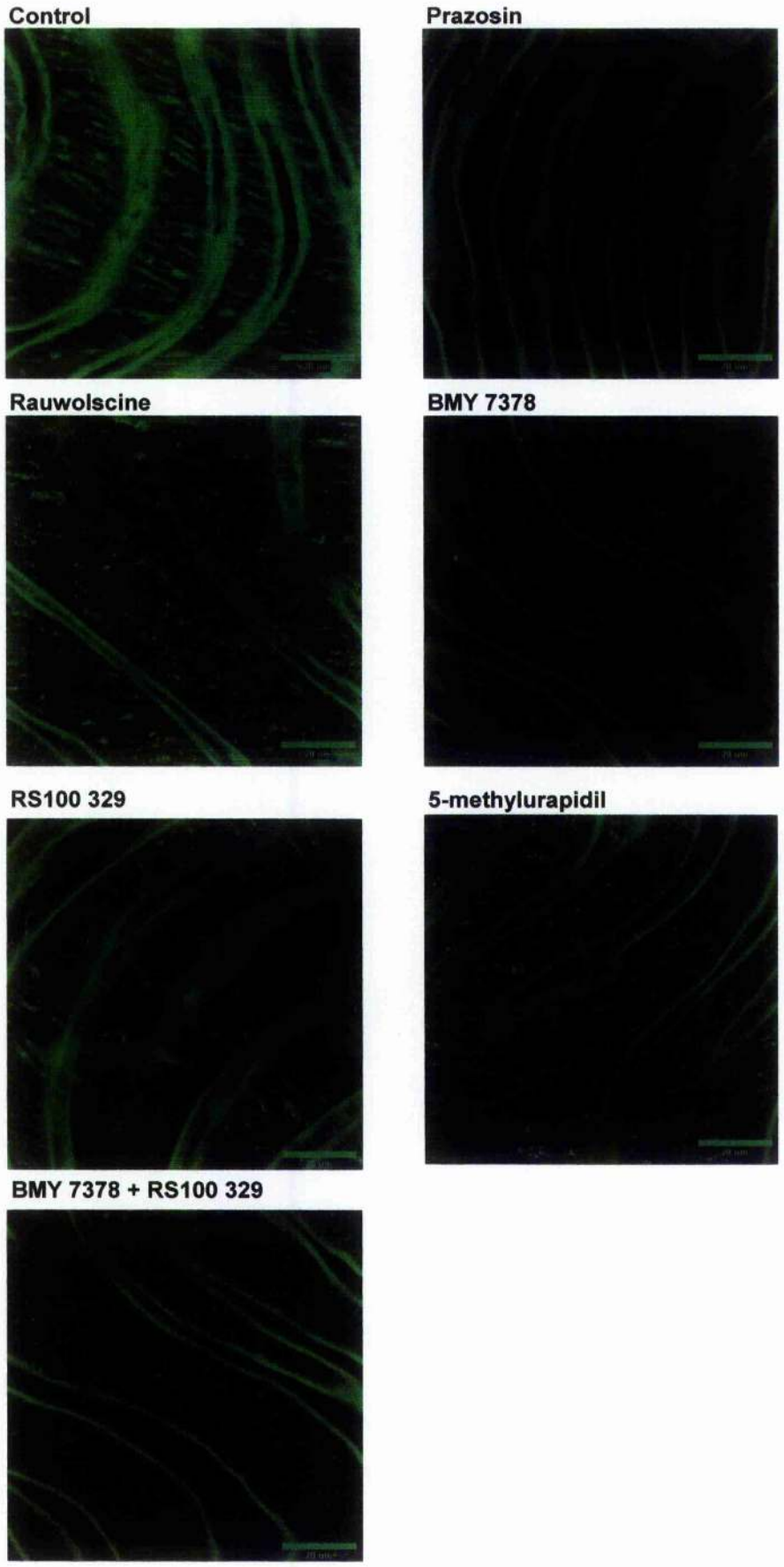

Figure 6.9. Low power view of SMCs in WT mouse: antagonists vs QAPB binding. Imaging settings: zoom three, laser 40, gain 12, iris 1.4.

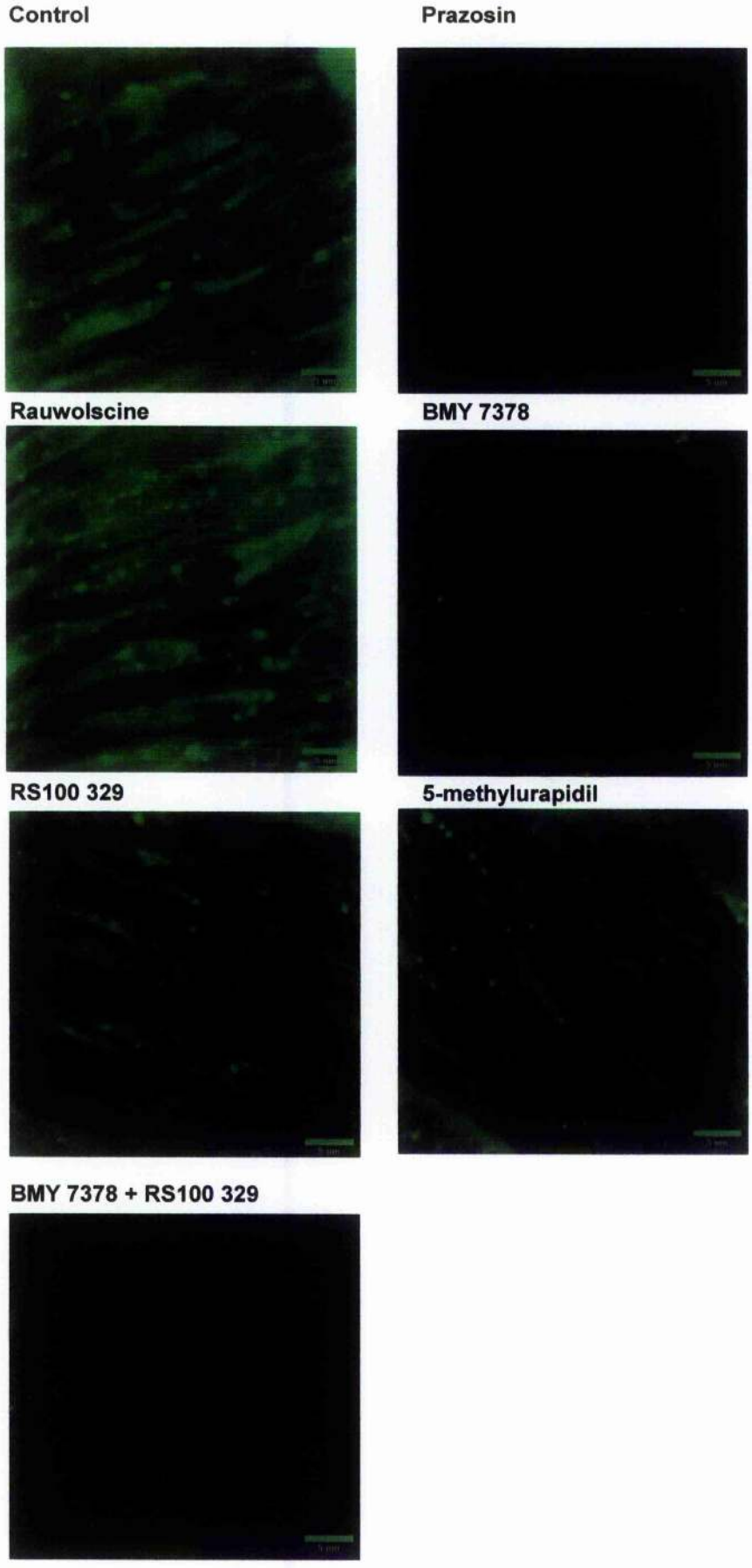

Figure 6.10. High power view of SMCs in WT mouse: antagonists vs QAPB binding. Imaging settings: zoom eight, laser 20, gain 22, iris 2.4.

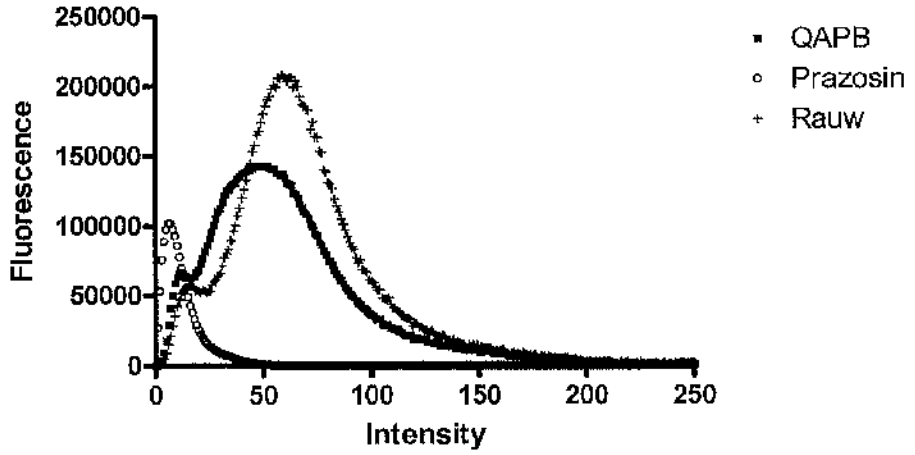

Figure 6.11 . Fluorescence against Intensity to QAPB in the WT mouse in the presence of prazosin and rauwolscine expressed as mean ± S.E. (n=4).

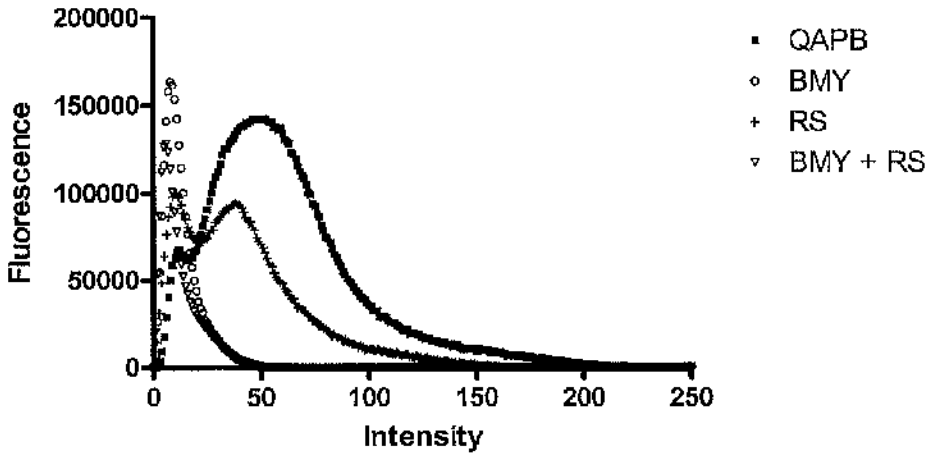

Figure 6.12. Fluorescence against intensity to QAPB in the WT mouse in the presence of BMY 7378, RS100 329 and BMY 7378/RS100 329 combination expressed as mean ± S.E. (n=4).

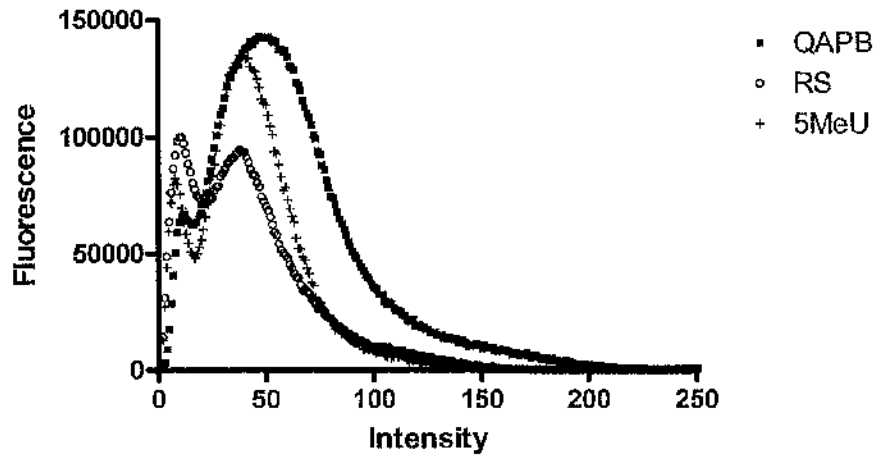

Figure 6.13. Fluorescence against intensity to QAPB in the WT mouse in the presence of 5-methylurapidil and RS100 329 expressed as mean ± S.E. (n=4).

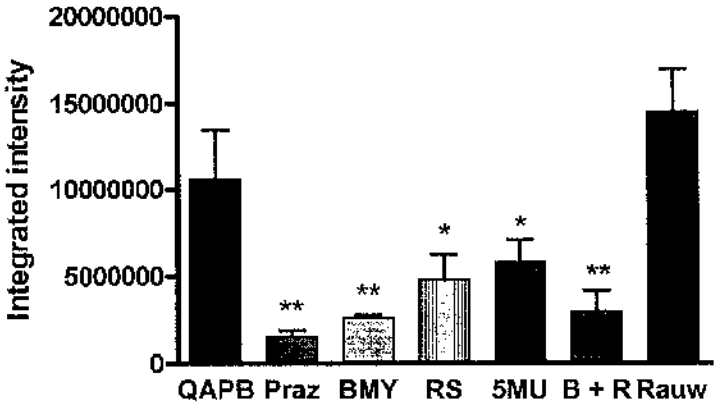

Figure 6.14. WT mouse: Integrated intensity of QAPB in the presence of antagonists (n=4).

Table 6.2. WT mouse: Comparison of integrated intensity for QAPB in the presence of antagonists.

Antagonist	Integrated intensity (± S.E.)
QAPB control	$1.06x10^{7} \pm 2.9x10^{6}$
QAPB + prazosin	$1.53x10^{6} \pm 3.7x10^{5}$ ***
QAPB + BMY 7378	$2.63x10^{6} \pm 1.5x10^{5}$ *
QAPB + RS100 329	$4.79x10^{6} \pm 1.2x10^{6}$ *
QAPB + 5-methylurapidil	$5.78x10^{6} \pm 1.3x10^{6}$ *
QAPB + BMY 7378 + RS100 329	$2.97x10^{6} \pm 1.2x10^{6}$ **
QAPB + Rauwolscine	$1.45x10^{7} \pm 2.4x10^{6}$ +

+p>0.05; *p<0.05; **p<0.01; ***p<0.001 compared to QAPB control (one-way ANOVA, Bonferroni's post test).

6.3.4.2. α_{1B}-KO

Like the WT mouse, in the α_{1B}-KO no QAPB binding was observed in the presence of prazosin (Figure 6.15; 6.16). With prazosin, the majority of QAPB fluorescence resulted from pixels of low intensity, thus the histogram for QAPB was displaced left (Figure 6.17) and integrated intensity was significantly reduced (Figure 6.20; Table 6.3).

In the presence of rauwolscine no change in fluorescence to QAPB was detected by eye (Figure 6.15; 6.16). The histogram mostly overlapped with that for QAPB alone although a small reduction in fluorescence was detected for pixels at intensities of approximately 30 to 60 in the α_{1B}-KO (Figure 6.17). In the presence of rauwolscine integrated intensity was not significantly different to the QAPB control (Figure 6.20; Table 6.3).

In the presence of BMY 7378 QAPB binding appeared markedly reduced but was still detectable (Figure 6.15; 6.16). Variations in fluorescence were observed between individual SMCs. Like the WT mouse, the reduction in fluorescence was demonstrated by the decrease in high intensity pixels resulting in the leftward displacement of the histogram (Figure 6.18) and the significant reduction in integrated intensity (Figure 6.20; Table 6.3).

Despite an apparent reduction in fluorescence and QAPB binding to SMCs, in the presence of RS100 329, both cell surface and intracellular staining remained (Figure 6.15; Figure 6.16). With RS100 329, a leftward shift in the histogram for QAPB was detected (Figure 6.18) and integrated intensity was significantly reduced (Figure 6.20; Table 6.3), following a similar trend as the WT mouse.

The presence of 5-methylurapidil appeared to cause a decrease in fluorescence to QAPB and SMCs were less defined but both binding to the cell membrane and intracellular compartments was observed (Figure 6.15; 6.16). 5-methylurapidil reduced fluorescence between intensities of approximately 25 to 50 but slightly increased fluorescence from high intensity pixels (Figure 6.19), which was not detected in the WT mouse. A significant reduction in integrated intensity was detected (Figure 6.20; Table 6.3).

Unlike the WT mouse, with the combination of BMY 7378 and RS100 329 QAPB binding appeared to be abolished (Figure 6.15; 6.16). The reduction in fluorescence was demonstrated by the leftward displacement of the histogram for QAPB in the presence of BMY 7378 and RS100 329 (Figure 6.18) and a significant reduction in integrated intensity was detected (Figure 6.20; Table 6.3).

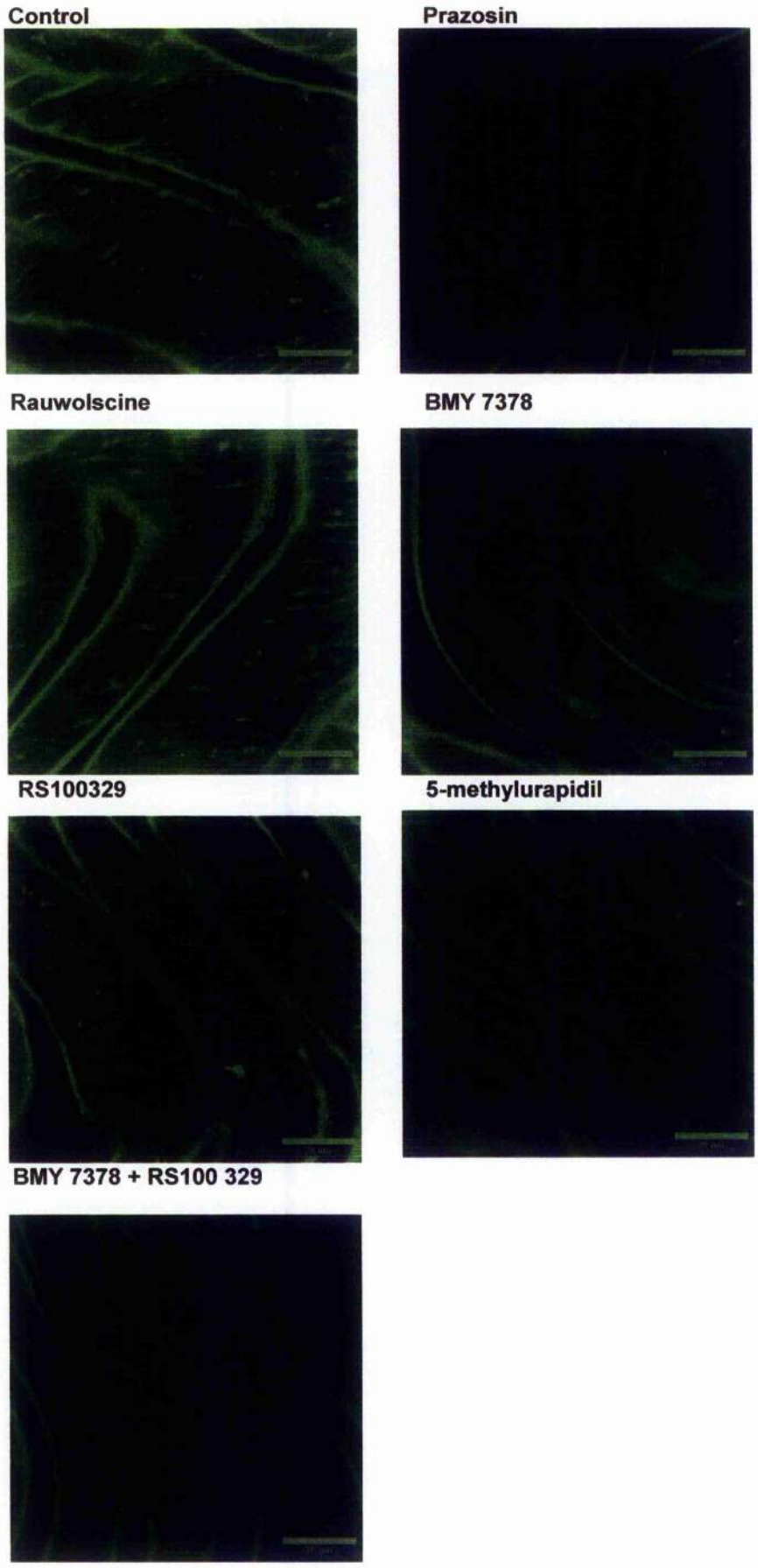

Figure 6.15. Low power view of SMCs in α_{1B}-KO: QAPB vs antagonists. Imaging settings: zoom three, laser 40, gain 12, iris 1.4.

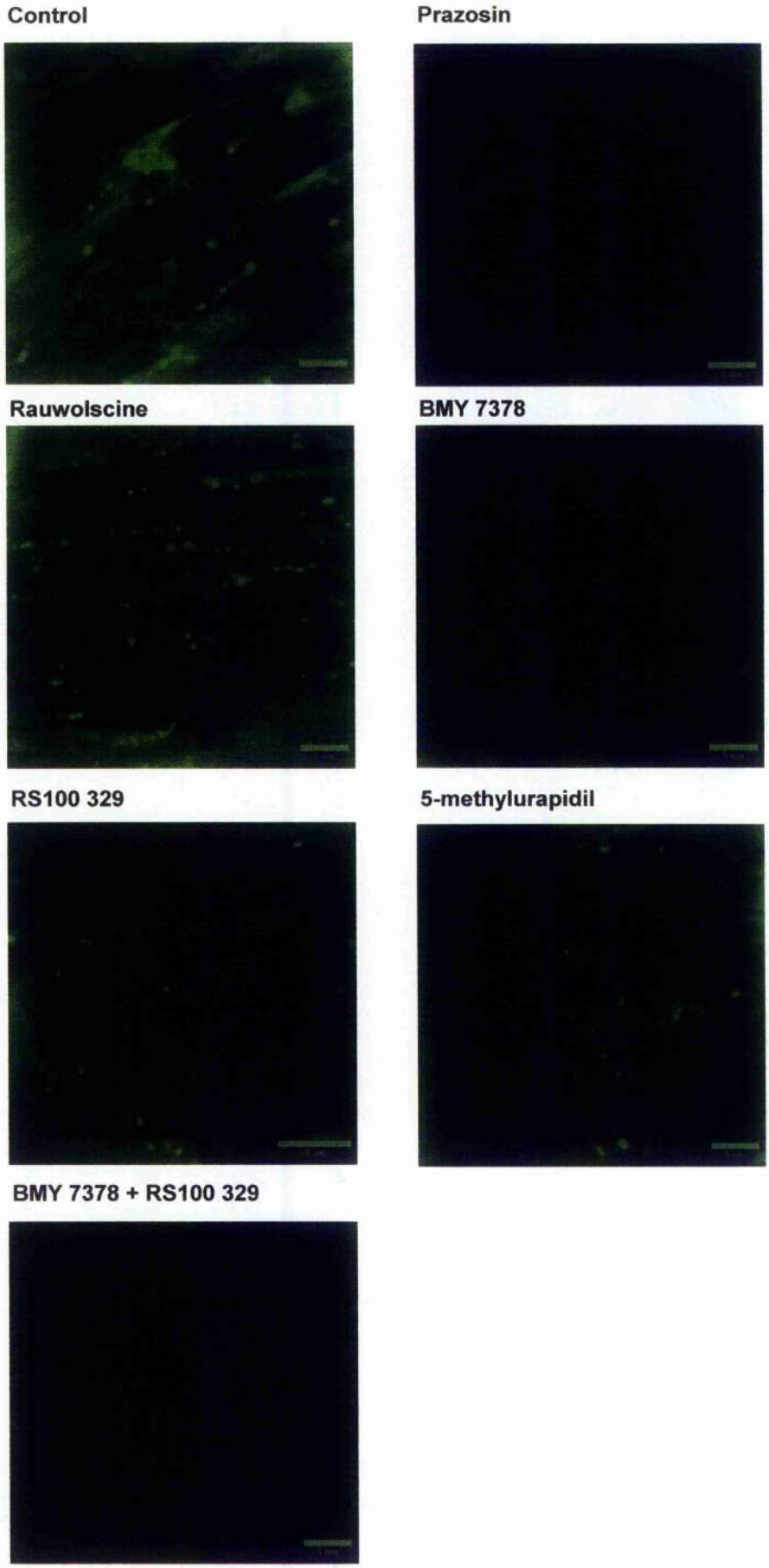

Figure 6.16. High power view of SMCs in α_{1B}-KO: QAPB vs antagonists. Imaging settings: zoom eight, laser 40, gain 22, iris 2.4.

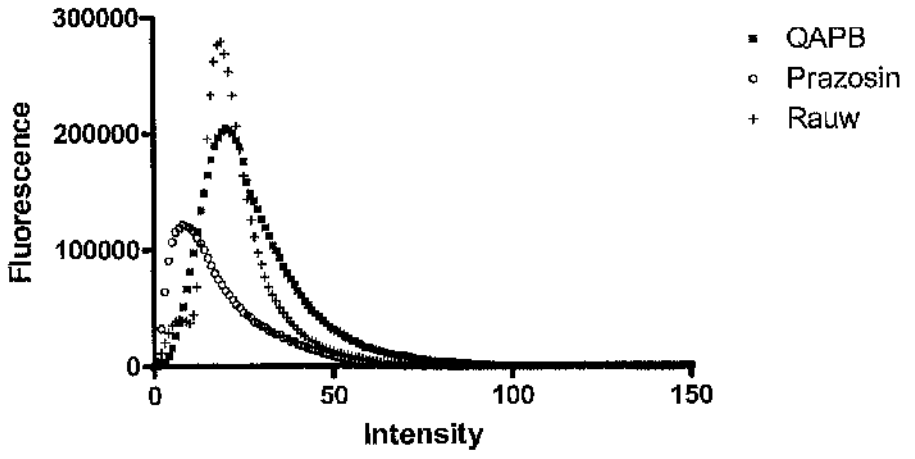

Figure 6.17 . Fluorescence against intensity to QAPB in the α_{1B}-KO in the presence of prazosin and rauwolscine expressed as mean ± S.E. (n=4).

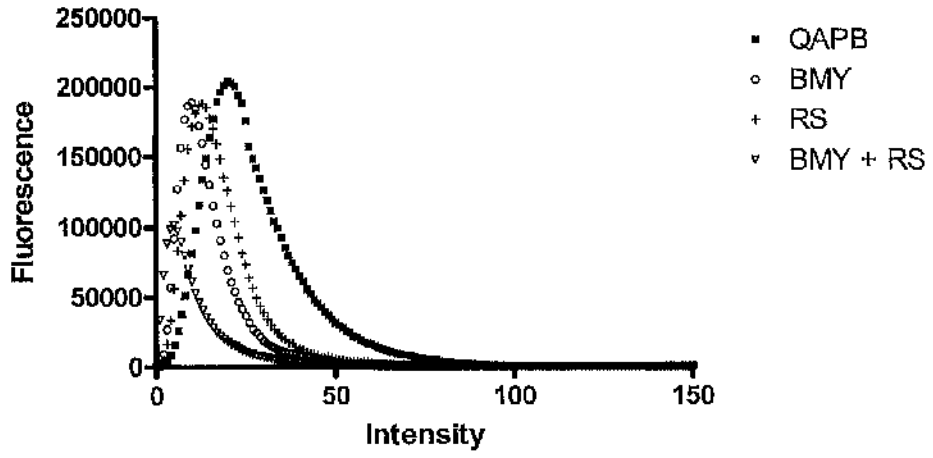

Figure 6.18. Fluorescence against intensity to QAPB in the α_{1B}-KO in the presence of BMY 7378, RS100 329 and BMY 7378/RS100 329 combination expressed as mean ± S.E. (n=4).

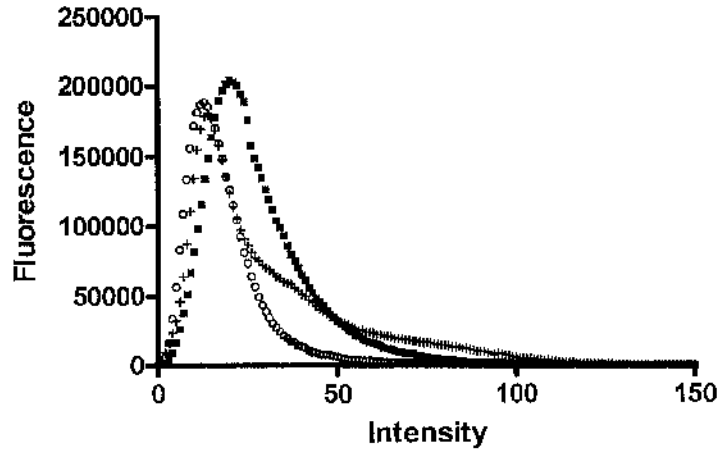

Figure 6.19. Fluorescence against intensity to QAPB in the α_{1B}-KO in the presence of 5-methylurapidil and RS100 329 expressed as mean ± S.E. (n=4).

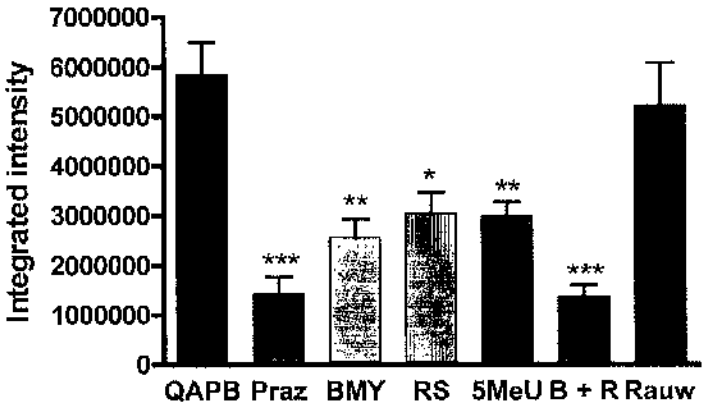

Figure 6.20. α_{1B}**-KO: Integrated Intensity of QAPB in the presence of selective antagonists (n=4).**

Table 6.3. α_{1B}**-KO: Comparison of Integrated Intensity for QAPB in the presence of selective antagonists.**

Antagonist	Integrated intensity (± S.E.)
QAPB control	$5.84x10^6 \pm 6.6x10^5$
QAPB + prazosin	$1.42x10^6 \pm 3.5x10^{5\,***}$
QAPB + BMY 7378	$2.56x10^6 \pm 3.7x10^{5\,**}$
QAPB + RS100 329	$3.05x10^6 \pm 4.1x10^{5\,*}$
QAPB + 5-methylurapidil	$2.98x10^6 \pm 2.9x10^{5\,**}$
QAPB + BMY 7378 + RS100 329	$1.37x10^6 \pm 2.3x10^{5\,***}$
QAPB + Rauwolscine	$5.21x10^6 \pm 8.6x10^{5\,+}$

+p>0.05; *p<0.05; **p<0.01; ***p<0.001 compared to QAPB control (one-way ANOVA, Bonferroni's post test).

6.3.4.3. α_{1D}-KO

Like the WT mouse, in the α_{1D}-KO in the presence of prazosin QAPB binding appeared to be abolished (Figure 6.21; 6.22). The histogram plot for QAPB in the presence of prazosin was shifted left showing the majority of fluorescence originating from pixels of low intensities (Figure 6.23) and integrated intensity was significantly reduced (Figure 6.26; Table 6.4).

In the presence of rauwolscine QAPB binding did not appear to be changed (Figure 6.21, 6.22). The histogram for QAPB with rauwolscine largely overlay the histogram for QAPB alone (Figure 6.23) and the increase in fluorescence detected in the WT mouse was not detected in the α_{1D}-KO. Integrated intensity was not significantly different to the QAPB control (Figure 6.26; Table 6.4).

QAPB binding was unaffected by the presence of BMY 7378, with no detectable differences in fluorescence in SMCs or subcellular distribution (Figure 6.21; 6.22). Unlike the WT mouse, the presence of BMY 7378 had little effect on the QAPB histogram, with the exception of a small increase in fluorescence from pixels at intensities of 30 to 40 (Figure 6.24). Integrated intensity was not significantly reduced compared to the QAPB control (Figure 6.26; Table 6.4).

No QAPB binding was observed in the presence of RS100 329 (Figure 6.21; 6.22). Following a similar trend to the WT mouse, RS100 329 caused fluorescence to decrease. This was shown by the leftward displacement of the histogram with the majority of fluorescence resulting from low intensity pixels (Figure 6.24), and a significant reduction in integrated intensity (Figure 6.26; Table 6.4).

In contrast to the WT mouse, in the presence of 5-methylurapidil no evidence of QAPB binding was observed in the α_{1D}-KO (Figure 6.21; 6.22). This was demonstrated by the leftward shift in intensity on the histogram (Figure 6.25) and the significant reduction in integrated intensity (Figure 6.26; Table 6.4).

Unlike the WT mouse, the combination of BMY 7378 and RS100 329 resulted in the abolition of QAPB binding (Figure 6.21; 6.22). The leftward displacement of the histogram (Figure 6.24) and the significant reduction in integrated intensity for QAPB (Figure 6.26; Table 6.4) demonstrated that fluorescence was decreased by the combination of BMY 7378 and RS100 329.

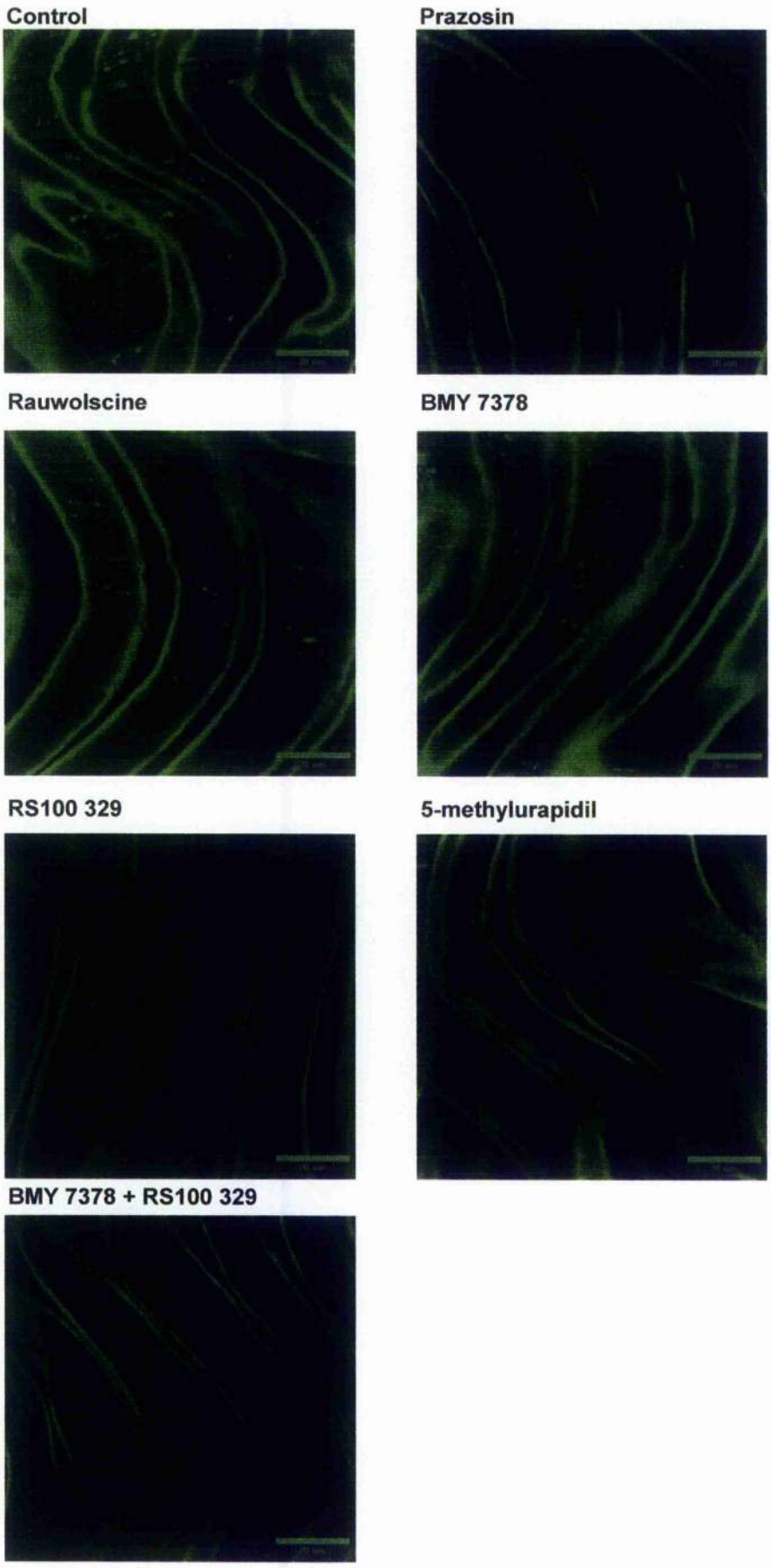

Figure 6.21. Low power view of SMCs in α_{1D}-KO: QAPB vs antagonists. Imaging settings: zoom three, laser 40, gain 12, iris 1.4.

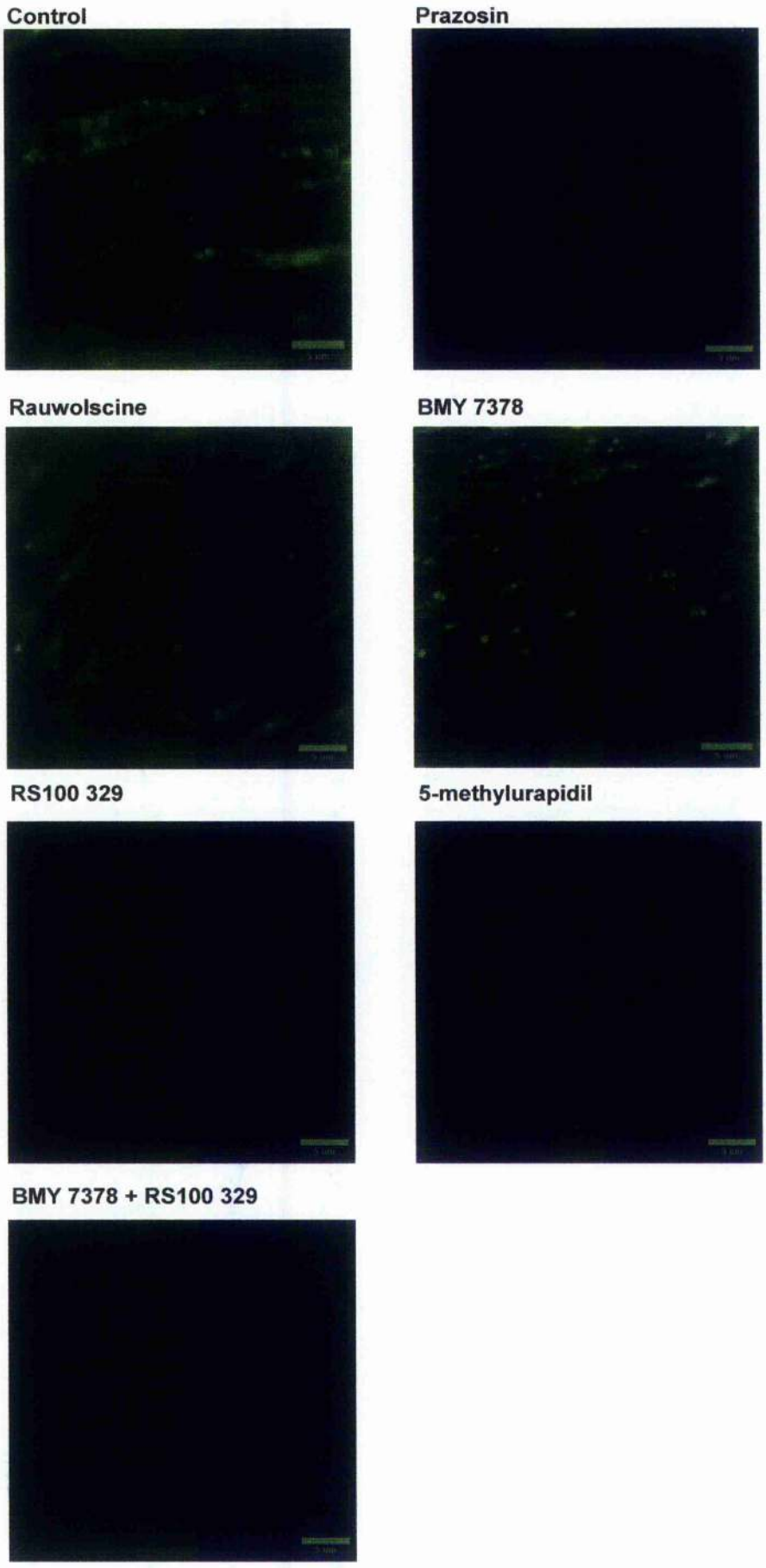

Figure 6.22. High power view of SMCs in α_{1D}-KO: QAPB vs antagonists. Imaging settings: zoom eight, laser 20, gain 22, iris 2.4.

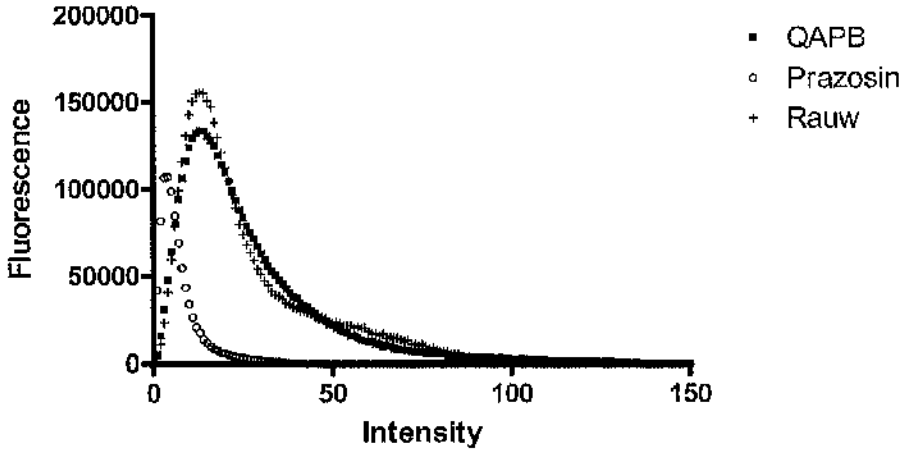

Figure 6.23 . Fluorescence against intensity to QAPB in the α_{1D}-KO in the presence of prazosin and rauwolscine expressed as mean ± S.E. (n=4).

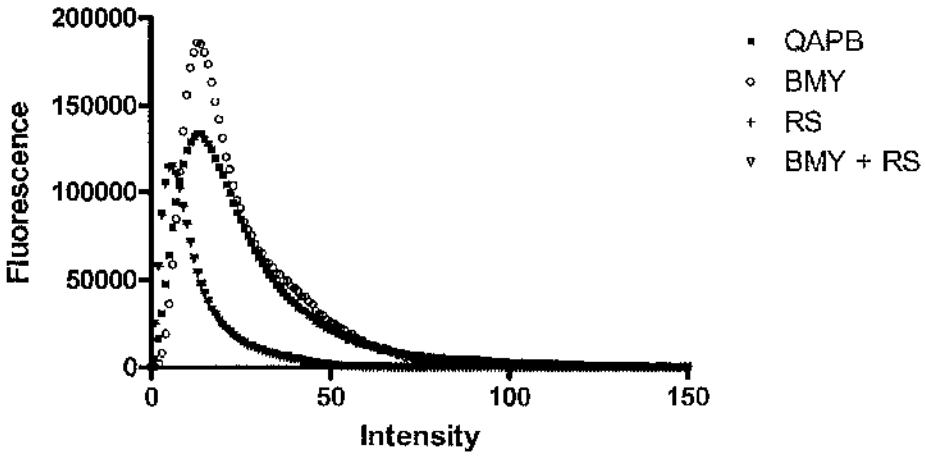

Figure 6.24. Fluorescence against intensity to QAPB in the α_{1D}-KO in the presence of BMY 7378, RS100 329 and BMY 7378/RS100 329 combination expressed as mean ± S.E. (n=4).

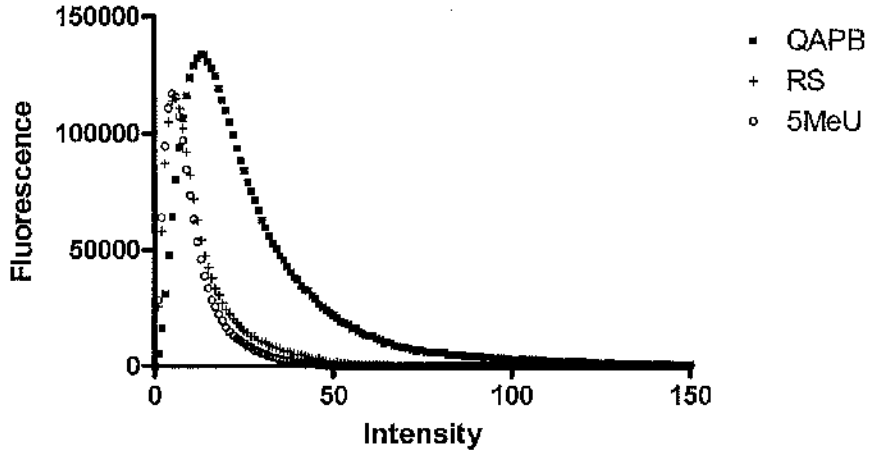

Figure 6.25. Fluorescence against intensity to QAPB in the α_{1D}-KO in the presence of 5-methylurapidil and RS100 329 expressed as mean ± S.E. (n=4).

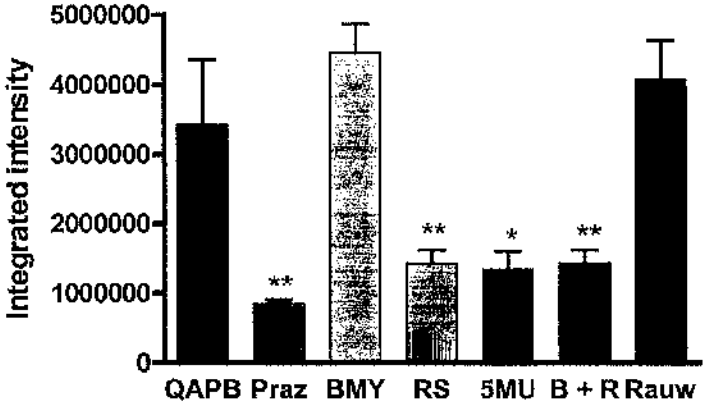

Figure 6.26. α_{1D}**-KO: Integrated intensity of QAPB in the presence of selective antagonists (n=4).**

Table 6.4. α_{1D}**-KO: Comparison of integrated intensity for QAPB in the presence of selective antagonists.**

Antagonist	Integrated intensity (± S.E.)
QAPB control	$3.43x10^6 \pm 9.3x10^5$
QAPB + prazosin	$8.53x10^5 \pm 5.1x10^{4\,**}$
QAPB + BMY 7378	$4.46x10^6 \pm 4.0x10^{5\,+}$
QAPB + RS100 329	$1.43x10^6 \pm 1.9x10^{5\,**}$
QAPB + 5-methylurapidil	$1.35x10^6 \pm 2.5x10^{5\,*}$
QAPB + BMY 7378 + RS100 329	$1.43x10^6 \pm 1.9x10^{5\,**}$
QAPB + Rauwolscine	$4.08x10^6 \pm 5.5x10^{5\,+}$

+p>0.05; *p<0.05; **p<0.01 compared to QAPB control (one-way ANOVA, Bonferroni's post test).

6.3.4.4. $\alpha_{1B/D}$-KO

Like the WT mouse, in the $\alpha_{1B/D}$-KO prazosin abolished QAPB binding (Figures 6.27; 6.28). In the presence of prazosin the leftward displacement of the histogram, the high number of low intensity pixels (Figure 6.29), and the significant reduction in integrated intensity (Figure 6.32; Table 6.5) demonstrated that fluorescence was decreased.

In the presence of rauwolscine no differences in QAPB binding were observed compared to the QAPB control (Figure 3.27; 6.28). The histogram indicated that in the presence of rauwolscine fluorescence to QAPB was decreased at intensities of approximately 30 to 50 but increased at intensities of 60 and above (Figure 6.29), following a similar trend to the WT mouse. Integrated intensity was not significantly different to the QAPB (Figure 6.32; Table 6.5).

Unlike the WT mouse, no changes to QAPB binding were observed in the presence of BMY 7378 (Figure 6.27; 6.28). However, the histogram indicated fluorescence to QAPB was reduced slightly at pixel intensities greater than 40 (Figure 6.30), although no significant change in integrated intensity was observed (Figure 6.32; Table 6.5).

In the presence of RS100 329 QAPB binding was completely abolished (Figure 6.27; 6.28). The histogram indicated that fluorescence was reduced at pixel intensities of 25 and above (Figure 6.30) and integrated intensity was significantly reduced (Figure 6.32; Table 6.5), following a similar trend as the WT mouse.

QAPB binding appeared markedly reduced and SMCs being less defined in the presence of 5-methylurapidil (Figure 6.27; 6.28). The histogram was shifted left with a high number of low intensity pixels (Figure 6.31) and a significant reduction in integrated intensity was detected in the presence of 5-methylurapidil (Figure 6.32; Table 6.5), following a similar trend as the WT mouse.

Unlike the WT mouse, with the combination of BMY 7378 and RS100 329 no QAPB binding was detected in the $\alpha_{1B/D}$-KO (Figure 6.27; 6.28). The histogram was shifted left indicating that the majority of fluorescence originated from low intensity pixels (Figure 6.30). Integrated intensity was significantly reduced (Figure 6.32; Table 6.5).

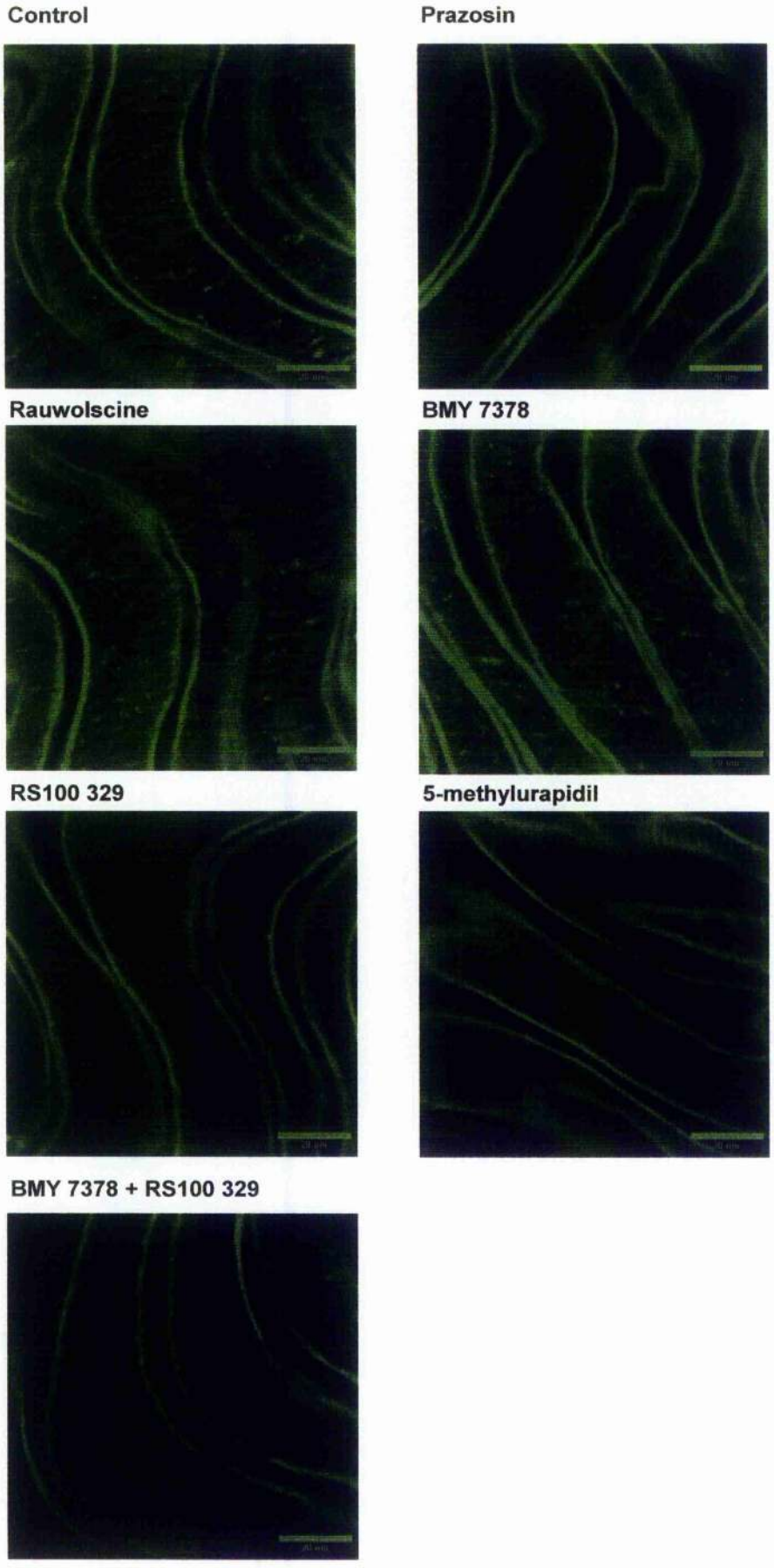

Figure 6.27. Low power view of SMCs in $\alpha_{1B/D}$-KO: QAPB vs antagonists. Imaging settings: zoom three, laser 40, gain 12, iris 1.4.

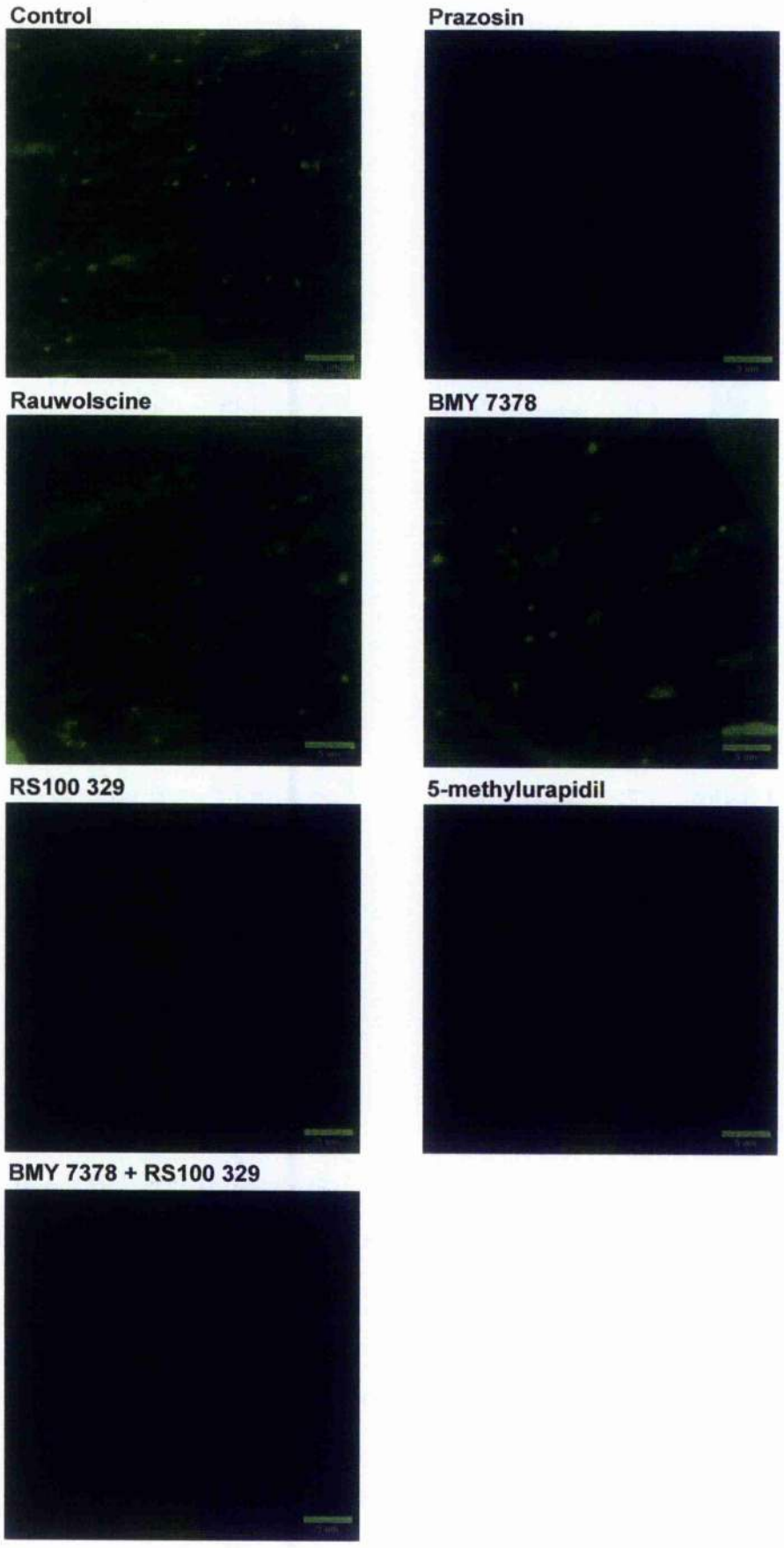

Figure 6.28. High power view of SMCs in $\alpha_{1B/D}$-KO: QAPB vs antagonists. Imaging settings: zoom eight, laser 20, gain 22, iris 2.4.

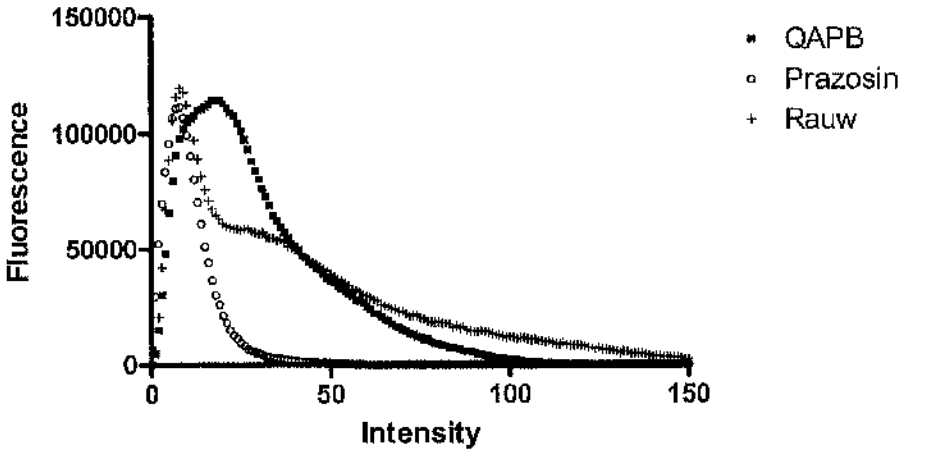

Figure 6.29. Fluorescence against intensity to QAPB in the $\alpha_{1B/D}$-KO in the presence of prazosin and rauwolscine expressed as mean ± S.E. (*n*=4).

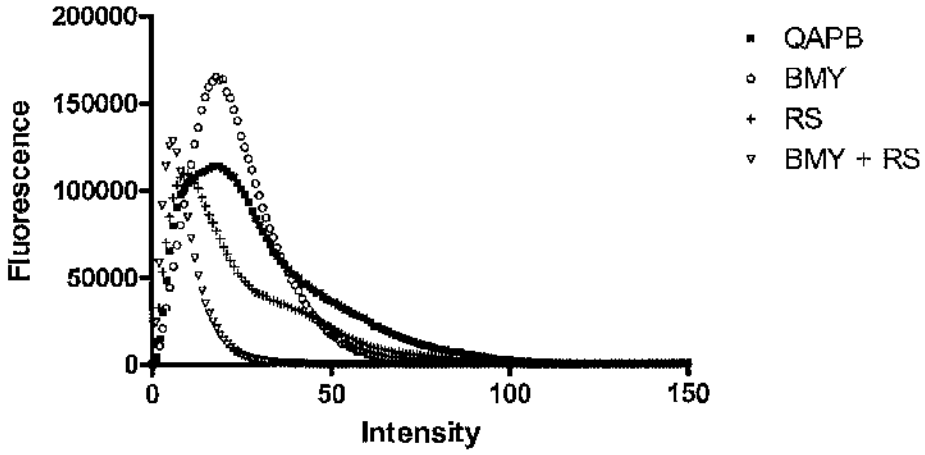

Figure 6.30. Fluorescence against intensity to QAPB in the $\alpha_{1B/D}$-KO in the presence of BMY 7378, RS100 329 and BMY 7378/RS100 329 combination expressed as mean ± S.E. (n=4).

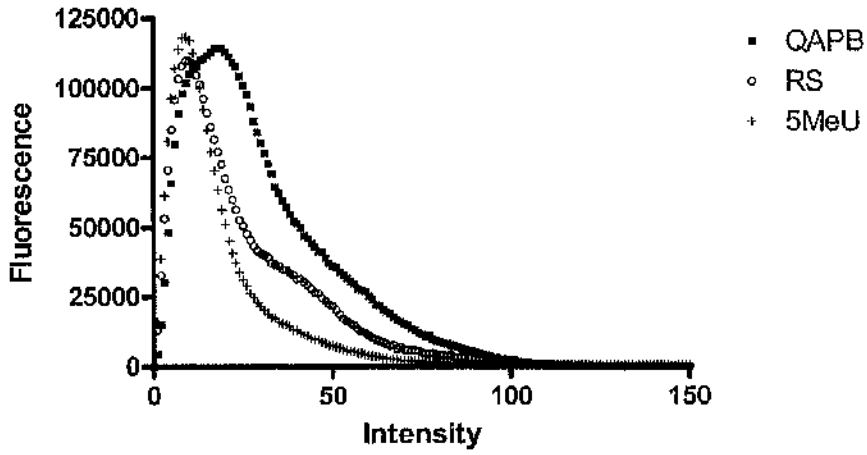

Figure 6.31. Fluorescence against intensity to QAPB in the $\alpha_{1B/D}$-KO in the presence of 5-methylurapidil and RS100 329 expressed as mean ± S.E. (n=4).

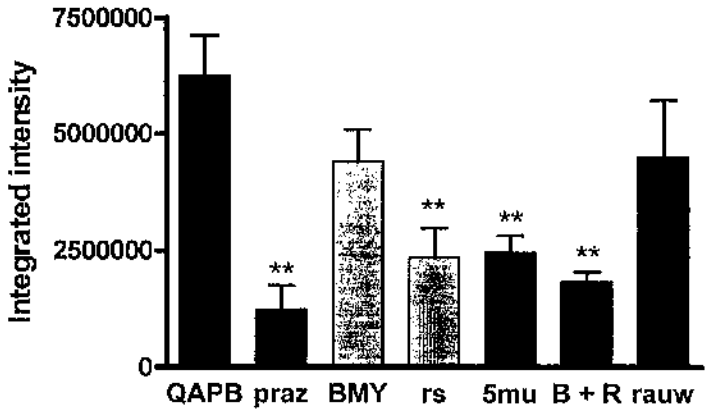

Figure 6.32. $\alpha_{1B/D}$-KO: Integrated intensity of QAPB in the presence of selective antagonists (n=4).

Table 6.5. $\alpha_{1B/D}$-KO: Comparison of integrated intensity for QAPB in the presence of selective antagonists.

Antagonist	Integrated intensity (± S.E.)
QAPB control	$6.25x10^6 \pm 8.7x10^5$
QAPB + prazosin	$1.24x10^5 \pm 5.0x10^{5\,**}$
QAPB + BMY 7378	$4.40x10^6 \pm 6.9x10^{5\,+}$
QAPB + RS100 329	$2.35x10^6 \pm 6.3x10^{5\,**}$
QAPB + 5-methylurapidil	$2.45x10^6 \pm 3.7x10^{5\,**}$
QAPB + BMY 7378 + RS100 329	$1.84x10^6 \pm 2.0x10^{5\,**}$
QAPB + Rauwolscine	$4.49x10^6 \pm 1.2x10^{6\,+}$

+p>0.05; **p<0.01 compared to QAPB control (one-way ANOVA, Bonferroni's post test).

6.4. Discussion

6.4.1. Protocol development

At the onset of this study a series of preliminary experiments was carried out to determine the most suitable vessel preparation and incubation conditions for the experimental protocol. The use of the open vessel preparation overcame the problems associated with the thick elastic wall of the carotid artery. Ideally QAPB incubations would have been performed at the physiological temperature of 37°C, but to prevent the calcium precipitating out of the PSS, incubations were carried out at room temperature (21°C). QAPB binding was concentration-dependent but the intermediate concentration of QAPB 0.1 μM was selected for use in the study due to insufficient definition at 10 nM and concerns over saturation and non-selectivity at QAPB 1 μM. In addition, QAPB 0.1 μM antagonised the α_1-AR-mediated response to phenylephrine, which further validated the use of this concentration for the visualisation study of α_1-ARs. The pK_B of 8.5 obtained for QAPB 0.1 μM also correlates with the affinity of QAPB for the α_1-AR subtypes (pK_i α_{1A}-AR 8.7, α_{1B}-AR 8.4, α_{1D}-AR 8.1) (Mackenzie *et al.*, 2000). QAPB has been successfully used in previous studies on cells at concentrations below 10nM (Pediani *et al.*, 2005;Woollhead, 2002). However, the present study has shown that in the intact vessel higher concentrations are required. This is supported by recent studies in the mouse mesenteric artery, which used QAPB 1 μM (McBride *et al.* Submitted for publication). The binding of QAPB 0.1 μM was time-dependent. An incubation time of 120 minutes was selected for use in this study since SMCs were insufficiently defined at the earlier time-points suggesting that QAPB had not reached equilibrium. This was surprising as incubations of 30 to 40 minutes are usually sufficient for an antagonist to reach equilibrium in functional experiments and previous studies using QAPB 1 μM have successfully imaged isolated cells and other vessels following an incubation of only 60-75 minutes (Pediani *et al.*, 2005;McBride *et al.* Submitted for publication). This suggests that the uptake of QAPB into the SMC is slower in the carotid artery than isolated SMCs or SMCs in the mouse first order mesenteric artery.

Control vessels were incubated in PSS alone to assess the fluorescence produced in the absence of QAPB. It has previously been demonstrated that QAPB was only fluorescent when bound to receptors (Daly *et al.*, 1998;Mackenzie *et al.*, 2000). This was confirmed in the present study by only autofluorescence from the elastic lamina being observed in the absence of QAPB and no fluorescence was detected in the smooth muscle layers. For this

reason the quantitative analysis was performed on the high power images, which excluded the elastic lamina.

6.4.2. Comparison of QAPB binding in WT mouse and knockouts

Clear differences in the binding distribution of QAPB were observed between mouse strains, which were supported by the quantitative analysis. The even distribution of clearly defined SMCs and bright fluorescence observed in the WT mouse and α_{1B}-KO contrasted with the variable binding pattern and reduced definition of SMCs in the α_{1D}-KO and $\alpha_{1B/D}$-KO. However, in all three knockouts a marked reduction in the fluorescence at high intensity pixels was detected. The reduction in the number of high intensity pixels in the α_{1B}-KO suggests that the total α_1-AR population in the carotid artery was reduced, thus in the WT mouse the α_{1B}-AR appears to be present in SMCs. Fluorescence in the α_{1D}-KO was reduced more than in the α_{1B}-KO, consistent with the expectation that the α_{1D}-AR would be a major component of the α_1-AR population. This suggests that a greater number of α_{1D}-ARs than α_{1B}-ARs are present in the media of the WT mouse. Like the α_{1D}-KO, the marked reduction in QAPB binding in the $\alpha_{1B/D}$-KO compared to the α_{1B}-KO confirms that a high proportion of the total α_1-AR population in the WT mouse is α_{1D}-ARs. Furthermore, the reduction in fluorescence compared to the α_{1D}-KO supports findings in the α_{1B}-KO that the α_{1B}-AR does appear to comprise a component of the α_1-AR population in the smooth muscle layers of the WT mouse carotid artery. It has been reported that when the α_{1B}-AR is coexpressed with either the α_{1A}-AR or α_{1D}-AR an increase in binding site density and protein expression is detected (Uberti *et al.*, 2003). Thus, the absence of the α_{1B}-AR may account for the decreased fluorescence in the α_{1B}-KO and $\alpha_{1B/D}$-KO by a reduction in the binding site density of the α_{1A}-AR and/or α_{1D}-AR., in addition to a reduction in the total α_1-AR population

6.4.3. Competition with non-fluorescent antagonists

The varying affinities of the non-fluorescent antagonists for the α_1-ARs were taken into consideration while evaluating how effectively the antagonists competed with QAPB (Table 6.6). In addition, affinity estimates from binding experiments at the α_2-AR subtypes (pK_i α_{2A}-AR 7.8; α_{2B}-AR 7.3; α_{2D}-AR 7.8) (McGrath & Daly, 2005) were used to select the concentration of rauwolscine used. Generally, the concentration of each

antagonist used was higher than indicated by the pK_i but was selected to have approximately ten-fold higher affinity than QAPB 0.1 μM at the subtype.

Table 6.6. Comparison of affinity estimates from rat-1-fibroblasts expressing human α_1-AR subtypes

Ligand	α_{1A}-AR pK_i	α_{1B}-AR pK_i	α_{1D}-AR pK_i
QAPB	8.7	8.4	8.1
Prazosin	9.0	9.0	9.0
BMY 7378	7.1	6.8	10.5
RS100 329	9.7	8.0	8.0
5-methylurapidil	9.2	7.2	7.9

Data from Table 2, Mackenzie et al. (2000).

6.4.3.1. Prazosin

In all four mouse strains prazosin abolished QAPB binding, or at least reduced fluorescence below a detectable level. This confirmed that the α_1-AR selectivity of QAPB was preserved at 0.1 μM. The observations were supported by the quantitative analysis, which showed prazosin caused a marked reduction in total intensity of QAPB. Furthermore, in the presence of prazosin the majority of fluorescence originated from low intensity pixels.

6.4.3.2. Rauwolscine

The α_2-AR selective antagonist, rauwolscine did not appear to reduce fluorescence when examined visually in any of the mice strains. However, the small reduction in low intensity pixels and the increase in high intensity pixels in both the WT mouse and $\alpha_{1B/D}$-KO indicated that caused an increase in fluorescence to QAPB. At present it is unclear why this would occur. In the α_{1B}-KO a small reduction in fluorescence to QAPB from high intensity pixels was detected. This raises the possibility that QAPB 0.1 μM may be binding α_2-ARs. Alternatively, this could also reflect the binding of rauwolscine to α_1-AR. However, in the α_{1D}-KO rauwolscine did not have an effect on QAPB binding and the total intensity to QAPB in all four mouse strains was not significantly different in the

presence of rauwolscine suggesting that QAPB binding was not greatly affected by the antagonist.

6.4.3.3. BMY 7378

Based on the binding affinities at the α_1-AR subtypes (Table 6.6), BMY 7378 0.1 μM could have potentially bound to all three α_1-AR subtypes. However, a decrease in fluorescence to QAPB was observed in the presence of BMY 7378 in the WT mouse and α_{1B}-KO, but not the α_{1D}-KO or $\alpha_{1B/D}$-KO. These observations were sustained in the quantitative analysis: integrated intensity and fluorescence from high intensity pixels were reduced in the WT mouse and α_{1B}-KO, but were largely unchanged in the α_{1D}-KO and $\alpha_{1B/D}$-KO. These findings are consistent with a previous study in isolated SMCS from the carotid artery also reported that BMY 7378 blocked QAPB binding in the majority of SMCs in the WT mouse and α_{1B}-KO. In agreement with the functional data in Chapters Three and Four, these findings suggest that the concentration of BMY 7378 used (0.1 μM) had higher affinity at the α_{1D}-AR than the α_{1A}-AR or α_{1B}-AR. The variations in fluorescence observed between individual SMCs in the presence of BMY 7378 in the WT mouse and α_{1B}-KO suggest that the α_{1D}-AR was not uniformly distributed throughout the media. Overall, these findings confirm that the α_{1D}-AR is present in the media of the WT mouse and α_{1B}-KO and is absent in the α_{1D}-KO and $\alpha_{1B/D}$-KO.

6.4.3.4. RS100 329

Relative to the binding affinity of RS100 329 at the α_1-AR subtypes, at a concentration of 0.1 μM, RS100 329 could prevent QAPB binding to all three α_1-AR subtypes (Table 6.6). In the WT mouse and α_{1B}-KO a decrease in fluorescence to QAPB was observed in the presence of RS100 329. This was supported by the significant reduction in integrated intensity and the reduction in the number of high intensity pixels. This suggested that the α_{1A}-AR was present in both the WT mouse and α_{1B}-KO. Some brighter cells remained stained, suggesting that the distribution of the α_{1A}-AR was intermittent. This is in agreement with an earlier study in isolated SMCS from the carotid artery, in which RS100 329 reduced QAPB binding in some cells in the WT mouse and α_{1B}-KO (Woollhead, 2002). The cell surface and intracellular binding observed in the presence of RS100 329 indicated that populations of other α_1-AR subtypes were present in these mice. In contrast, in the α_{1D}-KO and $\alpha_{1B/D}$-KO QAPB binding appeared to be abolished by RS100 329. The observations were supported by the significant reduction in integrated intensity and the

majority of fluorescence being detected at low intensity pixels. This suggests that the α_{1A}-AR was also present in the SMCs of the α_{1D}-KO and the $\alpha_{1B/D}$-KO. In these two mouse strains, where it was shown that the α_1-AR response is mediated by the α_{1A}-AR (Chapter Four), the abolition of QAPB binding was consistent with RS100 329 showing higher binding affinity at the α_{1A}-AR than the α_{1B}-AR or α_{1D}-AR. The residual QAPB binding detected in the WT mouse and α_{1B}-KO, where the α_1-AR response is predominantly α_{1D}-AR-mediated, is in agreement with RS100 329 having lower affinity at the α_{1D}-AR. There is no evidence from this data that α_{1B}-ARs are present in the α_{1D}-KO. This was unexpected since the α_{1B}-AR appears to be present in the WT mouse. This may be due to either the absence of α_{1B}-ARs in the α_{1D}-KO or the α_{1B}-ARs are present but are being blocked by RS100 329. This may be a difference that exists between the α_1-AR populations in WT mouse and α_{1D}-KO. Overall, these findings indicate that α_{1A}-ARs are present in the media of the carotid artery of the four mice.

6.3.4.5. 5-methylurapidil

Based on the binding affinities at the α_1-AR subtypes, 5-methylurapidil 0.1 μM could prevent QAPB binding to the α_{1B}-AR and α_{1D}-AR in addition to the α_{1A}-AR (Table 6.6). A marked reduction in QAPB binding was observed in the presence of 5-methylurapidil in the WT mouse, α_{1B}-KO and $\alpha_{1B/D}$-KO, with SMCs being less defined. Furthermore, in the α_{1D}-KO QAPB binding was abolished. The reduction in QAPB binding observed was in agreement with the significant reduction in integrated intensity and the reduction in fluorescence from high intensity pixels at high intensities in all four mouse strains. However, the residual binding detected in the WT mouse and α_{1B}-KO and the functional evidence in Chapters Three and Four suggest that at this concentration 5-methylurapidil has retained selectivity for the α_{1A}-AR. The effect of 5-methylurapidil on QAPB binding is comparable to that observed in the presence of RS100 329 and suggests that α_{1A}-ARs were present in the murine carotid artery of the four mouse strains, although there was no evidence of the α_{1B}-AR in the α_{1D}-KO.

6.3.4.6. BMY 7378 and RS100 329 combination

In the presence of both BMY 7378 and RS100 329 QAPB binding appeared markedly reduced in the WT mouse but was abolished in the α_{1B}-KO, α_{1D}-KO and $\alpha_{1B/D}$-KO. Quantitative analysis revealed a marked reduction in total intensity in all four strains of mouse and in all mice there was no evidence of fluorescence at the higher intensities. The

residual QAPB binding in the WT mouse suggests that all three α_1-AR subtypes may exist in the smooth muscle of the carotid artery of the WT mouse. As no QAPB binding was observed in the α_{1D}-KO, this may reflect that no α_{1B}-ARs are present in this strain.

In summary, QAPB appears to have selectively bound to α_1-ARs in the mouse carotid artery. In the $\alpha_{1B/D}$-KO the only possible α_1-AR subtype, the α_{1A}-AR, appears to be present. Evidence of the α_{1A}-AR but not the α_{1B}-AR was observed in the α_{1D}-KO. Both the α_{1A}-AR and the α_{1D}-AR appear to exist in the α_{1B}-KO. In the WT mouse evidence of all three α_1-AR subtypes was apparent. The findings in the WT mouse and α_{1B}-KO are in agreement with those in isolated SMCs from the carotid artery, in which evidence of all three α_1-ARs was reported in the WT and the α_{1A}-AR and α_{1D}-AR appeared to be present in the α_{1B}-KO (Woollhead, 2002).

6.3.5. QAPB subcellular distribution

Comparison of the distribution of QAPB binding in individual SMCs indicated that differences between α_1-AR subtypes may exist. In the WT mouse QAPB binding was observed on the cell membrane and in intracellular compartments. Inside the cell, diffuse QAPB binding existed in the perinuclear regions, while clusters of QAPB binding were also identified. This is consistent with previous studies, which reported QAPB bound to the cell surface and in punctate intracellular sites in isolated cells (Daly *et al.*, 1998;McGrath *et al.*, 1999;Mackenzie *et al.*, 2000) and in SMCs *in situ* (McBride *et al.* Submitted for publication). The subcellular distribution of QAPB binding in the α_{1B}-KO was similar to the WT mouse but there appeared to be more clustered intracellular binding, although this was not reflected in the number of high intensity pixels measured. In contrast, there appeared to be less punctate binding in the α_{1D}-KO and binding was generally more diffuse. However, in the $\alpha_{1B/D}$-KO, there was little evidence of diffuse QAPB binding to the cell surface and perinuclear region and binding was mostly in punctate compartments. These differences in QAPB binding between the mouse strains suggest that the subcellular distribution of α_1-ARs may differ or at least that changes occur when an α_1-AR subtype is not present.

Differences in α_1-AR subcellular distribution have been reported in previous studies. The α_{1A}-AR was located mainly intracellularly, while the α_{1B}-AR was predominantly located on the cell surface (Hirasawa *et al.*, 1997;Sugawara *et al.*, 2002;McCune *et al.*, 2000). In the present study in mice lacking the α_{1B}-AR (α_{1B}-KO and $\alpha_{1B/D}$-KO), QAPB binding

appeared to be more punctate. In contrast in the mice where the α_{1B}-AR was present (WT mouse and α_{1D}-KO), QAPB binding was more diffuse. This indicates that the α_{1B}-AR may have a regulatory role within the cell. It was recently reported that the α_{1B}-AR formed heterodimers with the α_{1A}-AR and α_{1D}-AR (Uberti *et al.*, 2003) and the α_{1B}-AR/α_{1D}-AR dimer was suggested to aid the transportation of the α_{1D}-AR to the cell surface (Hague *et al.*, 2004b). Thus, the increase in punctate binding in the α_{1B}-KO and $\alpha_{1B/D}$-KO may be due to a reduction in the transportation of α_{1A}-ARs or α_{1D}-ARs to the cell surface. Furthermore, the lack of intracellular clusters in the α_{1D}-KO could indicate that the α_{1D}-AR is predominantly located inside the cell, while the reduced binding on the cell surface of the α_{1B}-KO and $\alpha_{1B/D}$-KO could point to the main location of the α_{1B}-AR.

The evidence in the present study may support the hypothesis that a difference in the subcellular distribution of α_1-ARs in the SMCs of the mouse carotid artery exists. In agreement with the studies of α_1-AR distribution in isolated cells (Hirasawa *et al.*, 1997;Sugawara *et al.*, 2002;McCune *et al.*, 2000), the α_{1B}-AR is mainly found at the cell surface, while in the absence of the α_{1B}-ARs the α_{1A}-AR and α_{1D}-AR are predominantly located at intracellular sites.

6.3.6. α_1-AR distribution and function

In Chapters Three and Four the α_1-AR-mediated contractile response of the mouse carotid artery was characterised pharmacologically. The α_{1D}-AR was the predominant mediator of contraction, supporting a previous study (Deighan C, 2002;Deighan C *et al.*, 2005), and an α_{1A}-AR-mediated secondary component to the contractile response was identified using a selective α_{1A}-AR agonist. The present study has shown evidence which may provide an insight to the role of the α_{1B}-AR in the mouse carotid artery. Despite the lack of evidence of α_{1B}-ARs in the α_{1D}-KO, the α_{1B}-AR appeared to be present in the smooth muscle layers of the WT mouse. The presence of an α_1-AR cannot be taken as evidence that it is functional. However, the presence of the α_{1B}-AR is in agreement with the functional data in Chapters Three and Four, in which comparison of the phenylephrine-induced response in the WT and knockout mice indicated a contractile α_{1B}-AR. Thus, the α_{1B}-AR appears to contribute to the contraction of the carotid artery in the WT mouse. In addition to a contractile role, the present study indicates that the α_{1B}-AR may regulate the cellular expression of the α_{1A}-AR and α_{1D}-AR in the carotid artery.

6.3.7. Conclusion

The experimental protocol developed enabled the distribution of α_1-ARs in the smooth muscle layers of the carotid artery to be examined. α_1-ARs were evenly distributed in the WT mouse and α_{1B}-KO but in the α_{1D}-KO and $\alpha_{1B/D}$-KO the distribution of α_1-ARs was variable. All three α_1-AR subtypes appear to exist in the WT mouse, while the α_{1A}-AR and α_{1D}-AR were present in the α_{1B}-KO and only the α_{1A}-AR was identified in both the α_{1D}-KO and $\alpha_{1B/D}$-KO. In the absence of the α_{1B}-AR (α_{1B}-KO and $\alpha_{1B/D}$-KO) an increase in clustered binding was observed, while in the presence of the α_{1B}-AR (WT mouse and α_{1D}-KO) binding was more diffuse.

Chapter Seven

Visualisation of α_1-ARs on the endothelium

7.1. Introduction

The intima is the innermost layer of the arterial wall. It consists of a single layer of endothelial cells (EC), which are in direct contact with plasma, and is separated from the media by the internal elastic lamina. It is well documented that the vascular endothelium has an important role in the regulation of vascular tone, through the release of contractile or vasorelaxant substances from EC (see Chapter One).

7.1.1. Endothelial α-ARs

It is well established that α_2-ARs exist in both the media and the intima (Vanhoutte, 2001;Cocks & Angus, 1983), while α_1-ARs have been considered to be present only in the media due to the lack of positive evidence.

There is substantial functional evidence of endothelial α_2-ARs in several arteries. For instance, Zschauer et al. (1997) proposed that noradrenaline acted on endothelial α_2-ARs to relax the rabbit brachial artery as no relaxation was observed in denuded vessels. It has also been demonstrated that the stimulation of α_2-ARs on the endothelium, with noradrenaline, induced the release of NO and the subsequent relaxation of the rat aorta (Kaneko & Sunano, 1993). Furthermore, Malekzadeh Shafaroudi et al. (2005) established that in the mouse aorta the activation of α_{2A}-ARs on the endothelium resulted in vasodilatation. It has also been shown that the stimulation of endothelial α_2-ARs accounted for the suppressed contractions to noradrenaline in the carotid artery of the pig (Ohgushi et al., 1993). In the mouse carotid artery L-NAME blocked relaxations to the α_2-AR agonist UK14304, indicating that α_2-ARs were involved in NO release (Malekzadeh Shafaroudi, 2005). Thus, in many studies the endothelium-dependent relaxations to catecholamines, or surrogates acting are their receptors, are attributed to α_2-ARs on the endothelium.

Functional evidence to suggest that α_1-ARs exist on the endothelium is now emerging (Boer *et al.*, 1999;Tuttle & Falcone, 2001;Zschauer *et al.*, 1997;Kaneko & Sunano, 1993;Filippi *et al.*, 2001;de Andrade *et al.*, 2006). The first study to demonstrate the existence of endothelial α_1-ARs reported that in the presence of an α_2-AR antagonist noradrenaline induced NO release in the rabbit bronchial artery (Zschauer *et al.*, 1997). Furthermore, a study of the rat mesenteric vascular bed provided evidence of endothelium-dependent relaxations to phenylephrine (Filippi *et al.*, 2001). It was also demonstrated that

in the presence of the selective α_{1D}-AR antagonist BMY 7378, no phenylephrine-induced relaxations were observed, consistent with the response being mediated by endothelial α_{1D}-ARs. Further evidence of an endothelium-dependent α_{1D}-AR-mediated relaxation to phenylephrine was recently reported in the rat carotid artery (de Andrade *et al.*, 2006). At present, there is no evidence of the existence of α_1-ARs on the endothelium of the mouse carotid artery.

7.1.2. Aims

It is clear that the role of α_1-ARs on the endothelium is an area of research which is currently expanding. It is possible that attempts to obtain functional evidence of endothelial α_1-ARs are hindered by the strong contractile response to α_1-AR agonists in the carotid artery. However, endothelial α_2-ARs were recently visualised on the endothelium for the first time using a fluorescent ligand (Malekzadeh Shafaroudi *et al.*, 2005). This demonstrated an alternative method to investigate the receptors present on the endothelium. Consequently, the aims of the present study were:

- To establish whether α_1-ARs exist on the endothelium of the carotid artery of the WT mouse and α_1-AR knockouts using visualisation techniques.

- To compare the proportion of EC with α_1-ARs between mouse strains, and in doing so:

    - Determine the α_1-AR subtypes present on the endothelium of the WT mouse carotid artery by investigating the effect of subtype selective antagonists on the number of EC with α_1-ARs.

    - Investigate the α_1-AR subtypes present on the endothelium of the α_{1B}-KO, α_{1D}-KO and $\alpha_{1B/D}$-KO by comparing the relative number of EC with α_1-ARs, in the absence and presence of selective antagonists, in the knockouts with the WT mouse.

7.2. Methods

7.2.1. Incubation conditions

This protocol has been described in detail in Chapter Three. In brief, 5mm segments of carotid artery were incubated at room temperature (21°C) with QAPB 0.1μM, in a PSS solution at room temperature for 30 minutes. The vessels were then co-incubated with the nuclear dye Syto 61 1 μM and QAPB 0.1 μM for 90 minutes. Syto 61 was used to identify the position of the EC.

In the WT mouse, additional experiments were carried out in which, following the QAPB incubation period, vessels were incubated in a QAPB 0.1μM /PSS solution containing Syto 61 1 μM and a subtype selective antagonist(s): prazosin 0.1 μM, (non-selective α_1-AR antagonist); RS100329 0.1 μM, (α_{1A}-AR selective antagonist); 5-methylurapidil 1 μM (α_{1A}-AR selective antagonist); BMY7378 0.1 μM (α_{1D}-AR selective antagonist); both BMY 7378 0.1 μM and RS100329 0.1 μM; or rauwolscine 0.1 μM (α_2-AR antagonist). Throughout the incubation period all solutions were replaced every 30 minutes to ensure the pH of the solution and glucose levels were maintained.

In all four mouse strains a series of experiments were also performed in which vessels were incubated with QAPB 0.1 μM for 60 minutes and then co-incubated for a further 60 minutes with a 0.1μM QAPB/PSS solution containing one of the subtype selective antagonists described above.

7.2.2. Slide mounting

At the end of the incubation period each carotid artery segment was sliced open with a single-edged razor blade and laid flat on a microscope slide with the endothelial side up (Miquel RM *et al.*, 2005) and coverslip (thickness 1.5) on top. Care was taken to preserve the endothelium.

All arteries were visualised using the Bio-Rad Radiance 2100 Confocal Laser Scanning System. A x40 oil immersion objective (NA 0.75) was used for all experiments. An argon-ion laser with an excitation wavelength of 488nm with an emission filter of 515nm was used for QAPB. Images were recorded at zoom three a laser intensity of 40, a gain of 12, offset 0.0 and pinhole setting of 1.4. A red diode, with an excitation/emission

wavelength of 628/645nm, was used for Syto 61. At a zoom of three, laser intensity was set to 30, with a gain of 12, offset 0.0 and an optimal pinhole of 1.4. The standard scan speed of 500 lines per second was used for all experiments. An image size of 515 x 512 pixels produced a field size of 289μm x 289μm.

Vessels were imaged from the internal elastic lamina through to the media. A minimum of three images were collected from random areas of each vessel. Each experiment was repeated four times for each strain of mouse.

Kalman (5 frames) was used to record individual 2D images. Z-series were also produced in stacks of 1μM slices, starting at the first smooth muscle layer and ending at the internal elastic lamina, producing a stack of approximately 15μm.

7.2.3. Image analysis

Following image capture, the images produced from the colocalisation experiments with QAPB and Syto 61 were overlaid using Lasersharpe software. Thus, the localisation of QAPB binding was directly compared with the nuclear binding of Syto 61. In all four mouse strains, using Metamorph software, the numbers of EC showing QAPB binding were counted for individual 2D images produced in each experiment and a mean number of EC was calculated and expressed as mean ± standard error. This was repeated for the number of EC identified by Syto 61 binding. The number of EC with QAPB binding was expressed as a percentage of the total number of EC (as identified by Syto 61). The proportion of EC stained with QAPB out of the number of EC stained with Syto 61 was compared between mouse strains using Student's t-test. In addition, the number of EC stained with QAPB in the presence of the subtype selective antagonists in the WT mouse mice was compared with the knockout mice. It should be noted that this method of quantitative analysis was dependent on the α_1-AR population varying among EC.

3D images were produced from a 3D projection of the stack of "optical sections" using Lasersharpe software.

7.3. Results

7.3.1. QAPB and Syto 61 binding

7.3.1.1. WT mouse

The membrane dye Syto 61 (1 μM) bound to the nucleus of cells on the endothelium of the carotid artery in the WT mouse. EC were located on the internal elastic lamina (Figure 7.2) and within the grooves formed by folds in the internal elastic lamina (Figure 7.1). QAPB (0.1 μM) bound to EC on the internal elastic lamina and within the folds of the internal elastic lamina in the WT mouse. QAPB binding on the endothelium overlapped with the Syto 61 binding as shown in the merged images. Evidence of both diffuse and clustered QAPB binding was observed on the cell membrane of the EC.

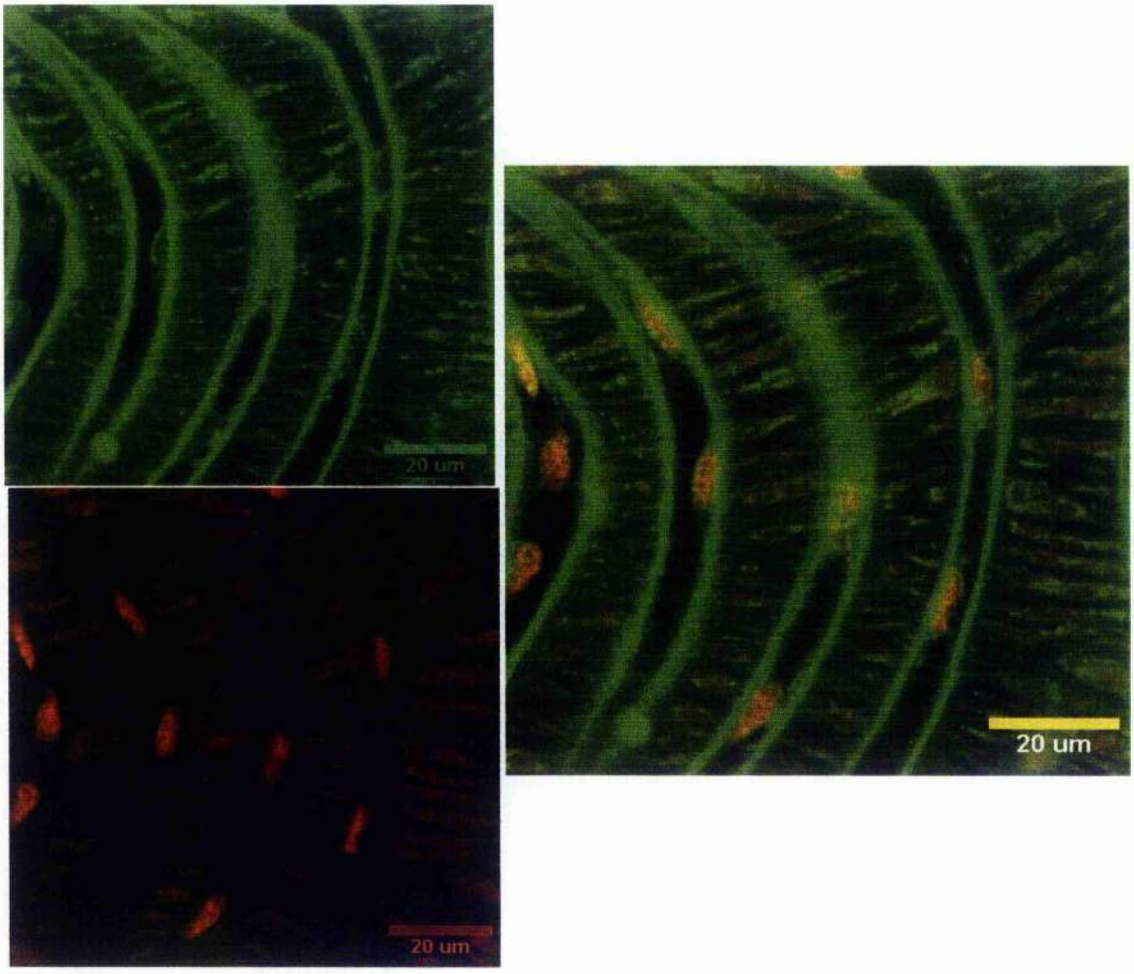

Figure 7.1. 2D image of EC in the WT mouse: EC attached to the folds in the internal elastic lamina and smooth muscle cells within the bands of elastic lamina. (QAPB binding in green; Syto 61 binding in red).

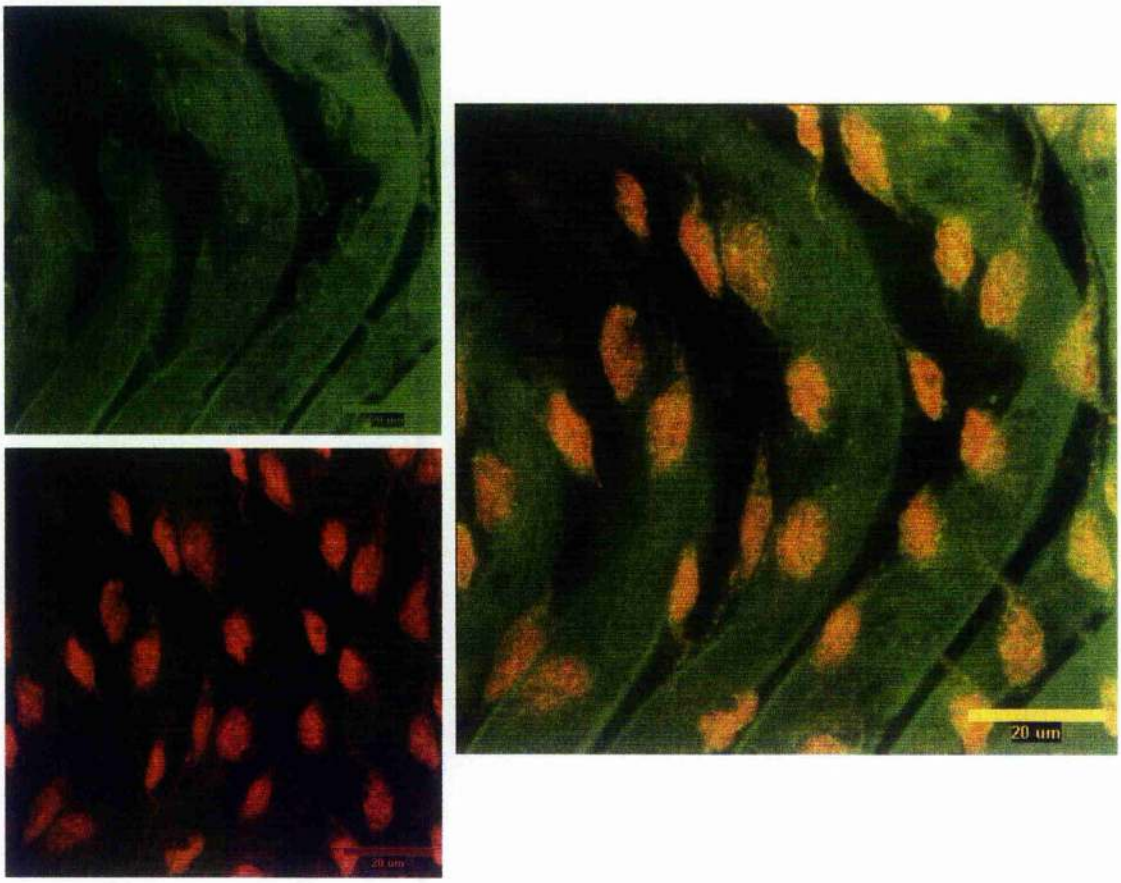

Figure 7.2. 3D reconstruction of EC in the WT mouse: EC attached to the folds in the internal elastic lamina. (QAPB binding in green; Syto 61 binding in red).

7.3.1.2. α_{1B}-KO

The nucleus of the EC in the carotid artery was stained with Syto 61 (Figure 7.3 and 7.4). EC were visualised on the surface of the internal elastic lamina as well as in the grooves formed by the folded internal elastic lamina. Evidence of co-staining with QAPB was observed on the cells stained with Syto 61. QAPB binding was observed on cells on the endothelium. Evidence of both diffuse and clustered QAPB binding was identified on the cell surface.

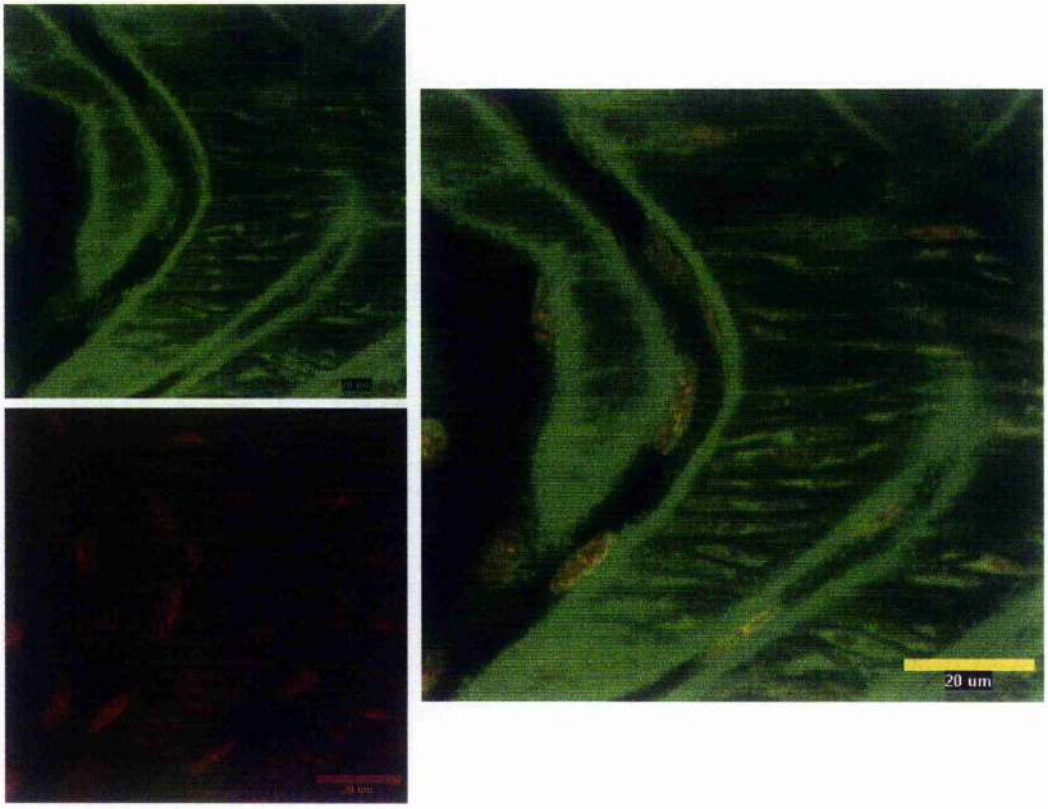

Figure 7.3. 2D image of EC in the α_{1B}-KO: EC attached to the folds in the internal elastic lamina and smooth muscle cells within the bands of elastic lamina. (QAPB binding in green; Syto 61 binding in red).

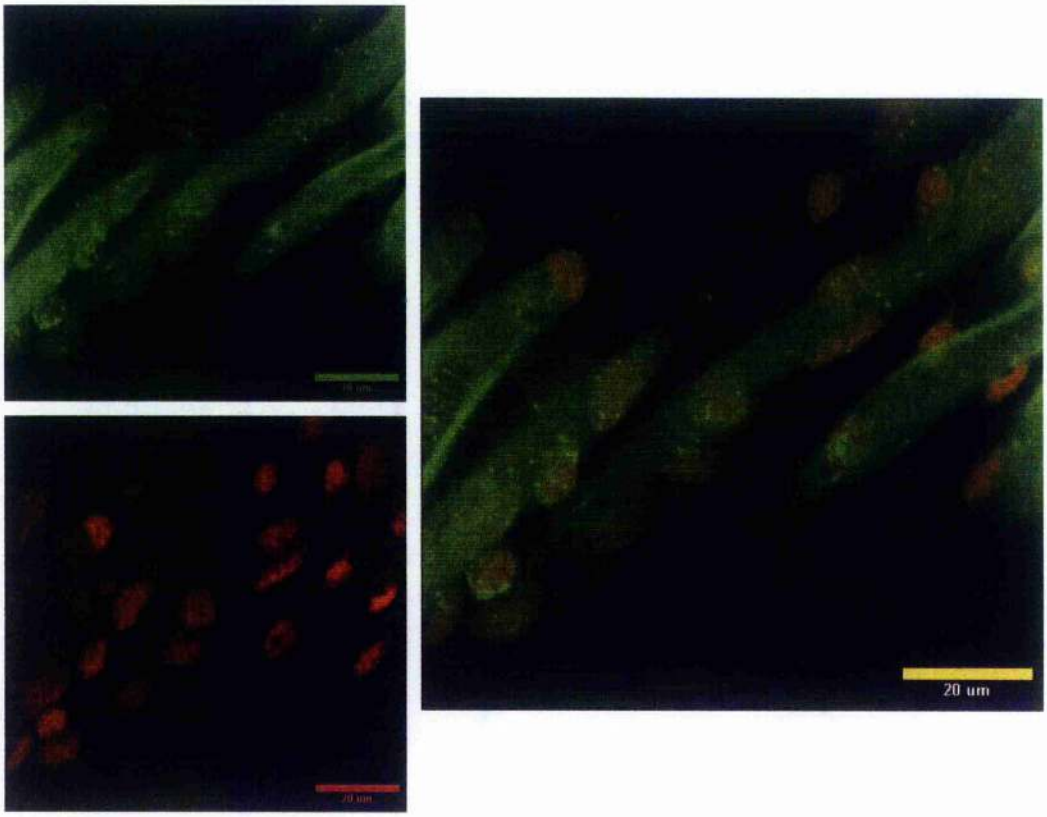

Figure 7.4. 3D reconstruction of EC in the α_{1B}-KO: EC attached to the folds in the internal elastic lamina. (QAPB binding in green; Syto 61 binding in red).

7.3.1.3. α_{1D}-KO

Syto 61 bound to the nucleus of the EC in the carotid artery and enabled the location of individual cells to be revealed in the α_{1D}-KO. EC were attached to the internal elastic lamina surface and within the grooves formed by the folds in the lamina (Figure 7.5 and 7.6). QAPB binding was observed on the EC in the α_{1D}-KO. Diffuse binding to the cell surface was visualised frequently, while punctate binding was observed on the cell surface occasionally.

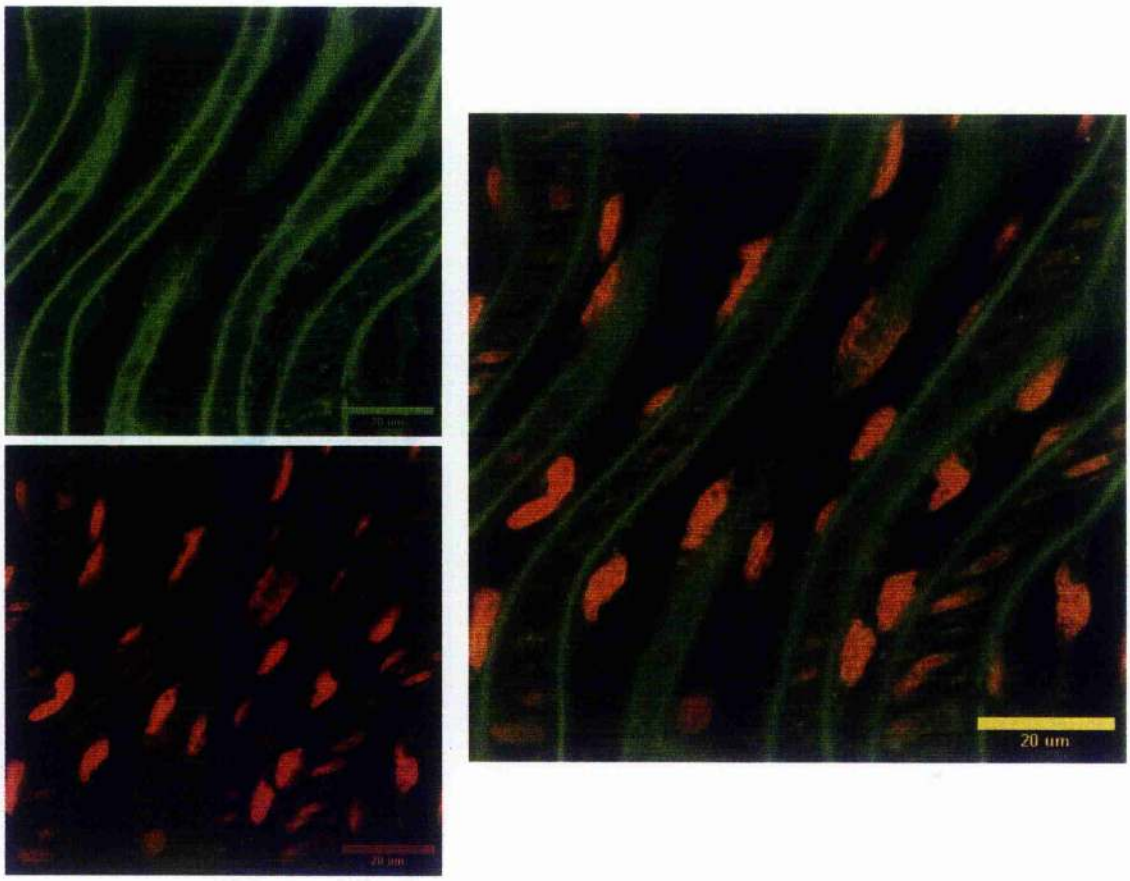

Figure 7.5. 2D image of EC in the α_{1D}-KO: EC attached to the folds in the internal elastic lamina and smooth muscle cells within the bands of elastic lamina. (QAPB binding in green; Syto 61 binding in red).

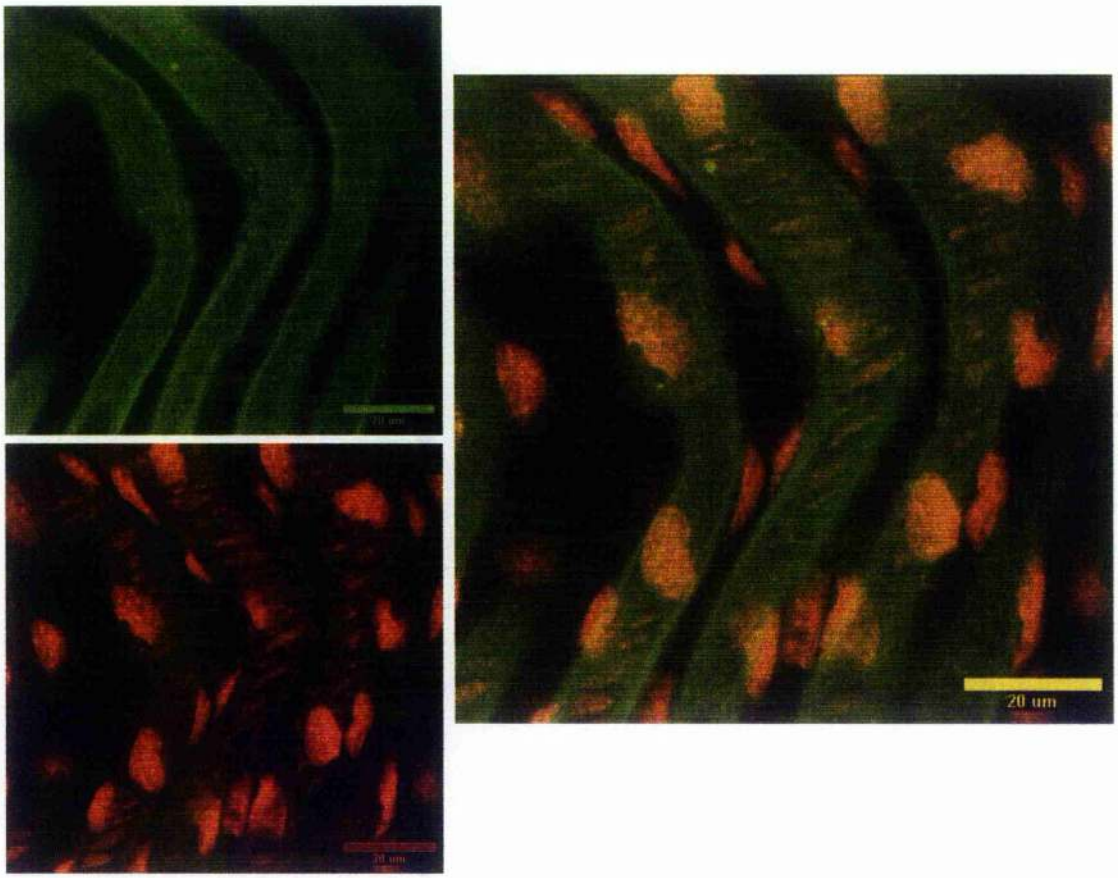

Figure 7.6. 3D reconstruction of EC in the α_{1D}-KO: EC attached to the folds in the internal elastic lamina. (QAPB binding in green; Syto 61 binding in red).

7.3.1.4. $\alpha_{1B/D}$-KO

In the $\alpha_{1B/D}$-KO the nucleus of the cells on the endothelium of the carotid artery was stained with Syto 61. EC were identified attached to the internal elastic lamina (Figure 7.8) including between the grooves created by the folds in the internal elastic lamina (Figure 7.7). Both diffuse and clustered QAPB binding was identified on the surface of the EC.

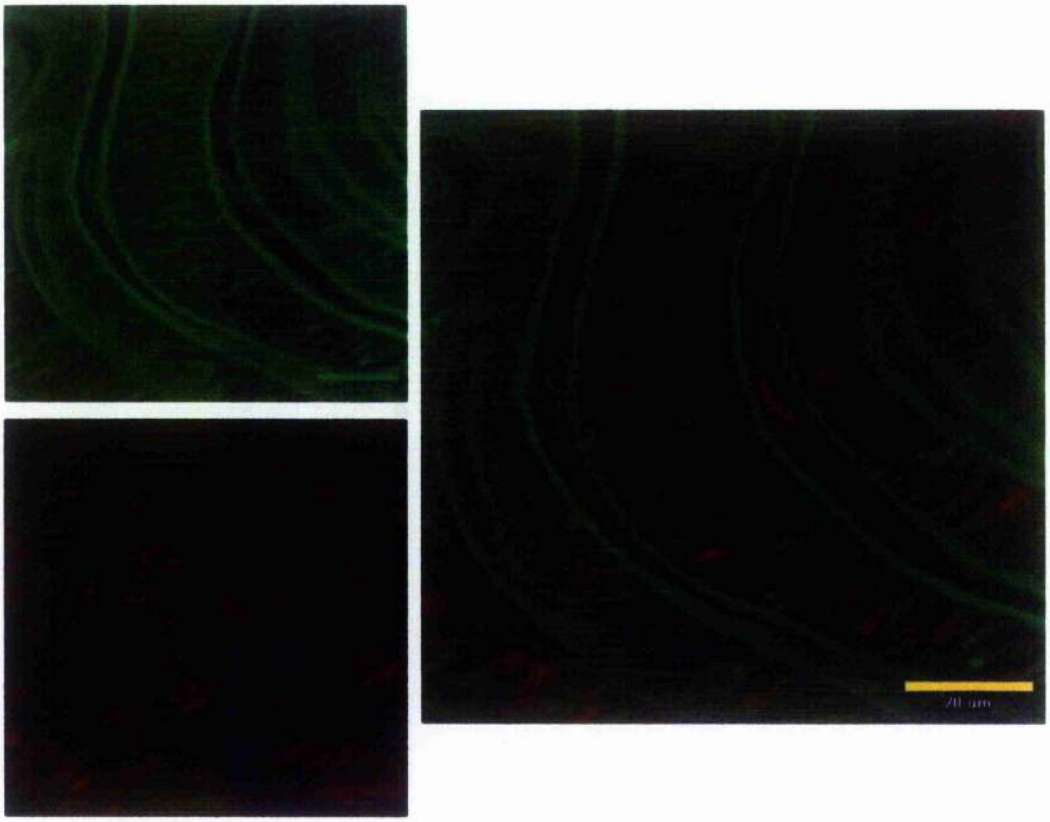

Figure 7.7. 2D image of EC in the $\alpha_{1B/D}$-KO: EC attached to the folds in the internal elastic lamina and smooth muscle cells within the bands of elastic lamina. (QAPB binding in green; Syto 61 binding in red).

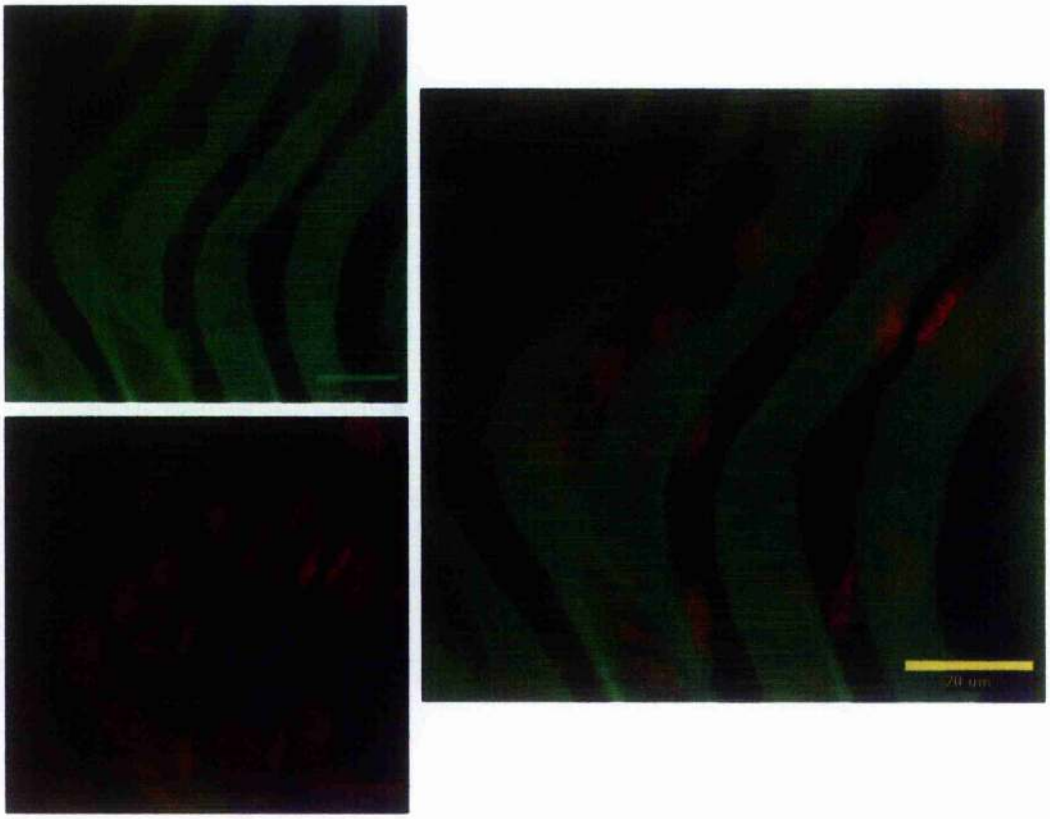

Figure 7.8. 3D reconstruction of EC in the $\alpha_{1B/D}$-KO: EC attached to the folds in the internal elastic lamina. (QAPB binding in green; Syto 61 binding in red).

7.3.2. Comparison of QAPB and Syto 61 binding in the wild type and knockout mice

In the WT mouse the mean number of EC showing QAPB binding was significantly lower than the total number of EC identified by nuclear staining (Table 7.1). The number of EC showing QAPB binding was 80.1% of the total number of EC.

In the α_{1B}-KO the apparent reduction in the number of EC showing QAPB binding did not reach significance (Table 7.1). On average 55.8% of the total number of EC were stained with QAPB.

In the α_{1D}-KO the number of EC identified with QAPB binding was significantly lower than the total number of EC identified by Syto 61 binding (Table 7.1). QAPB bound to 68.9% of the total number of EC.

In the $\alpha_{1B/D}$-KO the apparent reduction in the number of EC with QAPB binding compared to the number of EC with Syto 61 binding did not reach significance (Table 7.1). QAPB bound to 46.0% of the total number of EC.

The number of EC with QAPB binding was highest in the WT mouse and the α_{1D}-KO, which were not significantly different (Table 7.1). The number of EC with QAPB binding in both the α_{1B}-KO and $\alpha_{1B/D}$-KO were significantly lower than the WT mouse.

Table 7.1. Comparison of number of EC bound with QAPB in the WT and knockout mice.

Mouse strain	n	Mean No. EC stained with QAPB	Mean No. EC stained with Syto 61	% of EC stained with QAPB
WT mouse	8	11.5±0.64	14.7±0.89**	80.1±2.34
α_{1B}-KO	7	5.2±1.90$^{▲▲}$	9.1±0.98^{+}	55.8±18.4$^{▲▲}$
α_{1D}-KO	8	9.2±1.14$^{▪}$	13.6±1.43*	68.9±4.61$^{▲}$
$\alpha_{1B/D}$-KO	8	7.0±1.73$^{▲}$	16.3±4.63^{+}	46.0±8.79$^{▲▲▲}$

7.3.3. Effect of subtype selective antagonists in the WT mouse

In the absence of a subtype selective antagonist QAPB binding to EC was observed as described in section 7.3.2. The number of EC stained with QAPB was significantly lower than EC stained with Syto 61 (Table 7.2).

In the presence of prazosin 0.1 μM, QAPB binding was abolished (Figure 7.9) with the exception of one experiment where QAPB binding to a limited number EC was observed. QAPB binding to EC in the presence of prazosin was significantly lower than the total number of EC identified by Syto 61 (Table 7.2). 14.3% of the total number of EC was stained with QAPB in the presence of prazosin.

QAPB binding to EC was observed in the presence of rauwolscine 0.1 μM (Figure 7.9). The number of EC with QAPB binding was not significantly different to the total number of EC observed with Syto 61 (Table 7.2). 86.9% of the total number of EC was stained with QAPB in the presence of rauwolscine.

A significant reduction in EC stained with QAPB was observed in the presence of BMY 7378 0.1 μM compared to EC identified by Syto 61 binding (Figure 7.9; Table 7.2). In the presence of BMY 7378 24.3% of the total number of EC were stained with QAPB.

In the presence of RS100 329, QAPB binding to EC was observed but was limited (Figure 7.9). The number of EC cells identified by QAPB binding was not significantly different to the total number of EC identified by Syto 61 staining (Table 7.2). With RS100 329 62.0% of the total number of EC was stained with QAPB.

The combination of BMY 7378 and RS100 329 markedly reduced the EC that were bound with QAPB compared to the number of EC identified with Syto 61 (Figure 7.9; Table 7.2). In the presence of both BMY 7378 and RS100 329 24.4% of the total number of EC was stained with QAPB.

Table 7.2. Number of EC bound with QAPB in the presence of subtype selective antagonists in the WT mouse.

	n	Mean No. EC stained with QAPB.	Mean No. EC stained with Syto 61	% of total EC
Control	8	11.5±0.64	14.7±0.89**	80.1±2.33
Prazosin	4	1.8±1.05▲▲▲	14.2±2.80**	14.3±7.39
Rauwolscine	4	14.5±1.61■	17.0±2.00+	86.9±3.97
BMY 7378	4	1.5±0.50▲▲▲	6.0±1.00**	24.3±4.30
RS100 329	4	9.7±1.87■	15.8±2.89+	62.0±7.79
BMY 7378 + RS100 329	4	3.2±1.01▲▲▲	12.9±1.36***	24.4±7.57

+p>0.05; **p<0.01; ***p<0.001 compared to EC stained with QAPB (Student's t-test). ■p>0.05; ▲▲▲p<0.001 compared to control (one-way ANOVA, Bonferroni's post test).

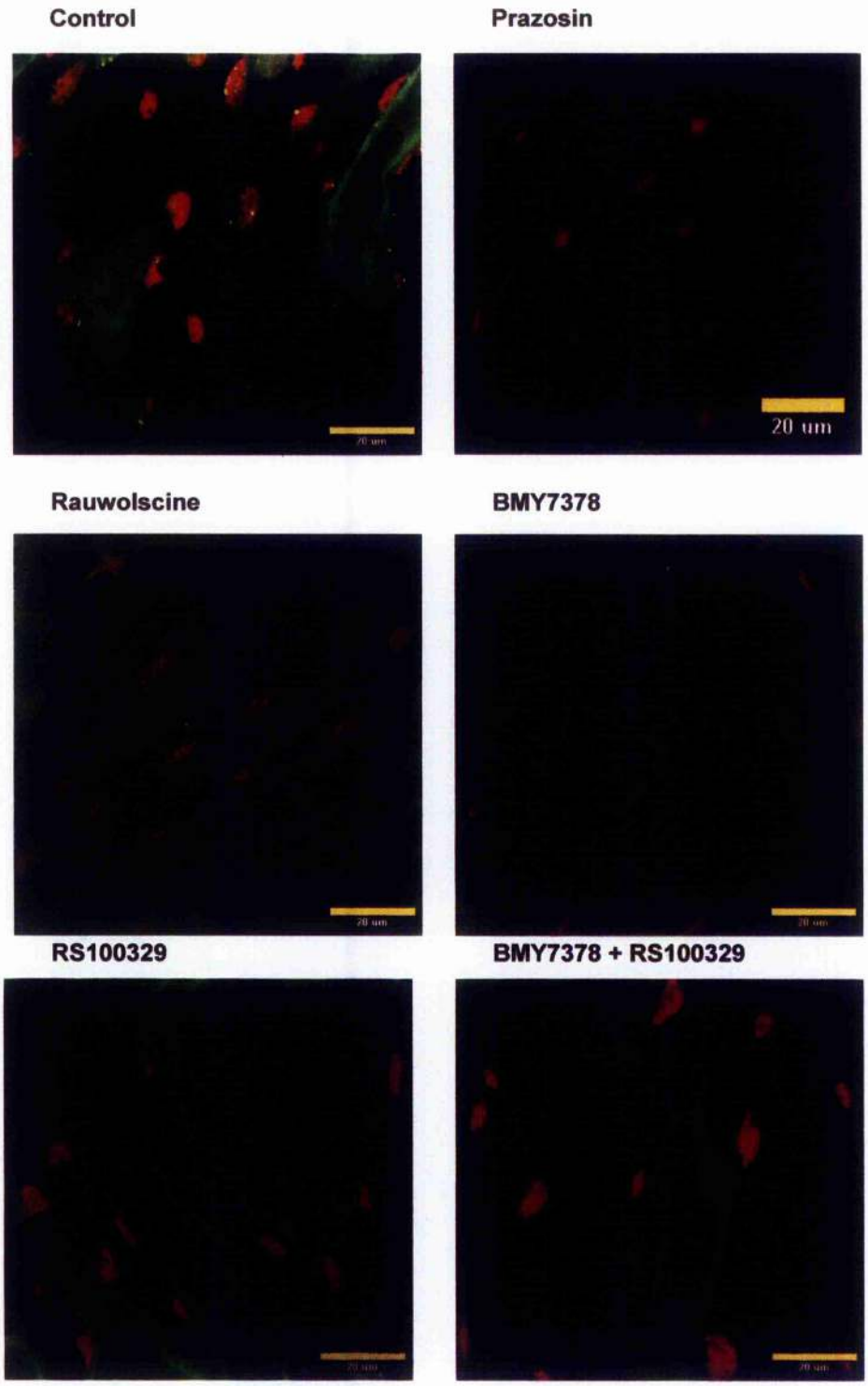

Figure 7.9. WT mouse: Effect of subtype selective antagonists on number of EC stained with QAPB (green) compared to the number of EC stained with Syto 61 (red).

7.3.4. Comparison of effect of subtype selective antagonists in wild type and knockout mice

7.3.4.1. Prazosin

QAPB binding to EC was frequently abolished by prazosin 0.1 μM in all strains of mice (Figure 7.10). However, in some experiments isolated EC with QAPB staining were observed in the presence of prazosin (Table 7.3). In the WT mouse the number of EC showing QAPB binding was significantly reduced to 14.7% in the presence of prazosin. In the α_{1B}-KO the number of EC stained with QAPB was significantly reduced by prazosin, which is 9.8% of the number of EC stained with QAPB. Prazosin significantly reduced the number of EC with QAPB binding from in the α_{1D}-KO, which was 28.1% of the number of EC stained with QAPB. In the $\alpha_{1B/D}$-KO no QAPB binding to EC was detected in the presence of prazosin.

Table 7.3. Comparison of number of EC bound with QAPB in the presence of prazosin in the wild type and knockout mice.

Mouse strain	n	Mean No. EC	Mean No. EC in presence prazosin	% EC in presence prazosin
WT mouse	4	12.5±1.27	1.8±1.05***	14.7
α_{1B}-KO	4	6.1±1.05	0.6±0.6***	9.8
α_{1D}-KO	4	8.4±0.44	2.4±0.96***	28.1
$\alpha_{1B/D}$-KO	4	4.2±0.79	0.0±0.00	0.0

***p<0.001 compared to EC stained with QAPB (Student's t-test).

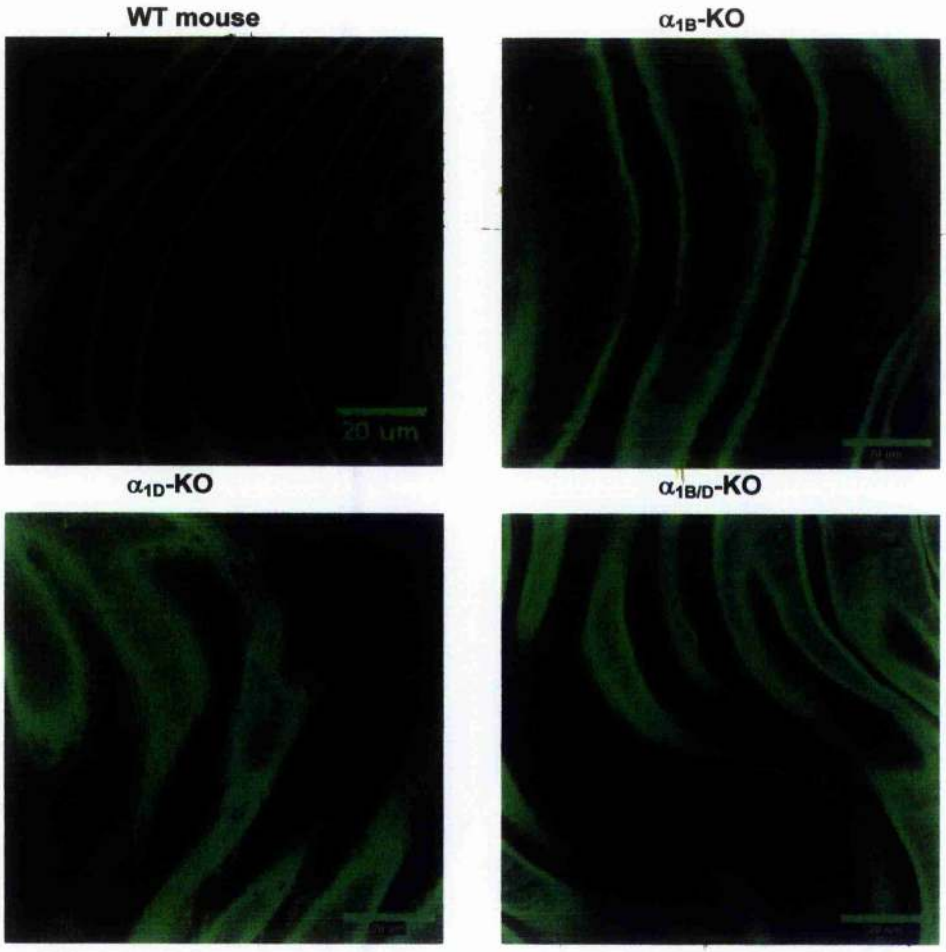

Figure 7.10. Comparison the WT and knockout mice: number of EC bound with QAPB in the presence of prazosin.

7.3.4.2. Rauwolscine

In all four stains of mouse the QAPB binding to EC was observed in the presence of rauwolscine 0.1 μM with evidence of both diffuse and punctate binding (Figure 7.11). In the WT mouse the number of EC stained with QAPB was not significantly different in the absence or presence of rauwolscine 0.1 μM. 93.5% of the number of EC stained with QAPB was identified in the presence of rauwolscine (Table 7.4). In the α_{1B}-KO, in the presence of rauwolscine 127.6% of the EC were stained with QAPB, which was not significantly different. The number of EC showing QAPB binding was not significantly different in the presence of rauwolscine in the α_{1D}-KO with 83.2% of the number of EC stained with QAPB. In the $\alpha_{1B/D}$-KO, 167.0% of the number of EC showing QAPB binding was identified in the presence of rauwolscine in the presence of rauwolscine compared to QAPB alone, but this was not significantly different.

Table 7.4. Comparison of the WT and knockout mice: number of EC bound with QAPB in the presence of rauwolscine.

Mouse strain	Mean No. EC	Mean No. EC in presence rauwolscine	% EC in presence rauwolscine
WT mouse	12.5±1.27	11.6±1.24^{+}	93.5
α_{1B}-KO	6.1±1.05	7.8±1.77^{+}	127.6
α_{1D}-KO	8.4±0.44	7.0±1.72^{+}	83.2
$\alpha_{1B/D}$-KO	4.2±0.79	7.0±2.28^{+}	167.0

+ p>0.05 compared to EC stained with QAPB (Student's t-test).

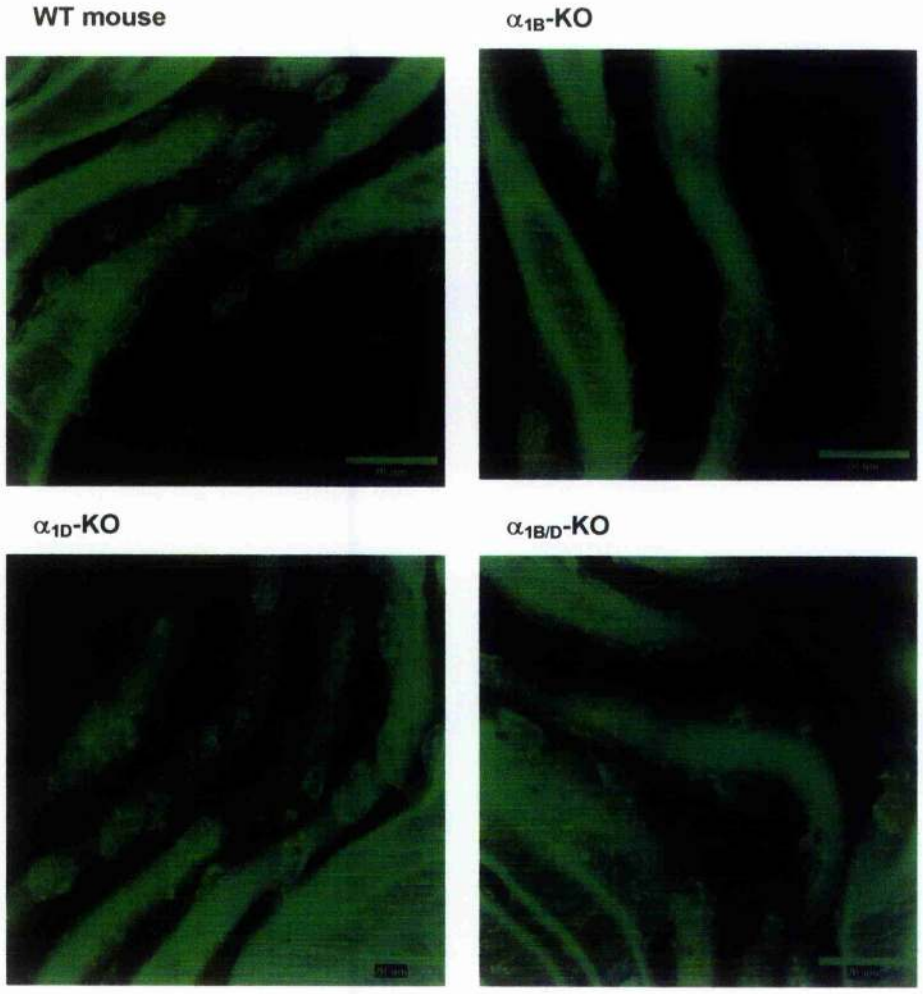

Figure 7.11. Comparison of the WT and knockout mice: number of EC bound with QAPB in the presence of rauwolscine.

7.3.4.3. BMY 7378

In both the WT mouse and α_{1B}-KO a reduction in EC stained with QAPB was visible in the presence of BMY 7378 0.1 μM (Figure 7.12). Cells which had been stained showed diffuse QAPB binding to the cell surface but there was less evidence of punctate binding. BMY 7378 significantly reduced the number of EC stained with QAPB to 38.6% and 35.5% of the number of EC stained with QAPB in the WT mouse and α_{1B}-KO, respectively (Table 7.5). In the α_{1D}-KO and $\alpha_{1B/D}$-KO, no difference in QAPB binding to EC was visible in the presence of BMY 7378 0.1 μM. However, in the α_{1D}-KO quantitative analysis revealed a small but significant reduction in the number of cells stained with QAPB, with 60.9% of EC showing QAPB binding with BMY 7378. In the $\alpha_{1B/D}$-KO 131.2% of EC showed QAPB binding with BMY 7378, which was not significantly different.

Table 7.5. Comparison of number of the WT and knockout mice: EC bound with QAPB in the presence of BMY 7378.

Mouse strain	n	Mean No. EC	Mean No. EC in presence *BMY 7378*	% EC in presence *BMY 7378*
WT mouse	4	12.5±1.27	4.8±1.93**	38.6
α_{1B}-KO	4	6.1±1.05	2.2±0.95*	35.5
α_{1D}-KO	4	8.4±0.44	5.1±1.48*	60.9
$\alpha_{1B/D}$-KO	4	4.2±0.79	5.5±0.56+	131.2

+p>0.05; *p<0.05; **p<0.01 compared to EC stained with QAPB (Student's t-test).

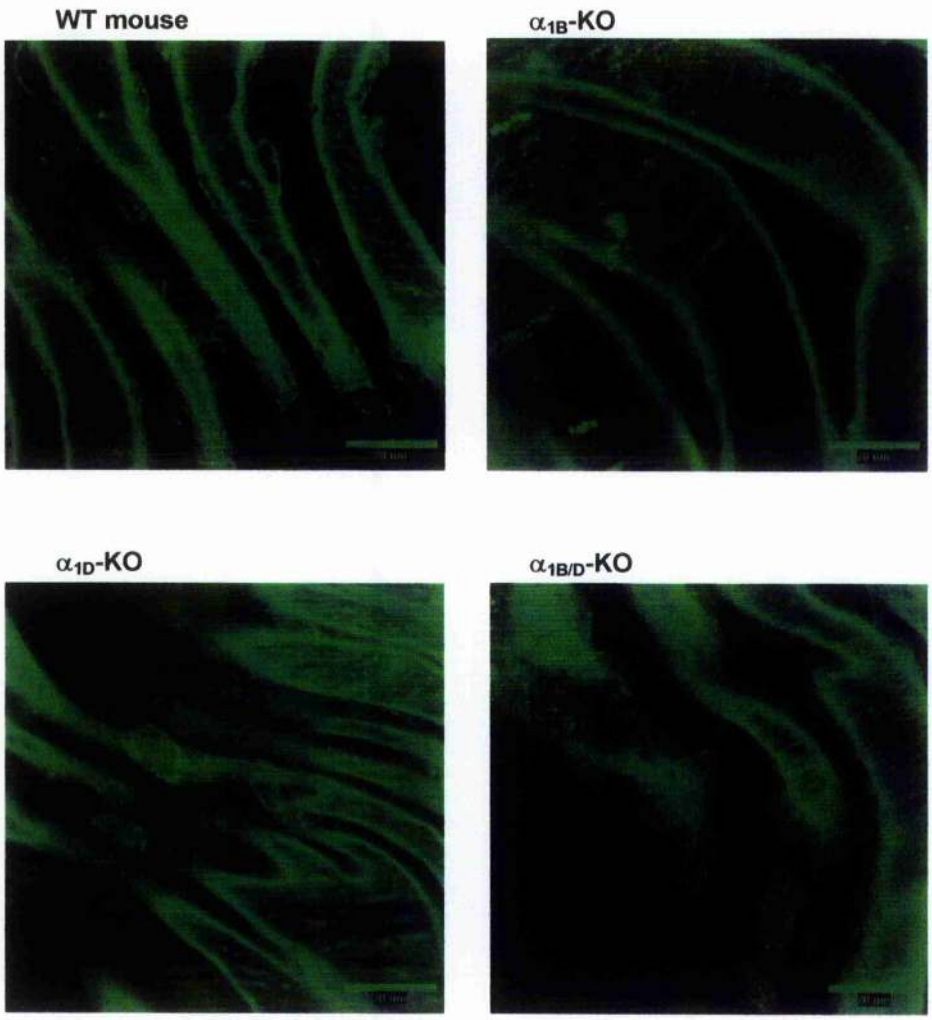

Figure 7.12. Comparison of the WT and knockout mice: number of EC bound with QAPB in the presence of BMY 7378.

7.3.4.4. RS100 329

In the presence of RS100 329, QAPB binding to EC was observed but appeared to be reduced in the WT mouse, α_{1B}-KO and α_{1D}-KO (Figure 7.13). QAPB binding to EC was largely diffuse but evidence of clustered binding was observed in some cells. In the WT mouse the number of EC showing QAPB binding was significantly in the presence of RS100 329, with 56.8% of EC showing QAPB binding with RS100 329 (Table 7.6). In the α_{1B}-KO 32.7% of EC showed QAPB, which was significantly reduced. In the α_{1D}-KO 33.7% of EC stained with QAPB in the presence of RS100 329, which was significantly reduced. In the $\alpha_{1B/D}$-KO QAPB binding to EC was not observed in the presence of RS100 329, with the exception of one experiment in which isolated EC were observed. The number of EC showing QAPB binding was significantly reduced in the presence of RS100 329, with 19.9% of EC showing QAPB binding with RS100 329.

Table 7.6. Comparison of the WT and knockout mice: number of EC bound with QAPB in the presence of RS100 329.

Mouse strain	Mean No. EC	Mean No. EC in presence RS100 329	% EC in presence RS100 329
WT mouse	12.5±1.27	7.1±1.03*	56.8
α_{1B}-KO	6.1±1.05	2.0±0.62**	32.7
α_{1D}-KO	8.4±0.44	2.8±0.70***	33.7
$\alpha_{1B/D}$-KO	4.2±0.79	0.83±0.40**	19.9

***p<0.05; **p<0.01; ***p<0.001 compared to EC stained with QAPB (Student's t-test).**

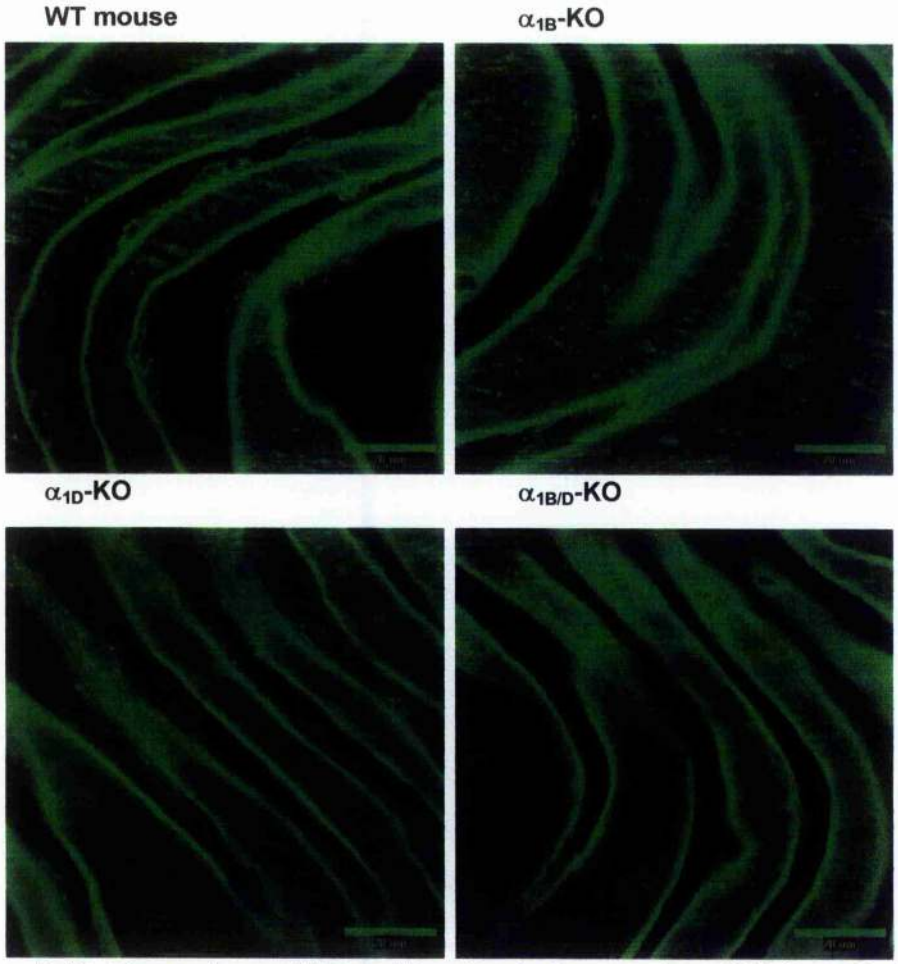

Figure 7.13. Comparison of WT and knockout mice: number of EC bound with QAPB in the presence of RS100 329.

7.3.4.5. BMY 7378 and RS100 329 combination

In the WT mouse and α_{1D}-KO some evidence of QAPB binding to EC was visible in the presence of the combination of BMY 7378 and RS100 329 (Figure 7.14). The number of EC stained with QAPB was significantly reduced by BMY 7378 and RS100 329, with 35.3% and 44.0% of EC showing QAPB binding for the WT mouse and α_{1D}-KO, respectively (Table 7.7). In the α_{1B}-KO and $\alpha_{1B/D}$-KO there was no evidence of QAPB binding to EC in the presence of the combination of BMY 7378 and RS100 329.

Table7.7. Comparison of the WT and knockout mice: number of EC bound with QAPB in the presence of a combination of BMY 7378 and RS100 329.

Mouse strain	n	Mean No. EC	Mean No. EC in presence BMY 7378 + RS100 329	% EC in presence BMY 7378 + RS100 329
WT mouse	4	12.5±1.27	4.4±1.10***	35.3
α_{1B}-KO	4	6.1±1.05	0.0±0.00	0.0
α_{1D}-KO	4	8.4±0.44	3.7±1.47**	44.0
$\alpha_{1B/D}$-KO	4	4.2±0.79	0.0±0.00	0.0

**p<0.01; ***p<0.001 compared to EC stained with QAPB (Student's t-test).

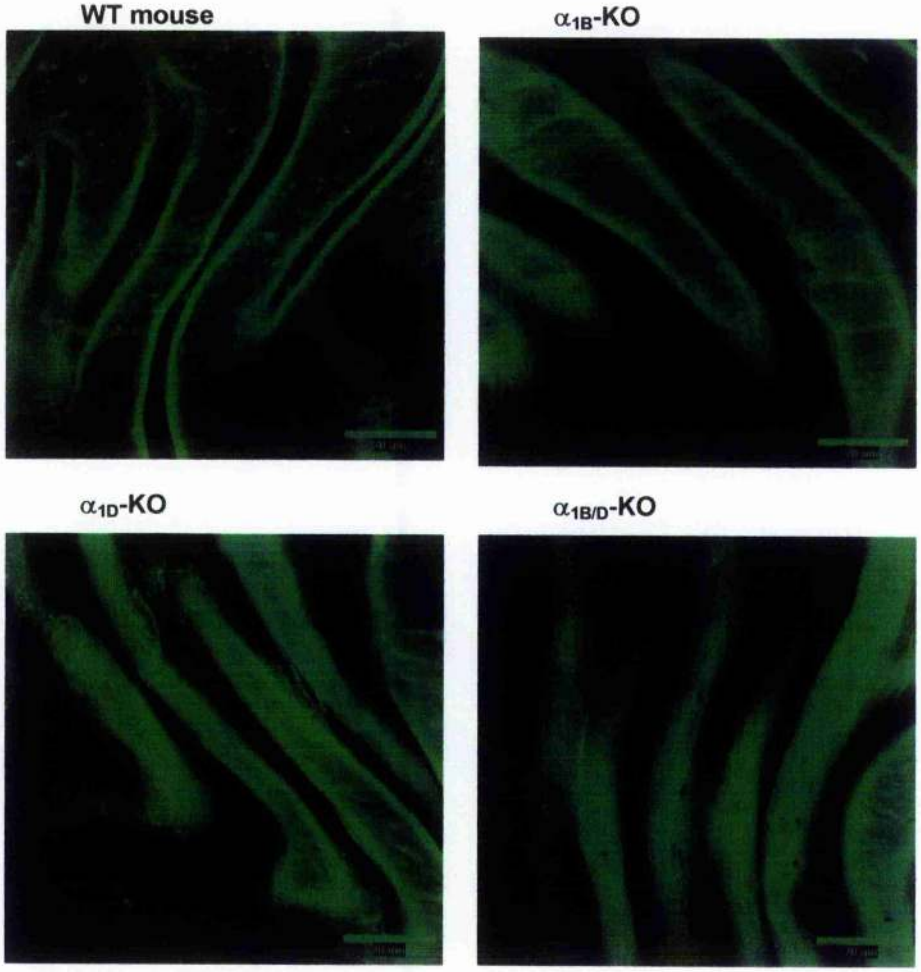

Figure 7.14. Comparison of the WT and knockout mice: number of EC bound with QAPB in the presence of BMY 7378 and RS100 329.

7.4. Discussion

7.4.1. α_1-AR subtypes on the endothelium

The nuclear membrane dye Syto 61 (1 μM) was used in the present study to confirm that the EC were preserved during slide mounting and to identify the position and shape of the EC. EC were attached to the surface of the internal elastic lamina, including within the grooves formed by the folds in the internal elastic lamina. In all four mouse strains, there was clear evidence that the position of the cells bound with QAPB, a fluorescent α_1-AR ligand, matched that of the EC identified by Syto 61. The binding of QAPB to cells on the endothelium indicated that α_1-ARs were present in all four strains of mouse. QAPB bound to EC in both a diffuse and punctate manner, which was evident in all four mice strains.

The relative number of EC stained with QAPB was examined quantitatively. Firstly, the proportion of EC stained with QAPB relative to Syto 61 was examined in the WT mouse and knockouts. The number of EC bound with QAPB was 80.1%, 55.8%, 68.9% and

46.0% of the total number of EC stained with Syto 61, for the WT mouse, α_{1B}-KO, α_{1D}-KO and $\alpha_{1B/D}$-KO, respectively. This indicates that α_1-ARs are not detectable in all EC. The reduction in the proportion of EC binding QAPB in the knockouts compared to the WT mouse is consistent with the loss of the entire α_1-AR population from a proportion of EC. Comparison of the number of EC identified with QAPB between the WT mouse and knockouts revealed a significant reduction in both the α_{1B}-KO and $\alpha_{1B/D}$-KO. This raises the possibility that endothelial α_{1B}-ARs are present in the WT mouse.

Secondly, in the WT mouse the effect of subtype selective antagonists on the number of endothelial α_1-ARs compared to the total number of EC (Syto 61 binding) was assessed. In the presence of prazosin (0.1 μM, nonselective α_1-AR antagonist) QAPB binding was detected in only 14.3% of the total number of EC. This marked reduction suggests that QAPB was binding α_1-ARs. The residual binding observed in some experiments may be due to QAPB binding α_2-ARs. Particularly in light of the evidence that α_2-ARs exist on the endothelium of the mouse carotid artery (Malekzadeh Shafaroudi, 2005). However, in the present study rauwolscine (nonselective α_2-AR antagonist) did not reduce the number of EC with QAPB binding, which opposes QAPB binding α_2-ARs at this concentration. The possibility of QAPB binding to α_2-ARs was an important consideration as, in addition to showing high affinity at α_1-ARs, QAPB has been shown to have moderate affinity for α_2-ARs (McGrath & Daly, 2005). It should be noted that Malekzadeh et al. (2005) used QAPB 0.1 μM in the presence of α_1-AR subtype selective antagonists to study α_2-ARs on the endothelium of the mouse aorta. In contrast to the present study, QAPB binding to EC was absent in the presence of rauwolscine. This highlights a difference in the endothelial cell population between the carotid artery and aorta.

Out of the total number of EC, only 24.3% were stained with QAPB in the presence of BMY 7378 (0.1 μM), consistent with QAPB binding to endothelial α_{1D}-ARs being inhibited, or at least reduced to a level that was not detectable. In the presence of RS100 329 the number of EC stained with QAPB was 62.0% of the total number of EC. This suggests that α_{1A}-ARs may be present on the endothelium of the WT mouse. The combination of BMY 7378 and RS100 329 reduced QAPB binding to only 24.4% of EC but QAPB binding was not completely abolished suggesting that endothelial α_{1B}-ARs may exist. Thus, all three α_1-AR subtypes may be present on the endothelium in the WT mouse.

The final part of the present study compared the effect of subtype selective antagonists on QAPB binding in the wild type and knockout mice. In the knockouts, QAPB binding to EC was almost completely abolished by prazosin confirming that QAPB was binding α_1-ARs, consistent with the WT mouse. This was further supported by the failure of rauwolscine to displace QAPB in the knockouts, which suggests that QAPB was not binding α_2-ARs on the endothelium at this concentration.

Endothelial α_{1D}-ARs were shown to exist in the α_{1B}-KO as only 35.5% of EC showed QAPB binding in the presence of BMY 7378, which was comparable to the WT mouse. With RS100 329, the number of EC with QAPB binding was 32.7%, 33.7% and 19.9% of the total number of α_1-ARs for the α_{1B}-KO, α_{1D}-KO and $\alpha_{1B/D}$-KO, respectively. This suggests that the α_{1A}-AR is present on the endothelium of the knockouts, which supports the evidence in the WT mouse. There is also evidence to suggest that endothelial α_{1B}-AR exist: in the presence of the combination of BMY 7378 and RS100 329 EC were identified in the WT mouse (35.3%) but not the α_{1B}-KO (0%). Comparison of the QAPB binding in the presence of subtype selective antagonists WT mouse and knockouts revealed that all three α_1-AR subtypes appear to exist on the endothelium of the mouse carotid artery.

7.4.2. Physiological significance

The predominance of the α_1-AR-mediated contractile response in the mouse carotid artery means that any attempt to functionally investigate the potential of endothelial α_1-ARs proves difficult. However, evidence of an α_1-AR stimulated release of NO has been shown in Chapter Five. As previously discussed it was unclear whether the release of NO was due to the direct stimulation of endothelial α_1-ARs or indirectly via the stimulation of α_1-ARs in the smooth muscle layers. The present study has shown that α_1-ARs do exist on endothelium of the mouse carotid artery. Therefore, it is likely that NO was released in response to the direct stimulation of endothelial α_1-ARs. This hypothesis is strengthened by other studies which have proposed that the activation of endothelial α_1-ARs induces NO release (Tuttle & Falcone, 2001;Zschauer *et al.*, 1997).

7.4.3. Conclusions

α_1-ARs were identified on the endothelium of the WT mouse and knockout mice using visualisation techniques. The proportion of EC with α_1-ARs was reduced in the knockout mice compared to the WT mouse. All three α_1-AR subtypes were present on the endothelium of the WT mouse.

Chapter Eight

General Discussion

The main objectives of the experiments described in the previous chapters were:

(i). To establish whether there is an α_{1A}-AR-mediated contractile response in the carotid artery of the WT mouse and also assess whether there is evidence of a functional α_{1B}-AR. This was achieved by using the α_{1A}-AR selective agonist A-61603 and range subtype selective antagonists, in addition to the α_1-AR non-selective agonist phenylephrine.

(ii). To determine whether an α_{1A}-AR-mediated contractile response could be identified in the carotid artery of α_1-AR knockout mice and, therefore, aid the characterisation of the α_1-AR response in the WT mouse. This was achieved using a similar approach to (i) to isolate the α_{1A}-AR in the α_{1B}-KO, α_{1D}-KO and $\alpha_{1B/D}$-KO.

(iii). To investigate the role of NO on the vascular response to phenylephrine and A-61603 in the mouse carotid artery. This was achieved by preventing NO release using the NOS inhibitor L-NAME.

(iv). To characterise the α_1-AR subtypes present in the media of the carotid artery by using subtype selective antagonists to compete with the fluorescent ligand QAPB in the WT mouse and α_1-AR knockout mice. In doing so, the distribution of the α_1-AR subtypes in SMC was examined.

(v). To establish whether α_1-ARs exist on the endothelium of the mouse carotid artery and to determine the α_1-AR subtypes present in EC. This was achieved using the fluorescent ligand QAPB in the WT mouse and α_1-AR knockout mice, as well as subtype selective antagonists.

In this final chapter, the findings and general conclusions of the studies described in this thesis are discussed.

8.1. α_1-AR function

The functional studies described in Chapters Three and Four investigated the contribution of the α_{1A}-AR and α_{1B}-AR to the α_1-AR-mediated contractile response in the mouse carotid artery, using a combination of pharmacological analysis and knockout technology.

This method enabled an α_{1A}-AR-mediated contractile response to be identified in the mouse carotid artery for the first time.

8.1.1. Phenylephrine and A-61603 selectivity

In general, the α_{1A}-AR selective agonist, A-61603, has been used to study vessels where the α_{1A}-AR is the predominant subtype. In Chapters Three and Four, A-61603 was used to isolate a minor α_{1A}-AR response in an artery in which the α_{1D}-AR is the main mediator of contraction: the mouse carotid artery. The agonist responses in the $\alpha_{1A/B}$-KO and $\alpha_{1B/D}$-KO provided good evidence that A-61603 is selective for the α_{1A}-AR over the α_{1B}-AR and α_{1D}-AR, and that phenylephrine has selectivity for the α_{1D}-AR over the α_{1A}-AR, in agreement with the findings of Knepper and colleagues (Knepper SM *et al.*, 1995;Meyer *et al.*, 1996). However, it was also demonstrated that the A-61603-induced response consisted of two components: an α_{1A}-AR-mediated component and an α_{1D}-AR-mediated component. In the murine thoracic aorta, A-61603 appeared to have an action on the α_{1D}-AR on the basis that an α_1-AR-mediated response was observed in the α_{1B}-KO but not the $\alpha_{1B/D}$-KO. Thus, the findings presented in Chapter Four and those reported by Ali (2004) provide evidence indicative of an α_{1D}-AR-mediated component to the A-61603-induced response.

8.1.2. α_{1D}-AR in the mouse carotid artery

The findings described in Chapters Three and Four confirmed previous reports that the α_{1D}-AR is the predominant contractile α_1-AR in the mouse carotid artery (Deighan C, 2002;Deighan *et al.*, 2005;Daly *et al.*, 2002a). The predominant contribution of the α_{1D}-AR in the WT mouse was illustrated by the limited phenylephrine-induced response in the α_{1D}-KO and $\alpha_{1B/D}$-KO. In the earlier study of the mouse carotid artery by Deighan (2002;Deighan *et al.*, 2005), a pK_B of 8.3 was produced for BMY 7378 against the phenylephrine-induced response, which was indicative of an α_{1D}-AR-mediated response in the WT mouse. Interestingly, there was evidence of α_1-AR heterogeneity in the WT mouse (Deighan C, 2002;Deighan *et al.*, 2005). In the present study, the higher pK_B of 9.1 obtained for BMY 7378 against phenylephrine, in preliminary results from the $\alpha_{1A/B}$-KO, appears to be representative of a 'pure' α_{1D}-AR population. This agrees with BMY 7378 acting on a low affinity site, in addition to the α_{1D}-AR, in the WT mouse. However, Deighan (2002;Deighan *et al.*, 2005) reported that in the α_{1B}-KO an even higher pK_B of

9.6 was produced for BMY 7378 against phenylephrine. It is unclear why BMY 7378 is more potent in the α_{1B}-KO than the $\alpha_{1A/B}$-KO, though further experiments are required in the $\alpha_{1A/B}$-KO before any firm conclusions can be drawn. The biphasic A-61603 CRC observed in the presence of BMY 7378 10nM in the WT mouse suggested that the A-61603 response was mediated by two α_1-AR subtypes. The pK_B of 8.3 was consistent with published potency values for the α_{1D}-AR and confirms the involvement of this subtype (see Chapter One). Together, these findings provide good evidence that the α_{1D}-AR is the predominant α_1-AR subtype and that the α_{1D}-AR plus either the α_{1A}-AR or α_{1B}-AR mediate the contractile response to phenylephrine and A-61603 in the carotid artery of the WT mouse.

These conclusions from both studies in the murine carotid artery are reinforced by studies in other mouse arteries. For instance, in a previous study in the thoracic aorta, the lack of contraction to both phenylephrine and A-61603 in the $\alpha_{1B/D}$-KO argues against an α_{1A}-AR-mediated response (Ali, 2004). Furthermore, the high potency and efficacy of phenylephrine, but not A-61603, in the α_{1D}-KO is consistent with phenylephrine acting on the α_{1B}-AR, as well as the α_{1D}-AR in the thoracic aorta. The absence of α_{1B}-AR potency for A-61603 in the thoracic aorta suggests that the two components observed in the present study arise from the α_{1D}-AR and the α_{1A}-AR.

8.1.3. α_{1A}-AR in the mouse carotid artery

Both 5-methylurapidil and RS100 329 were used to distinguish the α_{1A}-AR from the α_{1B}-AR and the α_{1D}-AR. The contractile role of the α_{1A}-AR was clear in the α_{1D}-KO and $\alpha_{1B/D}$-KO, in which both A-61603 and the α_{1A}-AR selective antagonists were potent. In the WT mouse and α_{1B}-KO, an α_{1A}-AR-mediated response was not identified from the phenylephrine-induced response (Deighan C, 2002;Deighan *et al.*, 2005); but 5-methylurapidil and RS100 329 showed increased potency against A-61603. Thus, there is evidence to suggest a contractile role for the α_{1A}-AR in these mice, although it appears to be masked by the predominant α_{1D}-AR. In the α_{1D}-KO, the reduced potency of RS100 329 against phenylephrine compared to A-61603 may be indicative of an α_{1B}-AR component to the phenylephrine-induced response. However, the use of the α_{1A}-AR selective antagonists confirmed that the α_{1A}-AR, but not the α_{1B}-AR, was mediating the A-61603 response.

In a recent study of the mouse first order mesenteric artery, in which the α_{1A}-AR is the predominant subtype, a biphasic phenylephrine CRC was observed in the presence of 5-methylurapidil (McBride *et al.* Submitted for publication). The 5-methylurapidil-resistant component to the response was lost in the presence of a combination of 5-methylurapidil and BMY 7378. This led to the conclusion that in addition to the predominant α_{1A}-AR, the α_{1D}-AR had a small contractile role in the mesenteric artery. Thus, evidence exists of a vessel, in which contraction is predominantly α_{1A}-AR, having a contribution from the α_{1D}-AR and now the present study has provided evidence of a vessel, which is predominantly α_{1D}-AR, having a contribution from the α_{1A}-AR.

8.1.4. α_{1B}-AR in the mouse carotid artery

In the absence of any α_{1B}-AR selective antagonists, there was no direct evidence of an α_{1B}-AR-mediated response in the WT mouse. However, the α_{1B}-KO could be used as a substitute for α_{1B}-AR selective antagonists. The findings presented in Chapters Three and Four suggested that the α_{1B}-AR may have a minor contractile role in mouse carotid artery, as proposed by Daly et al. (2002a). The existence of a small α_{1B}-AR component to the phenylephrine-induced response was also suggested in the previous study in the mouse carotid artery (Deighan C, 2002;Deighan *et al.*, 2005), in which BMY 7378 had higher affinity in the α_{1B}-KO than the WT mouse. An α_{1B}-AR response would account for the difference in the phenylephrine-induced response between the α_{1D}-KO and $\alpha_{1B/D}$-KO, identified in Chapter Four of this thesis. Comparison of the agonist responses in the knockout mice with the WT mouse suggested that the phenylephrine-induced response may be mediated by all three α_1-AR subtypes. However, comparison of the A-61603-induced response in the $\alpha_{1A/B}$-KO and the $\alpha_{1B/D}$-KO with the WT mouse suggested that the α_{1A}-AR and the α_{1D}-AR, but not the α_{1B}-AR, mediate the A-61603 response in the WT mouse. Furthermore, the visualisation study in Chapter Six provided evidence that the α_{1B}-AR was present in the media of the mouse carotid artery, suggesting that an α_{1B}-AR-mediated response is plausible. The findings presented in this thesis and those reported by Deighan and colleagues (Deighan C, 2002;Deighan *et al.*, 2005;Daly *et al.*, 2002a) are in agreement that the α_{1B}-AR does have a small contractile role in the mouse carotid artery.

8.1.5. Comparison with the aorta

Both the carotid artery and thoracic aorta are conductance arteries and the α_{1D}-AR is the predominant α_1-AR subtype (Daly *et al.*, 2002a;Ali, 2004;Yamamoto & Koike, 2001b;Tanoue *et al.*, 2002c;Tanaka *et al.*, 2004;Hosoda *et al.*, 2005a;Deighan C, 2002;Deighan *et al.*, 2005). The balance of evidence suggests that the mouse thoracic aorta has a contribution from the α_{1B}-AR, but there is a lack of evidence for a contractile α_{1A}-AR, in contrast to the evidence presented in Chapters Three and Four in the mouse carotid artery. For instance, no contractile response to phenylephrine or A-61603 was observed in the thoracic aorta of the $\alpha_{1B/D}$-KO (Ali, 2004). Furthermore, receptor protection studies failed to find any evidence of either an α_{1A}-AR or α_{1B}-AR-mediated response (Ali, 2004). This suggests that an α_{1A}-AR-mediated contractile response does not exist in the thoracic aorta of the WT mouse. To date, however, two studies have reported that the α_{1A}-AR has a functional role in the thoracic aorta in knockout mice. Firstly, Hosoda et al. (2005b) reported an α_1-AR-mediated contractile response to noradrenaline in the aorta of the $\alpha_{1B/D}$-KO, based on the high potency of prazosin. The noradrenaline-induced contraction was very small (approximately 16% of the WT mouse response) and significantly less potent in comparison to that obtained in the WT mouse and single knockouts. Thus, the $\alpha_{1B/D}$-KO infers that the contribution of the α_{1A}-AR in the mouse thoracic aorta is very limited (Hosoda et al., 2005b) but may exist in the aorta of the WT mouse. This study in the aorta of the $\alpha_{1B/D}$-KO shares similarities with the findings in Chapter Four in the carotid artery of the $\alpha_{1B/D}$-KO. However, unlike the carotid artery, there is no evidence of an α_{1A}-AR-mediated response in the WT mouse thoracic aorta. Secondly, Lazaro-Suarez et al. (2006) reported an α_{1A}-AR-mediated response in the aorta of the α_{1D}-KO. It should be noted that the conclusions of this receptor protection study were reached using the α_{1B}-AR antagonist, AH11110A, and the alkylating agent, chloroethylclonidine, and the reliability of both has been questioned (Eltze *et al.*, 2001;Hirasawa *et al.*, 1997). Thus, the evidence to date suggesting that the α_{1A}-AR has a role in the thoracic aorta of the mouse is less compelling than in the carotid artery.

Despite the contraction of both the thoracic aorta and carotid artery being predominantly α_{1D}-AR-mediated, an α_{1A}-AR-mediated response exists in the carotid artery, but is less likely to be present in the thoracic aorta. The α_1-AR subtypes vary in the abdominal aorta: like the thoracic aorta, the upper abdominal aorta is predominantly α_{1D}-AR-mediated, but contraction in the lower abdominal aorta is predominantly α_{1A}-AR-mediated (Yamamoto

& Koike, 2001a). Thus, differences between the minor subtypes in the thoracic aorta and the carotid artery are entirely plausible. Furthermore, differences exist in the α_1-AR subtypes present in the branches of the aorta. For instance, this study has shown that the contraction of the carotid artery is predominantly α_{1D}-AR-mediated, with a contribution from the α_{1A}-AR, while in the iliac artery, a branch of the lower abdominal aorta, the α_{1A}-AR is predominant (Shibano *et al.*, 2002). It is apparent that as the distance from the aortic arch increases the predominance of the α_{1D}-AR decreases and the predominance of the α_{1A}-AR increases.

It is clear from the studies of conductance arteries that the characterisation of α_1-AR subtypes other than the dominant α_{1D}-AR is difficult. The utilisation of α_1-AR knockout mice clearly aids the study of the α_1-AR subtypes, particularly by enabling the contractile response to be studied in the absence of the dominant contractile receptor. Thus, the minor subtypes can be characterised without the dominant α_1-AR subtype masking their function. The findings of Chapters Three and Four demonstrate that it is not accurate to assign one α_1-AR subtype to a specific vessel. Furthermore, α_1-AR heterogeneity is an important consideration when assessing the selectivity of α_1-AR compounds, and would be of particular importance when testing potential clinical drugs.

8.2. Effect of NO

In Chapter Five, the final functional study examined the effect of NO on the contraction of mouse carotid artery and demonstrated that the α_1-AR-mediated contractile response was suppressed by NO. This was evident from the increase in contraction and/or sensitivity to both phenylephrine and A-61603 in the presence of L-NAME.

There was no evidence that NO was being released spontaneously. For instance, it was demonstrated that without prior agonist stimulation basal tone was unaffected. At resting tone L-NAME has been shown to produce a contraction when spontaneous NO release is occurring (Shimokawa H *et al.*, 1996), which suggests that this was not the case in the mouse carotid artery. Furthermore, the contractile response to 5-HT was unaffected by L-NAME. This is different to findings in the mouse thoracic aorta in which the 5-HT contractile response was attenuated by L-NAME in a concentration-independent manner and suggested that NO was released spontaneously (Ali, 2004). Thus, there was no positive evidence of spontaneous NO release in the mouse carotid artery.

With prior stimulation to either phenylephrine or A-61603, L-NAME caused an increase in basal tone. In addition, it was evident from the phenylephrine and A-61603 CRCs in the presence of L-NAME that NO appeared to have a greater effect with increasing agonist concentrations. Thus, these findings suggest that NO was released in response to α_1-AR stimulation, and are in agreement with those in the rat carotid artery (de Andrade C *et al.*, 2006) and mouse thoracic aorta (Tabernero *et al.*, 1999;Kaneko & Sunano, 1993;Gurdal *et al.*, 2005), in which NO release has been shown to be stimulated by phenylephrine.

It was not clear whether NO was released through the activation of smooth muscle cells and stimulation of EC via myo-endothelial junctions, or the direct activation of endothelial α_1-ARs. To date, there is evidence of myo-endothelial junctions in small arteries such as the mesenteric artery of the rat (Dora K, 2001;Gonzalez Unpublished observations), though they have been identified in the rabbit carotid artery (Spagnoli *et al.*, 1982). However, there is no positive evidence that these structures exist in the carotid artery of other species or other conductance arteries. Nevertheless, phenylephrine-induced relaxatory responses were recently reported for the first time (Filippi *et al.*, 2001) and have now also been observed in the rat carotid artery (de Andrade C *et al.*, 2006). The above functional evidence of α_1-ARs on the endothelium, together with the identification of endothelial α_1-ARs in the mouse carotid artery in Chapter Seven, suggests that NO release through the direct stimulation of α_1-ARs on the endothelium is entirely plausible.

8.3. α_1-AR distribution

The visualisation studies in Chapters Six and Seven examined the distribution of α_1-AR subtypes in the media and SMC of the mouse carotid artery. These studies were intended to be analysed in conjunction with the findings of the functional data in Chapters Three to Five.

8.3.1. Smooth muscle cells

In Chapter Six,the distribution of the α_1-AR subtypes in the SMC were studied for the first time in the mouse carotid artery. A protocol was developed to enable the distribution of α_1-ARs in the media of the carotid artery to be examined at the tissue and subcellular level. Intact carotid arteries were incubated with QAPB 0.1 μM for 120 minutes at room temperature. Ideally, an even lower concentration of QAPB would be preferred as used in isolated cells (Pediani *et al.*, 2005), but 0.1 μM was required for suitable definition of the

SMC in the intact tissue. Incubations were performed at room temperature rather than physiological temperature due to pH problems associated with the PSS. A buffer that was not dependent on pH, such as HEPES, could have enabled a more physiological incubation temperature, but PSS was selected for use to complement the functional experiments.

SMC in both the WT mouse and α_{1B}-KO were evenly distributed and clearly defined, but analysis revealed that the total α_1-AR population in the α_{1B}-KO was reduced. In the α_{1D}-KO and $\alpha_{1B/D}$-KO, QAPB binding was reduced suggesting that a high proportion of the α_1-AR population is α_{1D}-AR. The detection of QAPB binding in the $\alpha_{1B/D}$-KO suggested the existence of the α_{1A}-AR. Comparison of QAPB fluorescence in the α_{1B}-KO and $\alpha_{1B/D}$-KO with the WT mouse indicated that the α_{1B}-AR was present in the media of the carotid artery. This correlates with the functional data, in which a small α_{1B}-AR-mediated contraction was apparent.

Non-fluorescent antagonists were used to compete for QAPB binding sites to obtain further information about the α_1-AR subtypes present in the media. The marked reduction or abolition of QAPB by the α_{1A}-AR antagonist indicated that α_{1A}-ARs were present in all mouse strains. This contrasts with a study in the α_{1A}-KO, in which β-galactosidase staining was used to indicate α_{1A}-AR expression, and was absent in the mouse carotid artery (Rokosh & Simpson, 2002). The inconsistencies in α_{1A}-AR expression between the two studies may be due to the different methods employed. In the present study, the presence of the α_{1A}-AR in the murine carotid artery was validated by the identification of the α_{1A}-AR-mediated response in the WT mouse, α_{1B}-KO, α_{1D}-KO and $\alpha_{1B/D}$-KO. The QAPB binding distribution in the α_{1A}-KO would provide valuable information to further investigate the presence of the α_{1A}-AR in the carotid artery. The presence of the α_{1D}-AR was confirmed in the WT mouse and α_{1B}-KO by the reduction in QAPB binding with the α_{1D}-AR selective antagonist. By blocking both the α_{1A}-AR and α_{1D}-AR the presence of the α_{1B}-AR was confirmed, since QAPB binding was still detectable in the WT mouse but not the α_{1B}-KO. Thus, it is evident that all three α_1-AR subtypes are present in the media of the carotid artery. The findings of the distribution study alone cannot be taken as evidence that the α_1-ARs are functional, but the presence of the α_{1A}-AR, α_{1B}-AR and α_{1D}-AR supports the functional data in Chapters Three and Four.

Consistent with previous studies in isolated cells (Daly *et al.*, 1998;McGrath *et al.*, 1999;Mackenzie *et al.*, 2000), and in SMCs *in situ* (McBride *et al.* Submitted for

publication), QAPB binding was identified on the cell surface and in punctate intracellular sites. The differences in the cellular distribution of QAPB between the mouse strains suggest that the cellular distribution of α_1-ARs may differ, or, at least, that changes occur when an α_1-AR subtype is not present. The lack of intracellular clusters in the α_{1D}-KO could indicate that the α_{1D}-AR is predominantly located inside the cell, while the reduced binding on the cell surface of the α_{1B}-KO and $\alpha_{1B/D}$-KO could point to the main location of the α_{1B}-AR. Similar conclusions were reached using fluorescent antibodies and GFP-tagged receptors in isolated cells (McCune *et al.*, 2000;Sugawara *et al.*, 2002). It is possible that the α_{1B}-AR may have a regulatory role as the increase in punctate binding observed in the α_{1B}-KO and $\alpha_{1B/D}$-KO may be due to a reduction in the transportation of α_{1A}-ARs or α_{1D}-ARs to the cell surface. Thus, in the absence of the α_{1B}-ARs, the α_{1A}-AR and α_{1D}-AR are predominantly located at intracellular sites.

8.3.2. Endothelial cells

Chapter Seven investigated whether α_1-ARs were present on the endothelium of the mouse carotid artery. QAPB binding to EC was confirmed by the use of nuclear dye Syto 61. It was apparent that α_1-ARs were present in all four mouse strains, but α_1-ARs were not detected in all EC identified. The inhibition of QAPB binding to EC by prazosin but not rauwolscine verified the presence of α_1-ARs.

The proportion of EC with α_1-ARs was compared between mouse strains and subtype selective antagonists were used to investigate the α_1-AR subtypes present on the endothelium of the WT mouse. The reduction of EC detected in the α_{1B}-KO, α_{1D}-KO and $\alpha_{1B/D}$-KO is consistent with loss of the respective α_1-AR populations. The presence of endothelial α_{1D}-ARs was suggested in the WT mouse and α_{1B}-KO by the inhibitory effect of BMY 7378. RS100 329 resulted in a reduction in the number of EC stained with QAPB in all four strains, suggesting the presence of α_{1A}-AR on the endothelium. The presence of α_{1B}-ARs was also suggested by blocking both α_{1A}-ARs and α_{1D}-ARs: in the WT mouse, but not the α_{1D}-KO, QAPB binding to EC was observed. Thus, all three α_1-ARs appear to exist on the endothelium of the mouse carotid artery.

Direct functional evidence of α_1-ARs on the endothelium has recently been reported (Filippi *et al.*, 2001;de Andrade C *et al.*, 2006). However, the strong α_1-AR-mediated contractile response makes it difficult to investigate an α_1-AR-mediated relaxatory

response in arteries, like the mouse carotid artery, and may account for the limited evidence of endothelial α_1-AR to date. It is possible that by following the protocol of Filippi et al. (2001) in the perfusion myograph, functional evidence of an α_1-AR-mediated relaxatory response could be obtained in the mouse carotid artery and warrants investigation. Despite no direct functional evidence, Chapter Seven demonstrates that α_1-ARs can be identified on the endothelium visually.

The evidence from Chapters Five and Seven collectively suggest that the direct activation of endothelial α_1-ARs triggers the release of NO. This is a more plausible explanation for NO release due to the existence of α_1-ARs on the endothelium of the mouse carotid artery and the lack of positive evidence for the presence of myo-endothelial junctions in this vessel.

8.4. Future research

Detailed pharmacological analysis is required in the carotid artery of the $\alpha_{1A/B}$-KO to validate the preliminary results presented in Chapter Four. In doing so, further information about the subtype selectivity of the α_1-AR antagonists employed in this thesis would be obtained. In the absence of any selective α_{1B}-AR antagonists, the α_{1B}-KO and $\alpha_{1B/D}$-KO provided some evidence that the α_{1B}-AR has a contractile role, but the $\alpha_{1A/D}$-KO would be the definitive test for an α_{1B}-AR-mediated response. $\alpha_{1A/D}$-KO, as well as the other double knockout mice, are being generated and studied in our laboratory. In addition, studying the QAPB binding distribution in the α_{1A}-KO would complete the examination of the three α_1-AR knockout mice.

8.5. General conclusions

A number of conclusions can be drawn from the studies presented in the previous chapters.

(i). An α_{1A}-AR-mediated contractile response was identified for the first time in the carotid artery of the WT mouse.

(ii). An α_{1A}-AR-mediated contractile response and an α_{1B}-AR-mediated response was identified in the carotid artery of α_1-AR knockout mice, which provided valuable information for the characterisation of the α_1-AR response in the WT mouse. The identification of all three α_1-AR subtypes in the WT mouse highlights that α_1-AR

heterogeneity is an important consideration when assessing the selectivity of α_1-AR compounds.

(iii). In the mouse carotid artery, phenylephrine and A-61603 induced NO release, which had a suppressant action on the contractile response to these α_1-AR agonists.

(iv). Evidence of all three α_1-AR subtypes was observed in the media of the carotid artery. The presence of the subtypes is consistent with their contractile roles identified in this vessel, though the α_{1B}-AR may also have a role in the regulation of the α_{1A}-AR and α_{1D}-AR.

(v). All three α_1-ARs exist on the endothelium of the mouse carotid artery. This unique evidence suggests that the mechanism of NO release in (iii) was through the direct stimulation of endothelial α_1-ARs.

Reference List

Aboud, R., Shafii, M., & Docherty, J. R. (1993). Investigation of the subtypes of alpha 1-adrenoceptor mediating contractions of rat aorta, vas deferens and spleen. *British Journal of Pharmacology.* **109**, 80-87.

Ali, Z. (2004). A study of murine vascular alpha-1-adrenoceptors: a functional knockout approach. University of Glasgow PhD Thesis.

Alosachie, I. & Godfraind, T. (1988). The modulatory role of vascular endothelium in the interaction of agonists and antagonists with alpha-adrenceptors in the rat aorta. *British Journal of Pharmacology* **95**, 619-629.

Amerini, S., Mantelli, L., & Ledda, F. (1995). Enhancement of the vasoconstrictor response to KCL by nitric oxide synthase inhibition: A comparison with noradrenaline. *Pharmacological Research* **31 (314)**, 175-181.

Angus, J., Cocks, T., & Satoh, K. (1986). The alpha adrenoceptors on endothelial cells. *Fed Proc* **45**, 2355-2359.

Arch, S., Ainsworth, A. T., Cawthorne, M. A., Piercy, V., Sennit, M. V., Thody, V. E., Wilson, C., & Wilson, S. (1984). Atypical beta-adrenoceptor on brown adipocytes as target for anti-obesity drugs. *Nature* **309**, 163-165.

Argyle, S. A. & McGrath, J. C. (2000). An alpha 1A/alpha 1L-Adrenoceptor Mediates Contraction of Canine Subcutaneous Resistance Arteries. *Journal of Pharmacology And Experimental Therapeutics* **295**, 627-633.

Balbatun, A., Louka, F., & Malinski, T. (2003). Dynamics of nitric oxide release in the cardiovascular system. *Acta Biochimica Polonica* **50**, 61-68.

Berthelsen, S. & Pettinger, W. A. (1977). A functional basis for classification of alpha-adrenergic receptors. *Life Sciences* **21**, 595-606.

Bevan, J. A. & Osher, J. (1972). A direct method for recording tension changes in the wall of small blood vessels in vitro. *Agents Actions* **2**, 257-260.

Black, J. W., Crowther, A. F., Shanks, R. G., Smith, L. H., & Dornhorst, A. C. (1964). A new adrenergic beta-receptor antagonist. *Lancet* **1**, 1080-1081.

Boer, C., Scheffer, G., de Lange, J. J., Westerhof, N., & Sipkema, P. (1999). alpha-1-adrenoceptor stimulation induces nitric oxide release in rat pulmonary arteries. *J Vasc Res* **36**, 79-81.

Boumaza, S., Arribas, S. M., Osborne-Pellegrin, M., McGrath, J. C., Laurent, S., Lacolley, P., & Challande, P. (2001). Fenestrations of the carotid internal elastic lamina and structural adaptation in stroke-prone spontaneously hypertensive rats. *Hypertension.* **37**, 1101-1107.

Brown, G. L. & Gillespie, J. E. (1957). The output of sympathetic transmitter from the spleen of the cat. *J Physiol* **138**, 81-102.

Buckner, S. A., Oheim, K. W., Morse, P. A., Knepper, S. M., & Hancock, A. A. (1996). Adrenoceptor-induced contractility in rat aorta is mediated by the alpha(1D) subtype. *European Journal of Pharmacology* **297**, 241-248.

Buscher, R., Heeks, C., Taguchi, K., & Michel, M. C. (1996). Comparison of guinea-pig, bovine and rat alpha 1-adrenoceptor subtypes. *British Journal of Pharmacology* **117**, 703-711.

Bylund, D. B., Eikenberg, D. C., Hieble, J. P., Langer, S. Z., Lefkowitz , R. J., Minneman , K. P., Molinoff, P. B., Ruffolo, R. R., & Trendelenburg, U. (1994). IV. International Union of Pharmacology Nomenclature of Adrenoceptors. *The American Society for Pharmacology and Experimental Therapeutics* **46 (2)**, 121-136.

Bylund, D. B., Ray-Prenger, C., & Murphy, T. J. (1988). Alpha-2A and 2B adrenergic receptor subtypes: antagonist binding in tissues and cell lines containing only one receptor subtype. *Journal of Pharmacology And Experimental Therapeutics* **245**, 600-607.

Cavalli, A., Lattion, A. L., Hummler, E., Nenniger, M., Pedrazzini, T., Aubert, J. F., Michel, M. C., Yang, M., Lembo, G., Vecchione, C., Mostardini, M., Schmidt, A., Beermann, F., & Cotecchia, S. (1997). Decreased blood pressure response in mice deficient of the alpha 1b-adrenergicáreceptor. *Proceedings of the National Academy of Sciences* **94**, 11589-11594.

Chalothorn, D., McCune, D. F., Edelmann, S. E., Tobita, K., Keller, B. B., Lasley, R. D., Perez, D. M., Tanoue, A., Tsujimoto, G., Post, G. R., & Piascik, M. T. (2003). Differential cardiovascular regulatory activities of the alpha 1B- and alpha 1D-adrenoceptor subtypes. *Journal of Pharmacology & Experimental Therapeutics.* **305**, 1045-1053.

Chalothorn, D., McCune, D. F., Edelmann, S. E., Garcia-Cazarin, M. L., Tsujimoto, G., & Piascik, M. T. (2002). Differences in the Cellular Localization and Agonist-Mediated Internalization Properties of the alpha 1-Adrenoceptor Subtypes. *Molecular Pharmacology* **61**, 1008-1016.

Chen, L., Xin, X., Eckhart, A. D., Yang, N., & Faber, J. E. (1995). Regulation of Vascular Smooth Muscle Growth by alpha(1)-Adrenoreceptor Subtypes in Vitro and in Situ. *Journal of Biological Chemistry* **270**, 30980-30988.

Chiba, S. & Tsukada, M. (2002). Existence of functional alpha1A- and alpha1D- but no alpha1B-adrenoceptor subtypes in rat common carotid arteries. *Jpn J Pharmacol* **88**, 146-150.

Cleary, L., Murad, K., Bexis, S., & Docherty, J. R. (2005). The alpha-1D-adrenoceptor antagonist BMY 7378 is also an alpha-2C-adrenoceptor antagonist. *Autonomic and Autacoid Pharmacology* **25**, 135-141.

Cleary, L., Vandeputte, C., & Docherty, J. R. (2003). Investigation of postjunctional alpha-1 and alpha-2-adrenoceptor subtypes in vas deferens from wild type and alpha-2A/D-adrenoceptor knockout mice. *British Journal of Pharmacology* **138**, 1069-1076.

Coats, P., Jarajapu, Y. P. R., Hillier, C., McGrath, J. C., & Daly, C. J. (2003). The use of fluorescent nuclear dyes and laser scanning confocal microscopy to study the cellular aspects of arterial remodelling in human subjects with critical limb ischaemia. *Exp Physiol* **88 (4)**, 547-554.

Cocks, T. & Angus, J. (1983). Endothelium-dependent relaxation of coronary arteries by noradrenaline and serotonin. *Nature* **305**, 627-630.

Cotecchia, S., Schwinn, D. A., Randall, R. R., Lefkowitz, R. J., Caron, M. G., & Kobilka, B. K. (1988). Molecular cloning and expression of the cDNA for the hamster alpha 1-adrenergic receptor. *Proceedings of the National Academy of Sciences of the United States of America.* **85**, 7159-7163.

Daly, C. J., Deighan, C., McGee, A., Mennie, D., Ali, Z., McBride, M., & McGrath, J. C. (2002a). A knockout approach indicates a minor vasoconstrictor role for vascular {alpha}1B-adrenoceptors in mouse. *Physiological Genomics* **9**, 85-91.

Daly, C. J., McGee, A., Vila, E., Briones, A., Giraldo, J., Arribas, S. M., Gonzalez, C., Gonzalez, J. M., Somoza, B., Pagakis, S., Adler, J., Provost, J. C., Merle, A., Maddison , J., Pederson, J., & McGrath, J. (2002b). Analysing the 3D structure of blood vessels using confocal microscopy. *Microscopy and Analysis* **92**, 5-8.

Daly, C. J., Milligan, C. M., Milligan, G., Mackenzie, J. F., & McGrath, J. C. (1998). Cellular Localization and Pharmacological Characterization of Functioning Alpha-1 Adrenoceptors by Fluorescent Ligand Binding and Image Analysis Reveals Identical Binding Properties of Clustered and Diffuse Populations of Receptors. *Journal of Pharmacology And Experimental Therapeutics* **286**, 984-990.

Daniel, E. E., Brown, R. D., Wang, Y. F., Low, A. M., Lu-Chao, H., & Kwan, C. Y. (1999). alpha -Adrenoceptors in Canine Mesenteric Artery Are Predominantly 1A

Subtype: Pharmacological and Immunochemical Evidence. *Journal of Pharmacology And Experimental Therapeutics* **291**, 671-679.

de Andrade, C., Fukada, S., Olivon, V., Godoy, M., Haddad, R., Eberlin, M., Cuhna, F., de Souza, H., Laurindo, F., & de Oliveria, A. (2006). Alpha-1D-adrenoceptor-induced relaxation on rat carotid artery is impaired during endothelial dysfunction evoked in the early stages of hyperhomocysteinemia. *European Journal of Pharmacology* **543**, 83-91.

de Oliveria, A., Campos-Mello, C., Leitao, M. C., & Correa, F. M. A. (1998). Maturation and aging-related differences in responsiveness of rat aorta and carotid arteries to alpha-1-adrenoceptor stimulation. *Pharmacology* **57**, 305-313.

Deighan, C., Woollhead, A., Colston, J., & McGrath, J. C. (2004). Hepatocytes from {alpha}1B-adrenoceptor knockout mice reveal compensatory adrenoceptor subtype substitution. *British Journal of Pharmacology* **142**, 1031-1037.

Deighan, C. (2002).Combined Pharmacological/Knockout Approach to Subtyping Alpha 1-Adrenoceptors in Murine Tissues. University of Glasgow PhD Thesis.

Deighan, C., Methven, L., Naghadeh, M. M., Wokoma, A., MacMillan, J., Daly, C. J., Tanoue, A., Tsujimoto, G., & McGrath, J. C. (2005). Insights into the functional roles of alpha1-adrenoceptor subtypes in mouse carotid arteries using knockout mice. *British Journal of Pharmacology* **144**, 558-565.

Dixon, R. A., Kobilka, B. K., Strader, D. J., Benovic, J. L., Dohlman, H. G., Frielle, T., Bolanowski, M. A., Bennett, C. D., Rands, E., Diehl, R. E., Mumford, R. A., Slater, E. E., Sigal, I. S., Caron, M. G., Lefkowitz, R. J., & Strader, C. D. (1986). Cloning of the gene and cDNA for mammalian beta-adrenergic receptor and homology with rhodopsin. *Nature* **321**, 75-79.

Doggrell, S. A. (1992). An analysis of the inhibitory effects of prazosin on the phenylephrine response curves of the rat aorta. *Naunyn-Schmiedebergs Archives of Pharmacology.* **346**, 294-302.

Dora, K. (2001). Cell-cell communication in the vessel wall. *Vascular medicine* **6**, 43-50.

Dora, K., Hinton, J., Walker, S., & Garland, C. (2000). An indirect influence of phenylephrine on the release of endothelium-derived vasodilators in rat small mesenteric artery. *British Journal of Pharmacology* **129**, 381-387.

Eltze, M., Konig, H., Ullrich, B., & Grebe, T. (2001). Failure of AH11110A to functionally discriminate between alpha-1-adrenoceptor subtypes A, B and D or between alpha-1 and alpha-2-adrenoceptors. *European Journal of Pharmacology* **415**, 265-276.

Faber, J. E. & Yang, N. (2006). Balloon injury alters alpha-adrenoceptor expression across rat carotid artery wall. *Clinical Exp Ph Physiol* **33**, 204-210.

Faber, J. E., Yang, N., & Xin, X. (2001). Expression of alpha -Adrenoceptor Subtypes by Smooth Muscle Cells and Adventitial Fibroblasts in Rat Aorta and in Cell Culture. *Journal of Pharmacology And Experimental Therapeutics* **298**, 441-452.

Faure, C., Gouhier, C., Langer, S. Z., & Graham, D. (1995). Quantification of [alpha]1-Adrenoceptor Subtypes in Human Tissues by Competitive RT-PCR Analysis. *Biochemical and Biophysical Research Communications* **213**, 935-943.

Faure, C., Pimoule, C., Arbilla, S., Langer, S. Z., & Graham, D. (1994a). Expression of alpha-1-adrenoceptor subtypes in rat tissues: implications for alpha-1-adrenoceptor classification. *European Journal of Pharmacology* **268**, 141-149.

Faure, C., Pimoule, C., Vallancien, G., Langer, S. Z., & Graham, D. (1994b). Identification of [alpha]1-adrenoceptor subtypes present in the human prostate. *Life Sciences* **54**, 1595-1605.

Filippi S, Parenti A, Donnini S, Granger H, Fazzini A, & Ledda F (2001). Alpha-1D Adrenoceptors cause endothelium-dependent vasodilation in the rat mesenteric vascular bed. *Journal of Pharmacology And Experimental Therapeutics* **296**, 869-875.

Filippi, S., Parenti, A., Donnini, S., Granger, H., Fazzini, A., & Ledda, F. (2001). Alpha-1D Adrenoceptors cause endothelium-dependent vasodilation in the rat mesenteric vascular bed. *Journal of Pharmacology And Experimental Therapeutics* **296**, 869-875.

Flavahan, N. A. & Vanhoutte, P. M. (1986). [alpha]1-Adrenoceptor subclassification in vascular smooth muscle. *Trends in Pharmacological Sciences* **7**, 347-349.

Fonseca, M. I., Button, D. C., & Brown, R. D. (1995). Agonist Regulation of Adrenergic Receptor Subcellular Distribution and Function. *Journal of Biological Chemistry* **270**, 8902-8909.

Ford, A. P. D. W., Chang, D., Clarke, D., Daniels, D. V., Eglen, R. M., Gever, J. R., Jasper, J. R., Kava, M. S., Lachnit, W., Lesnick, J., Melov, T., Stepan, G., & Williams, T. J. (1998). Alpha-1A versus alpha-1L-adrenoceptors: a pharmacological comparison. *Journal of Pharmacology & Experimental Therapeutics* **238**, 139-147.

Ford, A. P. D. W., Williams, T. J., Blue, D. R., & Clarke, D. E. (1994). [alpha]1-Adrenoceptor classification: sharpening Occam's razor. *Trends in Pharmacological Sciences* **15**, 167-170.

Frielle, T., Collins, S., Daniel, K. W., Caron, M. G., Lefkowitz, R. J., & Kobilka, B. K. (1987). Cloning of the cDNA for the human beta 1-adrenergic receptor. *Proceedings of the National Academy of Sciences* **84**, 7920-7924.

Furchgott , R. F. & Zawadzki , J. V. (1980). The obligatory role of endothelial cells in the relaxation of arterial smooth muscle by acetylcholine. *Nature* **288**, 373-376.

Furchgott, R. F. (1967). The pharmacological differentiation of adrenergic receptors. *Ann N Y Acad Sci* **139**, 553-570.

Furchgott, R. F. & Vanhoutte, P. M. (1989). Endothelium-derived relaxing and contracting factors. *FASEB J* **3**, 2007-2018.

Garcia-Sainz, J. A., Casas-Gonzalez, P., Romero-Avila, M., & Gonzalez-Espinosa, C. (1994). Characterization of the hepatic [alpha]1B-adrenoceptors of rats, mice and hamsters. *Life Sciences* **54**, 1995-2003.

Garcia-Sainz, J. A., Vazquez-Prado, J., & Villalobos-Molina, R. (1999). Alpha-1-adrenoceptors: subtypes, signalling, and roles in health and disease. *Arch of Med Res* **30**, 449-458.

Garcia-Sainz, J. A. & Villalobos-Molina, R. (2004). The elusive alpha1d-adrenoceptor: molecular and cellular characteristics and integrative roles. *European Journal of Pharmacology* **500**, 113-120.

Giardina, D., Crucianelli, M., Romanelli, R., Leonardi, A., Poggesi, E., & Melchiorre, C. (1996). Synthesis and biological profile of the enantiomers of [4-(4-amino-6,7-dimethoxyquinazolin-2-yl)-cis-octahydroquinoxalin-1-yl]furan-2-ylmethanone (cyclazosin), a potent competitive alpha 1B-adrenoceptor antagonist. *J medical chemistry* **39**[23], 4602-4607.

Giardina, D., Polimanti, O., Sagratini, G., Angeli, P., Gulini, U., Marucci, G., Melchiorre, C., Poggesi, E., & Leonardi, A. (2003). Searching for cyclazosin analogues as [alpha]1B-adrenoceptor antagonists. *Il Farmaco* **58**, 477-487.

Gisbert, R., Madrero, Y., Sabino, V., Noguera, M. A., Ivorra, M. D., & D'Ocon, P. (2003). Functional characterization of alpha 1-adrenoceptor subtypes in vascular tissues using different experimental approaches: a comparative study. *British Journal of Pharmacology.* **138**, 359-368.

Gisbert, R., Noguera, M. A., Ivorra, M. D., & D'Ocon, P. (2000). Functional Evidence of a Constitutively Active Population of alpha 1D-Adrenoceptors in Rat Aorta. *Journal of Pharmacology And Experimental Therapeutics* **295**, 810-817.

Goetz, A. S., King, H. K., Ward, S. D. C., True, T. A., Rimele, T. J., & Saussy, J. (1995). BMY 7378 is a selective antagonist of the D subtype of [alpha]1-adrenoceptors. *European Journal of Pharmacology* **272**, R5-R6.

Goetz, A. S., Lutz, M. W., Rimele, T. J., & Saussy, D. L. J. (1994). Characterisation of alpha-1-adrenoceptor subtypes in human and canine prostate membrane. *Journal of Pharmacology And Experimental Therapeutics* **271**, 1228-1233.

Gornik HL & Creager MA. (2004). Arginine and endothelial and vascular health. *J Nutr.* **134**, 2880S-2887S.

Graham, R. M., Perez, D. M., Hwa, J., & Piascik, M. T. (1996). {alpha}1-Adrenergic Receptor Subtypes : Molecular Structure, Function, and Signaling. *Circulation Research* **78**, 737-749.

Granneman, J. G. (2001). The putative beta4-adrenergic receptor is a novel state of the beta1-adrenergic receptor. [Review] [33 refs]. *American Journal of Physiology - Endocrinology & Metabolism.* **280**, E199-E202.

Gross, G., Hanft, G., & Rugevics, C. (1988). 5-Methyl-urapidil discriminates between subtypes of the [alpha]1-adrenoceptor. *European Journal of Pharmacology* **151**, 333-335.

Guarino, R. D., Perez, D. M., & Piascik, M. M. Recent advances in the molecular pharmacology of the alpha-1 adrencergic receptor. *Cell Signalling* **8**[5], 323-333. 1996.

Guimaraes, S. & Moura, D. (2001). Vascular Adrenoceptors: An Update. *Pharmacological Reviews* **53**, 319-356.

Gurdal, H., Can, A., & Ugar, M. (2005). The role of nitric oxide synthase in reduced vasocontractile responsiveness induced by prolonged alpha-1 adrenergic receptor stimulation in rat thoracic aorta. *British Journal of Pharmacology* **145**, 203-210.

Hague, C., Chen, Z., Pupo, A. S., Schulte, N. A., Toews, M. L., & Minneman, K. P. (2004a). The N terminus of the human alpha1D-adrenergic receptor prevents cell surface expression. *Journal of Pharmacology & Experimental Therapeutics.* **309**, 388-397.

Hague, C., Uberti, M., Chen, Z., Hall, R., & Minneman, K. P. (2004b). Cell surface expressin of alpha 1D-adrenergic receptors is controlled by heterodimerization with alpha 1B-adrenergic receptors. *Journal of Biological Chemistry* **279 (15)**, 15541-15549.

Han, C., Abel, P. W., & Minneman, K. P. (1987). Alpha 1-Adrenoceptor subtypes likned to different mechanismsfor increaseing intracellular calcium in smooth muscle. *Nature* **329**, 333-335.

Hanft, G. & Gross, G. (1989). Subclassification of alpha 1-adrenoceptor recognition sites by urapidil derivatives and other selective antagonists. *British Journal of Pharmacology* **97**, 691-700.

Hedemann, J. & Michel, M. C. (2002). Alpha1A-adrenoceptors mediate contraction of mouse mesenteric artery. *Receptors and Channels* **8**, 125-126.

Hieble, J. P., Bylund, D. B., Clarke, D. E., Eikenburg, D. C., Langer, S. Z., Lefkowitz, R. J., Minneman, K. P., & Ruffolo, R. R., Jr. (1995a). International Union of Pharmacology.

X. Recommendation for nomenclature of alpha 1-adrenoceptors: consensus update. *Pharmacological Reviews.* **47**, 267-270.

Hirasawa, A., Sugawara, T., Awaji, T., Tsumaya, K., Ito, H., & Tsujimoto, G. (1997). Subtype-Specific Differences in Subcellular Localization of alpha 1-Adrenoceptors: Chlorethylclonidine Preferentially Alkylates the Accessible Cell Surface alpha 1-Adrenoceptors Irrespective of the Subtype. *Molecular Pharmacology* **52**, 764-770.

Honner, V. & Docherty, J. R. (1999). Investigation of the subtypes of alpha-1 adrenoceptor mediating contractions of rat vas deferens. *British Journal of Pharmacology* **128**, 1323-1331.

Horvath, B., Orsy, P., & Benyo, Z. (2005). Endothelial NOS-mediated relaxations of isolated thoracic aorta of the C57BL/6J mouse. *J Cardiovasc Pharmacol* **45**, 225-231.

Hosoda, C., Koshimizu, T. a., Tanoue, A., Nasa, Y., Oikawa R, Tomabechi T, Fukuda S, Shinoura, H., Takeo, S., Kitamura T, Cotecchia, S., & Tsujimoto, G. (2005a). Two alpha1-adrenergic receptor subtypes regulating the vasopressor response have differential roles in blood pressure regulation. *Molecular Pharmacology* **67**, 912-922.

Hosoda, C., Tanoue, A., Shibano, M., Tanaka, Y., Hiroyama, M., Koshimizu, T. A., Cotecchia, S., Tadaichi, K., Tsujimoto, G., & Koike, K. (2005b). Correlation between vasoconstrictor roles and mRNA expression of a1-adrenoceptor subtypes in blood vessels of genetically engineered mice. *British Journal of Pharmacology* **146**, 456-466.

Hrometz, S. L., Edelmann, S. E., McCune, D. F., Olges, J. R., Hadley, R. W., Perez, D. M., & Piascik, M. T. (1999). Expression of Multiple alpha 1-Adrenoceptors on Vascular Smooth Muscle: Correlation with the Regulation of Contraction. *Journal of Pharmacology And Experimental Therapeutics* **290**, 452-463.

Ibarra, M., Pardo, J. P., Lopez-Guerrero, J. J., & Villalobos-Molina, R. (2000). Differential response to chloroethylclonidine in blood vessels of normotensive and spontaneously hypertensive rats: role of {alpha}1D- and {alpha}1A-adrenoceptors in contraction. *British Journal of Pharmacology* **129**, 653-660.

Jarajapu, Y. P. R., Johnston, F., Berry, C., Renwick, A., McGrath, J. C., MacDonald, A., & Hillier, C. (2001a). Functional characterization of alpha 1-adrenoceptor subtypes in human subcutaneous resistance arteries. *Journal of Pharmacology & Experimental Therapeutics* **299**, 729-734.

Jarajapu, Y. P. R., Coats, P., McGrath, J. C., Hillier, C., & MacDonald, A. (2001b). Functional characterization of {{alpha}}1-adrenoceptor subtypes in human skeletal muscle resistance arteries. *British Journal of Pharmacology* **133**, 679-686.

Kallal, L. & Benovic, J. L. (2000). Using green fluorescent proteins to study G-protein-coupled receptor localization and trafficking. *Trends in Pharmacological Sciences* **21**, 175-180.

Kamikihara, S., Mueller, A., Lima, V., Silva, A., de Costa, I., Buratini, J., & Pupo, A. S. (2005). Differential distribution of functional alpha-1-adrenergic receptor subtypes along rat tail artery. *Journal of Pharmacology & Experimental Therapeutics* **314**, 753-761.

Kaneko, K. & Sunano, S. (1993). Involvement of [alpha]-adrenoceptors in the endothelium-dependent depression of noradrenaline-induced contraction in rat aorta. *European Journal of Pharmacology* **240**, 195-200.

Kenny, B. A., Chalmers, D. H., Philpott, P. C., & Naylor, A. M. (1995). Characterization of an alpha 1D-adrenoceptor mediating the contractile response of rat aorta to noradrenaline. *British Journal of Pharmacology* **115**, 981-986.

Knepper, S. M., Buckner, S. A., Brune, M. E., DeBernardis, J. F., Meyer, M. D., & Hancock, A. A. (1995). A-61603, a potent alpha 1-adrenergic receptor agonist, selective for the alpha 1A receptor subtype. *Journal of Pharmacology & Experimental Therapeutics* **274**, 97-103.

Kong, J. Q., Taylor, D. A., & Fleming, W. W. (1994). Functional distribution and role of alpha-1 adrenoceptor subtypes in the mesenteric vasculature of the rat. *Journal of Pharmacology And Experimental Therapeutics* **268**, 1153-1159.

Lachnit, W., Trun, A., Clarke, D., & Ford, A. P. D. W. (1997). Pharmacological characterization of an alpha-1A-adrenceptor mediating contractile responses to noradrenaline in isolated caudal artery of rat. *British Journal of Pharmacology* **120**, 819-826.

Lands, A. M., Arnold, A., McAuliff, J. P., Luduena, F. P., & Brown, T. (1967). Differentiation of receptor systems activated by sympathomimetic amines. *Nature* **214**, 597-598.

Langer, S. Z. (1974). Presynaptic regulation of catecholamine release. *Biochem Pharmacol* **23**, 1793-1800.

Laz, T. M., Forray, C., Smith, K. E., Bard, J. A., Vaysse, P. J., Branchek, T. A., & Weinshank, R. L. (1994). The rat homologue of the bovine alpha 1c-adrenergic receptor shows the pharmacological properties of the classical alpha 1A subtype. *Molecular Pharmacology* **46**, 414-422.

Lazaro-Suarez, M., Gomez-Zamudio, J., Gallardo-Ortiz, I., Tanoue, A., Tsujimoto, G., Farias-Rodriguez, V., & Villalobos-Molina, R. (2006). Chloroethylclonidine reveals that alpha-1A-adrenoceptors mediate contraction in aorta of alpha-1D-adrenoceptor knockout mice. *Autonomic and Autacoid Pharmacology* **25**, 183.

Leech, C. J. & Faber, J. E. (1996). Different alpha-adrenoceptor subtypes mediate constriction of arterioles and venules. *American Journal of Physiology - Heart & Circulatory Physiology* **270**, H710-H722.

Lin, F., Owens, W. A., Chen, S., Stevens, M. E., Kesteven, S., Arthur, J. F., Woodcock, E. A., Feneley, M. P., & Graham, R. M. (2001). Targeted alpha(1A)-adrenergic receptor overexpression induces enhanced cardiac contractility but not hypertrophy. *Circulation Research.* **89**, 343-350.

Lomasney, J. W., Cotecchia, S., Lorenz, W., Leung, W.-Y., Schwinn, D. A., Yang-Feng, T. L., Brownstein, M., Lefkowitz, R. J., & Caron, M. G. (1991). Molecular cloning and expression of the cDNA for the alpha-1A adrenergic receptor: the gene for which is isolated on human chromosome 5. *J Biol Chem* **266**, 6365-6369.

Mackenzie, J. F., Daly, C. J., Pediani, J. D., & McGrath, J. C. (2000). Quantitative Imaging in Live Human Cells Reveals Intracellular alpha 1-Adrenoceptor Ligand-Binding Sites. *Journal of Pharmacology And Experimental Therapeutics* **294**, 434-443.

MacLean, M. R., Clayton, R. A., & Hillis, S. W. (1994). Increased contractile response to 5-hydroxtryptamine$_1$-receptor stimulation in pulmonary arteries from chronic hypoxic rats: role of pharmacological synergy. *Pulm Pharmacol* **7**, 65-72.

Malekzadeh Shafaroudi, M. (2005). Interaction between angiotensin II receptors and alpha-adrenoceptors in the murine vascular system. University of Glasgow PhD Thesis.

Malekzadeh Shafaroudi, M., McBride, M., Deighan , C., Wokoma , A., MacMillan , J., Daly, C. J., & McGrath, I. (2005). Two knockout mouse models demonstrate that aortic vasodilatation is mediated via alpha-2a-adrenoceptors located on the endothelium. *Journal of Pharmacology And Experimental Therapeutics.*

Marti, D., Miquel, R. M., Ziani, K., Gisbert, R., Ivorra, M. D., Anselmi, E., Moreno, L., Villagrasa, V., Barettino, D., & D'Ocon, P. (2005). Correlation between mRNA levels and functional role of alpha-1-adrenoceptor subtypes in arteries: evidence of alpha-1L as a functional isoform of the alpha-1A-adrenoceptor. *AJP - Heart and Circulatory Physiology* **289**, H1923-H1932.

Martin, W., Furchgott, R. F., Villani, G., & Jothianandan, D. (1986). Depression of contractile responses in rat aorta by spontaneously released endothelium-derived relaxing factor. *J Pharmacol Exp Ther.* **237**, 529-538.

Martinez, L., Carmona , L., & Villalobos-Molina, R. (1999). Vascular alpha1D-adrenoceptor function is maintained during congestive heart failure after myocaridal infarction in the rat. *Arch of Med Res* **30**, 290-297.

McBride, M., MacMillan, J., Methven, L., Tanoue, A., Tsujimoto, G., Daly, C. J., & McGrath, I. (2006a). The alpha-1B/D-adrenerigc receptor knockout mouse permits isolation and visualisation of the alpha-1A subtype in vascular smooth muscle. *Molecular Pharmacology.*

McCloskey, D. T., Turnbull, L., Swigart, P., O'Connell, T. D., Simpson, P. C., & Baker, A. J. (2003). Abnormal Myocardial Contraction in [alpha]1A- and [alpha]1B-adrenoceptor double-knockout mice. *Journal of Molecular and Cellular Cardiology* **35**, 1207-1216.

McCune, D. F., Edelmann, S. E., Olges, J. R., Post, G. R., Waldrop, B. A., Waugh, D. J. J., Perez, D. M., & Piascik, M. T. (2000). Regulation of the Cellular Localization and Signaling Properties of the alpha 1B- and alpha 1D-Adrenoceptors by Agonists and Inverse Agonists. *Molecular Pharmacology* **57**, 659-666.

McGrath, I. & Daly, C. J. (2005). The use of fluorescent ligands and proteins to visualise adrenergic receptors. In *The adrenergic receptors in the 21st century*, ed. Perez, D. M..

McGrath, J. C. (1982a). Evidence for more than one type of post-junctional [alpha]-Adrenoceptor. *Biochemical Pharmacology* **31**, 467-484.

McGrath, J. C. (1982b). Is there more than one alpha-1 adrenoceptor or is this the wrong question? *British Journal of Pharmacology* **76**, 210P.

McGrath, J. C., Mackenzie, J. F., & Daly, C. J. (1999). Pharmacological implications of cellular localization of alpha1-adrenoceptors in native smooth muscle cells. *Journal of Autonomic Pharmacology.* **19**, 303-310.

McGrath, J. C., Pediani, J. D., MacMillan, J., Mackenzie, J. F., Deighan, C., Woollhead, A., McGrory, S., McBride, M., Ali, Z., Malekzadeh Shafaroudi, M., Cotecchia, S., Arribas, S. M., Vila, E., Briones, A., Perez, D. M., Mullins, J. J., Tsujimoto, G., & Daly, C. J. (2002). Adventitial cells are identified as the major location of vascular alpha 1B-adrenoceptors and may drive vascular remodelling. *British Journal of Pharmacology* **137**, 21P.

Meyer, M. D., Altenbach, R. J., Hancock, A. A., Buckner, S. A., Knepper, S. M., & Kerwin , J. F. (1996). Synthesis and in vitro characterization of N-[5-(4,5-dihydro-1H-imidazol-2-yl)-2-hydroxy-5,6,7,8-tetrahydronaphthalen-1-yl]methanesulfonamide and its enantiomers: a novel selective alpha-1a receptor agonist. *J medical chemistry* **39**, 4116-4119.

Michel, A., Loury, D., & Whiting, R. (1989). Identification of a single alpha-1-adrenoceptor corressponding to alpha-1A subtype in rat submaxillary gland. *British Journal of Pharmacology* **98**, 883-889.

Michel, M. C., Kerker, J., Branchek, T. A., & Forray, C. (1993). Selective irreversible binding of chloroethylclonidine at alpha 1- and alpha 2-adrenoceptor subtypes. *Molecular Pharmacology* **44**[6], 1165-1170.

Milano, C. A., Dolber, P. C., Rockman, H. A., Bond, R. A., Venable, M. E., Allen, L. F., & Lefkowitz, R. J. (1994). Myocardial expression of a constitutively active alpha 1B-adrenergic receptor in transgenic mice induces cardiac hypertrophy. *Proceedings of the National Academy of Sciences of the United States of America.* **91**, 10109-10113.

Miller, J. W., Zhuo-Wei, H., Okazaki, M., Fujinaga, M., & Hoffman, B. B. (1996). Expression of [alpha]1 adrenergic receptor subtype mRNAs in the rat cardiovascular system with aging. *Mechanisms of Ageing and Development* **87**, 75-89.

Minneman , K. P., Theroux, T. L., Hollinger, S., Han, C., & Esbenshade, T. A. (1994). Selectivity of agonists for cloned alpha-1-adrenergic receptor subtypes. *Molecular Pharmacology* **46**[5], 929-936.

Minneman, K. P. (1988). Alpha-1-adrenergic receptor subtypes, inositol phosphates, and sources of cell calcium. *Pharmacological Reviews* **40**, 87-119.

Minneman, K. P., Han, C., & Abel, P. W. (1988). Comparison of alpha 1-adrenergic receptor subtypes distinguished by chlorethylclonidine and WB 4101. *Molecular Pharmacology* **33**, 509-514.

Miquel, R. M., Segura, V., Ali, Z., D'Ocon, P., McGrath, J. C., & Daly, C. J. (2005). 3-D image analysis of fluorescent drug binding. *Mol Imaging* **4**, 1-13.

Morrow, A. L. & Creese, I. (1986). Characterisation of alpha-1 adrenergic receptor subtrypes in rat brain: a reevaluation of 3H-prazosin binding. *Molecular Pharmacology* **29**, 321-333.

Morton, J. S. Novel in vitro models to investigate pharmacological targets in genital resistance vasculature. 2006. University of Glasgow PhD Thesis.

Mulvany, M. J. & Halpern, W. (1976). Mechanical properties of vascular smooth muscle cells in situ. *Nature* **260**, 617-618.

Muramatsu, I. (1991). Relation between adrenergic neurogenic contraction and alpha 1-adrenoceptor subtypes in dog mesenteric and carotid arteries and rabbit carotid arteries. *British Journal of Pharmacology* **102**, 210-214.

Muramatsu, I., Ohmura, T., Kigoshi, S., Hashimoto, S., & Oshita, M. (1990). Pharmacological subclassification of alpha1-adrenoceptors in vascular smooth muscle. *British Journal of Pharmacology* **99**, 197-201.

Naghadeh, M. M. (1996). Vasomodulator mechanisms in rat carotid artery and in vessels from an experimental model of heart failure. University of Glasgow PhD Thesis.

O'Connell, T. D., Ishizaka, S., Nakamura, A., Swigart, P. M., Rodrigo, M. C., Simpson, G. L., Cotecchia, S., Rokosh, D. G., Grossman, W., Foster, E., & Simpson, P. C. (2003). The {alpha}1A/C- and {alpha}1B-adrenergic receptors are required for physiological cardiac hypertrophy in the double-knockout mouse. *Journal of Clinical Investigation* **111**, 1783-1791.

Oshita, M., Kigoshi, S., & Muramatsu, I. (1993). Pharmacological characterization of two distinct alpha 1-adrenoceptor subtypes in rabbit thoracic aorta. *British Journal of Pharmacology*. **108**, 1071-1076.

Palmer , R. M. J., Ferrige, A., & Moncada , S. (1987). Nitric oxide release accounts for the biological activity of endothelium-derived relaxing factor. *Nature* **327**, 524-526.

Palmer, R. M., Rees, D., Ashton, D., & Moncada , S. (1988). L-arginine is the physiological precursor for the formation of nitric oxide in endothelium-dependent relaxation. *Biochem Biophy Res Commun.* **153**[3], 1251-1256.

Papay, R., Gaivin, R., Jha, A., McCune, D. F., McGrath, J. C., Rodrigo, M. C., Simpson, P. C., Doze, V. A., & Perez, D. M. (2006). Localization of the mouse alpha 1A-adrenergic receptor (AR) in the brain: alpha 1A-AR is expressed in neurons, GABAergic interneurons, and NG2 oligodendrocyte progenitors. *The Journal of Comparitive Neurology* **497**, 209-222.

Papay, R., Gaivin, R., McCune, D. F., Rorabaugh, B., Macklin, W., McGrath, J. C., & Perez, D. M. (2004). Mouse alpha 1B-adrenergic receptor is expressed in neurons and NG2 oligodendrocytes. *The Journal of Comparitive Neurology* **478**, 1-10.

Pediani, J., Mackenzie, J. F., Heeley, RP., Daly, C. J., & McGrath, J. C. (2000). Single-cell recombinant pharmacology: bovine alpha-1a adrenoceptors in rat-1 fibroblasts release intracellular calcium, display subtype-characteristic agonism and antagonism and exhibit an antagonist-reversible inverse concentration-response phase. *Journal of Pharmacology And Experimental Therapeutics* **293**, 895.

Pediani, J. D., Colston, J. F., Caldwell, D., Milligan, G., Daly, C. J., & McGrath, J. C. (2005). Beta-arrestin-dependent spontaneous alpha-1a-adrenoceptor endocytosis causes intracellular transportation of alpha-blockers via recycling compartments. *Molecular Pharmacology* **67**, 1004.

Perez, D. M., DeYoung, M. B., & Graham, R. M. (1993). Coupling of expressed alpha 1B- and alpha 1D-adrenergic receptor to multiple signaling pathways is both G protein and cell type specific. *Molecular Pharmacology* **44**, 784-795.

Perez, D. M., Piascik, M. M., Malik, N., Gaivin, R., & Graham, R. M. (1994). Cloning, expression and tissue distribution of the rat homolog of the bovine alpha-1C receptor provides evidence for its classification as the alpha-1A subtype. *Molecular Pharmacology* **46**, 823-831.

Perez, D. M., Piascik, M. T., & Graham, R. M. (1991). Solution-phase library screening for the identification of rare clones: isolation of an alpha 1D-adrenergic receptor cDNA. *Molecular Pharmacology* **40**, 876-883.

Perry, B. D. & UPrichard, D. C. (1981). [3H]rauwolscine (alpha-yohimbine): a specific antagonist radioligand for brain alpha 2-adrenergic receptors. *European Journal of Pharmacology* **76**, 461-464.

Piascik, M. T. & Perez, D. M. (2001). alpha 1-Adrenergic Receptors: New Insights and Directions. *Journal of Pharmacology And Experimental Therapeutics* **298**, 403-410.

Piascik, M. T., Hrometz, S. L., Edelmann, S. E., Guarino, R. D., Hadley, R. W., & Brown, R. D. (1997). Immunocytochemical Localization of the Alpha-1B Adrenergic Receptor and the Contribution of This and the Other Subtypes to Vascular Smooth Muscle Contraction: Analysis with Selective Ligands and Antisense Oligonucleotides. *Journal of Pharmacology And Experimental Therapeutics* **283**, 854-868.

Pimoule, C., Langer, S. Z., & Graham, D. (1995). Further evidence that the classical alpha(1A)- and cloned alpha(1c)-adrenoceptors are the same subtype. *European Journal of Pharmacology-Molecular Pharmacology Section* **290**, 49-53.

Powell, C. E. & Slater, I. H. (1958). Blocking of inhibitory adrenergic receptors by a dichloro analog of isoproterenol. *J Pharmacol Exp Ther.* **122**, 480-488.

Price, D. T., Chari, R. S., Berkowitz, D. E., Meyers, W. C., & Schwinn, D. A. (1994a). Expression of alpha 1-adrenergic receptor subtype mRNA in rat tissues and human SK-N-MC neuronal cells: implications for alpha 1-adrenergic receptor subtype classification. *Molecular Pharmacology* **46**, 221-226.

Price, D. T., Lefkowitz, R. J., Caron, M. G., Berkowitz, D., & Schwinn, D. A. (1994b). Localization of mRNA for three distinct alpha 1-adrenergic receptor subtypes in human tissues: implications for human alpha-adrenergic physiology. *Molecular Pharmacology* **45**, 171-175.

Rees, D., Palmer, R. M., Schulz, R., Hodson, H. F., & Moncada, S. (1990). Characterisation of three inhibitors of endothelial nitric oxide synthase in vitro and in vivo. *British Journal of Pharmacology* **101**, 746-752.

Regan, J. W., Kobilka, T. S., Yang-Feng, T. L., Caron, M. G., Lefkowitz, R. J., & Kobilka, B. K. (1988). Cloning and expression of a human kidney cDNA for an alpha-2-adrenergic receptor subtype. *Proceedings of the National Academy of Sciences* **85**, 6301-6305.

Rohrer, D. K. & Kobilka, B. K. (1998). Insights from in vivo modification of adrenergic receptor gene expression. *Annual Review of Pharmacology & Toxicology* **38**, 351-373.

Rokosh, D. G., Bailey, B. A., Stewart, A. F. R., Karns, L. R., Long, C. S., & Simpson, P. C. (1994). Distribution of [alpha]1C-Adrenergic Receptor mRNA in Adult-Rat Tissues by RNase Protection Assay and Comparison with [alpha]1B and [alpha]1D. *Biochemical and Biophysical Research Communications* **200**, 1177-1184.

Rokosh, D. G. & Simpson, P. C. (2002). Knockout of the alpha 1A/C-adrenergic receptor subtype: The alpha 1A/C is expressed in resistance arteries and is required to maintain arterial blood pressure. *Proceedings of the National Academy of Sciences* **99**, 9474-9479.

Ruan, Y., Parmentier, J., Fatima, S., Allen, L., & Malik, K. (1998). Alpha-1A-adrenergic receptor stimulation with phenylephrine promotes arachidonic acid release by activation of phospholipase D in rat-1 fibroblasts: inhibition by protein kinase A. *J Pharmacol Exp Ther.* **284**, 576-585.

Saussy, D. J., Goetz, A. S., Queen, K. L., King, H. K., Lutz, M. W., & Rimele, T. J. (1996). Structure activity relationships of a series of buspirone analogs at alpha-1 adrenoceptors: further evidence that rat aorta alpha-1 adrenoceptors are of the alpha-1D-subtype. *Journal of Pharmacology And Experimental Therapeutics* **278**, 136-144.

Schwinn, D. A., Johnston, G., Page, S., Mosley, M., Wilson, K., Worman, N., Campbell, S., Fidock, M., Furness, L., & Parry-Smith, D. J. (1995). Cloning and pharmacological characterization of human alpha-1 adrenergic receptors: sequence corrections and direct comparison with other species homologues. *Journal of Pharmacology And Experimental Therapeutics* **272**[1], 134-142.

Schwinn, D. A., Lomasney, J. W., Lorenz, W., Szklut, P. J., Fremeau, R. T., Jr., Yang-Feng, T. L., Caron, M. G., Lefkowitz, R. J., & Cotecchia, S. (1990). Molecular cloning and expression of the cDNA for a novel alpha 1- adrenergic receptor subtype. *Journal of Biological Chemistry* **265**, 8183-8189.

Schwinn, D. A., Page, S., Middleton, J., Lorenz, W., Liggett, S., Yamamoto, K., Lapetine, E., Caron, M., Lefkowitz, R., & Cotecchia, S. (1991). The alpha 1C-adrenergic receptor: characterization of signal transduction pathways and mammalian tissue heterogeneity. *Molecular Pharmacology* **40**, 619-626.

Scofield, M. A., Liu, F., Abel, P. W., & Jeffries, W. B. (1995). Quantification of steady state expression of mRNA for alpha-1 adrenergic receptor subtypes using reverse transcription and a competitive polymerase chain reaction. *Journal of Pharmacology And Experimental Therapeutics* **275**, 1035-1042.

Scotland, R. S., Madhani , M., Chauhan, S., Moncada , S., Andresen , J., Nilsson , H., Hobbs, A., & Ahluwalia, A. (2005). Investigation of vascular responses in endothelial nitric oxide synthase/cyclooxygenase-1 double-knockout mice. *Circulation* **111**, 796-803.

Semwogerere, D. & Weeks, E. (2005). Confocal Microscopy. In *Encyclopedia of Biomaterials and Biomedical Engineering*, eds. Wnek, G. & Bowlin, G., pp. 1-10. Marcel Dekker Ltd..

Shibano, M., Yamamoto, Y., Horinouchi, T., Tanaka, Y., & Koike, K. (2002). Pharmacological characterization of alpha1-adrenoceptor in mouse iliac artery. *European Journal of Pharmacology.* **456**, 77-79.

Shibata, K., Foglar, R., Horie, K., Obika, K., Sakamoto, A., Ogawa, S., & Tsujimoto, G. (1995). KMD-3213, a novel, potent, alpha 1a-adrenoceptor-selective antagonist: characterization using recombinant human alpha 1-adrenoceptors and native tissues. *Molecular Pharmacology* **48**[2], 250-258.

Shimokawa, H., Yasutake, H., Fujii , K., Owada , K. M., Nakaike, R., Fukumoto , Y., Takayanagi, T., Nagao, T., Egashira , K., Fujishima, M., & Takeshita, A. (1996). The importance of the hyperpolarizing mechanism increases as the vessel size decreases in endothelium-dependent relaxations in rat mesenteric circulation. *J Cardiovasc Pharmacol* **28 (5)**, 703-711.

Simpson, P. C. (2006). The alpha-1 adrenergic receptors: lessons from knockouts. In *The adrenergic receptors in the 21st century*, ed. Perez, D. M., pp. 207-239. Humana Press.

Sleight, A., Koek, W., & Bigg, D. (1993). Binding of antipsychotic drugs at alpha 1A- and alpha 1B-adrenoceptors:risperidone is selective for the alpha 1B-adrenoceptors. *European Journal of Pharmacology* **238**, 407-410.

Spagnoli, L., Villaschi, S., Neri, L., & Palmieri, G. (1982). Gap junctions in myo-endothelial bridges of rabbit carotid arteries. *Experientia* **38**, 124-125.

Stam, W. B., Van der Graaf, P. H., & Saxena, P. R. (1998). Functional characterisation of the pharmacological profile of the putative alpha1B-adrenoceptor antagonist, (+)-cyclazosin. *European Journal of Pharmacology.* **361**, 79-83.

Starke, K. (1972). Alpha sympathomimetic inhibition of adrenergic and cholinergic transmission in the rabbit heart. *Naunyn-Schmiedebergs Archives of Pharmacology.* **274**, 18-45.

Stassen, F. R., Maas, R. G., Schiffers, P. M., Janssen, G. M., & De Mey, J. G. (1998). A Positive and Reversible Relationship Between Adrenergic Nerves and Alpha-1A Adrenoceptors in Rat Arteries. *Journal of Pharmacology And Experimental Therapeutics* **284**, 399-405.

Stassen, F. R., Williamsen, M., Janssen, G., & De Mey, J. G. (1997). Alpha1-adrenoceptor subtypes in rat aorta and mesenteric small arteries are preserved during left ventricular dysfunction post-myocardial infarction. *Cardiovascular Research* **33**, 706-713.

Stelzer, E. (1995). The intermediate optical system of laser-scanning confocal microscopes. In *The Handbook of Biological Confocal Microscopy*, ed. Pawley, J. B..

Sugawara, T., Hirasawa, A., Hashimoto K, & Tsujimoto, G. (2002). Differences in the subcellular localization of a1-adrenoceptor subtypes can affect the subtype selectivity of drugs in a study with the fluorescent ligand BODIPY FL-prazosin. *Life Sciences* **70**, 2113-2124.

Tabernero, A., Giraldo, J., & Vila, E. (1999). Modelling the changes due to the endothelium and hypertension in the a-adrenoceptor-mediated responses of rat aorta. *Journal of Autonomic Pharmacology.* **19**, 219-228.

Tabernero, A. & Vila, E. (1995). Effect of age on noradrenaline responses in rat tail artery and aorta: role of endothelium. *Journal of Autonomic Pharmacology.* **15**, 327-333.

Taguchi, K., Yang, M., Goepel, M., & Michel, M. C. (1998). Comparison of human alpha1-adrenoceptor subtype coupling to protein kinase C activation and related signalling pathways. *Naunyn-Schmiedebergs Archives of Pharmacology.* **357**[2], 100-110.

Tanaka, T., Zhang, L., Suzuki, F., & Muramatsu, I. (2004). Alpha-1 adrenoceptors: evaluation of receptor subtype-binding kinetics in intact arterial tissues and comparison with membrane binding. *British Journal of Pharmacology* **141**, 468-476.

Tanoue, A., Koshimizu, T. A., & Tsujimoto, G. (2002a). Transgenic studies of [alpha]1-adrenergic receptor subtype function. *Life Sciences* **71**, 2207-2215.

Tanoue, A., Koba, M., Miyawaki, S., Koshimizu, T. a., Hosoda, C., Oshikawa, S., & Tsujimoto, G. (2002b). Role of the {alpha}1D-Adrenegric Receptor in the Development of Salt-Induced Hypertension. *Hypertension* **40**, 101-106.

Tanoue, A., Nasa, Y., Koshimizu, T., Shinoura, H., Oshikawa, S., Kawai, T., Sunada, S., Takeo, S., & Tsujimoto, G. (2002c). The {alpha}1D-adrenergic receptor directly regulates arterial blood pressure via vasoconstriction. *Journal of Clinical Investigation* **109**, 765-775.

Terasaki, M. & Dailey, M. (1995). Confocal microscopy of living cells. In *The handbook of biological confocal microscopy*, ed. Pawley, J. B., pp. 327-346.

Testa, R., Guarneri, L., Angelico, P., Poggesi, E., Taddei, C., Sironi, G., Colombo, D., Sulpizio, A. C., Naselsky, D. P., Hieble, J. P., & Leonardi, A. (1997). Pharmacological Characterization of the Uroselective Alpha-1 Antagonist Rec 15/2739 (SB 216469): Role of the Alpha-1L Adrenoceptor in Tissue Selectivity, Part II. *Journal of Pharmacology And Experimental Therapeutics* **281**, 1284-1293.

Theroux, T. L., Esbenshade, T. A., Peavy, R., & Minneman , K. P. (1996). Coupling efficiencies of human alpha 1-adrenergic receptor subtypes: titration of receptor density and responsiveness with inducible and repressible expression vectors. *Molecular Pharmacology* **50**[5], 1376-1387.

Turnbull, L., McCloskey, D. T., O'Connell, T. D., Simpson, P. C., & Baker, A. J. (2003). alpha 1-Adrenergic receptor responses in alpha 1AB-AR knockout mouse hearts suggest the presence of alpha 1D-AR. *AJP - Heart and Circulatory Physiology* **284**, H1104-H1109.

Tuttle, J. L. & Falcone, J. C. (2001). Nitric oxide release during alpha1-adrenoceptor-mediated constriction of arterioles. *American Journal of Physiology - Heart & Circulatory Physiology.* **281**, H873-H881.

Uberti, M., Hall, R., & Minneman, K. P. (2003). Subtype-specific dimerization of alpha1-adrenoceptors: effects on receptor expression and pharmacological properties. *Molecular Pharmacology* **64**, 1379-1390.

Van der Graaf, P. H., Deplanne, V., Duquenne, C., & Angel, I. (1997). Analysis of alpha1-adrenoceptors in rabbit lower urinary tract and mesenteric artery. *European Journal of Pharmacology* **327**[1], 25-32.

Van der Graaf, P. H., Shankley, N. P., & Black, J. W. (1996). Analysis of the activity of alpha 1-adrenoceptor antagonists in rat aorta. *British Journal of Pharmacology.* **118**, 299-310.

Vanhoutte, P. M. (2001). Endothelial adrenoceptors. [Review] [138 refs]. *Journal of Cardiovascular Pharmacology.* **38**, 796-808.

Vanhoutte, P. M. & Miller, V. M. (1989). Alpha-2-adrenoceptors and endothelium-derived relaxing factor. *Am J Med.* **87**, 1S-5S.

Vargas, H. M. & Gorman, A. J. (1995). Vascular alpha-1 adrenergic receptor subtypes in the regulation of arterial pressure. *Life Sciences* **57**, 2291-2308.

Vecchione, C., Fratta, L., Rizzoni, D., Notte, A., Poulet, R., Porteri, E., Frati, G., Guelfi, D., Trimarco, V., Mulvany, M. J., Agabiti-Rosei, E., Trimarco, B., Cotecchia, S., & Lembo, G. (2002). Cardiovascular Influences of {alpha}1b-Adrenergic Receptor Defect in Mice. *Circulation* **105**, 1700-1707.

Villalobos-Molina, R. & Ibarra, M. (1996). [alpha]1-Adrenoceptors mediating contraction in arteries of normotensive and spontaneously hypertensive rats are of the [alpha]1D or [alpha]1A subtypes. *European Journal of Pharmacology* **298**, 257-263.

Weinberg, D. H., Trivedi, P., Tan, C. P., Mitra, S., Perkins-Barrow, A., Borkowski, D., Strader, C. D., & Bayne, M. (1994). Cloning, expression and characterization of human alpha adrenergic receptors alpha 1a, alpha 1b and alpha 1c. *Biochem Biophy Res Commun.* **201**[3], 1296-1304.

Weitzell, R., Tanaka, T., & Starke, K. (1979). Pre and postsynaptic effects of yohimbine stereoisomers on noradrenergic transmission in the pulmonary artery of the rabbit. *Naunyn-Schmiedebergs Archives of Pharmacology.* **308**, 127-136.

Willems, E. W., Heiligers, J. P., De Vries, P., Tom, B., Kapoor, K., Villalon, C. M., & Saxena, P. R. (2001). A61603-induced vasoconstriction in porcine carotid vasculature:

involvement of a non-adrenergic mechanism. *European Journal of Pharmacology.* **417,** 195-201.

Williams, N., Zhong, H., & Minneman , K. P. (1998). Differential coupling of alpha 1-, alpha 2- and beta-adrenergic receptors to MAP kinase pathways and differentiation in transfected PC12 cells. *J Biol Chem* **273,** 24624-24632.

Williams, T. J., Blue, D. R., Daniels, D. V., Davis, B., Elworthy, T., Gever, J. R., Kava, M. S., Morgans, D., Padilla, F., Tassa, S., Vimont, R. L., Chapple, C. R., Chess-Williams, R., Eglen, R. M., Clarke, D. E., & Ford, A. P. D. W. (1999). In vitro {alpha}1-adrenoceptor pharmacology of Ro 70-0004 and RS-100329, novel {alpha}1A-adrenoceptor selective antagonists. *British Journal of Pharmacology* **127,** 252-258.

Woollhead, A. (2002). Design of a molecular strategy to analyse the subcellular distribution of alpha 1-adrenoceptors in recombinant and native systems. University of Glasgow PhD Thesis.

Wu, D., Katz, A., Lee, C. H., & Simon, M. I. (1992). Activation of phospholipase C by alpha 1-adrenergic receptors is mediated by the alpha subunits of Gq family. *Journal of Biological Chemistry* **267,** 25798-25802.

Xin, X., Yang, N., Eckhart, A. D., & Faber, J. E. (1997). alpha 1D-Adrenergic Receptors and Mitogen-Activated Protein Kinase Mediate Increased Protein Synthesis by Arterial Smooth Muscle. *Molecular Pharmacology* **51,** 764-775.

Yamamoto, Y. & Koike, K. (2001a). alpha(1)-Adrenoceptor subtypes in the mouse mesenteric artery and abdominal aorta. *British Journal of Pharmacology.* **134,** 1045-1054.

Yamamoto, Y. & Koike, K. (2001b). Characterization of alpha1-adrenoceptor-mediated contraction in the mouse thoracic aorta. *European Journal of Pharmacology.* **424,** 131-140.

Yang, M., Reese, J., Cotecchia, S., & Michel, M. C. (1998). Murine alpha1-adrenoceptor subtypes. I. Radioligand binding studies. *Journal of Pharmacology & Experimental Therapeutics.* **286,** 841-847.

Yoshio, R., Taniguchi, T., Itoh, H., & Muramatsu, I. (2001). Affinity of serotonin receptor antagonists and agonists to recombinant and native alpha1-adrenoceptor subtypes. *Jpn J Pharmacol* **86,** 189-195.

Zacharia, J., Hillier, C., & MacDonald, A. (2004). Alpha-1-adrenoceptor subtypes involved in vasoconstrictor responses to exogenous and neurally released noradrenaline in rat femoral resistance arteries. *British Journal of Pharmacology* **141,** 915-924.

Ziani, K., Gisbert, R., Noguera, M. A., Ivorra, M. D., & D'Ocon, P. (2002). Modulatory role of a constitutively active population of alpha 1D-adrenoceptors in conductance arteries. *AJP - Heart and Circulatory Physiology* **282**, H475-H481.

Zschauer, A., Sielczak, M., Smith, D., & Wanner, A. (1997). Norepinephrine-induced contraction of isolated rabbit bronchial artery: role of alpha-1 and alpha-2 adrenoceptor activation. *journal of applied physiology* **82 (6)**, 1918-1925.

Zuscik, M. J., Chalothorn, D., Hellard, D., Deighan, C., McGee, A., Daly, C. J., Waugh, D. J. J., Ross, S. A., Gaivin, R. J., Morehead, A. J., Thomas, J. D., Plow, E. F., McGrath, J. C., Piascik, M. T., & Perez, D. M. (2001). Hypotension, Autonomic Failure, and Cardiac Hypertrophy in Transgenic Mice Overexpressing the alpha 1B-Adrenergic Receptor. *Journal of Biological Chemistry* **276**, 13738-13743.